**Oceano Dunes State Vehicular Recreation Area (ODSVRA) Dust Control Program
Draft 2024 Annual Report and Work Plan (ARWP)**

ATTACHMENTS

Attachment 01: 2011 to 2024 Dust Control Projects

Attachment 02: 2023/2024 ODSVRA Dust Control Program Vegetation Restoration Projects
(State Parks' ARWP Work Product)

Attachment 03: Report of Findings: ODSVRA Meteorological and PM_{10} Monitoring Network, 2023

- Report of Findings: ODSVRA Meteorological and PM_{10} Monitoring Network, 2023 (DRI Document)

- SAG Review of Desert Research Institute (DRI) "Report of Findings: ODSVRA Meteorological and PM_{10} Monitoring Network, 2023" (SAG Memo)

Attachment 04A: UCSB 2022-2023 ODSVRA Foredune Restoration UAS Survey Report

- UCSB 2022-2023 ODSVRA Foredune Restoration UAS Survey Report (UCSB Report)

- SAG Review of UCSB Report "Foredune Restoration UAS Survey Report" (UCSB 2022-2023 ODSVRA) (SAG Memo)

Attachment 04B: UCSB 2023-2024 ODSVRA Foredune Restoration UAS Survey Report

- UCSB 2023-2024 ODSVRA Foredune Restoration UAS Survey Report (UCSB Report)

- SAG Review of UCSB Report "2023-2024 ODSVRA Foredune Restoration UAS Monitoring Report" (SAG Memo)

Attachment 05: 2022-2023 Time-Lapse Photography Report Documents:

- Preliminary Analysis of Time-Lapse Photo Monitoring at the Oceano Dunes Foredune Restoration Site (UCSB Report)

- SAG Review of UCSB Report "Preliminary Analysis of Time-Lapse Photo Monitoring at the Oceano Dunes Foredune Restoration Site" (SAG Memo)

Attachment 06: Summary of Vegetation Monitoring of Restoration Sites at ODSVRA (2023)
(State Parks' ARWP Work Product)

ODSVRA Dust Control Program Draft 2024 ARWP

ATTACHMENT 01

2011 to 2024 Dust Control Projects

THIS PAGE WAS INTENTIONALLY LEFT BLANK

Total Acres of Dust Control

- Vegetation projects (399.9 acres)
- Straw treatment projects (12.3 acres)

Total dust control project acreage: 412.2 acres

- Additional dust reduction benefit area (293.3 acres)
- Seasonally closed foredune beach and corridor area (34.6 acres)

Total dust control program acreage: 740.1 acres

Source: CDPR, MIG   Imagery: 2014 NAIP

5/14/2024

Feet
0   500 1,000   2,000

A01-01: Cumulative Dust Control as of 7/31/24

2024 ARWP

- ● Marker post
- ▢ Park boundary
- Existing fenced vegetated islands
- — - — Open riding and camping area boundary fence

Labels on map:
2020-WF-01 / 2023-VG-01
2022-ST-01
2022-VG-01
2018-SB-01 / 2019-VG-01
2022-VG-02
2018-WF-01
2018-VG-01
2018-VG-02
2020-SB-02 / 2021-VG-02
2020-WF-02 / 2022-VG-03
2021-TV-01 / 2022-VG-06
2022-VG-07
2014-SB-01 / 2015-VG-01 / 2016-VG-01 / 2017-VG-01
2021-WF-01 / 2024-VG-01
2021-ST-04 / 2022-VG-12
2021-ST-05 / 2022-VG-13
2013-VG-01
2012-VG-01
2013-VG-02
2021-VG-05
2021-VG-07
2021-VG-06
2021-ST-03 / 2022-VG-11
2020-VG-01
2020-VG-02
2020-VG-03
2018-WF-02 / 2020-VG-04 / 2020-SB-01 / 2021-VG-01
2021-ST-01 / 2022-VG-04
2018-SB-02 / 2019-VG-02
2021-ST-02 / 2022-VG-05
2018-WF-04 / 2021-VG-03
2018-WF-05 / 2021-VG-04
2021-TV-02 / 2022-VG-08
2022-ST-02 / 2023-VG-02 / 2024-VG-02
2021-WF-02 / 2024-VG-03
2022-VG-10
2022-VG-09

Place names: Pavillion Hill, Worm Valley, Foredune North, Foredune Central, Foredune South, Bigfoot, La Grille Hill, North Eucalyptus Tree, Eucalyptus Tree, Schnauzer, Boy Scout Camp, Pipeline

Numbers on map: 65, 50, 51, 27, 24, 28, 30, 34, 18, 19, 35, 53, 54, 25, 55, 56, 58, 57, 67, 59, 66, 68, 69, 61, 62, 63, 64, 47, 48, 49, 14, 3, 2, 4, 5, 6, 7, 8, 4

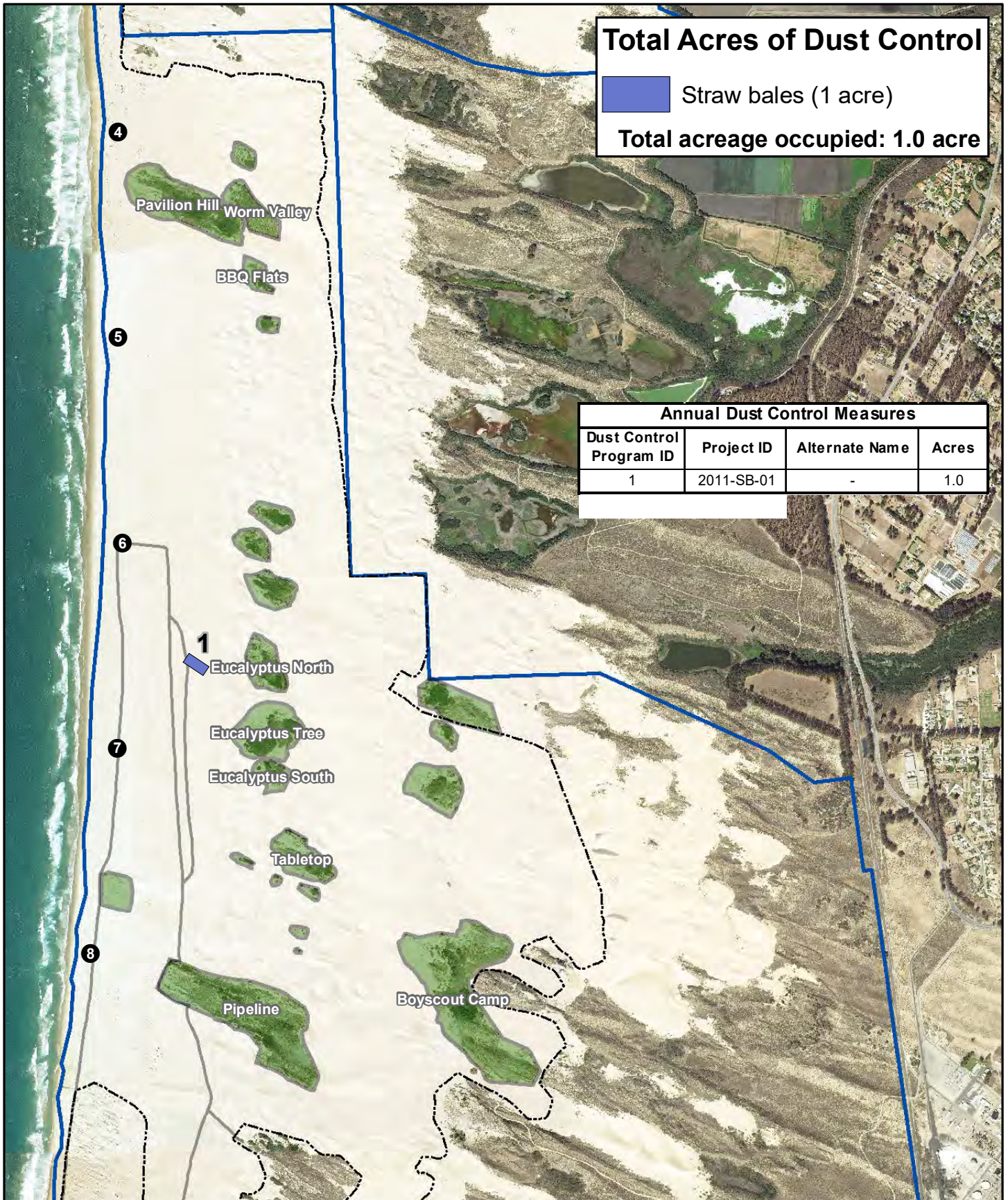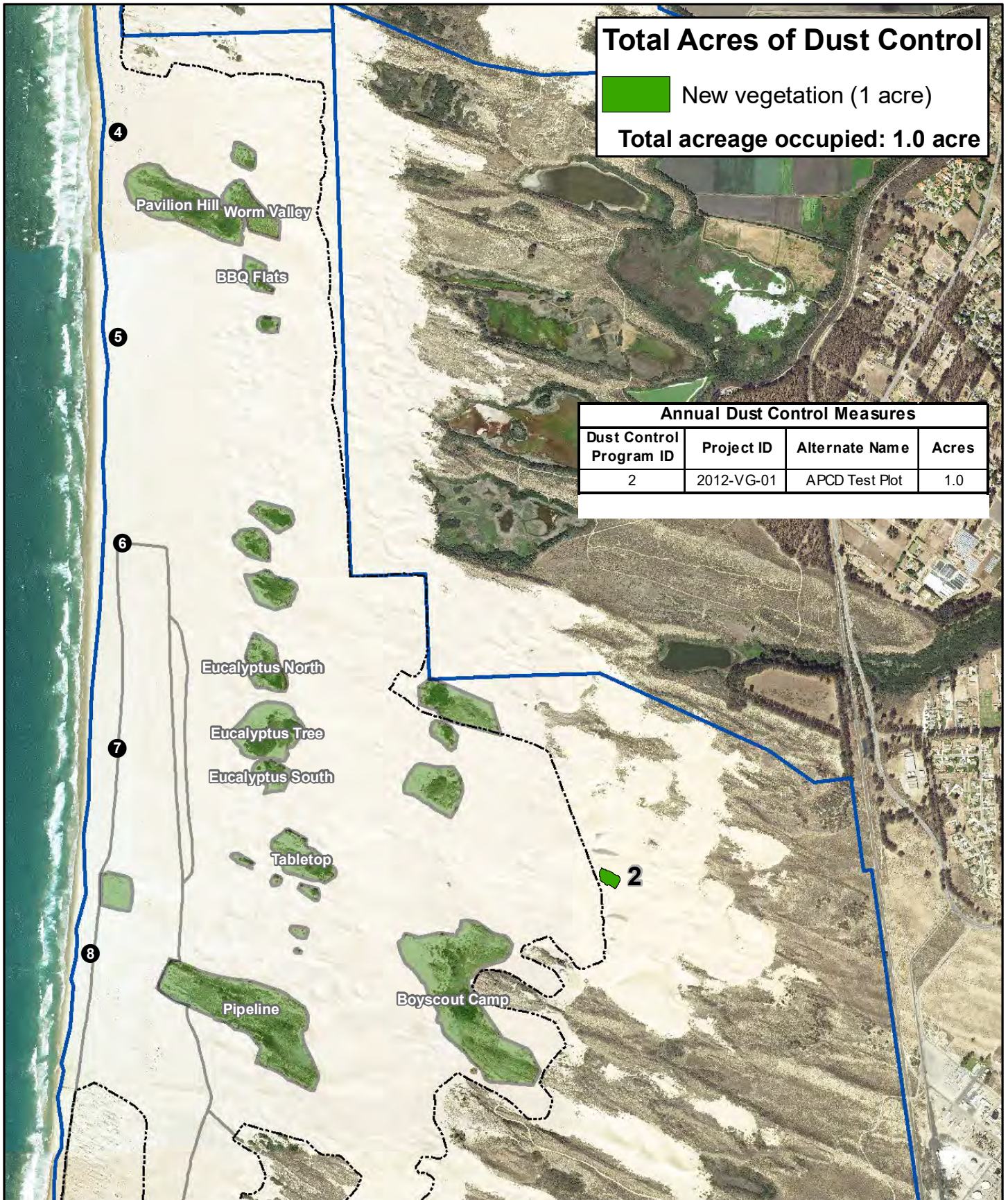CALIFORNIA STATE PARKS SINCE 1864 · OHV

N

Total Acres of Dust Control

Straw bales (1 acre)

Total acreage occupied: 1.0 acre

Annual Dust Control Measures

Dust Control Program ID	Project ID	Alternate Name	Acres
1	2011-SB-01	-	1.0

Pavilion Hill
Worm Valley
BBQ Flats

Eucalyptus North
Eucalyptus Tree
Eucalyptus South
Tabletop
Pipeline
Boyscout Camp

Source: CDPR, MIG   Imagery: 2014 NAIP

9/13/2021

Feet
0 500 1,000   2,000

A01-02: 2011 Dust Control Treatment Areas

2024 ARWP

● Marker post

Existing fenced vegetated islands

Park boundary

Nesting exclosure from 2020

Open riding and camping area boundary fence

N

Total Acres of Dust Control

New vegetation (1 acre)

Total acreage occupied: 1.0 acre

Annual Dust Control Measures			
Dust Control Program ID	Project ID	Alternate Name	Acres
2	2012-VG-01	APCD Test Plot	1.0

Pavilion Hill
Worm Valley
BBQ Flats
Eucalyptus North
Eucalyptus Tree
Eucalyptus South
Tabletop
Pipeline
Boyscout Camp

Source: CDPR, MIG   Imagery: 2014 NAIP

9/13/2021

Feet
0 500 1,000   2,000

N

A01-03: 2012 Dust Control Treatment Areas
2024 ARWP

● Marker post

▬ Nesting exclosure from 2020

■ Existing fenced vegetated islands

–∙–∙– Open riding and camping area boundary fence

▭ Park boundary

**Total Acres of Dust Control**

New vegetation (3.7 acres)

Previous vegetation projects (1 acre)

Total acreage occupied: 4.7 acres

Pavilion Hill Worm Valley

BBQ Flats

Eucalyptus North

Eucalyptus Tree

Eucalyptus South

Tabletop

Pipeline

Boyscout Camp

Annual Dust Control Measures			
Dust Control Program ID	Project ID	Alternate Name	Acres
3	2013-VG-01	Enigma	1.9
4	2013-VG-02	Crescent	1.8
		Total:	3.7
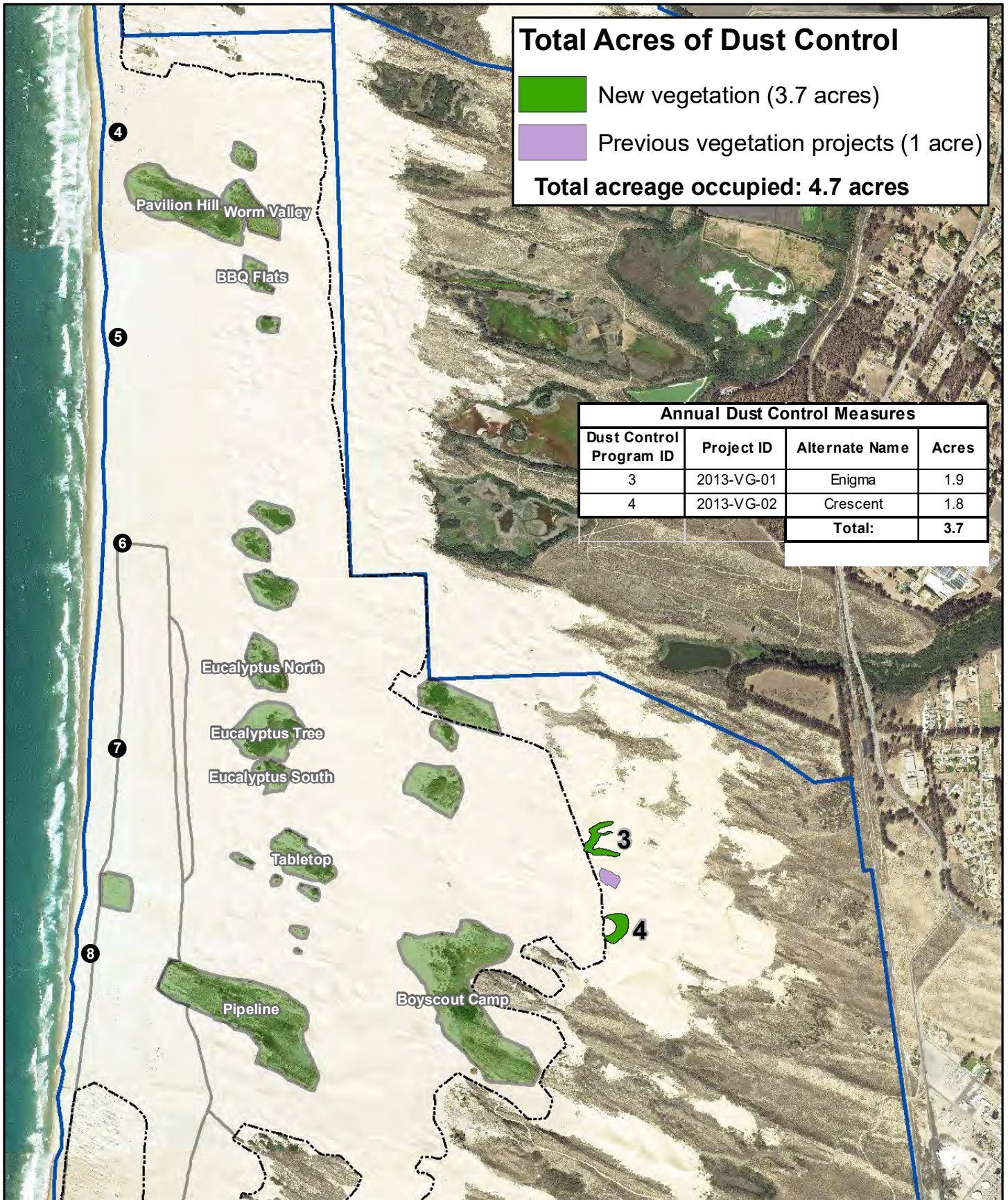
Source: CDPR, MIG Imagery: 2014 NAIP

9/13/2021

Feet

0 500 1,000 2,000

A01-04: 2013 Dust Control Treatment Areas

2023 ARWP
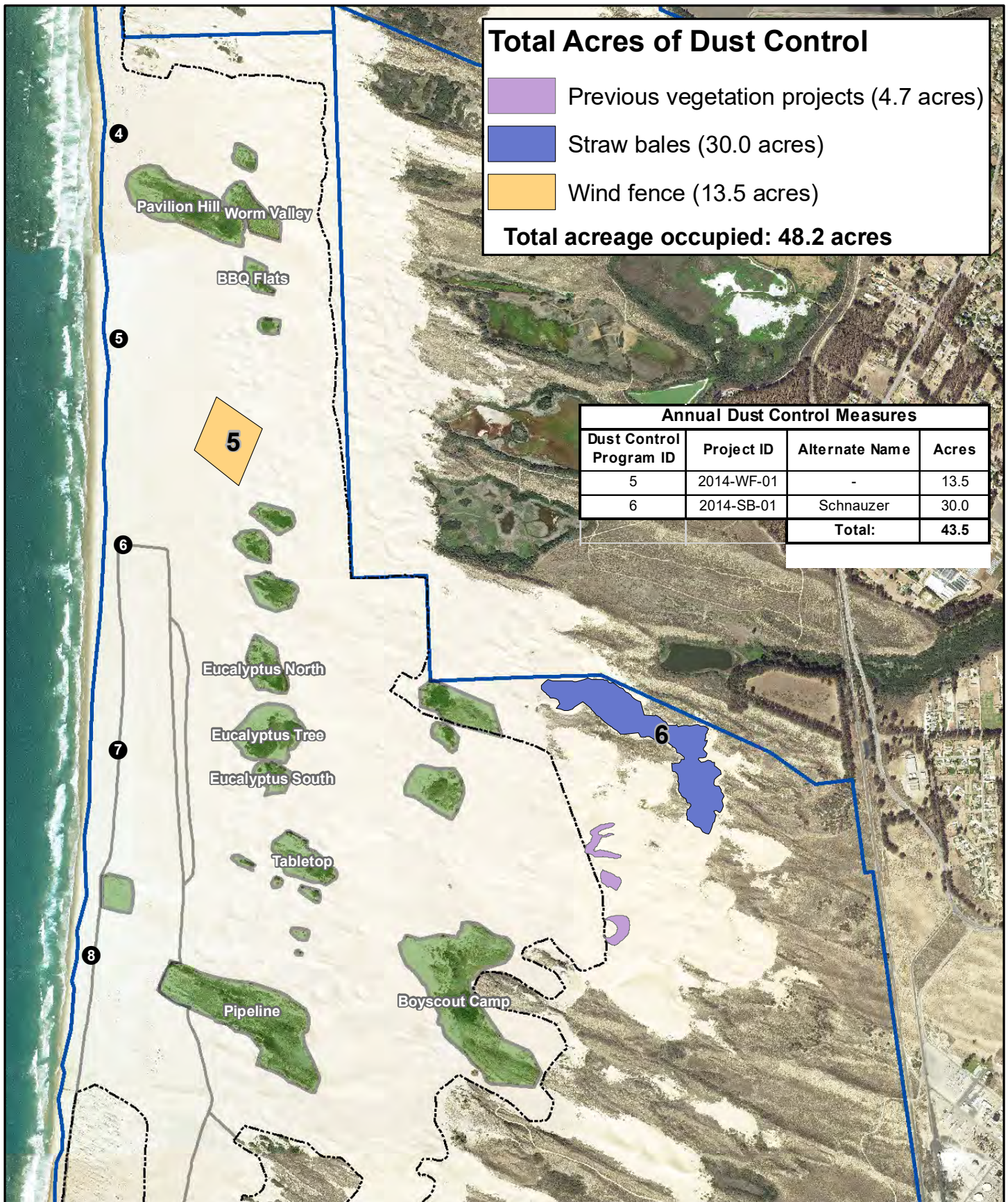
N

● Marker post

Nesting exclosure from 2020

Existing fenced vegetated islands

Open riding and camping area boundary fence

Park boundary

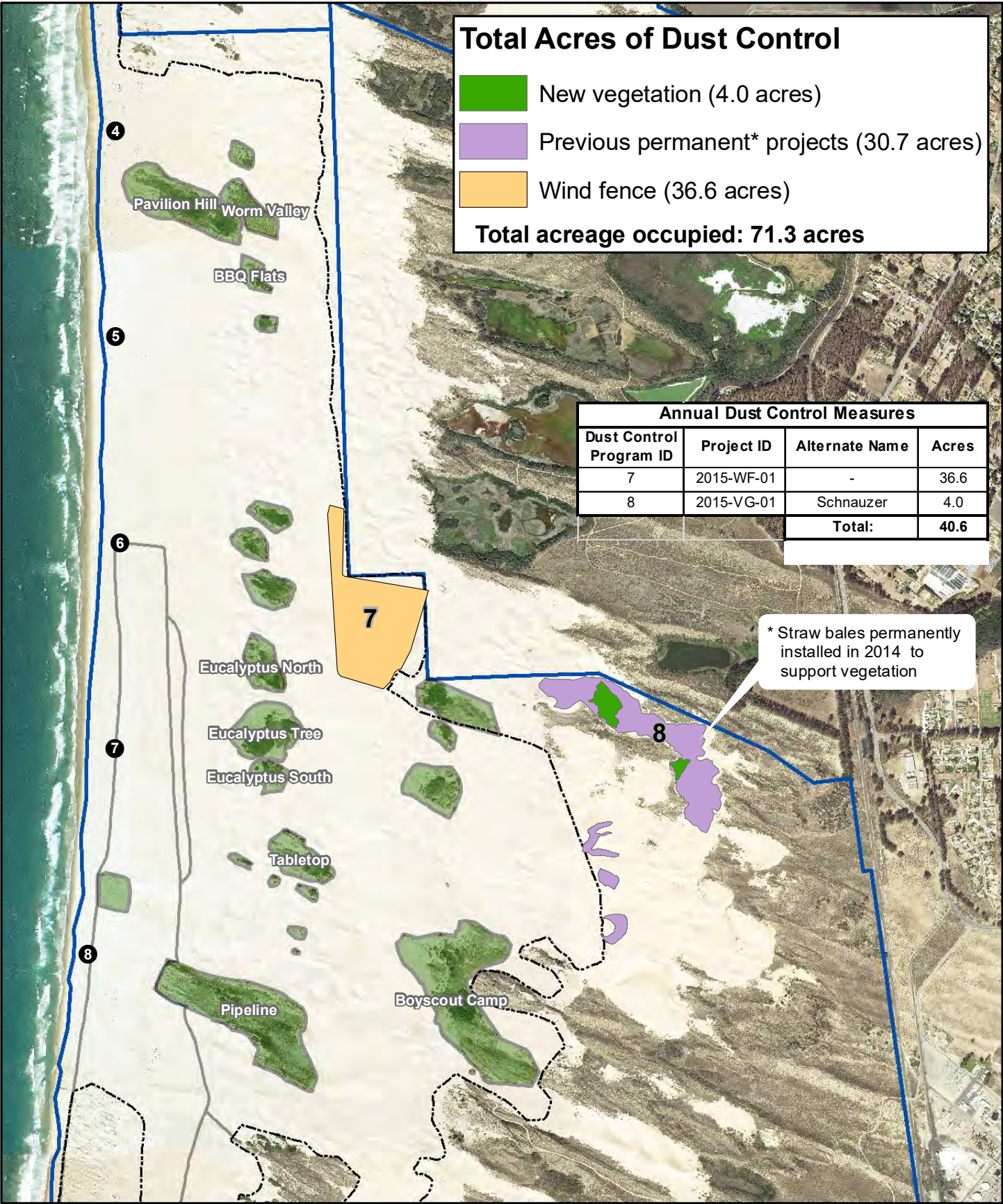## Total Acres of Dust Control

▩ (purple)	Previous vegetation projects (4.7 acres)
▩ (blue)	Straw bales (30.0 acres)
▩ (yellow)	Wind fence (13.5 acres)

Total acreage occupied: 48.2 acres

Annual Dust Control Measures

Dust Control Program ID	Project ID	Alternate Name	Acres
5	2014-WF-01	-	13.5
6	2014-SB-01	Schnauzer	30.0
		Total:	43.5

Map labels: Pavilion Hill, Worm Valley, BBQ Flats, Eucalyptus North, Eucalyptus Tree, Eucalyptus South, Tabletop, Pipeline, Boyscout Camp

Source: CDPR, MIG   Imagery: 2014 NAIP

9/13/2021

Feet
0   500 1,000   2,000

A01-05: 2014 Dust Control Treatment Areas

2024 ARWP

● Marker post   ▩ Existing fenced vegetated islands   ▭ Park boundary

—— Nesting exclosure from 2020   —·—·— Open riding and camping area boundary fence

N

Total Acres of Dust Control

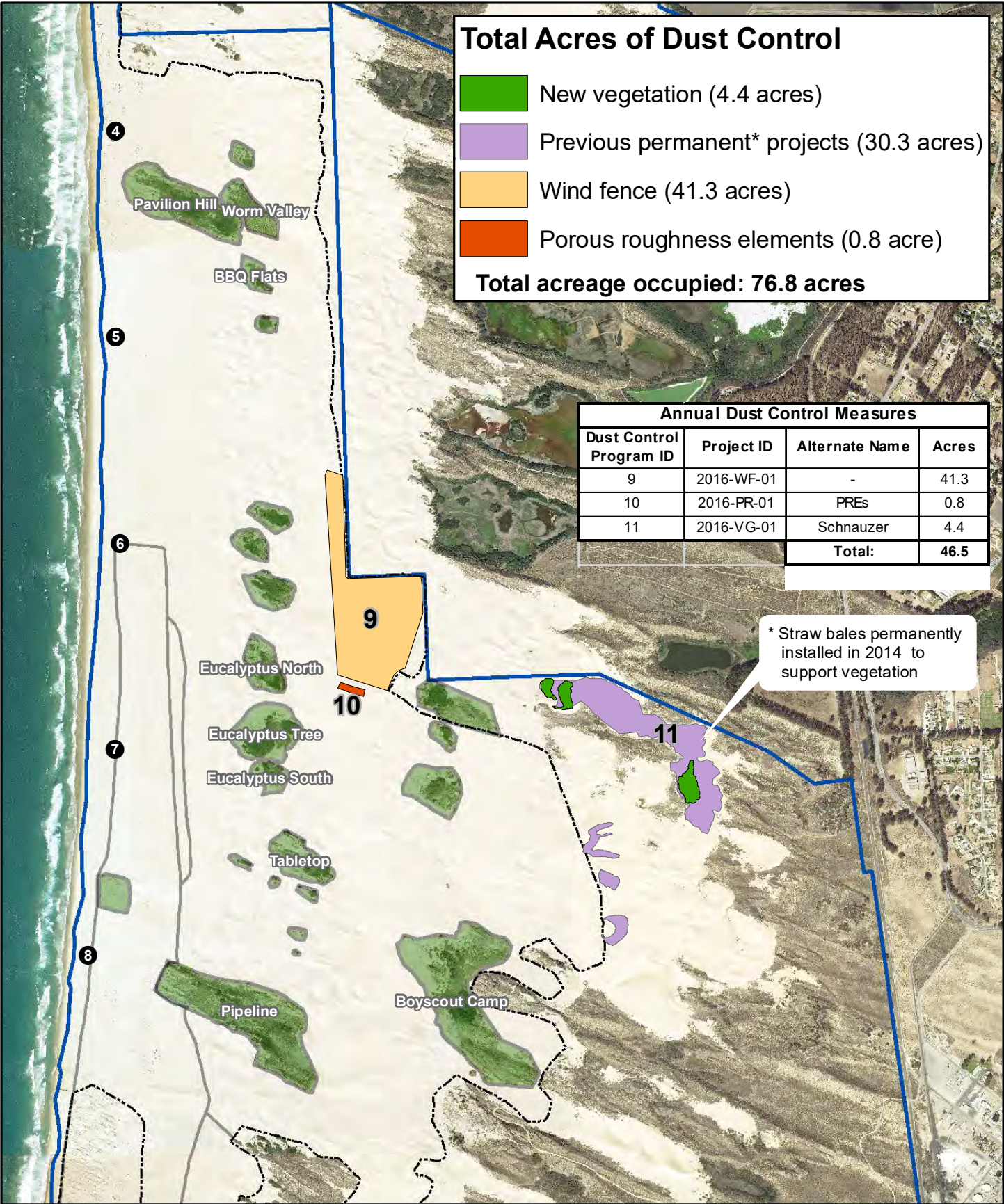|	
🟩	New vegetation (4.0 acres)
🟪	Previous permanent* projects (30.7 acres)
🟧	Wind fence (36.6 acres)

Total acreage occupied: 71.3 acres

Annual Dust Control Measures

Dust Control Program ID	Project ID	Alternate Name	Acres
7	2015-WF-01	-	36.6
8	2015-VG-01	Schnauzer	4.0
		Total:	**40.6**

* Straw bales permanently installed in 2014 to support vegetation

Pavilion Hill
Worm Valley
BBQ Flats
Eucalyptus North
Eucalyptus Tree
Eucalyptus South
Tabletop
Pipeline
Boyscout Camp

Source: CDPR, MIG   Imagery: 2014 NAIP

9/13/2021

Feet
0 500 1,000   2,000
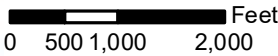
A01-06: 2015 Dust Control Treatment Areas

2024 ARWP

N

● Marker post

🟩 Existing fenced vegetated islands

▭ Park boundary

Nesting exclosure from 2020

Open riding and camping area boundary fence

Total Acres of Dust Control

- New vegetation (4.4 acres)
- Previous permanent* projects (30.3 acres)
- Wind fence (41.3 acres)
- Porous roughness elements (0.8 acre)

Total acreage occupied: 76.8 acres

Annual Dust Control Measures

Dust Control Program ID	Project ID	Alternate Name	Acres
9	2016-WF-01	-	41.3
10	2016-PR-01	PREs	0.8
11	2016-VG-01	Schnauzer	4.4
		Total:	46.5

* Straw bales permanently installed in 2014 to support vegetation

Pavilion Hill
Worm Valley
BBQ Flats
Eucalyptus North
Eucalyptus Tree
Eucalyptus South
Tabletop
Pipeline
Boyscout Camp

Source: CDPR, MIG   Imagery: 2014 NAIP

9/13/2021

A01-07: 2016 Dust Control Treatment Areas
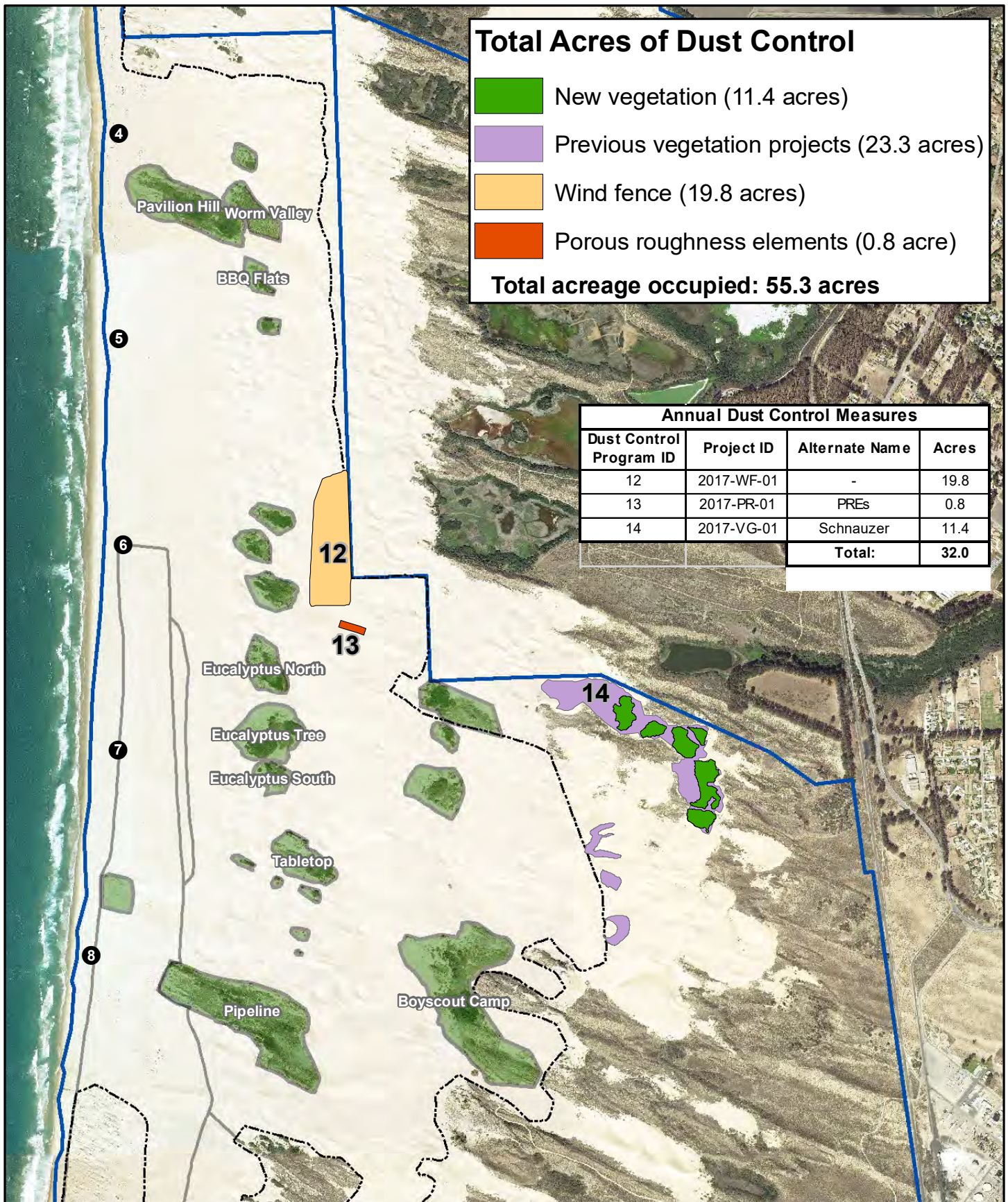
2024 ARWP

Feet
0 500 1,000   2,000

N

- Marker post
- Nesting exclosure from 2020
- Existing fenced vegetated islands
- Open riding and camping area boundary fence
- Park boundary

Total Acres of Dust Control

- New vegetation (11.4 acres)
- Previous vegetation projects (23.3 acres)
- Wind fence (19.8 acres)
- Porous roughness elements (0.8 acre)

Total acreage occupied: 55.3 acres

Annual Dust Control Measures			
Dust Control Program ID	Project ID	Alternate Name	Acres
12	2017-WF-01	-	19.8
13	2017-PR-01	PREs	0.8
14	2017-VG-01	Schnauzer	11.4
		Total:	32.0

Source: CDPR, MIG   Imagery: 2014 NAIP

9/13/2021

Feet
0 500 1,000   2,000

A01-08: 2017 Dust Control Treatment Areas
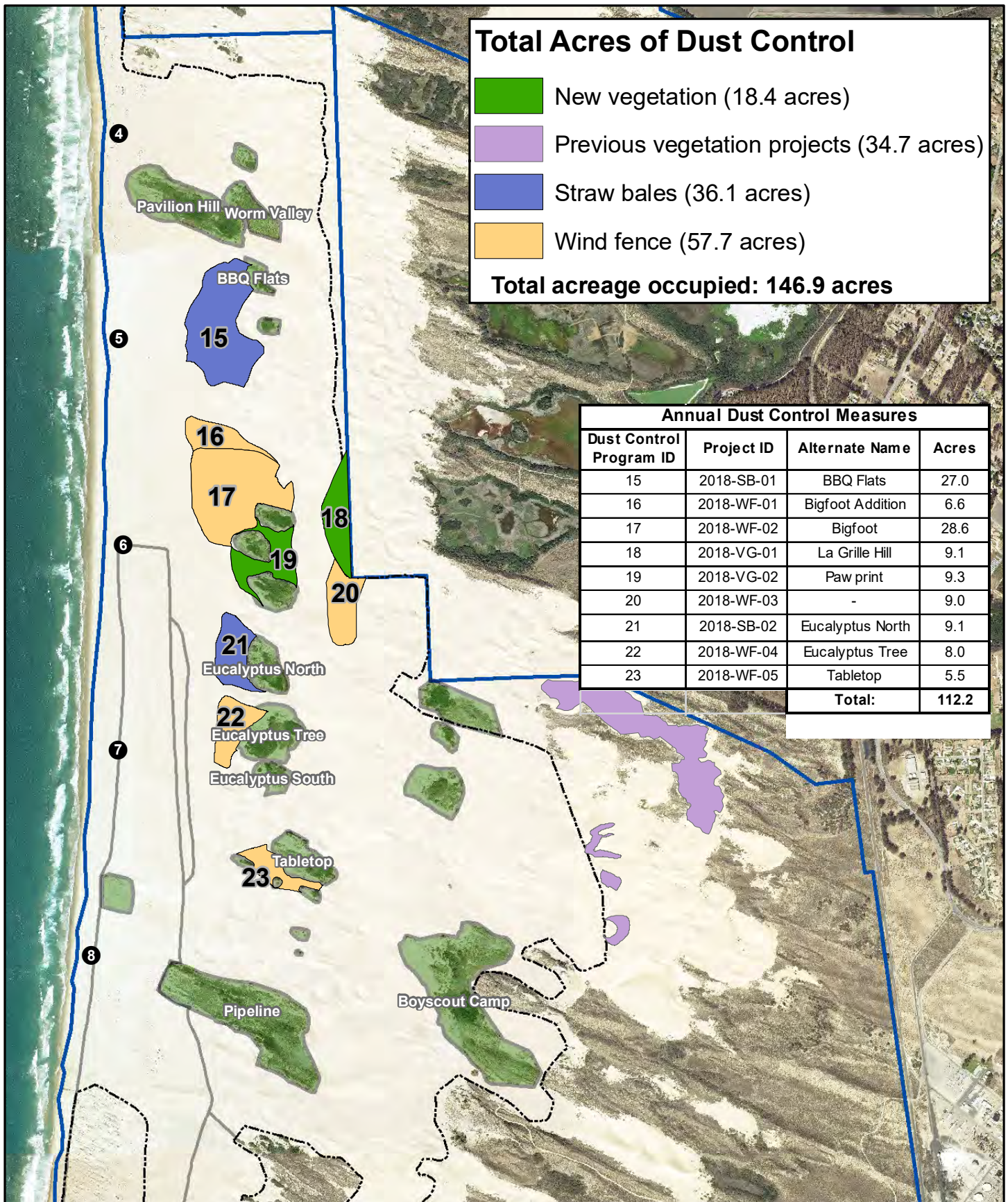
2024 ARWP

● Marker post

Existing fenced vegetated islands

Park boundary

—— Nesting exclosure from 2020

–·–·– Open riding and camping area boundary fence

N

Total Acres of Dust Control

- New vegetation (18.4 acres)
- Previous vegetation projects (34.7 acres)
- Straw bales (36.1 acres)
- Wind fence (57.7 acres)

Total acreage occupied: 146.9 acres

Annual Dust Control Measures

Dust Control Program ID	Project ID	Alternate Name	Acres
15	2018-SB-01	BBQ Flats	27.0
16	2018-WF-01	Bigfoot Addition	6.6
17	2018-WF-02	Bigfoot	28.6
18	2018-VG-01	La Grille Hill	9.1
19	2018-VG-02	Paw print	9.3
20	2018-WF-03	-	9.0
21	2018-SB-02	Eucalyptus North	9.1
22	2018-WF-04	Eucalyptus Tree	8.0
23	2018-WF-05	Tabletop	5.5
		Total:	**112.2**

Source: CDPR, MIG   Imagery: 2014 NAIP

9/13/2021

Feet
0 500 1,000   2,000

A01-09: 2018 Dust Control Treatment Areas

2024 ARWP

N

- Marker post
- Nesting exclosure from 2020
- Existing fenced vegetated islands
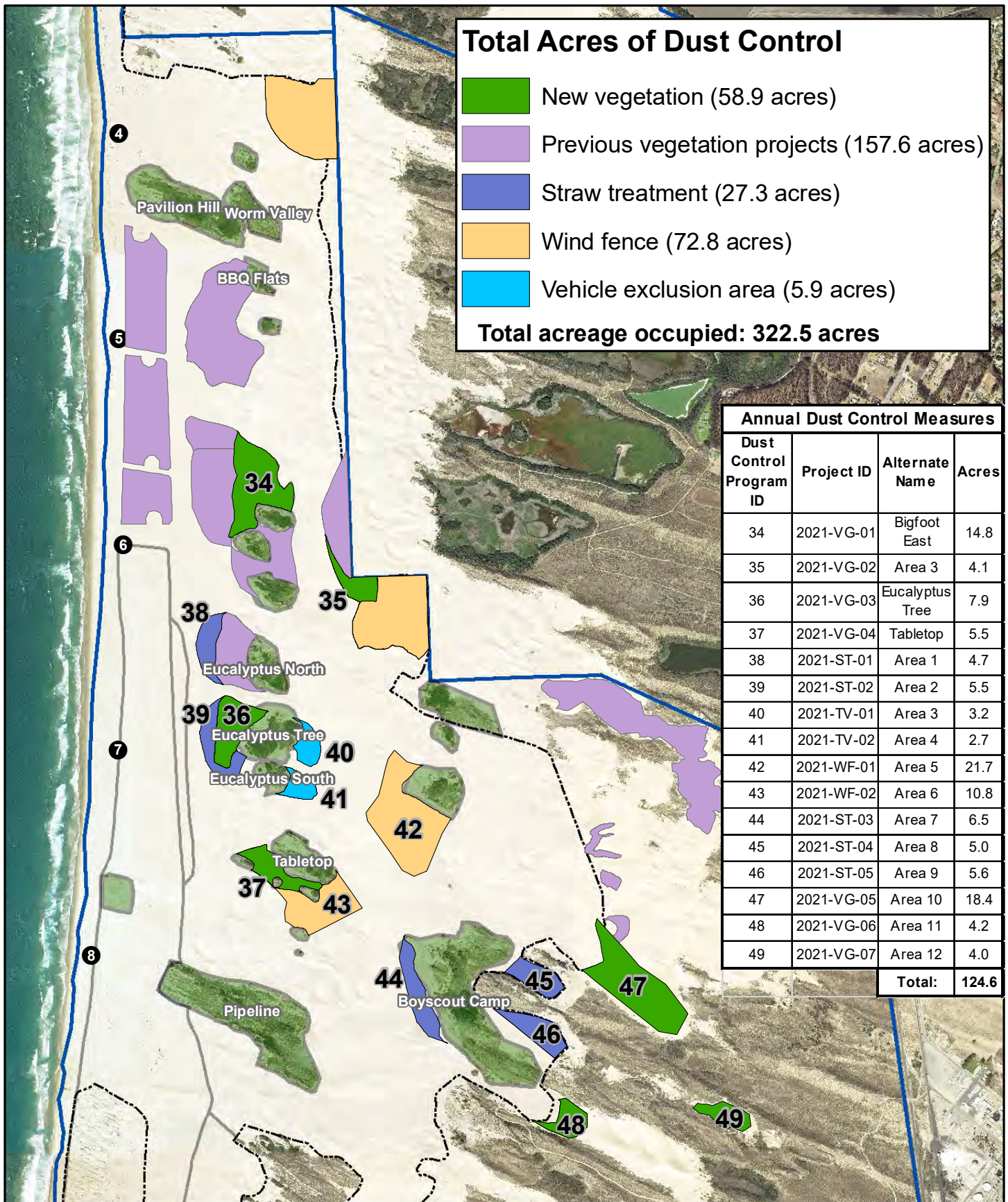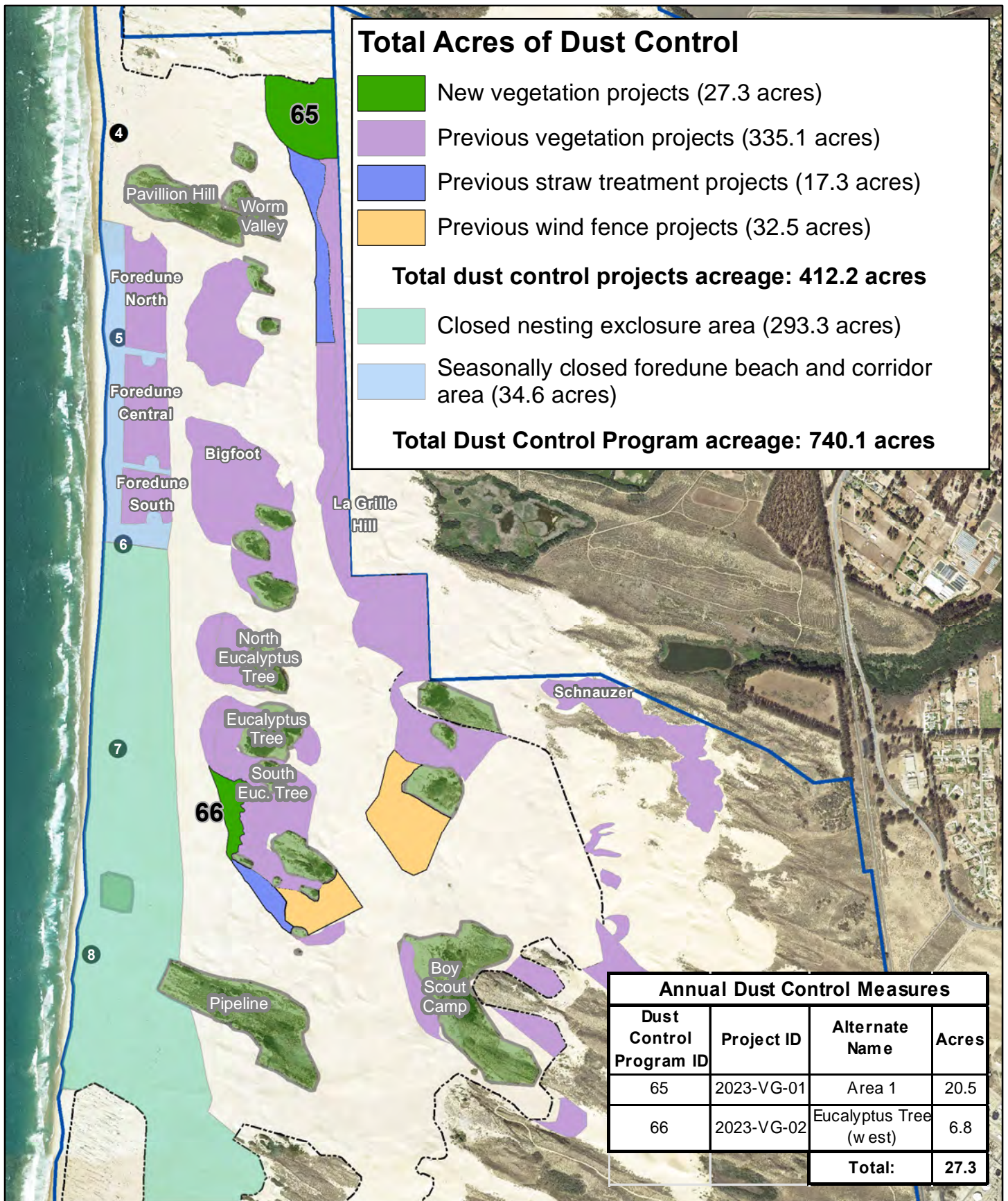- Open riding and camping area boundary fence
- Park boundary

Labels on map: Pavilion Hill, Worm Valley, BBQ Flats, Eucalyptus North, Eucalyptus Tree, Eucalyptus South, Tabletop, Pipeline, Boyscout Camp

Total Acres of Dust Control

- New vegetation (36.1 acres)
- Previous vegetation projects (53.1 acres)
- Wind fence (48.6 acres)
- Foredune fence installed December 2019

Total acreage occupied: 137.8 acres

Annual Dust Control Measures			
Dust Control Program ID	Project ID	Alternate Name	Acres
24	2019-VG-01	BBQ Flats	27.0
25	2019-VG-02	Eucalyptus North	9.1
		Total:	36.1

Pavilion Hill
Worm Valley
BBQ Flats
24
25
Eucalyptus North
Eucalyptus Tree
Eucalyptus South
Tabletop
Pipeline
Boyscout Camp

Source: CDPR, MIG   Imagery: 2014 NAIP

9/14/2021

Feet
0 500 1,000   2,000

A01-10: 2019 Dust Control Treatment Areas
2024 ARWP

N

- ● Marker post
- Nesting exclosure from 2020
- Existing fenced vegetated islands
- Open riding and camping area boundary fence
- Park boundary
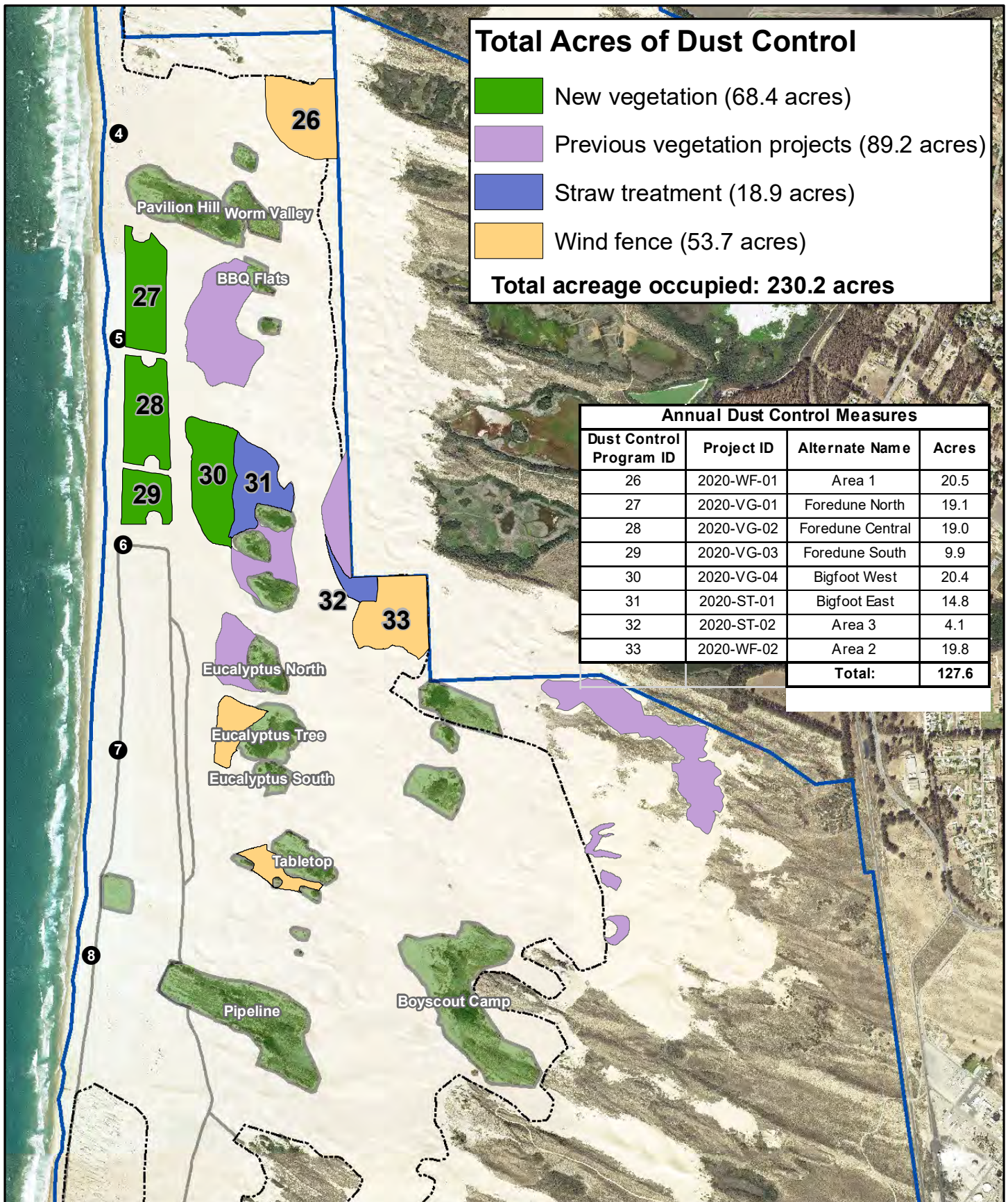
Total Acres of Dust Control

- New vegetation (68.4 acres)
- Previous vegetation projects (89.2 acres)
- Straw treatment (18.9 acres)
- Wind fence (53.7 acres)

Total acreage occupied: 230.2 acres

Annual Dust Control Measures			
Dust Control Program ID	Project ID	Alternate Name	Acres
26	2020-WF-01	Area 1	20.5
27	2020-VG-01	Foredune North	19.1
28	2020-VG-02	Foredune Central	19.0
29	2020-VG-03	Foredune South	9.9
30	2020-VG-04	Bigfoot West	20.4
31	2020-ST-01	Bigfoot East	14.8
32	2020-ST-02	Area 3	4.1
33	2020-WF-02	Area 2	19.8
		Total:	127.6

Source: CDPR, MIG   Imagery: 2014 NAIP
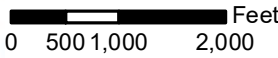
9/14/2021

Feet
0 500 1,000   2,000

A01-11: 2020 Dust Control Treatment Areas

2024 ARWP

N

● Marker post

Existing fenced vegetated islands

Park boundary

— Nesting exclosure from 2020   ----- Open riding and camping area boundary fence

Map labels: Pavilion Hill, Worm Valley, BBQ Flats, Eucalyptus North, Eucalyptus Tree, Eucalyptus South, Tabletop, Pipeline, Boyscout Camp

Total Acres of Dust Control

- **New vegetation (58.9 acres)**
- **Previous vegetation projects (157.6 acres)**
- **Straw treatment (27.3 acres)**
- **Wind fence (72.8 acres)**
- **Vehicle exclusion area (5.9 acres)**

Total acreage occupied: 322.5 acres

Pavilion Hill
Worm Valley
BBQ Flats
Eucalyptus North
Eucalyptus Tree
Eucalyptus South
Tabletop
Pipeline
Boyscout Camp

Annual Dust Control Measures

Dust Control Program ID	Project ID	Alternate Name	Acres
34	2021-VG-01	Bigfoot East	14.8
35	2021-VG-02	Area 3	4.1
36	2021-VG-03	Eucalyptus Tree	7.9
37	2021-VG-04	Tabletop	5.5
38	2021-ST-01	Area 1	4.7
39	2021-ST-02	Area 2	5.5
40	2021-TV-01	Area 3	3.2
41	2021-TV-02	Area 4	2.7
42	2021-WF-01	Area 5	21.7
43	2021-WF-02	Area 6	10.8
44	2021-ST-03	Area 7	6.5
45	2021-ST-04	Area 8	5.0
46	2021-ST-05	Area 9	5.6
47	2021-VG-05	Area 10	18.4
48	2021-VG-06	Area 11	4.2
49	2021-VG-07	Area 12	4.0
		Total:	**124.6**

Source: CDPR, MIG   Imagery: 2014 NAIP

9/13/2021

Feet
0 500 1,000   2,000

A01-12: 2021 Dust Control Treatment Areas

2024 ARWP

N

● Marker post

Existing fenced vegetated islands

Park boundary

Nesting exclosure from 2020

Open riding and camping area boundary fence

CALIFORNIA STATE PARKS SINCE 1864

OHV

Total Acres of Dust Control

- New vegetation (118.5 acres)
- Previous vegetation projects (216.6 acres)
- Previous straw treatment projects (24.1 acres)
- Previous wind fence projects (53.0 acres)

Total dust control projects acreage: 412.2 acres

- Additional dust reduction benefit area (293.3 acres)

Total Dust Control Program acreage: 705.5 acres

Pavillion Hill
Worm Valley
Foredune North
Foredune Central
Bigfoot
Foredune South
La Grille Hill
North Eucalyptus Tree
Eucalyptus Tree
Schnauze
Boy Scout Camp

Annual Dust Control Measures

Dust Control Program ID	Project ID	Alternate Name	Acres
50	2022-ST-01	East Moy Mell	12.3
51	2022-VG-01	Sand Highway (east)	14.6
52	2022-VG-02	Sand Highway (west)	11.3
53	2022-VG-03	La Grille Hill	19.9
54	2022-VG-04	North Eucalyptus Tree	4.6
55	2022-VG-05	Eucalyptus Tree (north)	5.5
56	2022-VG-06	Eucalyptus Tree (east)	3.3
57	2022-VG-07	La Grille Hill (south)	22.7
58	2022-VG-08	Eucalyptus Tree	2.9
59	2022-VG-09	Eucalyptus Tree (center)	14.9
60	2022-ST-02	Eucalyptus Tree (west)	11.8
61	2022-VG-10	Eucalyptus Tree (south)	2.4
62	2022-VG-11	Boy Scout Camp	6.3
63	2022-VG-12	North Orion	4.9
64	2022-VG-13	South Orion	5.7
		Total:	143.1

Source: CDPR, MIG   Imagery: 2014 NAIP

6/7/2022

Feet
0   500 1,000   2,000

CALIFORNIA STATE PARKS SINCE 1864

OHV

N

A01-13: 2022 Dust Control Treatment Areas
2024 ARWP

- Marker post
- Existing fenced vegetated islands
- Park boundary
- Open riding and camping area boundary fence

Total Acres of Dust Control

- New vegetation projects (27.3 acres)
- Previous vegetation projects (335.1 acres)
- Previous straw treatment projects (17.3 acres)
- Previous wind fence projects (32.5 acres)

Total dust control projects acreage: 412.2 acres

- Closed nesting exclosure area (293.3 acres)
- Seasonally closed foredune beach and corridor area (34.6 acres)

Total Dust Control Program acreage: 740.1 acres

Map labels: Pavillion Hill, Worm Valley, Foredune North, Foredune Central, Foredune South, Bigfoot, La Grille Hill, North Eucalyptus Tree, Eucalyptus Tree, South Euc. Tree, Schnauzer, Boy Scout Camp, Pipeline

Annual Dust Control Measures

Dust Control Program ID	Project ID	Alternate Name	Acres
65	2023-VG-01	Area 1	20.5
66	2023-VG-02	Eucalyptus Tree (west)	6.8
		Total:	27.3

Source: CDPR, MIG   Imagery: 2014 NAIP

6/27/2023

Feet
0   500 1,000   2,000

Figure A01-14: 2023 Dust Control Treatment Areas

2024 ARWP

- ● Marker post
- Existing fenced vegetated islands
- ▢ Park boundary
- – · – Open riding and camping area boundary fence

CALIFORNIA STATE PARKS · SINCE 1864 · OHV

N

Total Acres of Dust Control

- New vegetation (37.5 acres)
- Previous vegetation projects (362.4 acres)
- Previous straw treatments projects (12.3 acres)

Total dust control projects acreage: 412.2 acres

- Closed nesting exclosure area (293.3 acres)
- Seasonal foredune beach and corridors (34.6 acres)

Total Dust Control Program acreage 740.1 acres
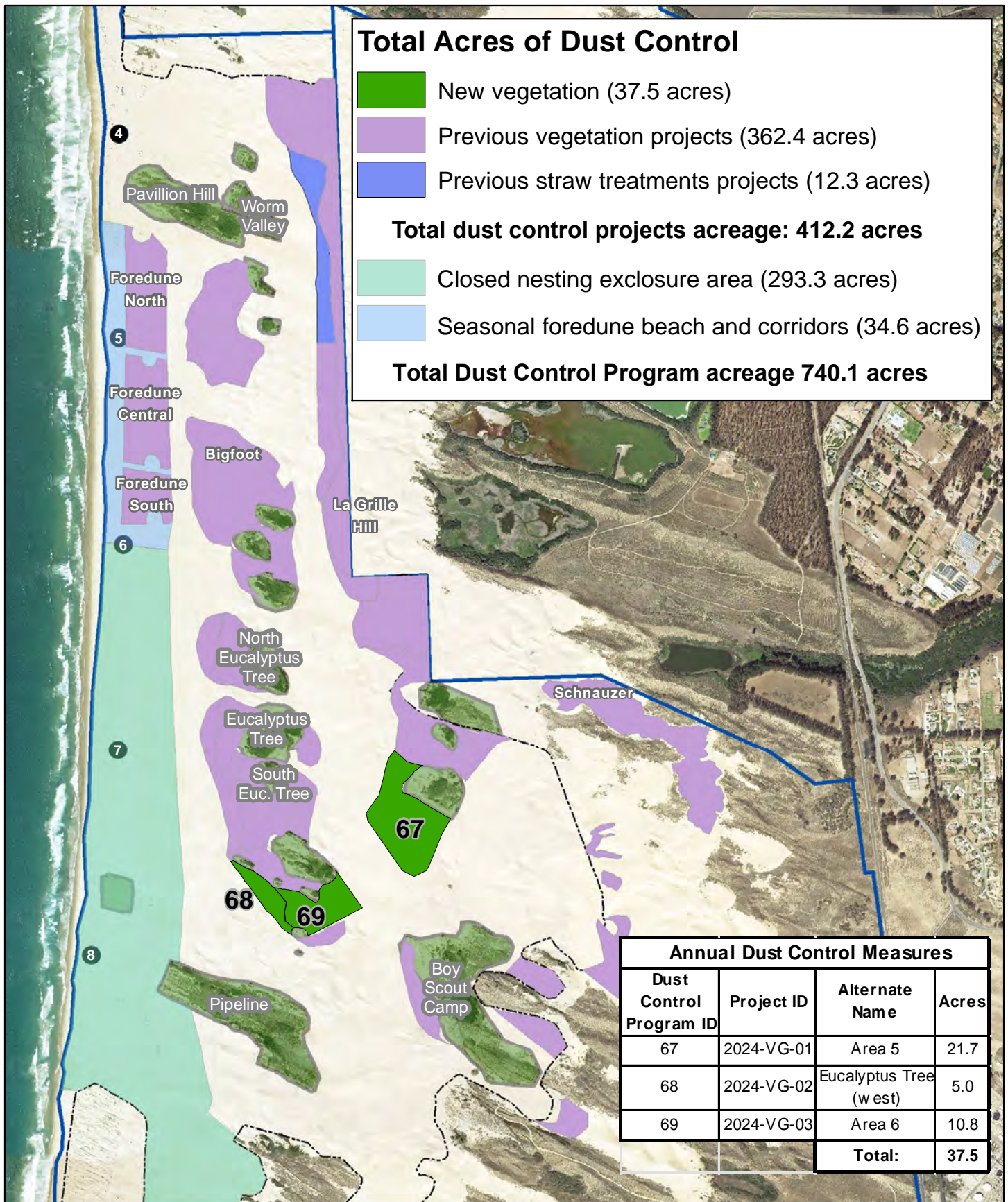
Annual Dust Control Measures			
Dust Control Program ID	Project ID	Alternate Name	Acres
67	2024-VG-01	Area 5	21.7
68	2024-VG-02	Eucalyptus Tree (west)	5.0
69	2024-VG-03	Area 6	10.8
		Total:	37.5

Source: CDPR, MIG   Imagery: 2014 NAIP

5/28/2024

Figure A01-15: 2024 Dust Control Treatment Areas

2024 ARWP

Feet
0   500 1,000   2,000

- ● Marker post
- Park boundary
- Existing fenced vegetated islands
- – · – Open riding and camping area boundary fence

N

THIS PAGE WAS INTENTIONALLY LEFT BLANK.

ODSVRA Dust Control Program Draft 2024 ARWP

ATTACHMENT 02

2023/2024 ODSVRA Dust Control Program Vegetation Restoration Projects

(State Parks' ARWP Work Product)

THIS PAGE WAS INTENTIONALLY LEFT BLANK.

Scientific Name / Common Name	Plant Counts / Native Seed (lbs)	Season Totals	Boy Scout North 2024-VG-01 (New Planting)	Eucalyptus Tree (west) 2024-VG-02 (New Planting)	Eucalyptus Tree (east) 2024-VG-03 (New Planting)	Eucalyptus Tree (south) 2022-VG-10 (Supplemental Planting)
2023/2024 ODSVRA Dust Control Program - Restoration Projects						
Acreage		39.9	21.7	5.0	10.8	2.4
Straw - (large bales)		504	264	56	151	33
Fertilizer (lbs) - 15-15-15		2025	1100	250	550	125
Triticale Seed (lbs) - sterile		2025	1100	250	550	125
Jute Netting (acres)		0.72	0.39	-	0.33	-
Total plants		116,112	62,795	13,377	32,832	7,110
Total Native Seed (lbs)		533.36	294.47	63.90	146.54	28.45
Abronia latifolia		343	294	49	-	-
Yellow sand verbena		2.00	1.50	0.50	-	-
Abronia maritima		294	147	147	-	-
Sticky sand verbena		28.00	21.00	7.00	-	-
Abronia umbellata		-	-	-	-	-
Beach sand verbena		1.20	0.76	-	0.44	-
Acmispon glaber		4,616	2,778	392	1,078	368
Deerweed		36.30	18.80	4.00	11.00	2.50
Acmispon heermannii		-	-	-	-	-
Heermann's lotus		0.87	0.57	0.08	0.22	-
Achillea millefolium		8,673	5,047	980	2,156	490
Common yarrow		26.50	14.00	3.00	8.25	1.25
Ambrosia chamissonis		1,176	882	294	-	-
Beach bur		40.00	30.00	10.00	-	-
Amsinckia spectabilis		-	-	-	-	-
Seaside fiddleneck		6.45	4.05	0.80	1.10	0.50
Astragalus nuttallii		2,424	1,027	196	1,078	123
Nuttall's milkvetch		1.39	0.84	0.20	0.35	
Castilleja affinis		1,216	358	196	539	123
Indian paintbrush		0.25	0.25	-	-	-
Camissoniopsis cheiranthifolia		3,790	2,026	441	1,078	245
Beach evening-primrose		1.16	0.63	0.12	0.33	0.08
Carex praegracilis		2,500	1,103	196	1,078	123
Field sedge		-	-	-	-	-
Camissoniopsis micrantha		-	-	-	-	-
Spencer primrose		0.10	0.10	-	-	-
Chenopodium californicum		-	-	-	-	-
California goosefoot		1.80	1.25	-	0.55	-
Cirsium occidentale		-	-	-	-	-
Cobweb thistle		2.64	2.64	-	-	-
Corethrogyne filaginifolia		2,360	1,821		539	
Common sandaster		23.05	14.30	2.00	5.50	1.25
Dudleya lanceolata		1,803	945	196	539	123
Southern California dudleya		-	-	-	-	-
Cryptantha clevelandii		-	-	-	-	-
Common cryptantha		3.20	1.90	0.20	1.10	-

	Plant Counts		Boy Scout North 2024-VG-01 (New Planting)	Eucalyptus Tree (west) 2024-VG-02 (New Planting)	Eucalyptus Tree (east) 2024-VG-03 (New Planting)	Eucalyptus Tree (south) 2022-VG-10 (Supplemental Planting)
2023/2024 ODSVRA Dust Control Program - Restoration Projects						
Scientific Name / Common Name	**Native Seed (lbs)**	Season Totals				
Erigeron blochmaniae	4,400	2,685	392	1,078	245	
Blochman's leafy daisy	8.25	4.75	0.80	2.20	0.50	
Eriastrum densifolium	1,849	991	196	539	123	
Giant eriastrum	4.98	2.55	0.40	1.65	0.38	
Ericameria ericoides	7,522	4,043	833	2,156	490	
Mock heather	75.38	36.00	9.00	24.75	5.63	
Eriogonum parvifolium	6,395	3,822	588	1,617	368	
Coastal buckwheat	55.98	30.10	2.00	22.00	1.88	
Eriophyllum staechadifolium	3,867	2,152	392	1,078	245	
Seaside golden yarrow	52.50	29.50	4.00	16.50	2.50	
Erysimum suffrutescens	6,334	3,761	588	1,617	368	
Suffrutescent wallflower	8.20	3.82	1.00	2.75	0.63	
Eschscholzia californica	-	-	-	-	-	
California poppy	0.10	0.10	-	-	-	
Horkelia cuneata	2,508	989	196	1,078	245	
Wedge leaved horkelia	3.55	1.80	0.40	1.10	0.25	
Juncus lescurii/breweri	-		-	-	-	
Dune rush	2.83	1.95	0.20	0.55	0.13	
Linanthus californicus	28	28	-	-	-	
Prickly phlox	-	-	-	-	-	
Lupinus chamissonis	30,380	15,876	3,920	8,624	1,960	
Dune bush lupine	12.88	7.00	2.50	2.75	0.63	
Malacothrix incana	-	-	-	-	-	
Dunedelion	0.40	0.30	0.10	-	-	
Morella californica	40	16	-	26	-	
Wax myrtle	-	-	-	-	-	
Monardella undulata ssp crisp	7,920	3,804	1,470	2,156	490	
Crisp monardella	16.00	7.70	2.40	4.40	1.50	
Penstemon centranthifolius	402	237	-	165	-	
Scarlet bugler	-	-	-	-	-	
Phacelia distans	-	-	-	-	-	
Common phacelia	2.81	1.93	0.20	0.55	0.13	
Phacelia ramosissima	6,066	3,346	735	1,617	368	
Branching phacelia	80.45	36.70	10.00	27.50	6.25	
Populus trichocarpa	168	97	22	49	-	
Black cottonwood	-	-	-	-	-	
Salix lasiolepis	228	114	27	87	-	
Arroyo willow	-	-	-	-	-	
Salvia columbariae	-	-	-	-	-	
Chia sage	0.29	0.29	-	-	-	
Senecio blochmaniae	8,428	4,189	931	2,695	613	
Dune ragwort	33.90	17.40	3.00	11.00	2.50	
Silene laciniata	382	217	-	165	-	
Cardinal catchfly	-	-	-	-	-	

ODSVRA Dust Control Program Draft 2024 ARWP

ATTACHMENT 03

Report on Findings: ODSVRA Meteorological and PM$_{10}$ Monitoring Network, 2023

- Report of Findings: ODSVRA Meteorological and PM$_{10}$ Monitoring Network, 2023 (DRI Document)

- SAG Review of Desert Research Institute (DRI) "Report of Findings: ODSVRA Meteorological and PM$_{10}$ Monitoring Network, 2023" (SAG Memo)

THIS PAGE WAS INTENTIONALLY LEFT BLANK.

Report of Findings: ODSVRA Meteorological and PM$_{10}$ Monitoring Network, 2023

J.A Gillies* and G. Nikolich**
Division of Atmospheric Sciences, Desert Research Institute, *Reno and **Las Vegas, Nevada

State Parks' meteorological and PM$_{10}$ monitoring network varies slightly from year to year depending on specific goals, objectives, and dust control measures identified in the annual ARWP cycle. From approximately April 1, 2023, to September 30, 2023, State Parks maintained the meteorological and PM monitoring network shown in Fig. 1, consisting of fifteen (15) sites located throughout and downwind of the ODSVRA. The network has been in operation since 2020 but prior to 2021 the number of stations was smaller and 2020 was the year for which there were COVID-related restrictions on OHV activity, March to September. The period of record with a full complement of stations and active OHV activity is restricted to 2021 through 2023. The expectation is that the network will be operational in 2024.

Each station has a MetSense instrument that measures wind speed and wind direction (ultrasonically), ambient temperature, atmospheric pressure, and relative humidity (RH), a MetOne 212 particle profiler to measure PM$_{10}$, and stations on open sand areas have Sensit saltation sensors (BBQ, Lagrande, Camping, Shoreline, Windfence, Acacia, Cottonwood, Tabletop, Pipeline, and Scout, Fig.1). The MetOne instrument is calibrated against a Beta Attenuation Monitor (BAM) in a dust chamber prior to deployment and after removal from the field in October. In 2023 no significant drift was observed between the pre- and post-deployment calibration relations.

The environmental data collected by these stations provides a means to examine spatial trends in PM$_{10}$ concentrations ($\mu g\ m^{-3}$) across the ODSVRA in relation to wind speed ($m\ s^{-1}$) and wind power density ($W\ m^{-2}$), and to evaluate if these relations have changed through time.

Wind power density (WPD, $W\ m^{-2}$) is defined as (e.g., Kalmikov, 2017):

$$WPD=0.5\ \rho_a\ u_z^3 \tag{1}$$

where ρ_a is air density at sea level (1.212 $kg\ m^{-3}$, and assumed constant), and u_z ($m\ s^{-1}$) is wind speed at the measurement height z (m) above ground level (AGL). For comparison among different locations and between different years, the height of measurement of wind speed and the lower limit of mean hourly wind speed for summation of Total Wind Power Density (TWPD) must be the same. To standardize the calculation of TWPD a lower limit of wind speed is chosen that corresponds with the lowest speed where the relation between increasing wind speed and simultaneous increase in PM$_{10}$ is observed at a monitoring station. For the in-Park stations this wind speed is chosen to be 5.5 $m\ s^{-1}$ measured at 3.5 m AGL. Figure 2 shows typical response relations between mean hourly wind speed measured at 3.5 m AGL for four in-Park stations, representing the north-south length of the network, in 2023 for the period April -through September.
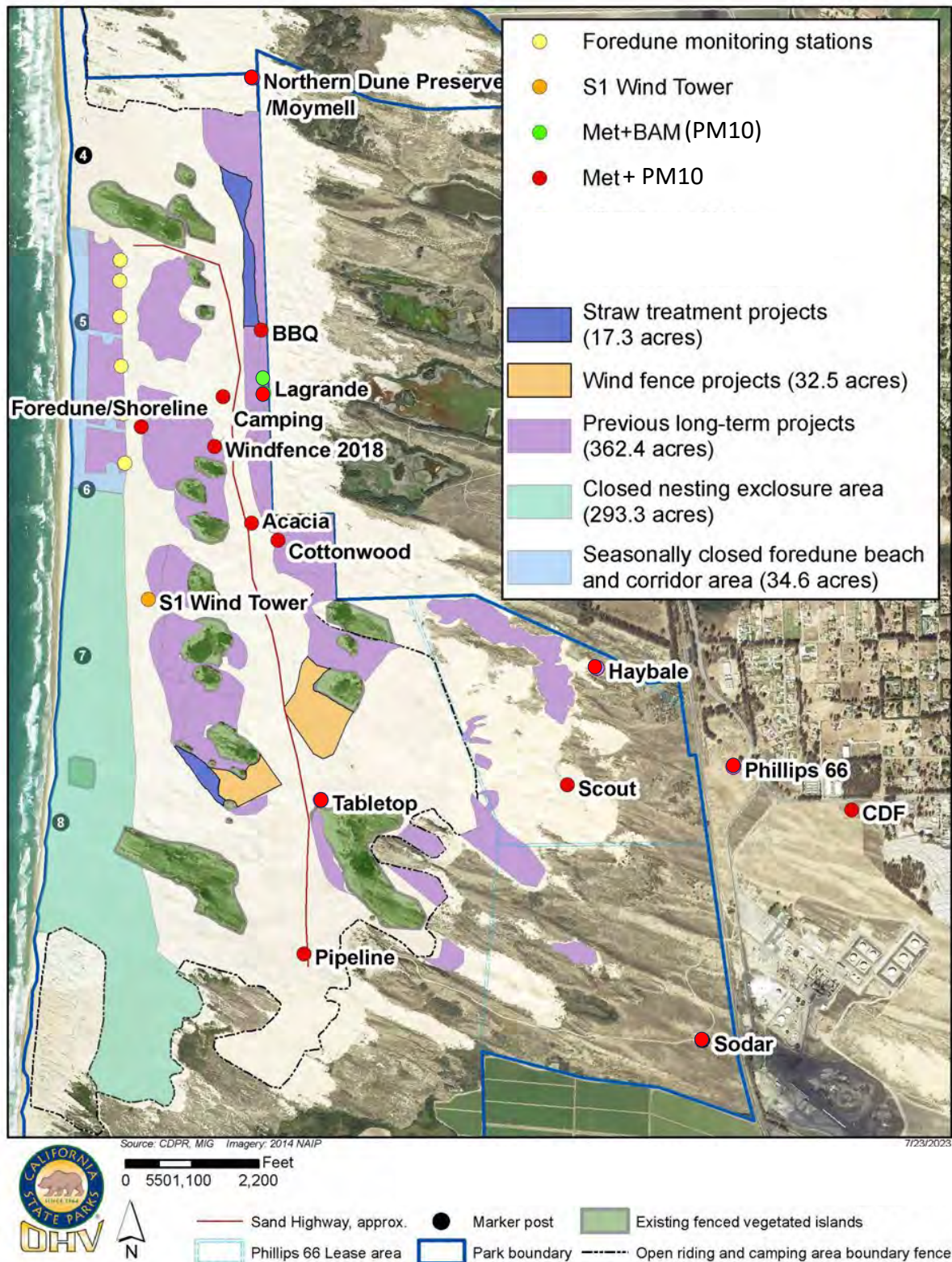
Figure 1. The locations of the monitoring stations. The Northern dune preserve station was not in place for 2023.
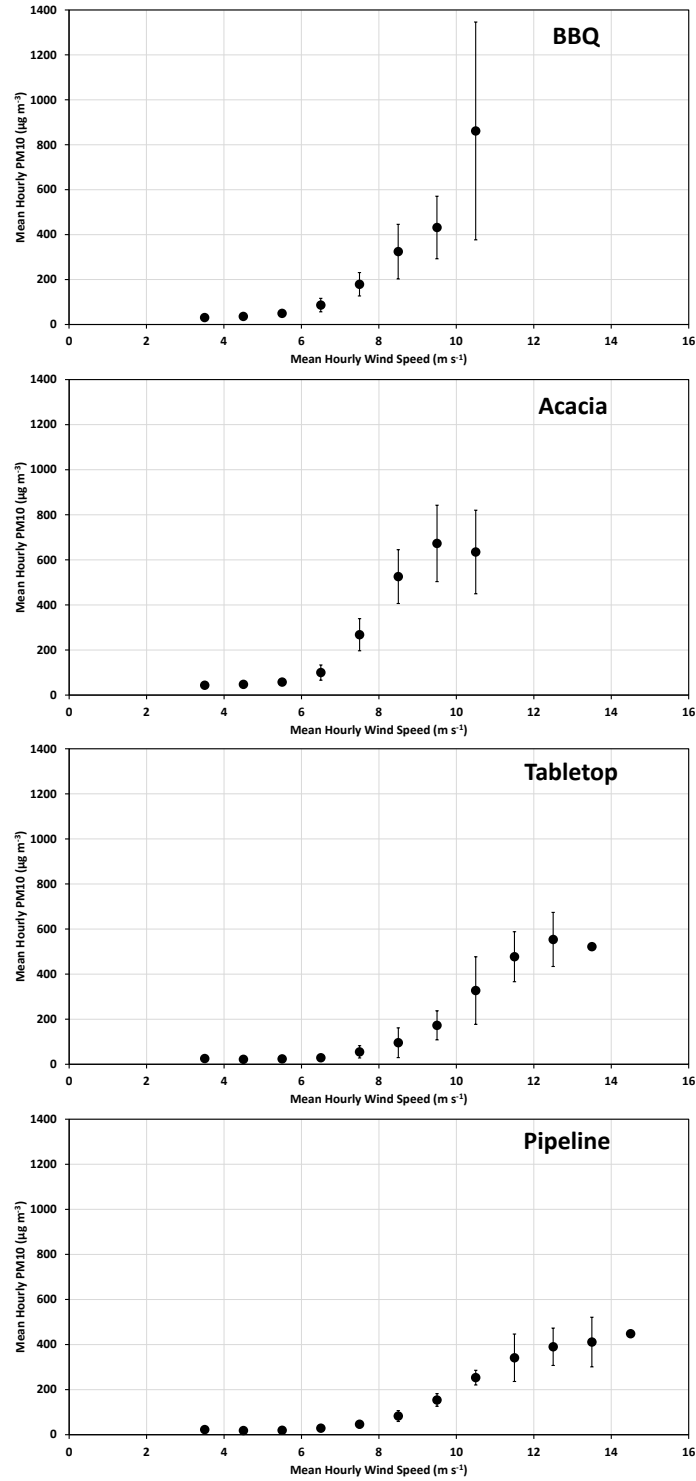
Figure 2. Relation between mean hourly wind speed and mean hourly PM_{10} concentration for four in-Park stations (April-September 2023) spanning the distance of the network, approximately equidistantly, from north to south. Error bars represent the standard deviation of the mean hourly PM_{10} associated with each 1 m s^{-1} wind speed bin.

Figure 2 also shows that along the north-south dimension of the network higher mean hourly PM_{10} concentrations are observed in the north (BBQ) than in the south (Pipeline) for lower wind speeds. The mean hourly PM_{10} concentration range at the BBQ station was 324 µg m^{-3} (±122 µg m^{-3}) to 861 µg m^{-3} (±485 µg m^{-3}), for the wind speed range 8.5 m s^{-1} to 10.5 m s^{-1}, respectively, while at the southern-most station, Pipeline, the PM_{10} concentration range was 83 µg m^{-3} (±24 µg m^{-3}) to 411 µg m^{-3} (±110 µg m^{-3}), for the wind speed range 8.5 m s^{-1} to 13.5 m s^{-1} (note there was only one PM_{10} reading for the mean hourly wind speed 14. 5 m s^{-1}). These wind and PM_{10} relations (Fig. 2) support previous reporting (e.g., Gillies and Etyemezian, 2014a) that wind speed increases from north to south and emissivity of PM_{10} from the sand surfaces decreases (e.g., Etyemezian et al., 2014; Gillies and Etyemezian, 2014b; SAG, 2023). The lower emissivity in the south is indicated by the lower PM_{10} concentrations associated with higher wind speeds in Fig. 2.

The total WPD (TWPD) and total PM_{10} (TPM$_{10}$) at each monitoring location quantified by summing the hourly mean values for the hours when MetOne 212 concentrations are paired with the station-measured wind speed. The lower limit for summation was set at 5.5 m s^{-1} for mean hourly wind speed, as this wind speed indicates that PM_{10} concentration will begin to increase and correlate with increasing wind speed with further increases in wind speed (Fig. 2) (Gillies et al., 2023). DRI did not apply a wind directional filter to in-Park measurement locations as these stations are surrounded by sand that can be mobilized from any direction. In contrast, for stations located downwind of the ODSVRA open riding and camping area (i.e., Haybale, Phillips 66, SODAR, and CDF), DRI filtered data by direction (236°to 326°) to ensure PM_{10} was originating from the direction of the ODSVRA, as the PM_{10} at these stations is being dispersed by the wind over mostly vegetation-covered surfaces and there is likely no additional contribution of PM_{10} from local saltation processes near these stations. Even though these stations were outside of the zone where saltation driven emissions of PM_{10} could occur, for consistency, the lower limit for summation was set at 5.5 m s^{-1} for mean hourly wind speed.

The Total Wind Power Density (TWPD) by month for the period April to September in 2021 through 2023 for each in-Park monitoring station is shown in Fig. 3. Through this period the greater TWPD values are observed in the months April, May, and June as compared with the summer months July, August, and September, and higher wind speeds in the south give rise to greater amounts of TWPD than is observed in the northern stations. A west to east pattern of wind power density was also observed. The TWPD was higher at the Shoreline station, compared to stations further east (e.g., Windfence and Camping) then TWPD increased at Cottonwood and then a notable decrease occurs beginning at Haybale.

The TWPD by month for the period April to September in 2021 through 2023 for each out-of-Park monitoring station are shown in Fig. 4. The same seasonal pattern, i.e., greater TWPD in April, May, and June as compared with the summer months July, August, and September, was
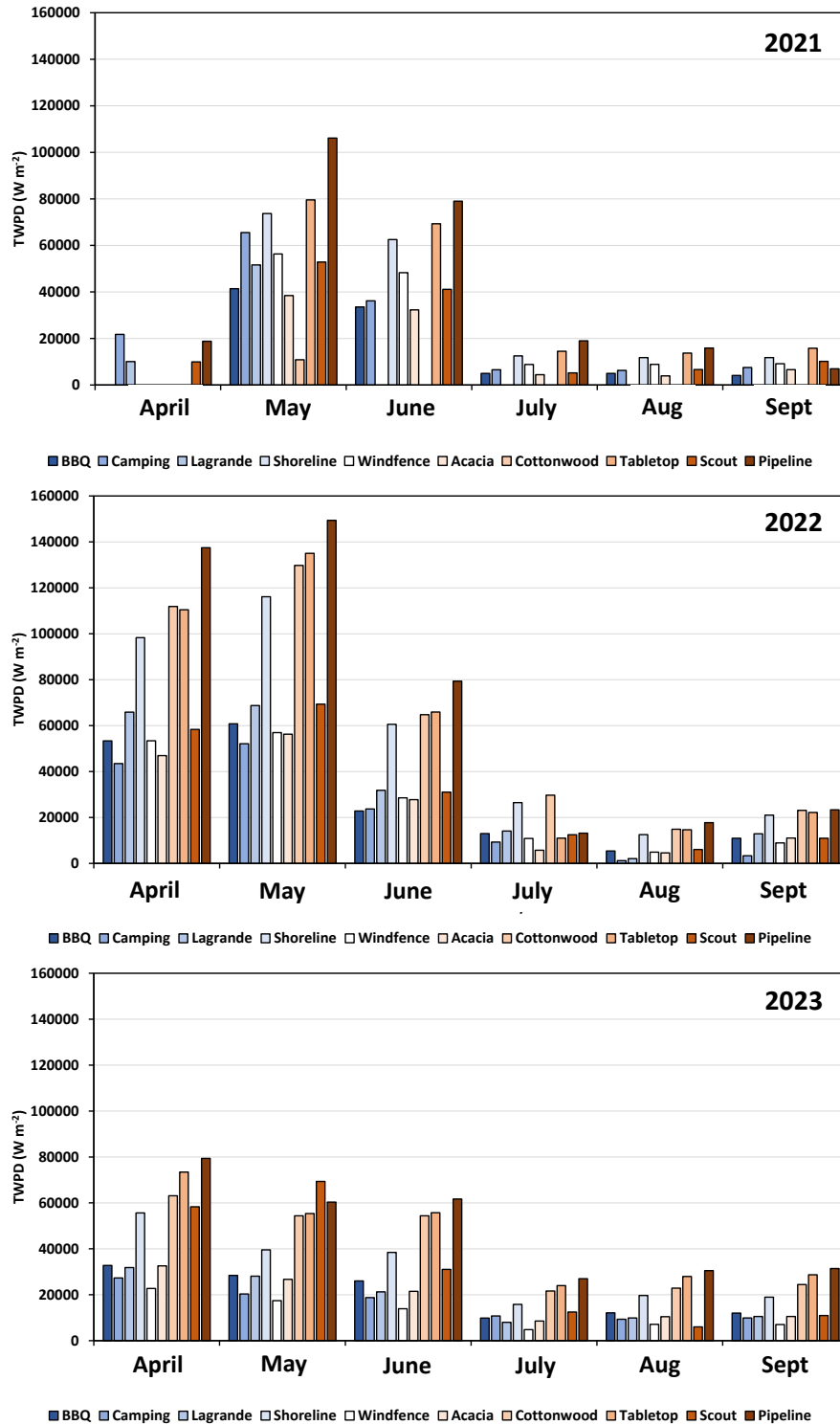
Figure 3. The monthly TWPD (W m^{-2}) for the in-Park stations. The order of stations is approximately north to south.
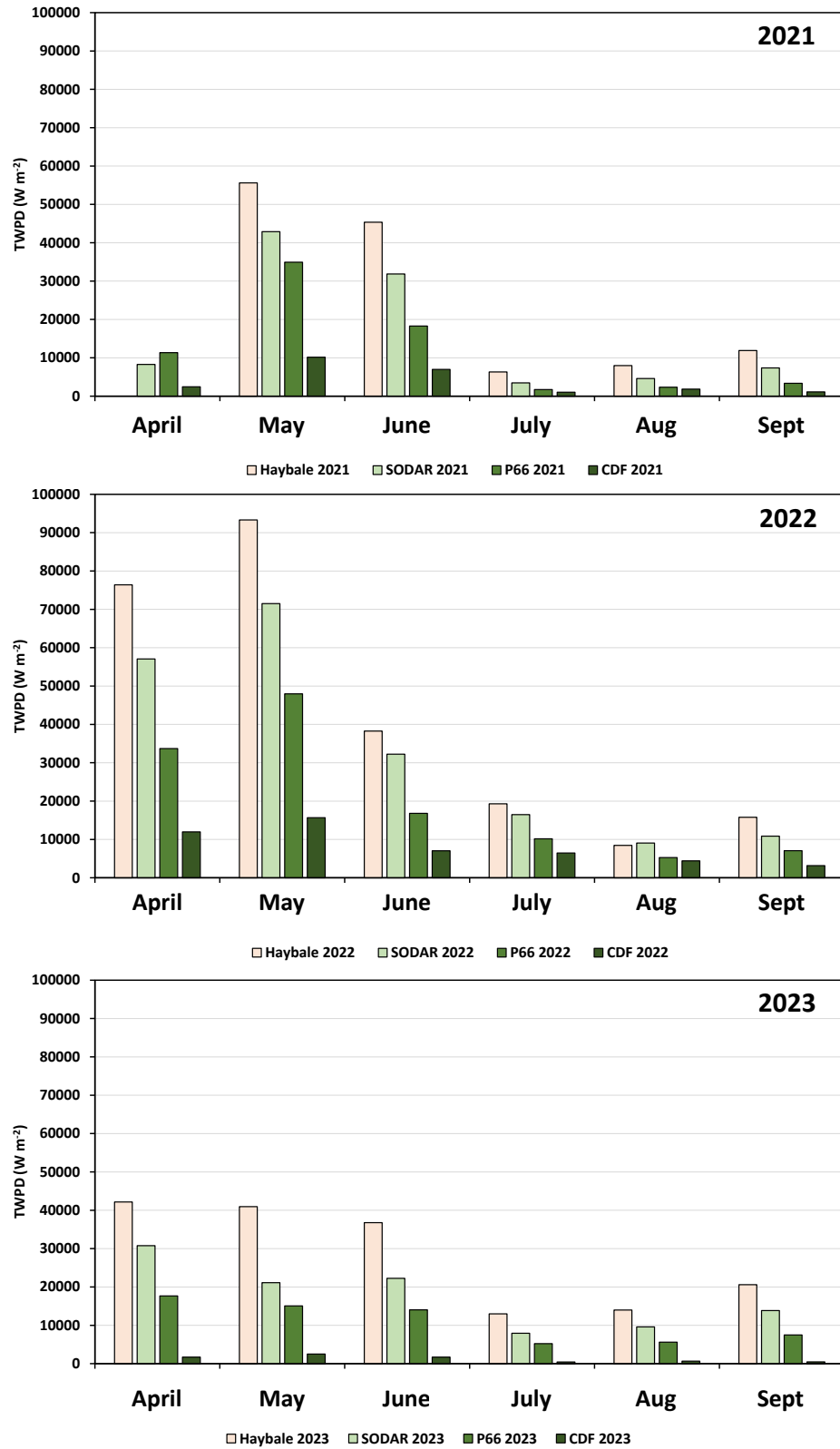
Figure 4. The monthly TWPD (W m^{-2}) for the out-of-Park stations. The order of stations is west to east.

observed in these stations as occurs for the in-Park stations. The TWPD range is smaller for the out-of-Park stations as the wind speed is slowed moving inland due to the frictional resistance of the vegetated surfaces. The CDF station farthest inland has the lowest range of TWPD compared with the other three stations that are farther to the west.

The change in TPM_{10}:TWPD for the in-park and out-of-park stations for available data from April/May to September 2021 through 2023 is shown in Fig. 5. As shown in this figure, for the period April to September 2022 and April to September 2023, the mean seasonal TPM_{10}:TWPD ratio for the in-park stations is variable as a function of position. The stations with the greatest TPM_{10}:TWPD ratio have consistently been the three northern stations BBQ, Camping, and Lagrande as well as Acacia. These stations are all on the downwind side of the "sand highway" route that is consistently used by OHV riders to access the ODSVRA riding areas.

The out-of-park stations (Haybale, Philips 66, Sodar, and CDF,) also show variability in the TPM_{10}:TWPD ratio across the three year record. CDF registers the highest TPM_{10}:TWPD ratio as it has the lowest TWPD values on a monthly basis, but still has PM_{10} concentration levels similar to the monitoring stations farther to the west that experience higher wind speeds. The in-Park network stations characterize the relation between wind speed and PM_{10} for more localized areas of the sand surface emitting PM_{10} during periods of saltation. The network based TPM_{10}:TWPD ratio for CDF is not directly comparable to the ratio reported in the Increments of Progress Reporting (Gillies et al., 2021, 2022, 2023)[1].

Spatial Trends in the Station PM10 and Wind Speed Data

The station data also provides a means to examine longitudinal and latitudinal trends in PM_{10} as well as changes upwind and in the lee of vegetation islands. The stations Shoreline, Windfence, Acacia, Cottonwood, Haybale, Phillips 66, and CDF define a west-east transect $\approx$4.2 km long at an azimuth of $\approx$300°. The spatial trend in normalized mean hourly PM_{10} concentration along this transect for wind in the directional range 246°-326° and when wind speed measured at the Shoreline station was $\geq$5.5 m s^{-1} (same as lower limit of wind speed for defining TPM_{10}:TWPD ratio), is shown in Fig. 6 for 2021, 2022, and 2023 for each of these station. Note that the PM_{10} has been normalized by dividing by mean hourly PM_{10} concentration at a station by the mean hourly PM_{10} concentration at the Acacia station, which consistently had the greatest PM10

---

[1] For the Increments of Progress Reporting the wind speed used in the denominator for the ratio is based on measurements at 10 m AGL at the S1 tower and PM10 is measured by a BAM at the CDF station ($\approx$3.5 m AGL). This provides a more robust indicator of the relation between the driving force of the wind creating emissions of PM_{10} from the sand surfaces of the ODSVRA and the PM_{10} concentrations observed at CDF with the Beta Attenuation Monitor (BAM). This pairing of wind power density and PM_{10} concentration represents the integrated effects of the turbulent transport processes and the surfaces (dust control areas, vegetation cover, etc.) on the dispersion of the PM_{10} prior to reaching the CDF station.
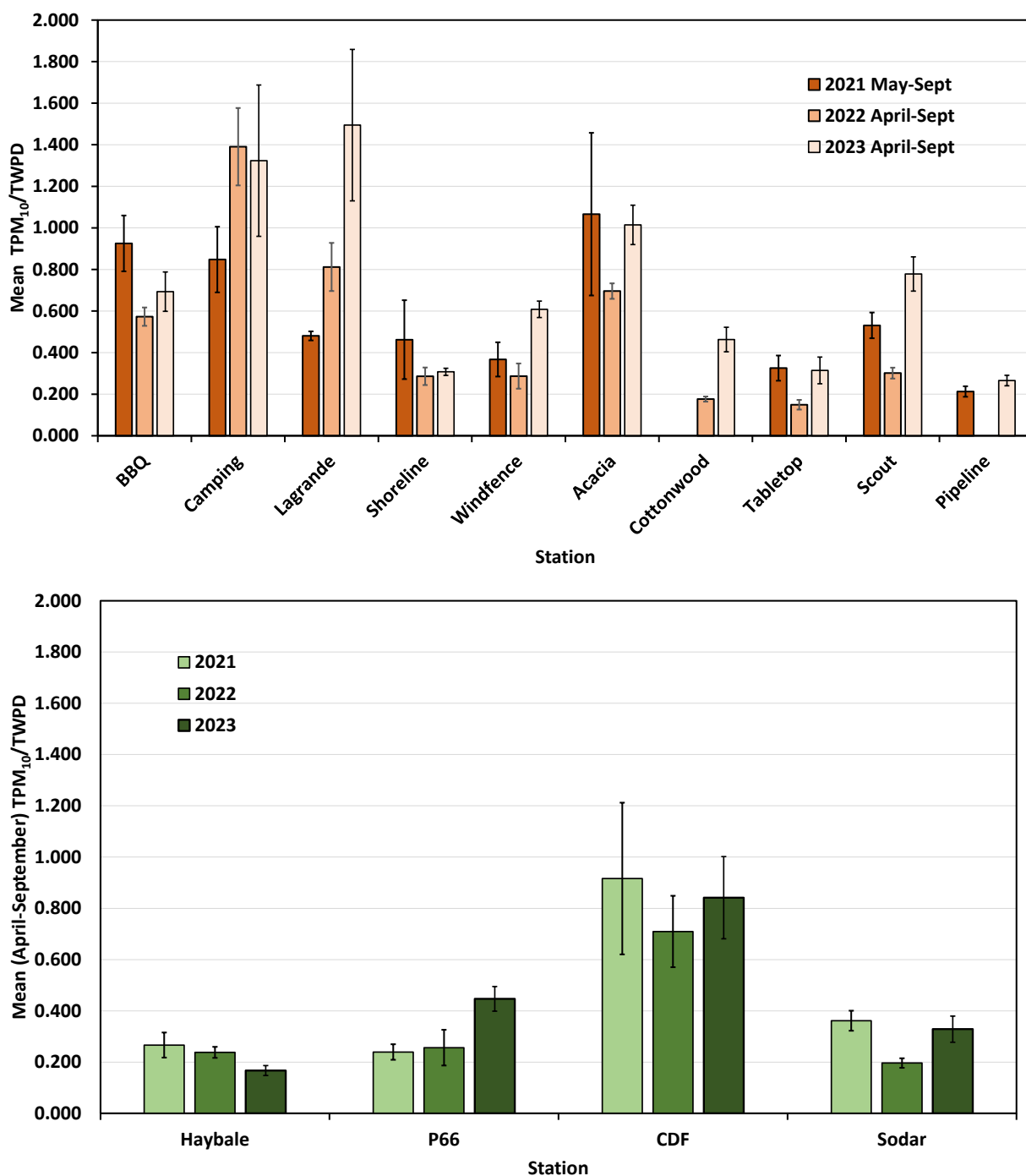
Figure 5. The monthly TPM$_{10}$:TWPD ratio (based on the summation of mean hourly data) for the in-Park stations (top panel) and the out-of-Park stations (bottom panel). The values represent the mean ratio based on the 6 (individual) monthly ratio values. The error bar represents the standard deviation of the mean value.

concentrations along this west to east transect. Although in 2021, Cottonwood station had a higher normalized mean PM_{10} value for the month of May compared to Acacia, this station did not record any data after May. The pattern of high PM_{10} values in the riding area of the ODSVRA as typified by the stations, Shoreline, Windfence, Acacia, and Cottonwood followed by a noticeable decrease beginning at the Haybale station is observed across the three years (Fig. 6).

Upon averaging the normalized mean hourly PM_{10} for the six months (i.e., April through September) for 2021, 2022, and 2023, Acacia consistently had the highest mean hourly PM_{10} concentration along this transect (Fig. 7). The highest concentrations of PM_{10} are observed at Acacia and Cottonwood, with an increase in mean concentration between the shoreline and these stations as the wind travels over the bare sand areas. For these three years of normalized mean hourly PM_{10} concentration, it is clear that the normalized concentration decreases appreciably beginning at Haybale, which marks the eastern edge of areas with open sand upwind of this station in a non-riding area.

Acacia station had the highest mean hourly PM_{10} concentrations in 2021, 2022, and 2023 (Fig. 7). Upwind of Acacia the normalized mean hourly values for Shoreline (0.67 ±0.12) and Windfence (0.48 ±0.07) stations are lower and downwind of Acacia there is a 15% decrease at Cottonwood (0.85 ±0.08), and then a more significant decrease in the normalized mean hourly
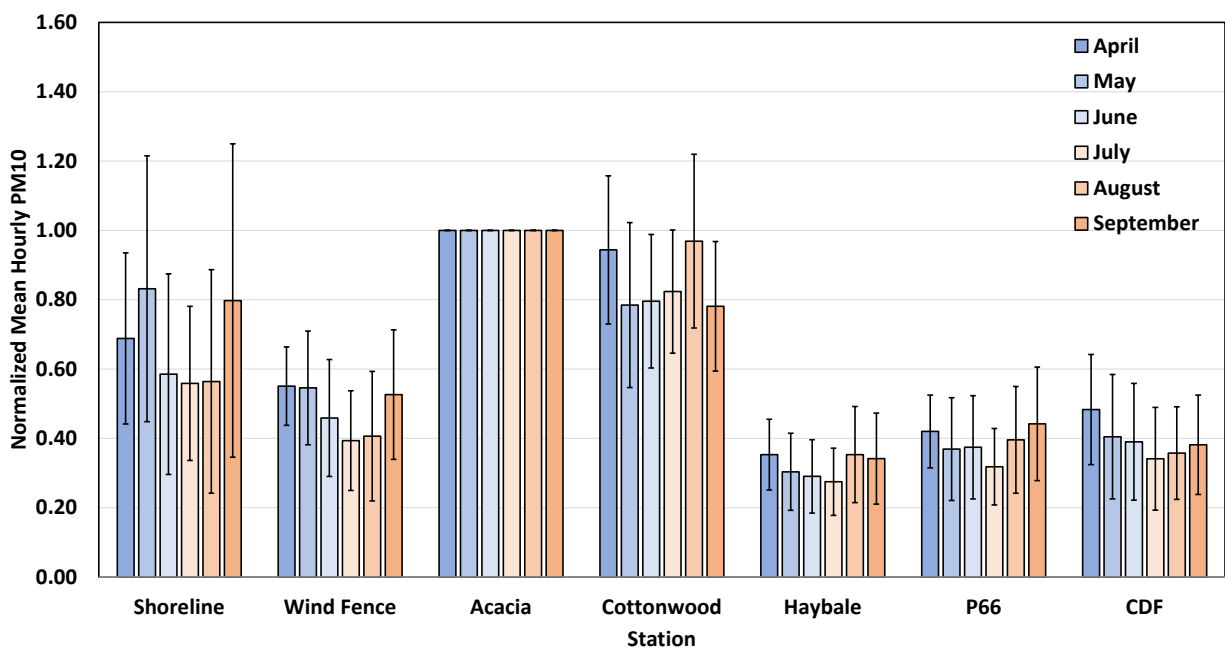
Figure 6. Normalized (by Acacia) mean hourly PM_{10} concentration for wind in the directional range 246°-326° and when wind speed measured at the Shoreline station was ≥5.5 m s^{-1}, April-September 2021, 2022, and 2023. The values represent the mean for all the hours in each month that met the data filter criteria for wind speed and wind direction. The error bar represents the standard deviation of the mean value.
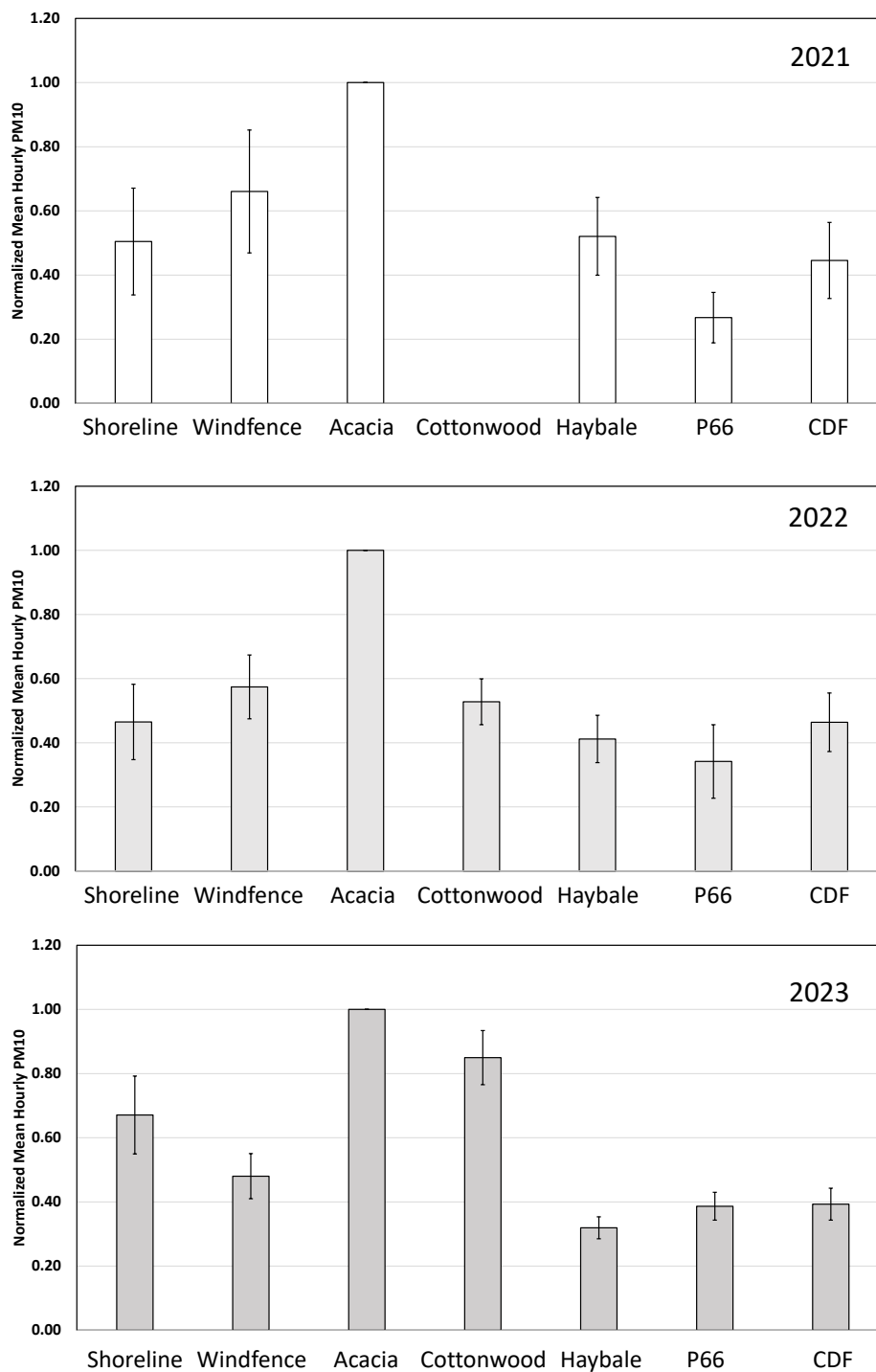
Figure 7. Normalized (by Acacia) mean hourly PM_{10} concentration for wind in the directional range 246°-326° and when wind speed measured at the Shoreline station was ≥5.5 m s⁻¹, for the combined period April-September 2021, 2022, and 2023. The values represent the mean for all the hours that meet the data filter criteria for wind speed and wind direction. The error bar represents the standard deviation of the mean value.

PM$_{10}$ values for the out-of-Park stations that are not located on emissive surfaces. These stations, i.e., Haybale, Phillips 66, and CDF, are in the zone where dispersion and deposition dominate the transport process affecting the concentration of PM$_{10}$. For Phillips 66 (0.39 ±0.04) and CDF (0.39 ±0.05), the normalized mean hourly PM$_{10}$ values under these wind direction and wind speed limitations are 60% lower than those at Acacia during active dust emission conditions. Why the Haybale station (0.32 ±0.03) is lower than Phillips 66 is not readily discernable, but it may be due to some effect of position in the landscape and the generally higher mean hourly wind speed at Haybale compared to Phillips 66 and CDF (Fig. 7) that induces more turbulent mixing.

North to South Trends in Station PM10 and Wind Speed Data

The in-Park stations BBQ, Lagrande, Acacia, Cottonwood, Tabletop, and Pipeline align in an approximate north-south direction (azimuth from Pipeline to BBQ is ≈356°). Along this series of stations, the increase in wind speed from north to south is demonstrated in Fig. 8, which shows the TWPD (six-month summation) for each station in 2023. Using the same six month summation period for TPM$_{10}$, the TPM$_{10}$:TWPD ratio for these six stations is shown in Fig. 9. Figure 9 illustrates that between Lagrande station in the north and Pipeline station in the south there is a consistent decrease in PM$_{10}$ concentration for equivalent wind power density levels, which indicates that the emissivity of the sand surface decreases towards the south. This further corroborates the PI-SWERL emissivity measurements spatial trend (SAG, 2023), which have also indicated the decrease in emissivity moving from north to south in the riding area.

Three of the network stations, Shoreline, Windfence, and Camping (Fig. 1) are positioned to examine the effect of a large area of vegetation on the concentration of PM$_{10}$ in an upwind-downwind configuration (Shoreline and Windfence) and in the absence of vegetation for an approximately equivalent length of fetch (Shoreline and Camping). The dust control/revegetation area identified as Bigfoot (Fig. 1, purple polygon with Shoreline on the west and Windfence on the east) was initiated in 2019. The mean hourly PM$_{10}$ concentrations at these stations for a constrained wind direction range of 284°-300° and for wind speed ≥5.5 m s^{-1}, for a period of overlapping time (April to July) was used to determine if the effect of vegetation on PM$_{10}$ concentrations could be demonstrated. Unfortunately, there was very limited data available with these constraints applied for 2021, which did not allow for further analysis.

If the hourly mean PM$_{10}$ concentrations (for matching hours following application of the wind speed and direction filters) for Shoreline and Windfence are normalized by dividing by the PM$_{10}$ concentrations at Camping, the change in concentration across the Bigfoot dust control area can be compared for the period April to July for 2022 and 2023 (Fig. 10). Figure 10 suggests that between 2022 and 2023 the mean hourly concentrations of PM$_{10}$ for the given wind speed and wind direction constraints across approximately the same west to east distance (or fetch) the difference between the Shoreline station and the Camping station in 2023 is less than between
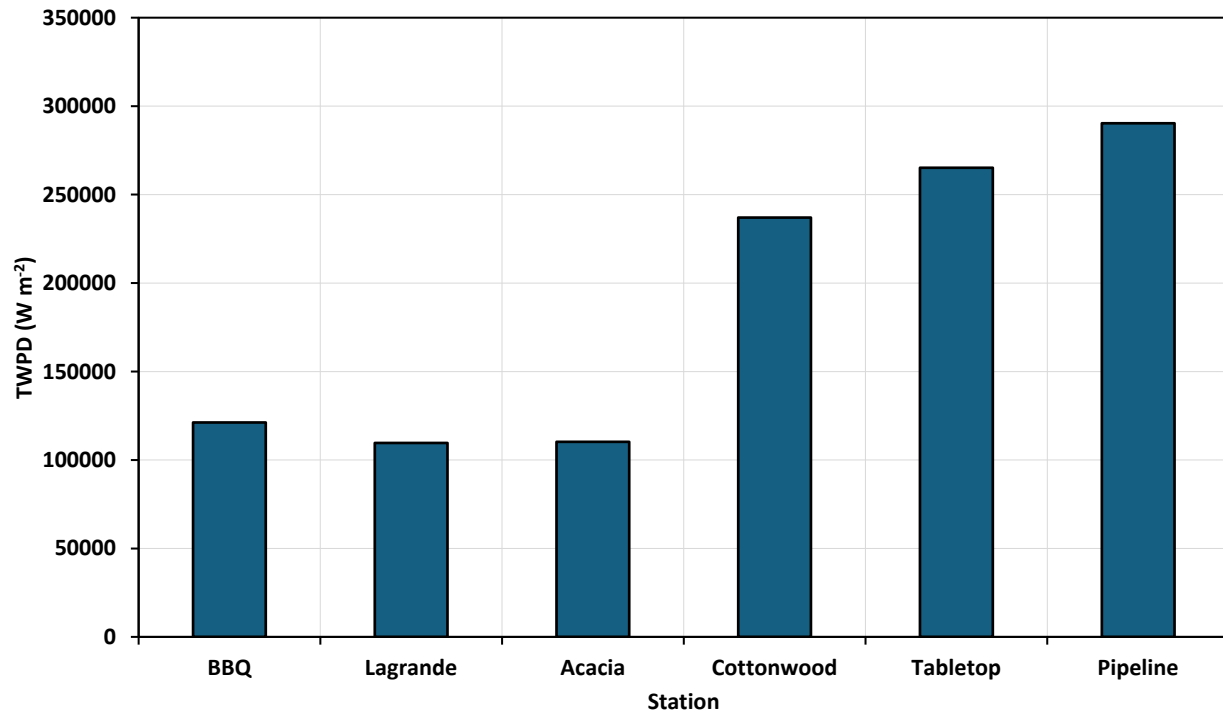
Figure 8. TWPD (W m^{-2}) (summed for April-September 2023) along a north to south transect from BBQ in the north to Pipeline in the south.
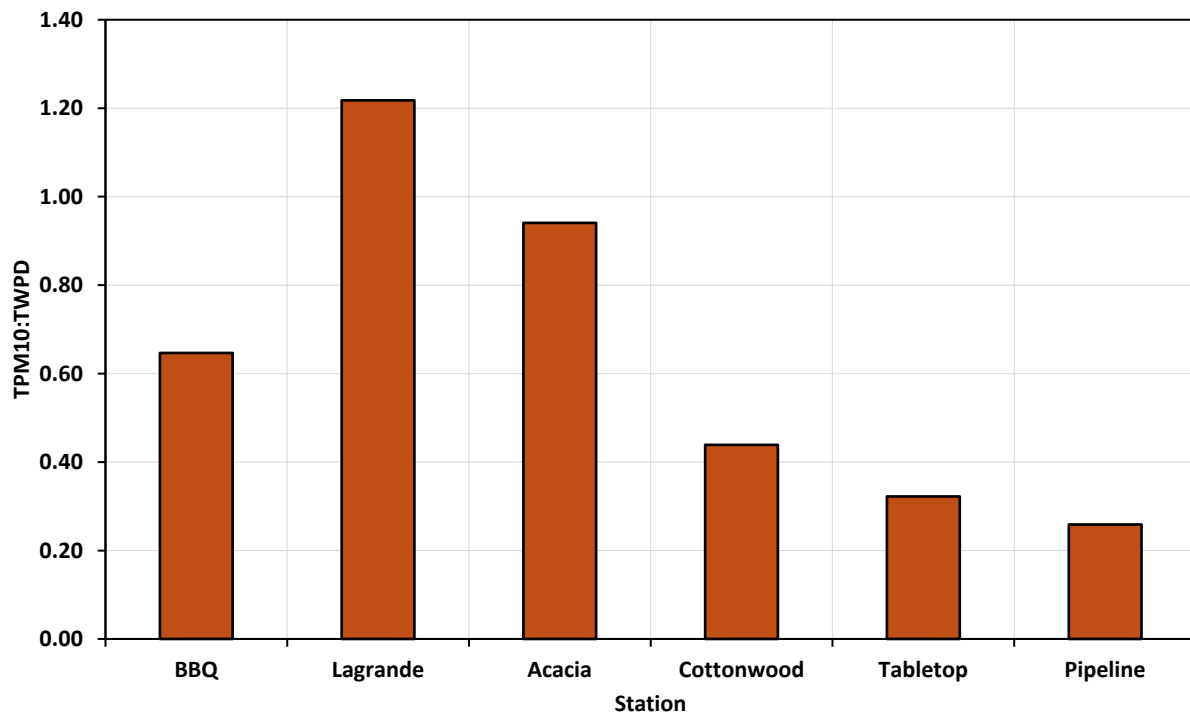
Figure 9. TPM$_{10}$:TWPD (summed for April-September 2023) along a north to south transect from BBQ in the north to Pipeline in the south.

Windfence and Camping. The variability in the mean monthly values is significant (standard deviation of the mean values are shown as error bars in Fig. 10), and it cannot be definitively stated that this effect is due to the maturation of the vegetation dust control. Figure 6 however, shows that for a wider range of wind direction and for PM_{10} concentrations normalized to the Acacia station, Windfence was lower than the Shoreline mean value in 2023. In previous years, Windfence had greater mean values than Shoreline. This comparison of PM_{10} concentrations among these three stations can be continued for 2024 to determine if the mean hourly PM_{10} values at Windfence continue to show lower values than Shoreline when compared with Camping. A continued decrease in normalized mean hourly PM_{10} at Windfence compared with Shoreline could signal the increasing effectiveness of the Bigfoot revegetation dust control area as the vegetation matures (i.e., increases in areal coverage and plant height) to influence the PM_{10} emitted upwind of Shoreline.

Conclusions

The concentration gradient of PM_{10} along an approximately 4.2 km long west to east transect (Shoreline to CDF) shows a consistent peak concentration occurring at the Acacia station in the years 2021 through 2023. This likely reflects the greater emissivity of the sand in this area that is highly influenced by the "sand highway". Following the peak in mean hourly PM10 at Acacia the mean hourly concentration of PM_{10} diminishes by, on average, 63% (±5%) for the stations Haybale, Phillips 66, and CDF compared to the Acacia station. These stations are east of the open sand areas of the riding and non-riding areas of the ODSVRA.

The 2023 wind speed and wind power density data (Fig. 8) show that for the north-south distance covered by the network (BBQ to Pipeline) the wind speed was higher in the south than the north, which corroborates what has previously been reported and indicates that this pattern has endured since monitoring was initiated. The station PM_{10} and wind speed data combined also show (Fig. 9) that the PM_{10} concentrations for the same wind power density are higher in the northern stations (BBQ, Lagrande, and Acacia) indicating that the emissivity of the sand surfaces upwind of these stations remains high in relation to the other stations and is still a rich source area for PM_{10} emissions. The high PM_{10} concentrations and emissivity in this area may be due to the presence of the "sand highway", which remains a high use area for OHV. The gradient of decreasing emissivity from north to south has also been observed in the PI-SWERL data. The 2023 TPM_{10}:TWPD data (Fig. 9) indicates that this pattern has endured since the monitoring was initiated.

Although the data are limited to 2022 and 2023, the difference in the PM_{10} concentration data between the stations Shoreline and Windfence, which lie on either side of a large re-vegetation area, show that for 2023 the downwind station Windfence has lower mean hourly PM_{10} concentrations than Shoreline. This may indicate that the re-vegetated area may now be of sufficient size, plant cover density, and low (or zero) emissivity to influence the dispersion and deposition processes such that the downwind concentrations are lower than the upwind. This comparison will be carried out for the 2024 station data to determine if this pattern persists.
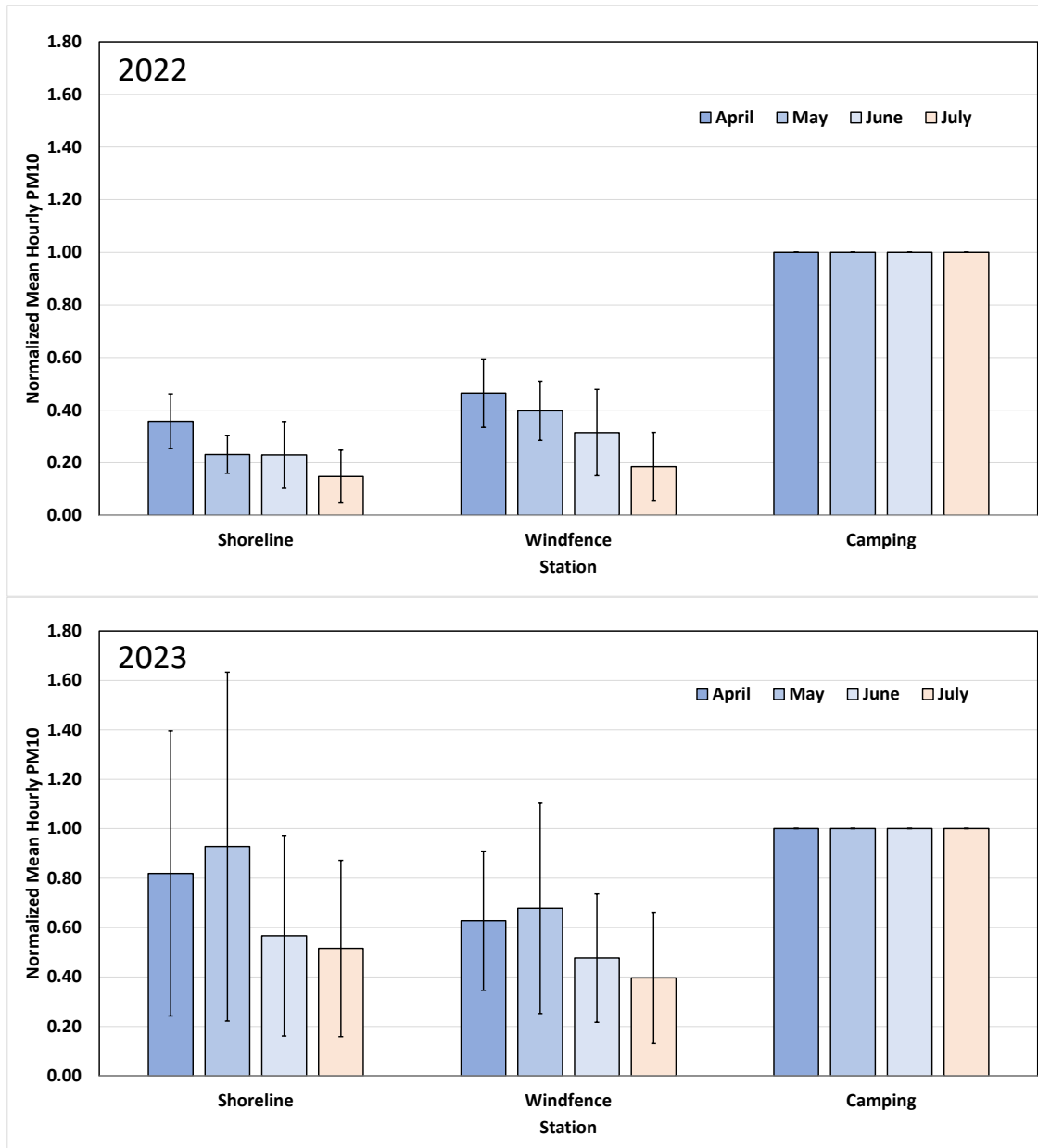
Figure 10. Normalized (by values at Camping) mean hourly PM_{10} concentration for wind in the directional range 284°-300° and when wind speed measured at the Shoreline station is ≥5.5 m s^{-1}, for the combined period April-July 2022 and 2023.

References

Etyemezian, V., J.A. Gillies, D. Zhu, A. Pokharel, G. Nikolich (2014). 2013 Intensive Wind Erodibility measurements at and Near the Oceano Dunes State Vehicular Recreation Area. Prepared for California State Parks, ODSVRA, Oceano, CA and OHMVR Division, Sacramento, CA, 07-08-2014.

Gillies, J.A., V. Etyemezian (2014a). Wind and PM10 Characteristics at the ODSVRA from the 2013 Assessment Monitoring Network. Prepared for California State Parks, ODSVRA, Oceano, CA and OHMVR Division, Sacramento, CA, 01-14-2014.

Gillies, J.A., G. Nikolich, E. Furtak-Cole (2023). Increments of Progress Towards Air Quality Objectives - ODSVRA Dust Controls, 2023 Update. Prepared for California State Parks, ODSVRA, Oceano, CA and OHMVR Division, Sacramento, CA, 11-27-2023.

Gillies, J.A., V. Etyemezian (2014b). Addendum to the PI-SWERL Report of Etyemezian et al. (2014): Particle Size Distribution Characteristics and PI-SWERL^{TM} PM10 Emission Measurements: Oceano Dunes State Vehicular Recreation Area. Prepared for California State Parks, ODSVRA, Oceano, CA and OHMVR Division, Sacramento, CA, 02-03-2015.

Kalmikov, A. (2017). Wind power fundamentals. In Wind Power Engineering, ed. T.M. Letcher. Elsevier Science Publishing Co., Inc.

Science Advisory Group [SAG] (2023). SAG Recommendations for Establishing Emissivity Grids to be used in Modeling of Pre-Disturbance Conditions and Future Excess Emissions Reductions. Memo submitted to California Department of Parks and Recreation and San Luis Obispo Co. Air Pollution Control District, 06-21-2023.

THIS PAGE WAS INTENTIONALLY LEFT BLANK.

May 28, 2024

Memo: <u>SAG Review of Desert Research Institute (DRI) "Report of Findings: ODSVRA Meteorological and PM$_{10}$ Monitoring Network, 2023"</u>

From: Scientific Advisory Group (SAG)

To: Jon O'Brien, California Department of Parks and Recreation

Cc: Ronnie Glick, California Department of Parks and Recreation

The Scientific Advisory Group (SAG) received a copy of the Desert Research Institute (DRI) "Report of Findings: ODSVRA Meteorological and PM$_{10}$ Monitoring Network, 2023" on June 2023, on May 14, 2024 via e-mail, and SAG members have had the opportunity to review the document. This memo provides feedback on the DRI report[1].

The report summarizes the latest results, acquired in 2023, from the wind and dust monitoring network, which comprises multiple stations distributed within the ODSVRA and supplemented with additional stations downwind of the ODSVRA. The results from 2023 are contextualized using similar data collected in 2021 and 2022. The data were presented in summary form using hourly values that are averaged over monthly and seasonal (April – September) periods.

Overall the report is very effective in communicating the spatial-temporal dimensions of mean wind conditions and PM$_{10}$ concentrations across the ODSVRA and the adjacent areas that are relevant to air quality monitoring and regulation. The key findings are that:

1. there is a general increase in wind speed from north to south (as represented by Total Wind Power Density, TWPD), consistent with findings from earlier studies;
2. there is a general decrease in normalized PM$_{10}$ concentrations from north to south (as represented by the ratio of (Total PM$_{10}$)/(Total Wind Power Density), TPM$_{10}$/TWPD), consistent with results from multiple PI-SWERL campaigns showing that surface dust emissivity decreases from north to south (likely due to grain size trends);
3. there is a persistent local maximum of normalized PM$_{10}$ concentrations at the Acacia station, located at the eastern margin of ODSVRA in the north-central zone, as well as at the northern stations known as BBQ, Camping, and Lagrande, all of which are situated immediately downwind of an intensely used OHV corridor known as the 'sand highway';
4. there is a general west-east trend in TPM$_{10}$/TWPD that indicates that dust emissions increase from the shoreline in the inland direction across the ODSVRA and then decrease beyond the Park boundary toward monitoring stations such as CDF; and,
5. there is preliminary evidence suggesting that dust concentrations immediately downwind of vegetated treatment zones are smaller than those measured upwind of the treatment zones, indicating the potential effectiveness of surface vegetation cover in both reducing

---

[1] Standard procedure for SAG review of DRI reports is for Dr. Jack Gillies to recuse himself from the discussions due to a potential conflict of interest. Despite being a SAG member in good standing, Dr. Gillies did not participate in this review in any manner nor was DRI consulted about any aspect of this review.

surface dust emissions and trapping or capturing near-surface dust coming from upwind sources.

SAG members have the following recommendations for possible improvement of the DRI report:

A. There are numerous places in the document where additional clarification would be useful and where various sentences and paragraphs could be re-phrased to make messaging more effective. A marked-up copy of the original PDF with editorial suggestions and marginal comments is attached to this review.

B. In future reports, it would be useful to provide a more in-depth discussion of how the PI-SWERL results (showing spatial trends in dust emissivity, especially the north-south gradient) are complementary to the measurements of wind speed and PM_{10} concentrations from the network. The PI-SWERL emissivity estimates are collected infrequently at specific times and are spatially sporadic, and therefore provide only snapshots into how dust is potentially emitted from the ODSVRA, but they are critical to modeling dust emissions for purposes of regulatory compliance. The wind and dust measurements, on the other hand, are temporally continuous thereby providing significant detail into the dynamics of dust emissions via wind shear. Despite quantifying different aspects of the dust emission process, they are very complementary, and this complementarity should be exploited.

C. In future reports (or as a separate exercise), an analysis should be undertaken of dust dynamics during specific wind events. This might involve using hourly values across a 24-hour period or perhaps 10-minute averages across an 8-hour period when dust concentrations are particularly high. The intent would be to understand how dust plumes are generated and eventually make there way to monitoring stations such as CDF.

D. In future reports, it would be useful to tie the metrics used in the current report (e.g., monthly averages of TWPD and TPM_{10}/TWPD) to measures used by regulatory agencies to define exceedance events (i.e., 24-hr PM_{10} concentrations). The objective is to use the scientific results to inform management and regulatory efforts directly in ways that are meaningful and easy to understand.

Overall, the report is a welcome addition to the body of knowledge that informs the air quality program at the ODSVRA, and DRI is to be commended for its efforts in this regard.

Respectfully,

The Scientific Advisory Group

Bernard Bauer (Chair), Carla Scheidlinger (Vice-Chair), Mike Bush, Jack Gillies, Jenny Hand, Leah Mathews, Ian Walker

ODSVRA Dust Control Program Draft 2024 ARWP

ATTACHMENT 04A

UCSB 2022-2023 ODSVRA Foredune Restoration UAS Survey Report

- UCSB 2022-2023 ODSVRA Foredune Restoration UAS Survey Report (UCSB Report)

- SAG Review of UCSB Report "Foredune Restoration UAS Survey Report" (UCSB 2022-2023 ODSVRA) (SAG Memo)

THIS PAGE WAS INTENTIONALLY LEFT BLANK.

UCSB 2022-2023 ODSVRA

Foredune Restoration UAS Survey Report

Prepared by: Zach Hilgendorf[1,2], Ian Walker[1,3], Nitzan Swet[1], and Madison Heffentrager[1]

[1] Department of Geography, University of California, Santa Barbara
[2] Department of Geography and Anthropology, University of Wisconsin-Eau Claire
[3] Member of the ODSVRA Scientific Advisory Group

June 2023

List of Acronyms:

California Department of Parks and Recreation – CDPR
Desert Research Institute – DRI
Digital Terrain Model – DTM
Geomorphic Change Detection – GCD
Ground Sampling Distance – GSD
Light Detection and Ranging - LIDAR
Near Infrared – NIR
Normalized Difference Red-Edge Index – NDRE
Normalized Difference Vegetation Index – NDVI
Oceano Dunes State Vehicular Recreation Area – ODSVRA
Off-Highway Vehicles – OHV
Particulate Matter – PM
Particulate Matter Reduction Plan - PMRP
Portable In-Situ Wind Erosion Laboratory – PI-SWERL
Post-Processing Kinematic - PPK
Red-Edge – RE
Red-Green-Blue Spectral Bands – RGB
San Luis Obispo Air Pollution Control District – SLO-APCD
Scientific Advisory Group – SAG
Structure-from-Motion – SfM
Stipulated Order of Abatement - SOA
Uncrewed Aerial Platform – UAS
University of California Santa Barbara – UCSB

EXECUTIVE SUMMARY

Five (5) different foredune restoration treatments and a control site were established in Feb. 2020 in a 48 acre region of the ODSVRA. Treatments included (north to south): 1) a minimal intervention control plot textured by a sheepsfoot roller only; 2) sheepsfoot texture and broadcast native seeds; 3) sheepsfoot texture and broadcast native plant and sterile rye grass seeds; 4) low-density straw planting circles with nodes of juvenile native plants; 5) high-density straw planting circles with nodes of juvenile native plants; 6) complete straw cover with high density of juvenile plants. Performance of the treatments is assessed using five (5) criteria that track the geomorphic and vegetation responses within the restoration areas (see below).

An uncrewed aerial system (UAS) with high resolution cameras was used to detect and map geomorphic and vegetation changes in the restoration plots and adjoining beach and back dune areas from eight (8) biannual flights in Oct. and Feb. dating back to Oct. 2019. Resulting datasets include georeferenced orthophoto mosaics, plant cover maps, digital terrain maps (DTMs), and geomorphic change detection (GCD) maps used to calculate volumes of sediment erosion/deposition across the restoration sites. These data are then used to identify and interpret dune development, sediment budget responses, and vegetation establishment. This report provides results from three years of wind seasons, plant growth and dune development.

To date, sand supply to the beach has been highly variable, as expected, due to seasonal trends in wave energy, beach erosion/rebuilding, and the movement of rip current embayments. Overall, however, sand supply to the beach has declined in front of the restoration sites, particularly in this past year in response to severe winter storms and widespread beach erosion. This was most pronounced in front of plots 1-3. Changes in beach width occur naturally and independently from the restoration efforts, yet they control responses of the treatments by modulating the supply of sand available for aeolian transport into the restoration plots. Dune development continued in all of five (5) treatment plots with 1 to >2 m tall nebkha observed, with the smallest and lowest extent of nebkha in treatments 6 and 2, respectively. The control plot 1 continues to show low, migrating unvegetated transverse ridges with negligible plant cover. Plots 2-6 all continue to show positive sediment budgets. Backdune units downwind of the restoration plots show differences related to location and treatment type, with a general north to south gradient of increasingly negative sand budgets. Plots 1-3 typically recorded similar trends in sand volume changes, often reflecting beach inputs. Plots 4-6, however, have a distinctly different, oscillating trend from near-neutral to negative change.

Plant cover has generally increased since implementation for all plots except the control site, which continues to show negligible cover. Plot 6, the most intensive initial restoration

treatment, shows the greatest net increase in plant cover (14.8%) by Feb. 2023, followed by (in decreasing order) plot 5 (9.7%), 3 (8.9%), 4 (5.5%), and 2 (2.7%). The peak observed historical cover at the restoration site and in the broader foredune zone (~400 m inland) in the OHV riding area, respectively, were about 3 and 6% in 1966[see footnote 3]. Interestingly, most plots showed a slight decline in plant cover over this past year, perhaps due to an unusually wet and stormy winter season and/or erosion along the seaward margins of the plots.

In terms of performance assessment criteria, the summary following this third year is as below:

1. **All foredune treatments continue to show net positive sediment budgets**. For the first time, however, the control plot 1 shifted to a negative (erosional) budget that relates partly to a lack of vegetation to promote accretion and nebkha development, as well as notable beach erosion in the winter of 2022-23. This said, beach erosion was greater fronting treatments 2 and 3, yet they maintained appreciable accretion. Generally, sediment budgets continued to increase in the vegetated treatment plots where nebkha dune development is enhancing sediment capture and providing downwind sheltering to the surface.

2. **Aeolian processes remained active in all treatments** shown by rippled sand transport corridors, dune development, coalescence and migration, and emergence of erosional deflation surfaces with coarse lag deposits on all sites, which is required to provide needed ecological disturbance gradients and processes required for plant growth and dune development.

3. **Plant cover since implementation continues to increase in all treatment plots** except for the control site, which continues to show negligible cover. Although the 3-year trend is positive, plant cover declined notably this past year in most plots perhaps due to the unusually wet and stormy winter and/or erosion along the seaward margins of the plots. The site-wide average of plant cover across all vegetation treatments (2-6) is ~8.2% with a maximum of 14.8% in plot 6 (parks classic) and a minimum of 2.7% in treatment 2 (native seed).

4. **Dune development continues in all treatment plots**, with the largest (>2 m) nebkha dunes in plots 3 and 5, smaller (1.0-1.5 m) nebkha in plots 2 and 4, and multiple smaller dunes in plot 6. This past year also saw increasing development of nebkha along the seaward edge of most plots.

5. **Assessing contributions of restoration treatments to reduced dust emissivity is underway**. A recent PI-SWERL campaign was conducted by DRI in Summer 2022 to assess the emissivity in the treatment plots for improved dust modeling and for monitoring emissivity response of the treatments.

1. Introduction:

To monitor and assess the performance of the foredune restoration dust emissions mitigation project at the ODSVRA, a team from UCSB and formerly Arizona State University, in collaboration with the CDPR, have been conducting UAS flights biannually since Oct. 2019. The UAS imagery datasets are then used to create the following main data products:

1. Georeferenced, orthorectified **aerial photo mosaics** of the study site in the visual (RGB) spectral bands,

2. Georeferenced, orthorectified **maps of vegetation cover** derived from RGB and multispectral imagery using NDVI and other spectral methods,

3. Three-dimensional **DTMs**[1] derived from the RGB imagery using SfM photogrammetry,

4. **Geomorphic Change Detection (GCD) maps** from consecutive time steps showing differences in elevation derived by comparison of DTMs using spatial statistics. The GCD maps are then used to calculate volumes of sediment change between surveys that can be used to identify and interpret dune development, evolution, erosion/deposition patterns, and sediment budgets.

Data collected during the UAS flights allows for high resolution, three-dimensional DTM surfaces to be constructed and compared over time to quantify sand volume changes and dune dynamics throughout the park. Other data collected allow for examination of the growth of vegetation and the development of dune forms within the foredune treatment plots. This report details the methods used for data collection, processing, as well as initial baseline conditions collected prior to the implementation of the restoration treatments (Oct. 2019) through to Feb. 2023 (3 years following the installation of restoration treatments in Feb. 2020).

Generally, the performance or 'success' of the restoration treatments at ODSVRA can be assessed using criteria that track the geomorphic, sediment transport, and vegetation characteristics and responses within the treatment areas. Walker et al. (2013)[2] identified several key indicators that can be used to assess the performance of coastal dune restoration projects using an approach that encourages re-establishment of dynamic ecological and geomorphic conditions that improve dune ecosystem form and function and promote a more resilient and

---

[1] DTMs differ from Digital Elevation Models (DEMs) in that they can include other elements on top of the surface, such as vegetation or structures. For the purposes of change detection modelling in this report, any structures (e.g., restroom buildings, fences, etc.) or other elements (e.g., vehicles) were removed during processing.

[2] Walker, I. J., Eamer, J. B., & Darke, I. B. (2013). Assessing significant geomorphic changes and effectiveness of dynamic restoration in a coastal dune ecosystem. Geomorphology, 199, 192-204. https://doi.org/10.1016/j.geomorph.2013.04.023

sustainable landform. These indicators have since been modified by Walker et al. (2023)[3] to suit the conditions and management needs at the Oceano Dunes. Key indicators include:

1. **Establish and maintain a positive sediment budget** (i.e., continued gains in sediment volume over time). This is particularly important during the first phase of foredune development in which small incipient nebkha dunes (mounds of windblown sand trapped in vegetation) establish and related downwind shadow dunes grow. Eventually, as nebkha and shadow dunes grow and coalesce and, in turn, alter onshore wind and sand transport patterns, volumetric gains may slow and/or plateau once the system reaches its fully developed state. Based on nearby natural foredune sites (e.g., Oso Flaco), this could take as long as several decades to occur.

2. **Maintain aeolian activity, namely sand transport (saltation) and open sand surfaces, within the treatments**. Saltation of sand, and related erosion and deposition patterns, are critical processes required for dune development and maintenance. In addition, these processes create fundamental ecological disturbances (abrasion, burial, exhumation, nutrient transport, etc.) and gradients required to maintain healthy foredune plant communities. Plant species found in backdune scrub ecosystems, however, are not necessarily well adapted to the same disturbance processes or gradients and, thus, care must be used in selecting appropriate plants for foredune vs. backdune restoration settings. Natural foredunes in this region are not characterized by a uniform foredune ridge with high plant cover, as is often the case further north in California and Oregon. Rather, a more hummocky, discontinuous form with active sand surfaces is the preferred ecosystem form.

3. **Increase foredune plant cover and survivorship**. Where a new foredune ecosystem is being developed, it is imperative that plants establish and survive to initiate sedimentation during the early stages of dune development. Eventually, however, plant cover density might plateau at an amount that is in balance with dune form/position, aeolian activity, soil nutrients, and regional climate conditions. As ecosystem re-establishment occurs, it is also anticipated that species richness would improve and, accordingly, initial planting palettes should reflect the range of species present in neighboring natural foredune ecosystems, such as the Oso Flaco reference site.

4. **Enhanced dune development**. The establishment and growth of foredunes and related dune forms (e.g., nebkha, blowouts, transverse or barchanoid ridges, parabolic dunes, etc.) and morphodynamics involving erosion and/or deposition of sediment in the

---

[3] Walker, I. J., Hilgendorf, Z., Gillies, J. A., Turner, C. M., Furtak-Cole, E., & Nikolich, G. (2023). Assessing performance of a "nature-based" foredune restoration project, Oceano Dunes, California, USA. Earth Surface Processes and Landforms, 48(1), 143-162.

landscape is a key sign of improved performance. Important feedback mechanisms exist between wind flow, sand transport, vegetation cover, and dune form that are required to build and maintain natural foredunes. As the system develops and evolves, the variety of dune forms is expected to change and will organize toward a morphology that reflects plant cover, aeolian activity, and regional climate controls.

5. **Contribute to a reduction in dust emissivity**. The main impetus for the foredune restoration project at ODSVRA was to implement a sustainable, nature-based dust emissions mitigation treatment that had both onsite and downwind impacts. The location for the project was determined by CDPR-ODSVRA staff and the SAG to target a highly emissive area of sand surface as identified by extensive Pi-SWERL testing by DRI. Prior to restoration, the ~48 acre site had been used for intensive camping and OHV activity close to the high water line, where a foredune system would naturally exist. The new terrain and vegetation roughness is designed to disrupt boundary layer airflow and surface shear stress patterns that drive saltation and dust emissions in this area. Due to secondary lee-side flow effects, it is anticipated that the new foredune will also have downwind benefits on reduced shear stress and dust emissions.

2. Methods:

UAS platforms and SfM photogrammetry have experienced widespread and rapid advancements in the last decade[4,5]. SfM photogrammetry refers to the reconstruction of a three-dimensional landscape from highly overlapped (≥70% frontal and side overlap) images. The quality and resulting products are dependent on the camera used, methods for georectification, and, in the case of UAS platforms, flight altitude, shutter speed, and stability[6]. UAS-SfM datasets have been used in a wide variety of landscapes and ecosystems, including those along the coast. Advantages for using such datasets for coastal monitoring and detecting change include the relative ease and low cost of data collection, compared to aerial LIDAR, and the high accuracy (mm-cm resolution) of the resulting maps.

---

[4]Anderson, K., Westoby, M. J., & James, M. R. (2019). Low-budget topographic surveying comes of age: Structure from motion photogrammetry in geography and the geosciences. Progress in Physical Geography: Earth and Environment, 43(2), 163–173. https://doi.org/10.1177/0309133319837454

[5]James, M. R., Chandler, J. H., Eltner, A., Fraser, C., Miller, P. E., Mills, J. P., Noble, T., Robson, S., & Lane, S. N. (2019). Guidelines on the use of structure-from-motion photogrammetry in geomorphic research. Earth Surface Processes and Landforms, 44(10), 2081–2084. https://doi.org/10.1002/esp.4637

[6] Singh, K. K., and A. E. Frazier. (2018). A meta-analysis and review of unmanned aircraft system (UAS) imagery for terrestrial applications. International Journal of Remote Sensing, 39(15–16), 5078–5098. https://doi.org/10.1080/01431161.2017.1420941

A fixed-wing, fully autonomous Wingtra One UAS platform was used at the ODSVRA from Oct. 2019 to Feb. 2023 to monitor and characterize changes in sediment volumes, geomorphic responses, and vegetation cover within and beyond the restoration treatments (Figure 1). The WingtraOne UAS is typically flown at altitudes over 100 m above ground level and is equipped with on board, survey-grade GPS with PPK correction capabilities. During data collection, a Trimble R10 (Oct. 2019 through Feb. 2022) or R12 (Oct. 2022 through present) base station is operated in static collection mode, which is then used to refine photo point locations from the UAS to within millimeters of their real-world location. As of the date of this report, eight collection campaigns have been flown at ODSVRA (Table 1) with multispectral data collected concurrently since Oct. 2020.

The primary camera payload, a Sony RX1RII 42 MP full-frame sensor, is used to produce high resolution (<2 cm) orthomosaic imagery that, in turn, is used with SfM to create three-dimensional point clouds of the underlying surface that can be compared between campaigns to quantify volumetric change (Table 2). Point clouds between campaigns are aligned to one another using static features in the landscape (e.g., structures, roads, etc.) and then the dataset is averaged to 10 cm point spacing. This point cloud is then used to create a gridded (rasterized) DTM that represents the surface topography.
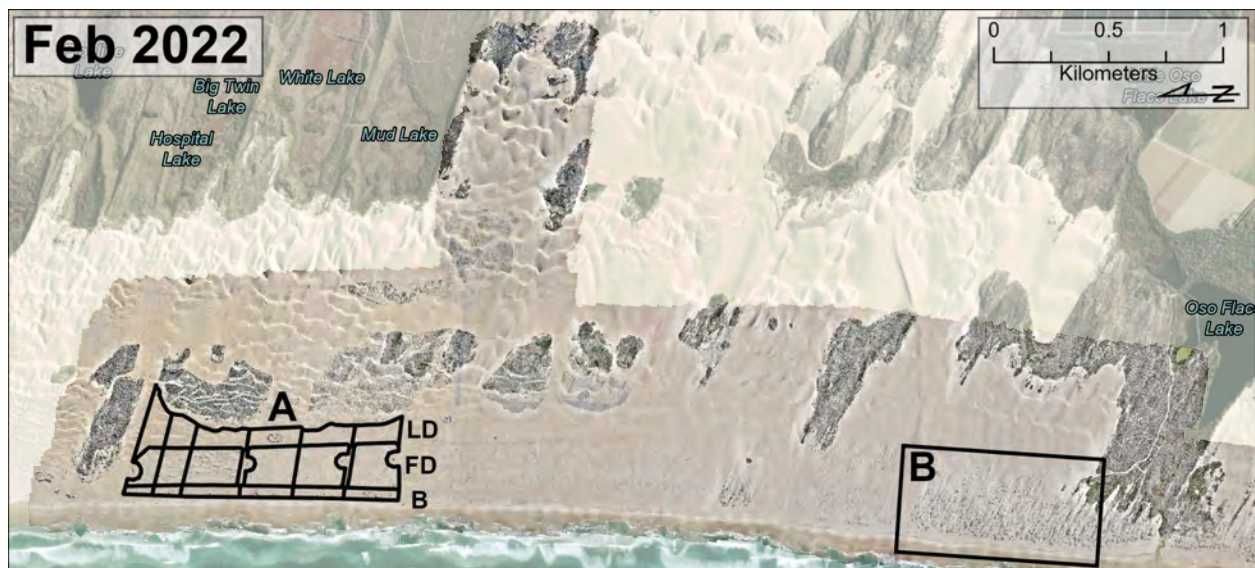
Figure 1. UAS orthophoto mosaic from Feb. 2022 showing the typical extent of the UAS mapping campaigns. North is oriented towards the left of the image. Box A shows the location of the six treatment plots, as well as the landward (LD) and beach (B) polygons. Box B shows the location or the reference plot, north of Oso Flaco Lake. All orthophotos are provided in Appendix A.

Successive DTMs are imported into the GCD toolset (Figure 2), developed by Riverscapes Consortium, which calculates volumes of change between collocated raster grid cells (pixels) and then applies a statistical filter to remove volumes of change that fall below a threshold uncertainty value with 95% confidence[7,8]. The threshold for realistically measurable change is determined by developing an uncertainty budget that includes the inherent accuracy of the GNSS station, the calculated uncertainty of the point cloud, and the root mean square error from the alignment of each point cloud with static features in the landscape. The uncertainty between two campaigns is propagated and pixels that exceed the minimum level of detection threshold (typically around 5 cm) are included. The results can be subset by specified units to monitor plot-based change over time.

Two multispectral sensors have been used: a Micasense RedEdge-MX (Oct. 2020 through Feb. 2022) and a Micasense RedEdge-P (Oct. 2022 through present). The RedEdge-MX features a 5-band camera payload that captures not only visual RGB, but also red edge (RE) and near-infrared (NIR) bands. The RedEdge-P contains the same five bands, but has an additional panchromatic (Pan) band that is used to improve the resolution of the dataset from ~7 cm/pix to ~3.5 cm/pix. Data from these payloads allow for improved vegetation extraction. A normalized difference vegetation index (NDVI) was created for each dataset, which was then thresholded to help extract vegetation from the surface (sand or straw) to quantify coverage across the treatment plots (Figure 3). NDVI expresses the difference between the reflectance values of NIR light (reflected strongly by plants) and red (R) light (absorbed by plants). NDVI values range from -1 to +1 and areas with dense vegetation will typically have positive values (~+0.3 to 0.8) while water surfaces or fog (that absorb both bands) will tend to have low positive to slightly negative values. Soil surfaces also tend to be characterized by small positive NDVI values (say 0.1 to 0.2), depending on color and moisture content.

---

[7] Wheaton, J. M., Brasington, J., Darby, S. E., & Sear, D. A. (2009). Accounting for uncertainty in DEMs from repeat topographic surveys: improved sediment budgets. Earth Surface Processes and Landforms, 35(2), 136-156. https://doi.org/10.1002/esp.1886

[8] Hilgendorf, Z., Marvin, M. C., Turner, C. M., & Walker, I. J. (2021). Assessing Geomorphic Change in Restored Coastal Dune Ecosystems Using a Multi-Platform Aerial Approach. Remote Sensing, 13(3), 354. https://doi.org/10.3390/rs13030354

Table 1. Collection specifications for the eight RGB UAS campaigns and the six multispectral (RGB, RE, NIR; RGB, RE, NIR, Pan) campaigns.

UAS Survey Campaign	Survey Date	Sensor Payload (spectral bands)	Coverage Area (km²)	Average Altitude (m)	Average Wind (m s⁻¹)
1: Baseline pre-restoration survey	Oct. 1-2, 2019	Sony RX1R II (42 MP, RGB)	3.83	114	7.00
2: Initial treatment installations	Feb. 10-11, 2020	Sony RX1R II (42 MP, RGB)	5.41	123	4.29
3: First post-treatment survey	Oct. 13-15, 2020	Sony RX1R II (42 MP, RGB)	5.98	121	4.16
	Oct. 16, 2020	Micasense RedEdge-MX (RGB, RE, NIR)	4.63	113	5.70
4: First year of treatment response	Feb. 17-18, 2021	Sony RX1R II (42 MP, RGB)	5.95	120	3.35
	Feb. 18-21, 2021	Micasense RedEdge-MX (RGB, RE, NIR)	5.79	118	6.68
5. Second growing season	Oct. 4-5, 2021	Sony RX1R II (42 MP, RGB)	5.98	121	1.83
	Oct. 5-7, 2021	Micasense RedEdge-MX (RGB, RE, NIR)	6.95	119	2.61
6. Second year of treatment response	Feb. 23-25, 2022	Sony RX1R II (42 MP, RGB)	7.56	112	3.13
	Feb. 25-26, 2022	Micasense RedEdge-MX (RGB, RE, NIR)	5.91	116	2.46
7. Third growing season	Oct. 17-18, 2022	Sony RX1R II (42 MP, RGB)	7.45	125	2.39
	Oct. 19-21, 2022	Micasense RedEdge-P (RGB, RE, NIR, Pan)	8.59	111	1.56
8. Third year of treatment response	Feb. 23, 2023	Sony RX1R II (42 MP, RGB)	4.64	121	3.04
	Feb. 20-21 2023	Micasense RedEdge-P (RGB, RE, NIR, Pan)	7.38	120	5.07
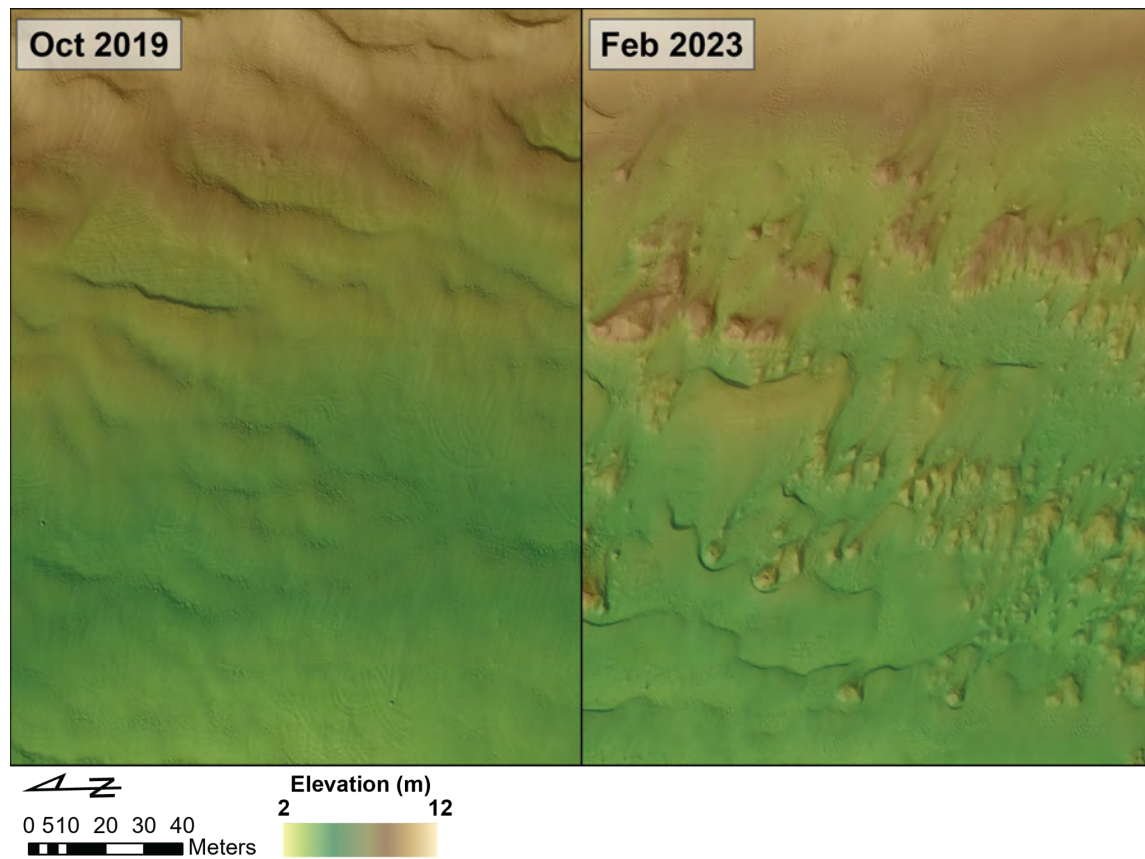
Figure 2. Example DTMs of from the Oct. 2019 and Feb. 2023 collection campaigns from treatment plot 3. The development of coalesced nebkha ridges are evident in the Feb. 2023 DTM. These differences are detected and quantified using the Geomorphic Change Detection toolset.
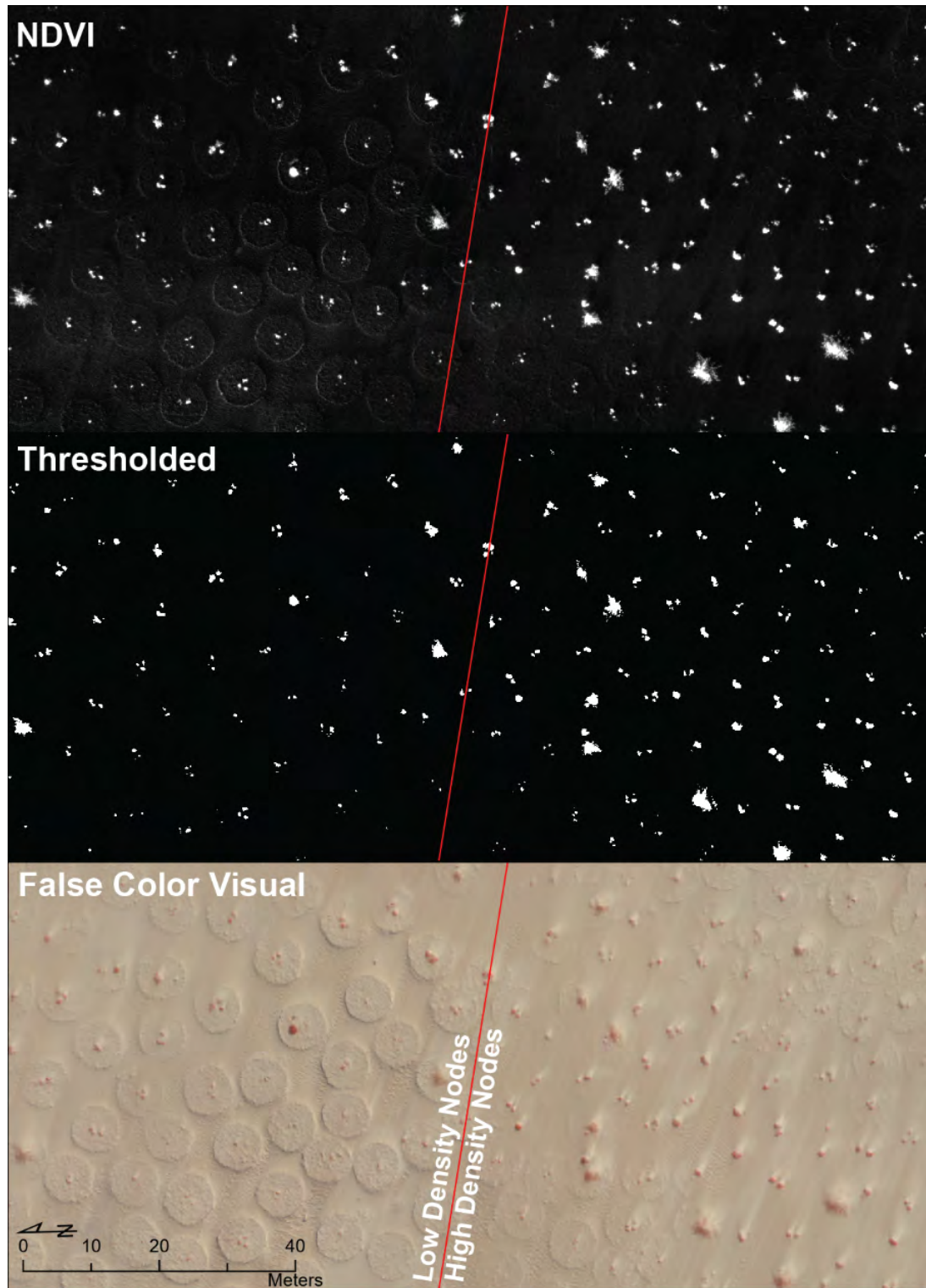
Figure 3. Example of the NDVI output, thresholded NDVI used to extract distinct vegetation pixels, and false color visual outputs (vegetation as red pixels) along the boundary of the low density planting node (treatment 4) and high density node (treatment 5) plots.

Table 2. SfM specifications for the RGB and multispectral UAS campaigns. GSD refers to the distance between the center of adjacent pixels and describes the cell size of each pixel in centimeters (i.e., pixel resolution). The RGB camera takes a single image per capture point, while the multispectral camera takes a picture in each band, hence the difference between RGB and multispectral images used. The Total Uncertainty column refers to the calculated vertical uncertainty for datasets used in DEM development and volumetric change detection mapping. As the multispectral datasets were not used for this purpose, a value of "NA" is shown.

UAS Survey Campaign	Survey Date	Images Used	GSD (cm/pix)	Total Uncertainty (m)
1. Baseline pre-restoration survey	Oct. 1-2, 2019	5,954	1.45	0.038
2. Initial treatment installations	Feb. 10-11, 2020	6,186	1.56	0.033
3. First post-treatment survey	Oct. 13-15, 2020	6,998	1.54	0.037
	Oct. 16, 2020	25,085	7.53	—
4. First year of treatment response	Feb. 17-18, 2021	7,312	1.52	0.030
	Feb. 18-21, 2021	57,315	7.89	—
5. Second growing season	Oct. 4-5, 2021	7,341	1.54	0.025
	Oct. 5-7, 2021	62,330	7.82	—
6. Second year of treatment response	Feb. 23-25, 2022	9,009	1.42	0.043
	Feb. 25-26, 2022	54,130	7.71	—
7. Third growing season	Oct. 17-18, 2022	8,554	1.66	0.026
	Oct. 19-21, 2022	93,366	3.67	—
8. Third year of treatment response	Feb. 23, 2023	5,950	1.59	0.034
	Feb. 20-21 2023	99,630	3.97	—

3. Results:

3.1. UAS visible (RGB) imagery and photomosaics

Figure 1 shows the typical extent of the eight (8) UAS visual (RGB) orthophoto campaigns between Oct. 2019 and Feb. 2023. Figures 4 and 5 show the UAS RGB orthophotos. The Feb. 2020 campaign included the collection of an eastward extending panhandle swath to monitor the rate of change of the landward dunes, and another eastward extent immediately north of Oso Flaco Lake and landward of more established foredunes. The Oct. 2020 campaign included the area between the southern landward extent and the eastern extent, south of the panhandle. The Feb. 2022 campaign included a flight south of Oso Flaco Lake to better understand how those dunes were developing. These changes were made to monitor restoration efforts and dune responses landward of the established foredune to the south, as an analog to compare against the foredune treatment plots to the north. In Feb. 2023 there was a smaller flight extent with the RGB sensor given challenging weather conditions and prioritization of the multispectral sensor, which was flown first and covered the entire domain.

The initial Oct. 2019 orthophoto mosaic represents the pre-restoration "baseline" of the site prior to any restoration treatments, which were implemented in Feb. 2020 as evident by the partial straw coverage in plots 5 and 6. The Oct. 2020 collection represents responses following the full first growing season, but also captures eight (8) months of park closure (no OHV activity) during the COVID-19 pandemic. The Feb. 2021 collection captures conditions after the first full year of plant growth and geomorphic response within the treatment plots. The Oct. 2021 collection represents the second full growing season. The Feb. 2022 collection captures the second full year of plant growth and geomorphic response. The Oct. 2022 collection represents the third full growing season. The Feb. 2023 collection captures the third year of plant growth and geomorphic response and represents the most recent collection at the site (see Appendix A for maps of the full extents of each flight).

3.2. UAS multispectral (RGB+RE+NIR+Pan) imagery and vegetation maps

To enhance the detection and monitoring of vegetation at the landscape scale in the restoration treatment areas, multispectral imagery collection was added, starting with the Oct. 2020 campaign (Figure 6). The Oct. 2020 collection primarily focused on the seaward extent of the site, including the foredune treatment zones, seasonal Western Snowy Plover exclosure, and established foredunes to the south near Oso Flaco Lake. The Feb. 2021 collection covered a larger extent to match that of the concurrent RGB campaign. Following Feb. 2021, nearly all collections matched the extent of the RGB collection (see Appendix A for maps of the full extents of each flight). All data are calibrated using a pre- and post-flight calibration panel so that, while the orthomosaics in Figure 6 may appear to have variable contrast, individual pixels are properly scaled so that the extracted indices are accurate.

NDVI indices were calculated for all multispectral datasets in order to detect pixels of vegetation cover from the imagery and monitor changes over time. After examining the histograms for each NDVI output, a threshold was used to remove pixels with high index values (representative of vegetation) (Figure 3). Results highlight a general increase in the percent vegetation cover (normalized by total treatment plot area) across all but the control plot 1 between Feb. 2020 (implementation) and Feb. 2023 (Figure 7, Table 3). Treatment 6 (broadcast straw + seedlings) exhibited the highest plant cover change, increasing from 2.5% in Oct. 2020 to 14.8% by Feb. 2023, followed by treatment 5 (high density nodes, 1.6 to 9.7%), treatment 3 (native seed + sterile grass seed, 2.7 to 8.9%), treatment 4 (low density nodes, 0.9 to 5.5%), and treatment 2 (native seed, 0.4 to 2.7%). Negligible vegetation cover has been observed in the control site 1 to date. Interestingly, most treatments showed a slight decline in plant cover over the most recent monitoring interval (Oct. 2022 - Feb. 2023). The cause of this decline is unknown, but could relate to an unusually wet and stormy winter and/or erosion along the seaward margins of the

plots. It is unclear if this downturn reflects a new equilibrium or plateau in the plant community, or simply just natural variability as the ecosystem continues to develop.
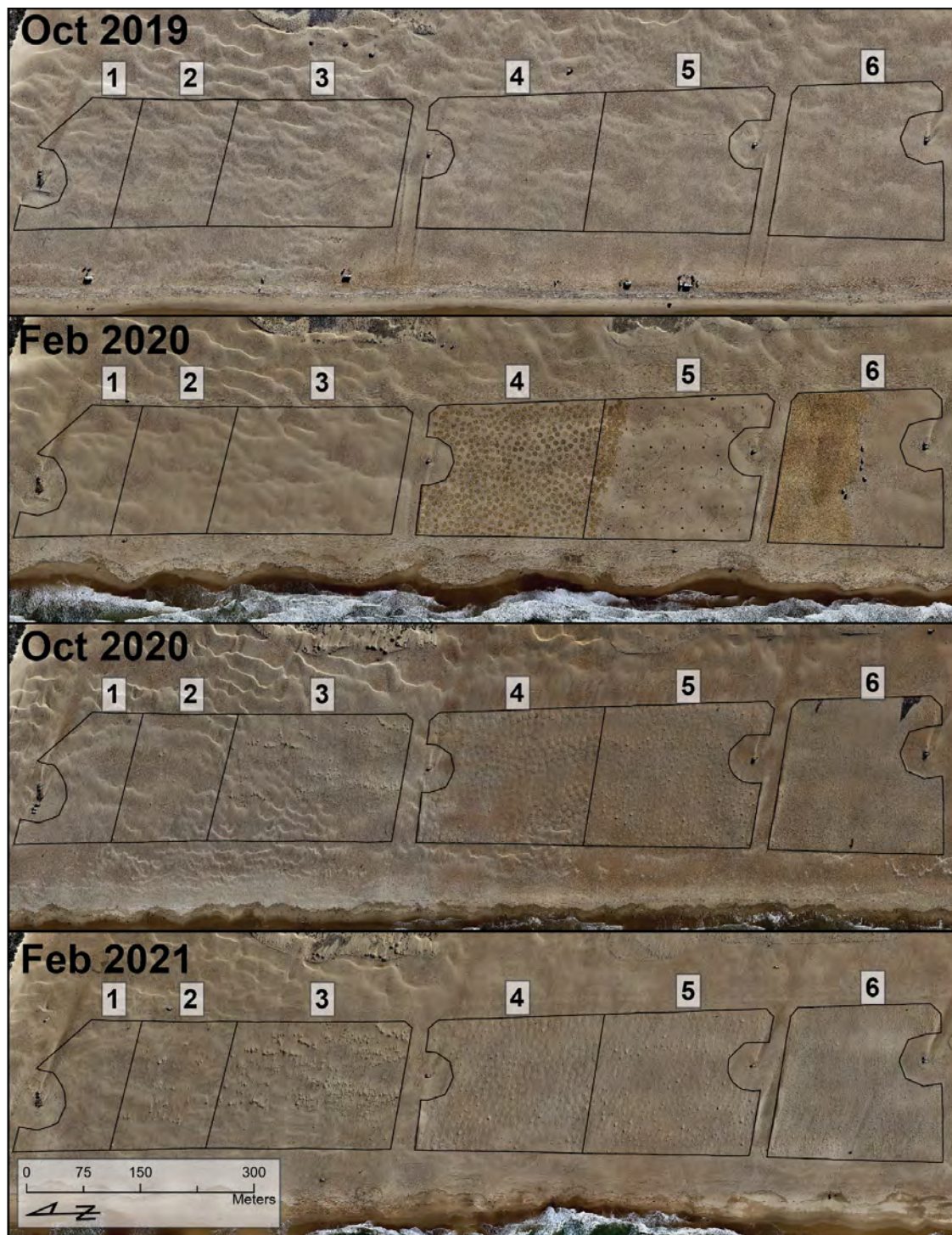
Figure 4. Foredune treatment plots as shown in the first four visible (RGB) UAS mapping campaigns (Oct. 2019, Feb. 2020, Oct. 2020, Feb. 2021). Numbers correspond to the following restoration treatments: 1) Sheepsfoot texturing only (control site), 2) native seeds, 3) native

seeds + sterile ryegrass seed, 4) low density straw planting nodes, 5) high density planting nodes, and 6) broadcast straw, randomly planted seedlings, and broadcast seed (aka "Parks Classic").

Figure 5. Foredune treatment plots from the second four visible (RGB) UAS mapping campaigns (Oct. 2021, Feb. 2022, Oct. 2022, Feb. 2023). Numbers correspond to the following restoration treatments: 1) Sheepsfoot texturing only (control site), 2) native seeds, 3) native seeds + sterile

ryegrass seed, 4) low density straw planting nodes, 5) high density planting nodes, and 6) broadcast straw, randomly planted seedlings, and broadcast seed (aka "Parks Classic").
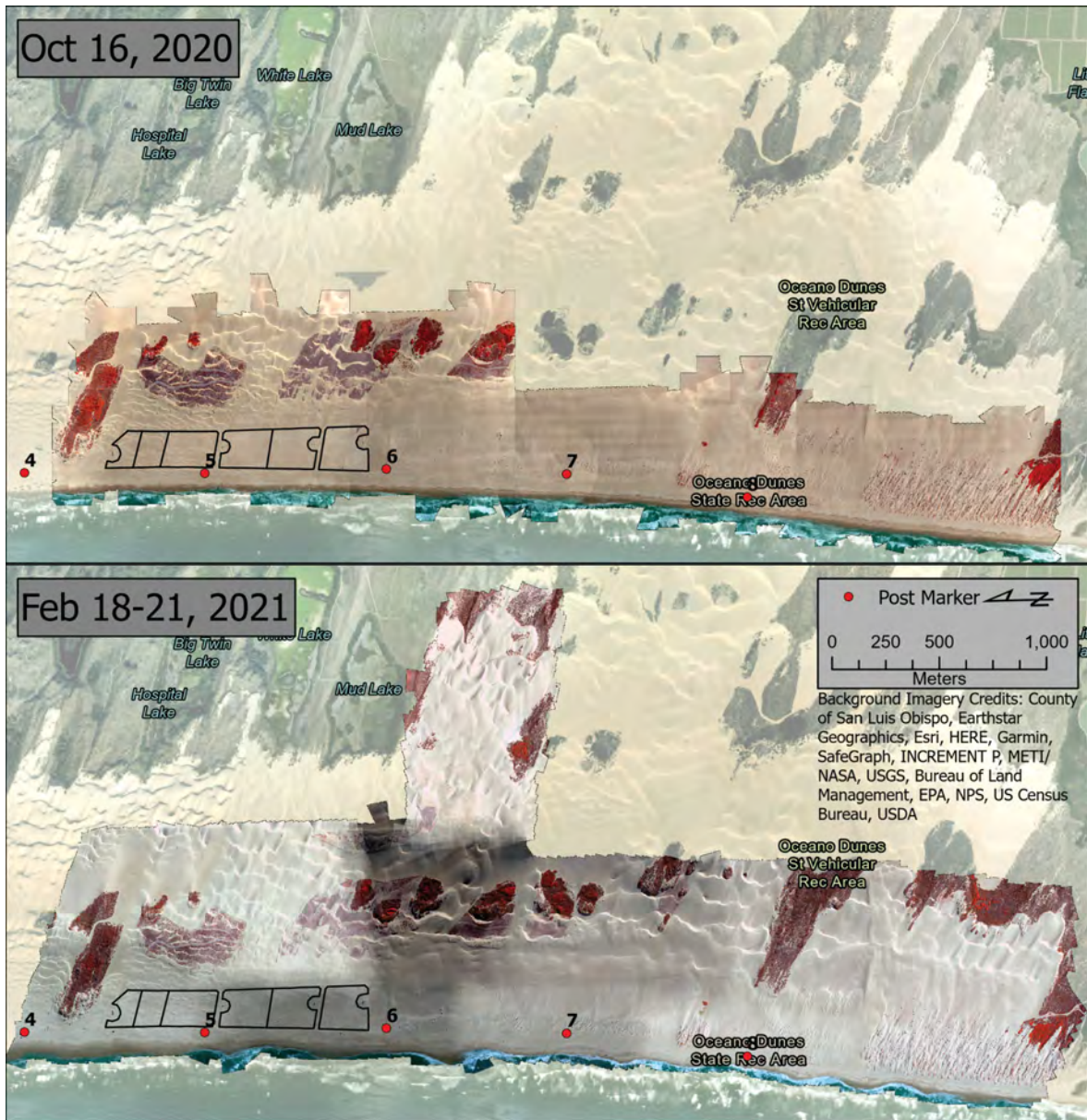
Figure 6. Examples of multispectral false-color (G+B+NIR) UAS orthomosaics captured from a Micasense RedEdge-MX 5-band sensor (R, G, B, RE, NIR) used to map vegetation cover for the first two collection campaigns. Contrast differences are only visual and do not impact the indices calculated from the values of compared bands. Remaining images are provided in Appendix A.
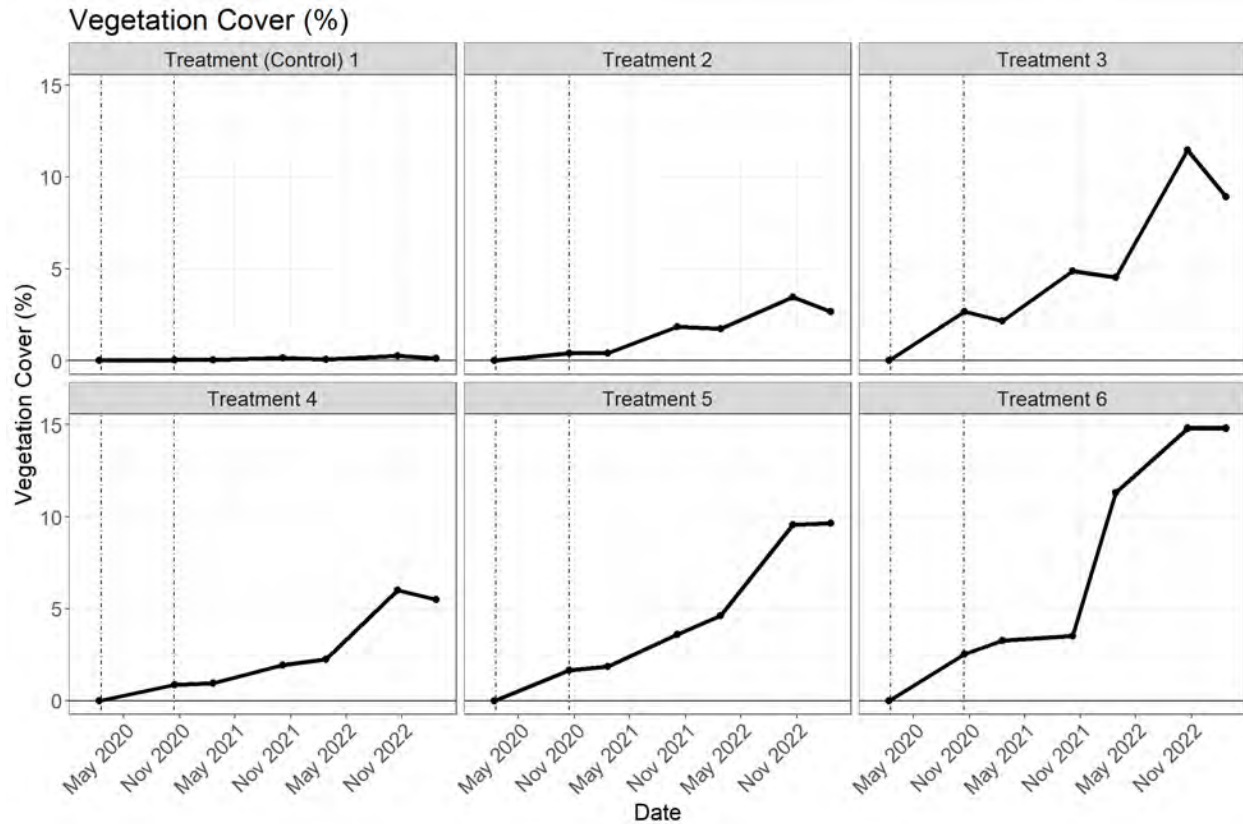
Figure 7. Line graph showing changes in percent cover of vegetation per treatment plot (as described in Figure 5) derived from the multispectral UAS datasets since implementation in Feb. 2020 through to Feb. 2023.

	Plot 1	Plot 2	Plot 3	Plot 4	Plot 5	Plot 6	Total
Feb-20	0.00	0.00	0.00	0.00	0.00	0.00	0.00
Oct-20	0.02	0.41	2.66	0.87	1.65	2.54	1.60
Feb-21	0.02	0.50	2.66	1.08	2.08	4.02	2.05
Oct-21	0.14	1.85	4.87	1.93	3.63	3.54	3.02
Feb-22	0.08	1.74	4.55	2.24	4.64	11.35	4.82
Oct-22	0.26	3.45	11.47	6.03	9.57	14.82	8.85
Feb-23	0.12	2.68	8.93	5.52	9.66	14.83	8.18

Table 3. Vegetation cover percentage (%) per treatment plot as shown in Figure 7. The Total values represent the plant coverage for each interval as a percentage of the entire restoration site area (plots 1 - 5).

At this point, vegetation cover estimates derived from the UAS campaigns do not identify particular plant species, only the presence/absence of plant cover. Coordination with CDPR vegetation transect monitoring datasets, coupled with ground truthing of distinct species against corresponding imagery and multi-spectral signatures, is recommended to improve species-level identification and track plant community changes over time.

For context, the historic vegetation cover observed in aerial imagery back to 1939 in the area of the restoration plots reached a maximum of 3.3% in 1949 and then declined to essentially zero (0) cover by 1985 (see report by Swet et al. 2022, UCSB Historical Vegetation Cover Change Analysis (1930-2020) within the Oceano Dunes SVRA). Since 1985, there was no detectable increase in plant cover at the foredune restoration site until after implementation of the restoration treatments in 2020 (Figure 8). Following restoration, plant cover increased from 0% in Feb. 2020 to about 8.18% (as averaged across treatment plots 2-6) by Feb. 2023 (Figure 8A, Table 3).

While the specific location of the foredune restoration site has historically been relatively sparsely vegetated, the rest of the foredune zone (~400 m inland from the shoreline) within the ODSVRA ranged from ~1.4% in 1939, over 10% by 1966, and up to 20% in 2010. Plant cover was even higher in more established, less disturbed foredunes at north and south Oso Flaco locations, reaching up to 25.6 and 36.2%, respectively (Figure 8B). It is important to state, however, that the Oso Flaco areas and other areas in the ODSVRA (e.g., Pavilion Hill) have hosted varying amounts of invasive species and, therefore, plant cover in those areas might be higher than expected in natural conditions.
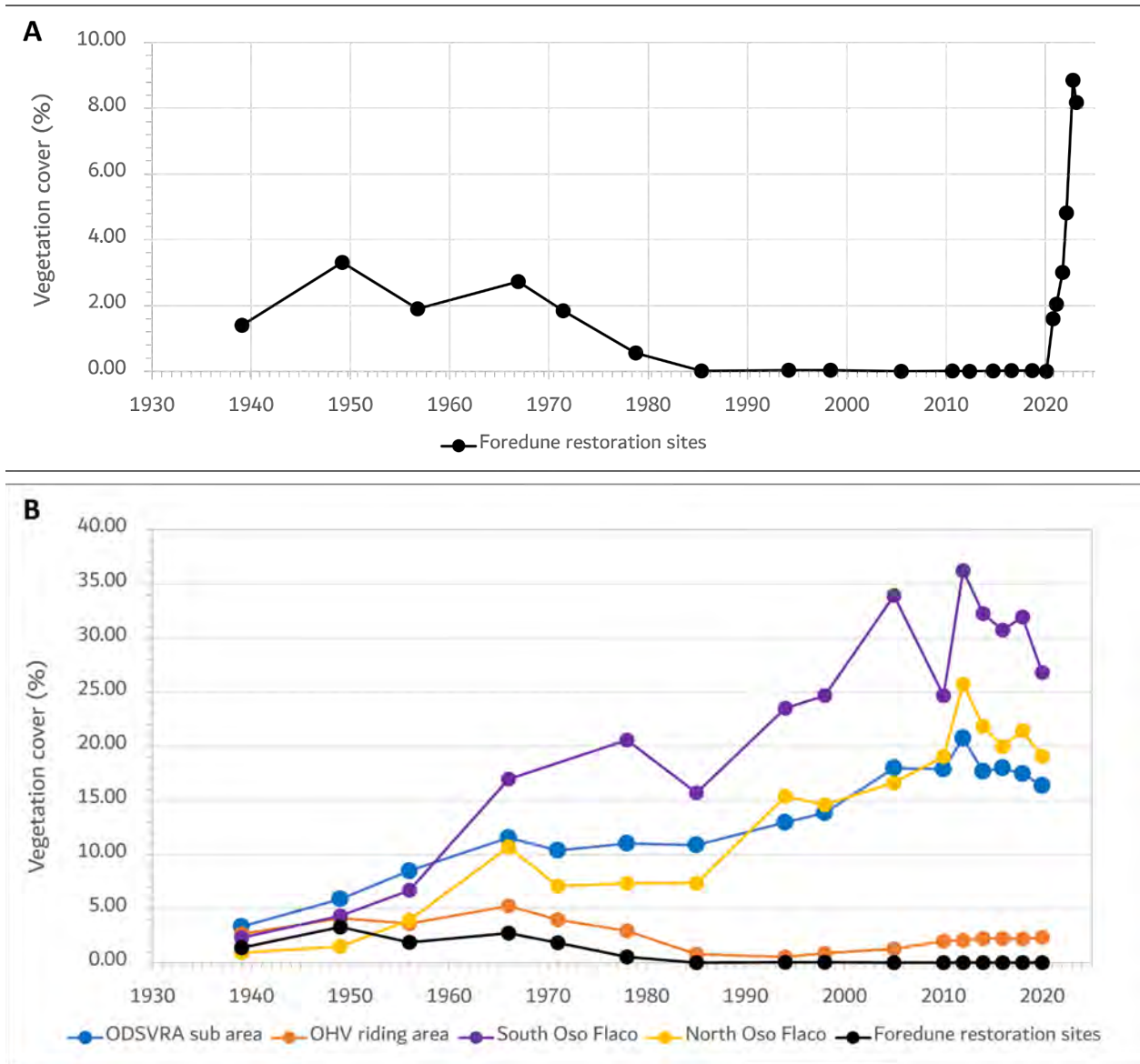
Figure 8. A) Plant cover within the foredune restoration zone between Feb. 1939 and Feb. 2023. Recent vegetation cover since Feb. 2020 were derived from the UCSB multispectral UAS datasets. B) Plant cover in the foredune zones of the broader ODSVRA (blue), the OHV riding area (orange), South Oso Flaco (purple), North Oso Flaco (yellow), and foredune restoration zone specifically (black) from 1939 to 2020. See UCSB Historical Vegetation Cover Change Analysis (1930-2020) within the Oceano Dunes SVRA (Swet et al., 2022).

3.3. Topographic Differencing and Volumetric Change Trends

Repeat DTMs derived from the UAS imagery are compared through time using spatial statistics to detect pixels of statistically significant elevation change (topographic differencing) and

corresponding geomorphic changes (Figure 2). The resulting GCD change maps (Figures 9, 10) show areas and quantities of significant change that are then used to calculate volumes of sediment erosion or deposition between surveys in cubic meters (m^3) or normalized by area (m^3 m^{-2}), which is effectively an average depth of change (m) over the entire area. The raster grid positioning and size (0.10 x 0.10 m) is fixed across all surveys, so the volume estimates are determined by changes in depth above/below the grid. Pixels of insignificant change are not shown in the resulting change detection maps (i.e., they are transparent) and are not used to calculate sediment volumes, but they are included in the uncertainty estimates for each interval.

Quantities of surface elevation (normalized volume) change can be used to identify and interpret dune development and evolution, erosion/deposition patterns, and sediment budgets for the restoration treatments and other areas within ODSVRA. Typically this is done by identifying distinct zones (e.g., the foredune treatment polygons) and interpreting changes relative to upwind beach areas, which provide sand supply, and inland dunes downwind/landward of the foredune treatments.

Figures 9 and 10 show the GCD maps for each survey interval between Oct. 2019 and Feb. 2023 with corresponding pixels of significant elevation (normalized volume) change. Foredune treatment polygons are identified as well as adjoining beach and inland backdune areas for each treatment plot. The first interval (Oct. 2019 to Feb. 2020) characterizes a baseline reference condition prior to implementation of the restoration treatments. The second interval (Feb. 2020 to Oct. 2020) shows the response of the treatments to the initial installation, first wind season, and first plant growth season. The third interval (Oct. 2020 to Feb. 2021) shows the responses associated with the first winter season (plant dormancy, increased rainfall and storms). The fourth (Feb. 2021 to Oct. 2021), fifth (Oct. 2021 to Feb. 2022), sixth (Feb. 2022 to Oct. 2022), and seventh (Oct. 2022 to Feb. 2023) intervals show the second and third growing seasons, as well as the second and third full years of development of the treatment plots.

To date, three (3) full years (Feb. 2020 to Feb. 2023) of geomorphic and sediment volume changes have been observed following restoration. As in Figures 9 and 10, the restoration treatments each exhibited different signals of geomorphic response and sediment volume change over this interval. Figure 11 and Table 4 provide a time series of normalized volumetric changes for each geomorphic unit.

One of the key controls on the sedimentation response of all treatments is the amount of sand that enters the upwind beach, which effectively provides the incoming supply of sand that could enter the treatment by aeolian transport between survey intervals. The beach units fronting

each of the restoration plots saw alternating natural cycles of positive and negative sediment volumes. Generally, the beach units fronting all of the restoration treatment plots have shown a declining trend, albeit variable, in sand volume inputs from positive values in the initial Oct. 2019 to Feb 2020 baseline interval to negative values by Feb. 2023. Beach erosion (deficit) patterns, shown as red, are evident in the GCD maps across the various sites and change detection intervals in Figures 9 and 10. Beach sand declines are most pronounced in front of treatment plots 1-3, particularly in the most recent Oct. 2022 to Feb. 2023 interval. This corresponds to pronounced beach erosion and cuspate rip current embayments that occurred during the stormy winter of 2022-23.

Two trends are prevalent within the restoration plots to date. Plots 1-3 exhibited positive budgets in the first couple of intervals, transitioning to neutral/negative from Oct. 2019 to Feb. 2021, neutral/positive from Feb. 2021 to Feb. 2022, and widespread erosion (net negative) in the latest two intervals (Oct. 2022 to Feb. 2023). Accordingly, the foredune unit for treatment plots 1/control and 2 showed some of the lowest rates of accumulation, suggesting that most sediment is bypassing the treatment zone and/or supply into the treatment plots declined. Plots 4-6 followed a similar progression of alternating depositional and erosional phases with one key difference: none of these southern three plots experienced the magnitude of erosion recorded by the three northern beach plots.

Plots 1 (control) and 2 (native seed) were the least altered by vegetation-induced sedimentation and maintained similar change patterns across all intervals. Sand transport in these plots generated low-lying (0.4-0.6 m), slowly migrating semi-continuous transverse and barchanoid dune ridges and protodunes. Negligible plant cover established in the control plot 1, except for a small amount near the seaward edge of the plot observed in Oct. 2022. Some shadow dunes were present in the landward half of these plots, but these were not nebkha as they were initiated by nodes of cemented sand and anthropogenic debris and not vegetation. Plot 2 exhibited a developing nebkha cluster within the center of the plot, but this did not expand appreciably by Feb. 2023. These two plots recorded the smallest net change between Oct. 2019 and Feb. 2023 (plot 1 = 0.121 $m^3 m^{-2}$; plot 2 = 0.092 $m^3 m^{-2}$).

Treatment plot 3 (native seed + sterile rye grass seed) developed significantly through seed germination, subsequent plant growth, and nebkha development, predominantly with *Abronia latifolia*. Nebkha dunes quickly coalesced to form ridges now over 2 m tall - the largest dunes across all of the treatment plots to date. This plot exhibited the highest normalized volumetric change per month across all treatments in the first year following installation (Oct. 2020 to Feb. 2021). Net sediment volume change has remained positive across all intervals and experienced

the second largest depositional interval (Feb. 2022 to Oct. 2022, 0.122 m^3 m^{-2}) and second greatest net deposition to date (Oct. 2019 to Feb. 2023, 0.285 m^3 m^{-2}).

Treatment plots 4 and 5 (low and high density straw planting nodes) were established by estimating the plant density and shadow dune coverage for more established nebkha fields to the south in both the seasonal Western Snowy Plover exclosure as well as in the north Oso Flaco foredune area. The two different densities are comparable to the spacing of earlier stage (treatment 4) and more developed nebkha foredunes (treatment 5), respectively, although without the associated depositional topography on installation. In the first interval following installation (Feb. 2020 to Oct. 2020) erosion occurred in plot 4 due to the development of erosional streets between the planting circles and these features persist, although nebkha are growing and slowly coalescing. As with many other plots, the Feb. 2022 to Oct. 2022 interval featured the greatest deposition for plot 4 (0.090 m^3 m^{-2}). This plot also has the fourth highest net positive budget (0.189 m^3 m^{-2}) to date. Nebkha dunes in plot 5 were larger than in the neighboring plot 4 and closer in height to the larger dunes in treatment 3, with some dunes over 1.5 m tall. Erosional streets and erosion upwind of the straw circles was not as common as in plot 4. Plot 5 has the third largest net positive budget (0.214 m^3 m^{-2}) to date.

Treatment 6 (broadcast straw + native seeds + plant seedlings) had the highest planting density and complete surface straw cover on installation. It maintains the highest plant coverage post-installation (Figure 7, Table 3) but, despite this, large nebkha are not developing in this plot, compared to plots 3-5. This said, plot 6 has shown consistent accretion with high deposition along the windward margins adjoining the beach and on the border to the north on the transportation corridor, which was lined with sand fencing for most of the observation period. The sand fence promotes appreciable drift development immediately downwind in the treatment plot, which does not technically reflect the effectiveness of the restoration treatment itself. The same fence-drift pattern is also observed on the north fence line of treatment 4. Treatment 6 consistently featured the greatest deposition between plots, with the highest recorded deposition (0.135 m^3 m^{-2}) during the Feb. 2022 to Oct. 2022 interval and overall greatest net positive sediment budget (0.343 m^3 m^{-2}) to date.
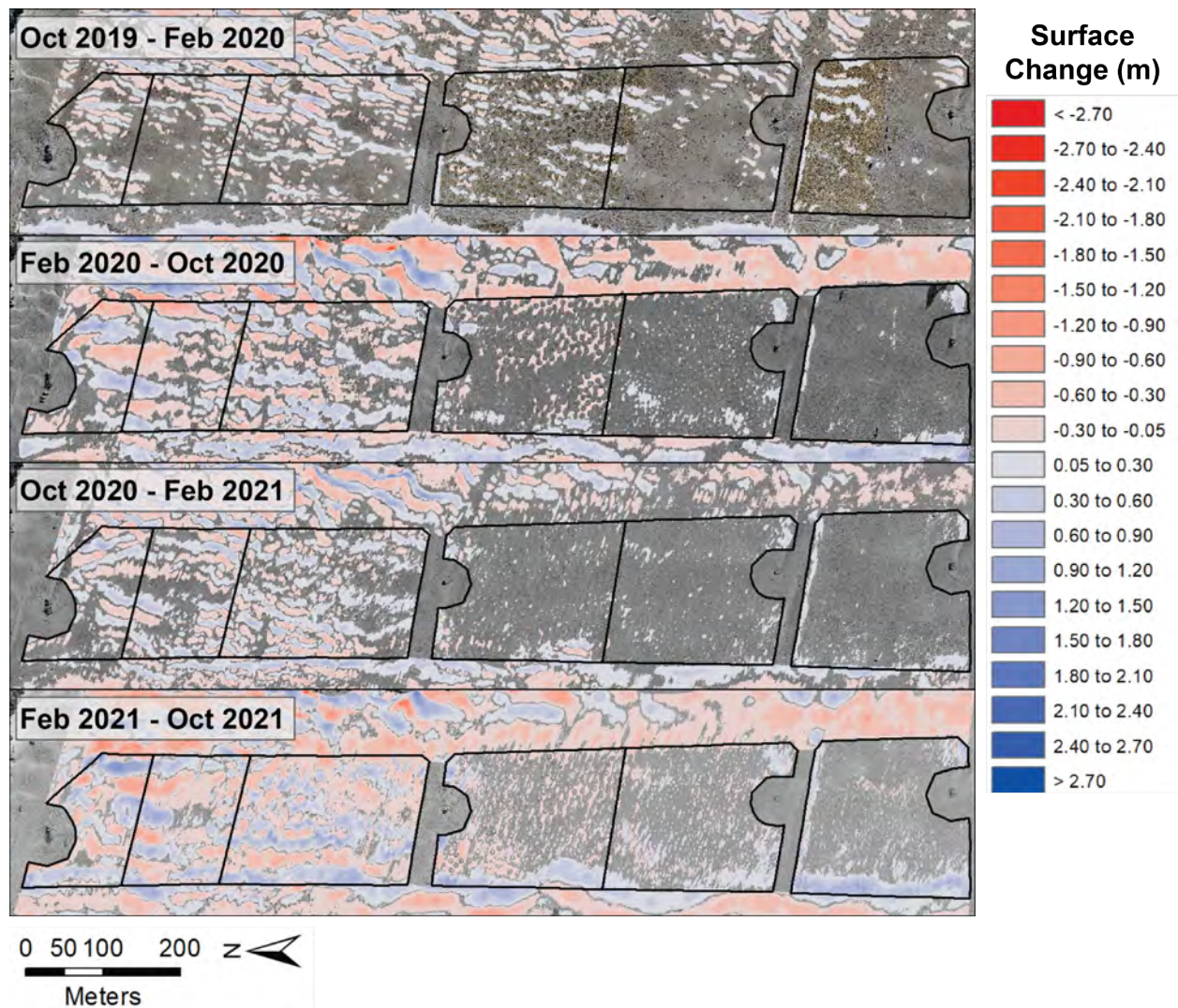
Figure 9. GCD maps with corresponding pixels of significant elevation change (reds = erosion, blues = deposition, insignificant change = transparent) for each survey interval between Oct. 2019 and Oct. 2021 overlain on the UAS photomosaics for the second time step in each interval. Foredune treatment polygons are outlined and numbered. Intervening transportation corridors, between plots 3 and 4, and 5 and 6, are not included in the analysis. Also included are the beach and landward backdune zones adjacent to each treatment plot.
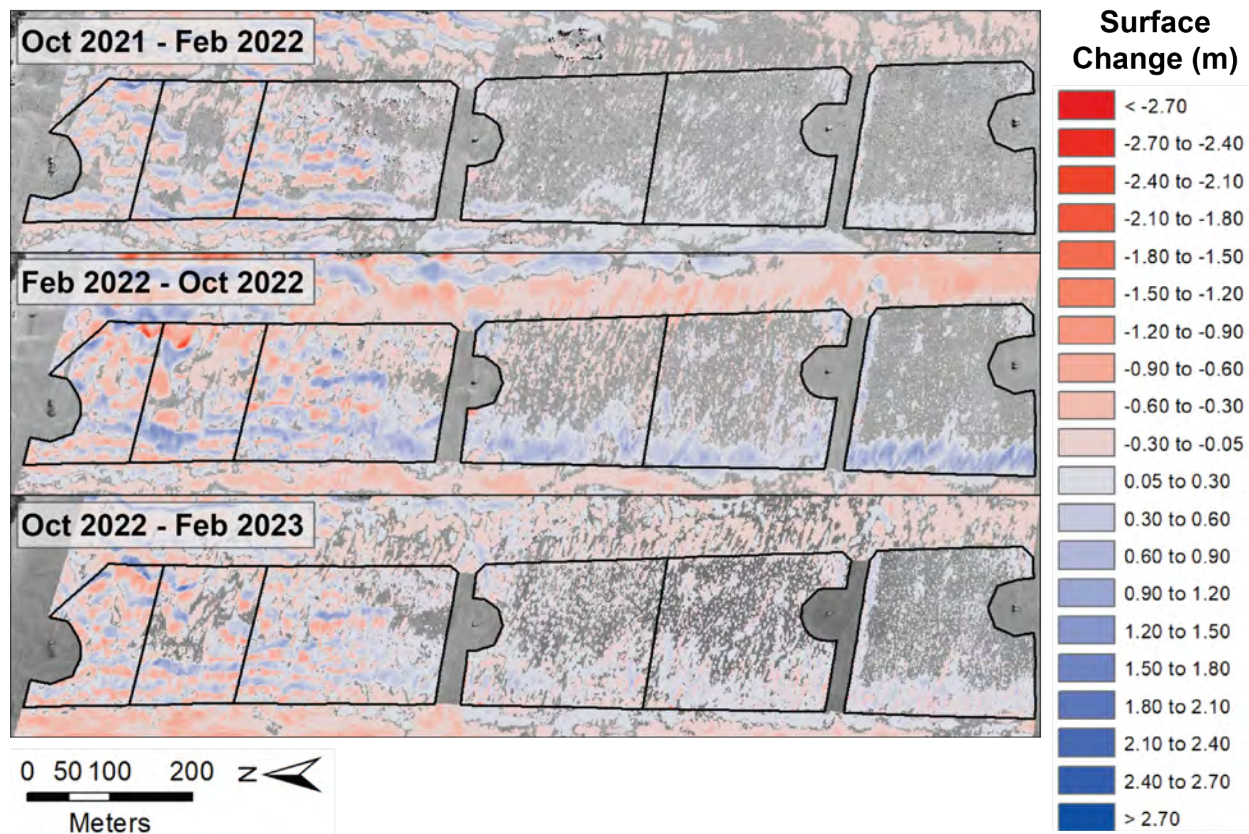
Figure 10. GCD maps with corresponding pixels of significant elevation change (reds = erosion, blues = deposition, insignificant change = transparent) for each survey interval between Oct. 2021 and Feb. 2023 overlain on the UAS photomosaics for the second time step in each interval. Foredune treatment polygons are outlined and numbered. Intervening transportation corridors, between plots 3 and 4, and 5 and 6, are not included in the analysis. Also included are the beach and landward backdune zones adjacent to each treatment plot.

Table 4. Normalized surface volumetric changes for the foredune treatment plots (FD, bold values) and adjoining beach (B) and landward dune (LD) zones. Blue cells indicate sand accumulation, red cells show erosion. The net change column represents change between the baseline (Oct. 2019) and most recent (Feb. 2023) intervals. Uncertainty values associated with individual measurement campaigns are provided in Table 2.

		Normalized Volumetric Change by Total Area (m³ / m²)							
Treatment Plot	Landscape Zone	Oct 2019 – Feb 2020	Feb 2020 – Oct 2020	Oct 2020 – Feb 2021	Feb 2021 – Oct 2021	Oct 2021 – Feb 2022	Feb 2022 – Oct 2022	Oct 2022 – Feb 2023	*Net Change (Oct 2019 – Feb 2023)*
Sheepsfoot (1)	B	0.075	-0.013	-0.045	-0.037	0.070	-0.050	-0.371	*-0.378*
	FD	**0.002**	**0.006**	**0.018**	**0.070**	**0.039**	**0.030**	**-0.027**	***0.121***
	LD	-0.004	0.020	0.024	-0.025	0.002	-0.010	0.007	*-0.002*
Sheepsfoot+ Seed (2)	B	0.050	0.052	0.005	0.016	-0.001	-0.039	-0.351	*-0.275*
	FD	**0.005**	**-0.014**	**0.022**	**0.019**	**0.035**	**0.021**	**0.024**	***0.092***
	LD	0.008	0.050	0.020	-0.017	-0.012	0.025	0.038	*0.100*
Sheepsfoot+ Seed+Rye (3)	B	0.088	0.043	0.017	-0.036	0.075	-0.137	-0.272	*-0.230*
	FD	**0.012**	**0.008**	**0.027**	**0.054**	**0.034**	**0.122**	**0.043**	***0.285***
	LD	0.010	-0.039	0.029	-0.010	0.017	-0.069	0.017	*-0.066*
Low Density (4)	B	0.155	0.096	-0.029	-0.025	0.053	-0.118	-0.050	*0.087*
	FD	**0.017**	**-0.016**	**0.010**	**0.033**	**0.021**	**0.090**	**0.031**	***0.189***
	LD	0.004	-0.104	-0.002	-0.103	0.000	-0.069	0.004	*-0.296*
High Density (5)	B	0.148	-0.008	0.026	-0.017	0.066	-0.020	-0.081	*0.157*
	FD	**0.008**	**0.008**	**0.006**	**0.023**	**0.016**	**0.087**	**0.034**	***0.214***
	LD	-0.005	-0.147	0.005	-0.104	0.000	-0.167	-0.021	*-0.483*
Parks Classic (6)	B	0.068	0.188	-0.058	-0.071	0.030	-0.069	-0.002	*0.098*
	FD	**0.010**	**0.016**	**0.013**	**0.083**	**0.018**	**0.135**	**0.033**	***0.343***
	LD	-0.003	-0.172	-0.013	-0.168	-0.020	-0.221	-0.037	*-0.693*
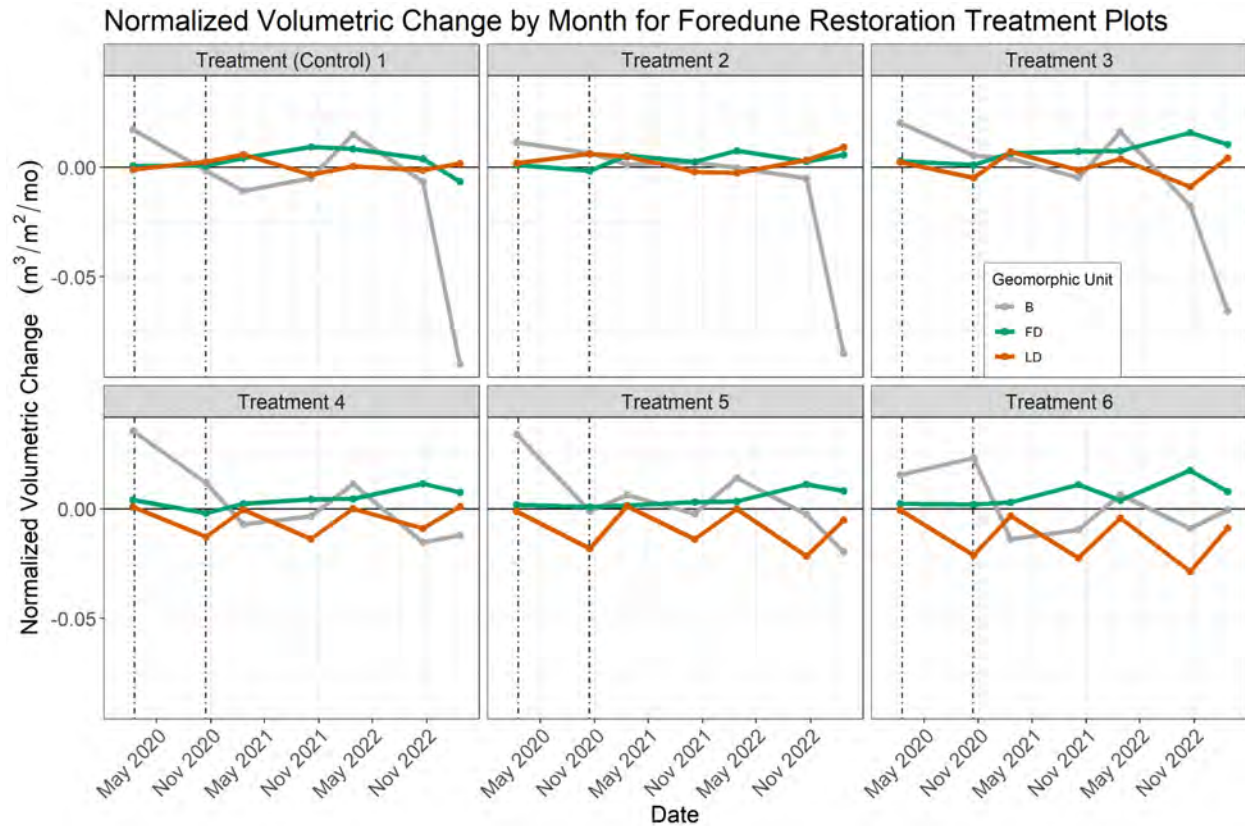
Figure 11. Time series of normalized volumetric changes (total volumetric change divided by total plot area divided by months between collections) derived by successive change intervals for each restoration treatment plot. Responses are shown for the foredune (FD), adjacent beach (B), and landward dune (LD) landscape units. Each point on the plot represents net results of volumetric change for the preceding interval (e.g., the first point represents net change between Oct. 2019 and Feb. 2020, etc.). Dashed lines delimit the COVID-19 closure period (March 2020 through Oct. 2020).

Generally, changes in the inland (eastern) dune units for all treatments are somewhat decoupled from those within the upwind foredune treatment plots due to the influence of OHV traffic and landscape scale secondary flow patterns that are generated by larger dunes (e.g., Pavilion Hill or larger barchanoid and transverse dunes). However, there are two primary groups of response in these units downwind of the treatment plots. Areas downwind of treatment plots 1-2 do not exhibit seasonally alternating (peak-valley) trends, whereas areas downwind of plots 3-6 all exhibit this trend, perhaps in response to the combined accretionary effects of the plant growth and wind/sand transport seasons within the upwind treatment plots. For instance, the inland dunes downwind of plot 3 alternated between positive budgets in each of the Oct. to Feb. (winter) intervals and negative budgets during the Feb. to Oct. (wind/plant growth) intervals where more sediment would be accreting in the upwind restoration plots. The trend of this cycle is predominantly neutral to slightly negative in treatment plots 4-6. In plot 6, the trend

26

has become increasingly negative. Net budgets were most negative for the southern three inland dune units (treatment 6 = -0.693 $m^3 m^{-2}$; treatment 5 = -0.483 $m^3 m^{-2}$; treatment 4 = -0.296 $m^3 m^{-2}$).

4. Discussion

4.1. Geomorphic and Sand Volume Change Trends

Geomorphic change within the treatment plots showed both seasonal and treatment-related responses. In addition to seasonal changes related to variations in moisture/precipitation (a supply-limiting factor, highest in winter months) and the frequency of transporting winds (a transport-limiting factor, highest in April through June), two other key factors control the variability in treatment responses over time, including: 1) variations in sand supply to the beach (inputs to the system), and 2) the extent of modifications of the treatments and their related influence on vegetation development and sand accretion.

The absolute volumes of sand inputs to the beach fronting the restoration plots differ (Figures 11, 12, Table 4) and have generally declined to negative values in recent observation intervals. Area-normalized volumes were variable but comparable across the treatment sites until this most recent winter interval (Figure 11, Oct. 2022 to Feb. 2023), during which the beach saw increasingly negative budgets from south to north. As of Feb. 2023, plots 1 through 3 had significant deficits in sand supply to the beach, which could have implications (i.e., reductions) for future sand supply to the adjoined foredune treatments in these areas. Since installation of the treatments in Feb. 2020, only foredune plots 4, 5 (greatest overall), and 6 have experienced net gains in sand volume, while plots 1 through 3 have seen net deficits. Despite this, all adjoining foredune restoration treatments (plots 2-6) have maintained net positive sediment budgets, while the control site (1) switched to a deficit in this most recent interval.

Seasonal establishment and movement of rip current embayments and consequent narrowing of beach width is common in the winter months (see Feb. imagery in Figures 4 and 5). These embayments and narrower beaches generally persist into the late spring when the wind season begins and, as a result, they can limit available fetch for aeolian transport and subsequent sand delivery into the foredune treatment plots. Such sand supply variations can have an appreciable and variable impact on geomorphic and sediment budget responses of the foredune treatments at this scale of observation. Seasonal to interannual variations, as well as other beach erosion events, such as those that occur during El Niño seasons, are natural, difficult to predict, and should be considered accordingly during interpretation of restoration responses and future adaptive management decisions. It is also quite likely that the response signals of the foredune

treatment plots lag behind the periods of decreased beach sand supply, but this is difficult to assess at this (biannual) scale of observation.
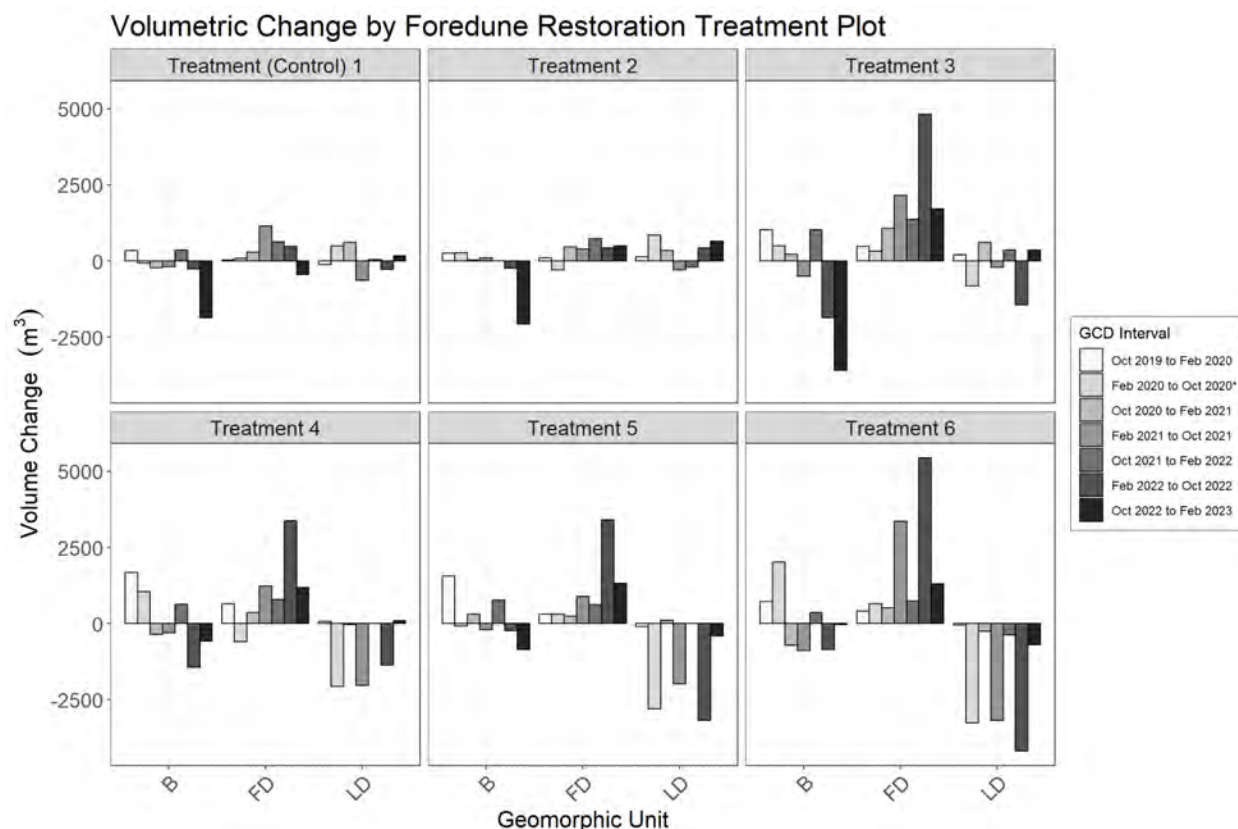
Figure 12. Bar graph of observed volumetric changes (m³) within the beach (B), foredune restoration plot (FD), and landward dunes (LD), for each treatment, across each GCD interval. Asterisk in the legend indicates the Feb. 2020 to Oct. 2020 COVID-19 closure period that occurred between Mar. and Oct. of 2020.

In the inland dune polygons downwind from the foredune restoration plots, the erosion/deposition trends are somewhat decoupled from the foredune and beach units for two main reasons. First, OHV traffic in the corridor behind the restoration plots has remained active, except for during the Mar. 2020 to Oct. 2020 COVID-19 closure. OHV traffic can displace sediment over time on beaches, modify or disrupt sand supply from beaches to landward foredunes, reorganize pre-existing dunes and protodunes, and enhance localized erosion[9,10].

---

[9] Defeo, O., McLachlan, A., Schoeman, D. S., Schlacher, T. A., Dugan, J., Jones, A., Lastra, M., & Scapini, F. (2009). Threats to sandy beach ecosystems: A review. Estuarine, Coastal and Shelf Science, 81(1), 1–12. http://dx.doi.org/10.1016/j.ecss.2008.09.022

[10] Houser, C., Labude, B., Haider, L., & Weymer, B. (2013). Impacts of driving on the beach: Case studies from Assateague Island and Padre Island National Seashores. Ocean & Coastal Management, 71, 33–45. http://dx.doi.org/10.1016/j.ocecoaman.2012.09.012

Second, as dunes evolve and protrude more into the atmospheric boundary layer, their roughness generates secondary flow patterns downwind that can have appreciable influence on shear stress, sand transport, and dune form[11,12]. At some length downwind, varying typically from 4-10 dune heights (for continuous dune ridges, not nebkha) wind flow reattaches to the surface and velocity increases (known as the flow separation zone). Within 30-100 dune heights downwind, turbulence and surface shear stress approach upwind values[13]. Thus, there is often a downwind 'sheltering' (i.e., shear stress reduction) effect immediately within the separation zone behind dunes that should experience reduced sand transport and dust emissions. Therefore, the restored foredune is expected to have dust emission mitigation effects that extend further downwind beyond the treatment area itself. Downwind of the separation zone, as the boundary layer redevelops and other deflected flow patterns converge, transport of fine-grained sands and surface deflation (erosion and lowering) can occur and coarsening and armoring of this downwind zone is possible on undisturbed surfaces over time. In situations where replenishment of fine particles to the surface is limited, progressive coarsening can make the entrainment of fines more difficult over time.
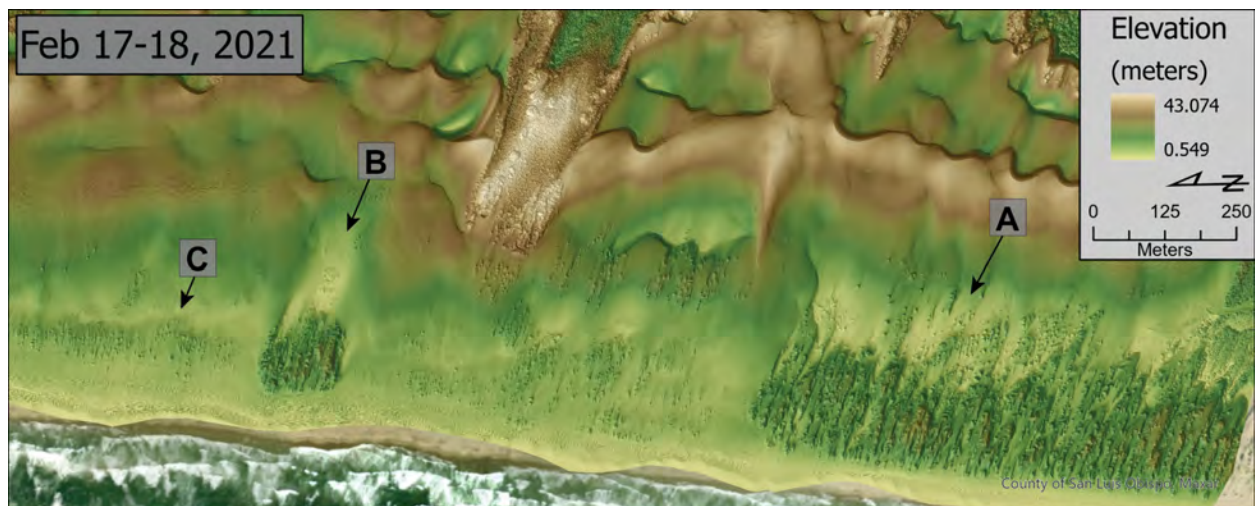
Figure 13. DTM from the Feb. 2021 UAS campaign located south of the foredune restoration plots near the Oso Flaco foredune reference site. Elevations range from 0.55 m (1.8 ft) to 43 m (141 ft) above sea level in the landward dunes. Downwind (leeward) deflation plains are

---

[11] Walker, I. J., & Hesp, P. A. (2013). 11.07 Fundamentals of Aeolian Sediment Transport: Airflow Over Dunes. In Treatise on Geomorphology, ed. J. F. Shroder, 109–133. Elsevier https://linkinghub.elsevier.com/retrieve/pii/B9780123747396003006

[12] Walker, I. J., & Shugar, D. H. (2013). Secondary flow deflection in the lee of transverse dunes with implications for dune morphodynamics and migration. Earth Surface Processes and Landforms, 38(14), 1642–1654. https://doi.org/10.1002/esp.3398

[13] Walker, I.J., & Nickling, W.G. (2002). Dynamics of secondary airflow and sediment transport over and in the lee of transverse dunes. Progress in Physical Geography, 26(1), 47-75. https://doi.org/10.1191%2F0309133302pp325ra

common behind dune topography as seen at A) leeward of the northern Oso Flaco foredune complex, B) leeward of the "7.5 Reveg" plot, and C) leeward of the nebkha field within the bird nesting exclosure. Figure 4 includes an inset box (A), to highlight the extent of area in Figure 13.

The established foredune landscape near Oso Flaco Lake and areas with larger nebkha and shadow dunes within the seasonal bird nesting exclosure provide local analogues for what the foredune restoration site could evolve towards. The established Oso Flaco foredunes are between 5-7 m tall. A deflation plain also exists downwind of the Oso Flaco foredune complex (see Figure 13 "A") as well as landward of the "7.5 Reveg" plot, near post marker 8 (Figure 13 "B") and, while this site has not had as long to develop as the Oso Flaco foredunes, it exhibits a similarly spaced foredune-deflation plain relationship. To the north in the seasonal nesting exclosure, nebkha can be up to 2 m tall and, toward the southern end of this exclosure, they are much more densely arranged and a small deflation plain can be seen (see immediately south of post marker 7 in Figure 13 "C"). Based on these observed geomorphic trends, it is likely that the more densely vegetated and faster evolving treatment plots 3-6 will evolve toward these neighboring stages of landscape development.

4.2. Dune Development

Dune development differed distinctly across treatment sites as evident in the geomorphic change maps (Figures 9-10) and site photographs of dune development (Figure 14). Low (0.2–0.4 m high) migrating protodunes and transverse/barchanoid ridges existed across the site prior to restoration (Figure 14b), but the types and/or sizes of dunes changed across all plots within the first few months following restoration treatment installation. At the plot 1 control site, protodunes and transverse/barchanoid ridges grew in height landward, from 0.3 m near the seaward edge, to 1.3 m at the landward edge of the plot, yet nebkha have not developed to date due to continued lack of vegetation cover (Figures 7 and 14a).

A similar pattern of migrating dune ridges was observed in plot 2 and 3, but with vegetated nebkha development near the center of plot 2 (0.2–1.2 m high) and much larger (up to 1.8 m) coalesced nebkha ridges in formed plot 3, predominantly with one plant species (*Abronia latifolia*). The size and spacing of the transverse/barchanoid dune ridges within plots 1–3 also increased during the wind season (Figures 9-10), yet plot 1 and 2 exhibited some of the lowest amounts of accumulation during initial intervals (Table 4, Figure 11), indicating that most sediment was bypassing the foredune zone early in the study period. For the first time since exclosure, the control plot 1 shifted to a negative sediment budget (Figures 11, 12 and Table 4), but all other treatment plots have maintained a positive sediment budgets associated with vegetation-induced deposition and dune development.

Treatment plots 2 and 4 were the only sites to show erosion (volumetric loss) in the foredune zone and, for both, this occurred by wind erosion that occurred in the interval following installation (Feb. - Oct. 2020). In plot 4, this resulted from the development of erosional streets between the straw planting circles for the lower density spacing (Figure 14 d,e). During the later two intervals, however, as plot 4 shifted back to a positive sediment budget, nebkha up to 0.6 m in height established near many of the planting nodes, despite a significant decline in sand supply from the beach. Plot 2 has been much slower to develop nebkha, largely due to the limited nature of the treatment (sheepsfoot texturing and scattered native seeds).

The straw planting circles of treatments 4 and 5 both developed widespread nebkha, mostly centered on the planting nodes, ranging from 0.2 to 1.2 m in height. Plot 5 had a greater number of larger nebkha that were distributed more broadly across the plot due to the closer spacing of the planting nodes, whereas in plot 4 nebkha were generally confined to the seaward half of the plot. Erosion around the straw planting circles was not as prevalent in plot 5 compared to the adjacent low density node treatment 4. Plot 6 (parks classic) has developed many small (0.2–0.3 m) nebkha, although larger nebkha developed along the seaward edge of the plot in recent intervals, and a large drift became established downwind of a sand drift fence along the north edge that was implemented to protect the intervening transportation corridor (Figures 9-10) as well as around a restroom structure in the southeast corner of the plot. As such, some of the accumulation and dune development in plot 6, and to a lesser degree in plots 1, 4, and 5, which also had drift fences along some margins, resulted from deposition around artificial structures and not the vegetation treatments themselves. To date, these artificial deposits have not been removed from the sediment budget analyses.
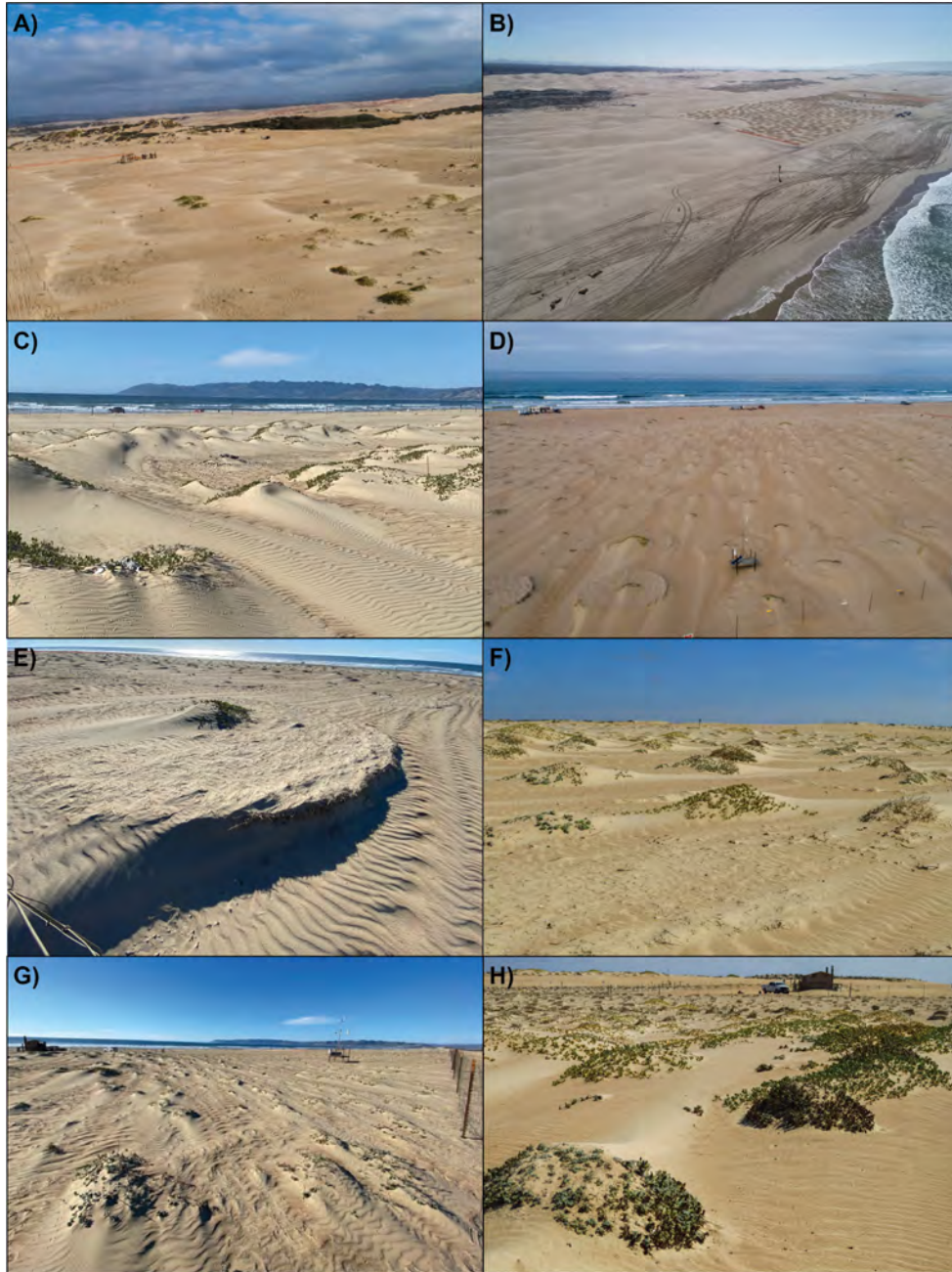
Figure 14. Geomorphology within the foredune restoration treatment plots. (a) UAS image of treatment plots 1 (control site) and 2 (native seed) plot from Oct. 2021. (b) UAS image of treatment plots 3 and 4 during installation in Feb. 2020. (c) Nebkha in plot 3 beginning to coalesce by May 2021. (d) UAS image looking upwind into treatment plot 4 showing prevalent erosional streets from Oct. 2021. (e) Flow steering and erosional street development around low density nodes in plot 4. (f) Developing nebkha in plot 5 associated with Abronia latifolia in Oct. 2021. (g) Full sand cover over the broadcast straw plot 6 within 2.5 months of installation (May 2020). (h) Low nebkha development in plot 6 from Oct. 2021. Photograph credits: I. Walker (c, e, g); Z. Hilgendorf (a, d); A. Hilgendorf (f, h); C. Turner (b).

5. Summary and Conclusions:

To monitor and assess the performance of the foredune restoration dust mitigation project at the ODSVRA, a team from UCSB, in collaboration with CDPR, has been conducting biannual UAS surveys of the foredune restoration treatment site from Oct. 2019 through to Feb. 2023. Primary data products, gathered with a WingtraOne fixed-wing UAS platform, include:

1. Eight (8) high resolution (~1.5 cm) visual (RGB) aerial orthomosaic images encompassing ongoing foredune restoration efforts and sites of landward interest between Pavilion Hill and Oso Flaco Lake,
2. Six (6) high resolution (~3.0-7.5 cm) multispectral (RGB-RE-NIR-Pan) orthomosaic images collected concurrently with the RGB datasets since Oct. 2020,
3. Six (6) high resolution (~3.0-7.5 cm) NDVI orthomosaics derived from the multispectral orthomosaic datasets used to assess vegetation extent and change,
4. Eight (8) high resolution (10 cm) three-dimensional point clouds reconstructing surface topography used to assess site geomorphic and,
5. Seven (7) GCD change maps of statistically significant locations of erosion and deposition as well as related quantities of sediment volumetric changes,

Prior to installation of the treatment plots (Oct. 2019 to Feb. 2020), there was negligible vegetation present in the foredune restoration treatment plots and change was primarily driven by: i) aeolian processes moving sand landward by saltation and low transverse dune migration, and ii) the impacts of vehicle activity and camping. Supply to the beach was variable, but net positive as all beach plots recorded net deposition. Deposition within the treatment plots and landward dune plots was low to negligible initially, as the eventual treatment plots were largely barren sand surfaces with little to no roughness elements to increase deposition and stimulate dune development.

Following treatment installations, continued sand accretion, plant growth, and resulting nebkha development has occurred within the treatment plots, with some (plots 3-6) featuring larger nebkha dunes (exceeding 2 m in plots 3, 5) with vegetation cover between ~9-15%. During this past year, development of nebkha along the seaward edge of most plots has been appreciable. These trends occur despite highly variable inputs to the beach that directly control sand supply to the treatment plots and landward units. While a north-to-south gradient in decreasing beach zone sediment budgets was observed, this was not reflected in the sand budgets of the adjoined foredune zones.

Trends in vegetation growth, dune evolution, and sediment budget responses in the foredune restoration zone at ODSVRA provide an opportunity to study and assess the effectiveness of the restoration project and, in turn, eventually inform adaptive management strategies. Following three (3) years of vegetation growth and dune development at the site, it is still apparent that

dune development is specific to treatment type and that the implications for longer term development and sustainability of the foredune remains uncertain. As the system continues to evolve, it will be necessary to evaluate performance using the indicators outlined in Section 1 to understand and quantify the effects that the restoration treatments are having on landscape evolution and dust mitigation in comparison to both the local control site (plot 1) and the nearby reference sites at Oso Flaco. Based on progress to Feb. 2023, the following indications of progress are assessed:

1. **All foredune treatments continue to show net positive sediment budgets**. For the first time, however, the control plot 1 shifted to a negative (erosional) budget that relates partly to a lack of vegetation to promote accretion and nebkha development, as well as notable beach erosion in the winter of 2022-23. This said, beach erosion was greater fronting treatments 2 and 3, yet they maintained appreciable accretion. Generally, sediment budgets continued to increase in the vegetated treatment plots where nebkha dune development is enhancing sediment capture and providing downwind sheltering to the surface.

2. **Aeolian processes remained active in all treatments** shown by rippled sand transport corridors, dune development, coalescence and migration, and emergence of erosional deflation surfaces with coarse lag deposits on all sites. Erosional responses are expected during dune development and do not necessarily reflect poor performance. Maintenance of aeolian processes is required to provide needed ecological disturbance gradients and processes required for plant growth and dune development.

3. **Plant cover since implementation continues an increasing trend in all treatment plots** except for the control site 1, which continues to show negligible vegetation. Although the 3-year trend is positive, plant cover declined in most plots this past observation period - markedly in plot 3, slightly in plots 2, 4, and 6, and remained similar in plot 5. The cause of this decline is unknown, but could relate to an unusually wet and stormy winter and/or erosion along the seaward margins of the plots. It is unclear if this downturn in plant cover reflects a plateauing of the ecosystem or just natural variability as the system continues to evolve. On average, plant cover across the site is 8.2% with a maximum of 14.8% (per plot area) in treatment 6 (broadcast straw + seedlings) and a minimum of 2.7% in treatment 2 (native seed). Some species, namely *Abronia latifolia*, have shown rapid establishment and growth, promoting development of taller nebkha. These observations of plant community development reinforce that more time is required to assess broader foredune ecosystem re-establishment and sustainability.

4. **Dune development continues in all treatment plots**, with the largest (>2 m) nebkha dunes emerging in plots 3 and 5, smaller (1.0-1.5 m) nebkha in plots 2 and 4, and multiple smaller dunes in plot 6. This past year also saw increasing development of

nebkha along the seaward edge of most plots. Dune growth and migration also occurred in the control plot immediately after exclosure and, until this latest interval, it maintained a positive sediment budget. Without vegetation, however, nebkha dunes and continued accretion might not occur in this site. This said, as the other treatments continue to evolve, it is important to maintain an adjoined control site that is not subject to OHV activity for comparison.

5. **Assessing contributions of restoration treatments to reduced dust emissivity is underway**. A recent PI-SWERL campaign was conducted by DRI in the foredune treatment plots and in the bird nesting exclosure in Summer 2022 to assess the emissivity in the treatment plots for improved dust modeling and for monitoring emissivity response of the treatments. See Section 2.3.5 for recent PI-SWERL results. In addition, computational fluid dynamics (CFD) modelling was conducted on the foredune treatments (see Section 2.3.4) and a peer-reviewed manuscript is in development. At this point, these results remain to be analysed collectively toward discrete assessment of the effectiveness of the foredune restoration treatments for reducing emissivity.

Appendix A: Full Extent of Visual (RGB) and Multi-spectral Imagery Collections

Visual (RGB) imagery:
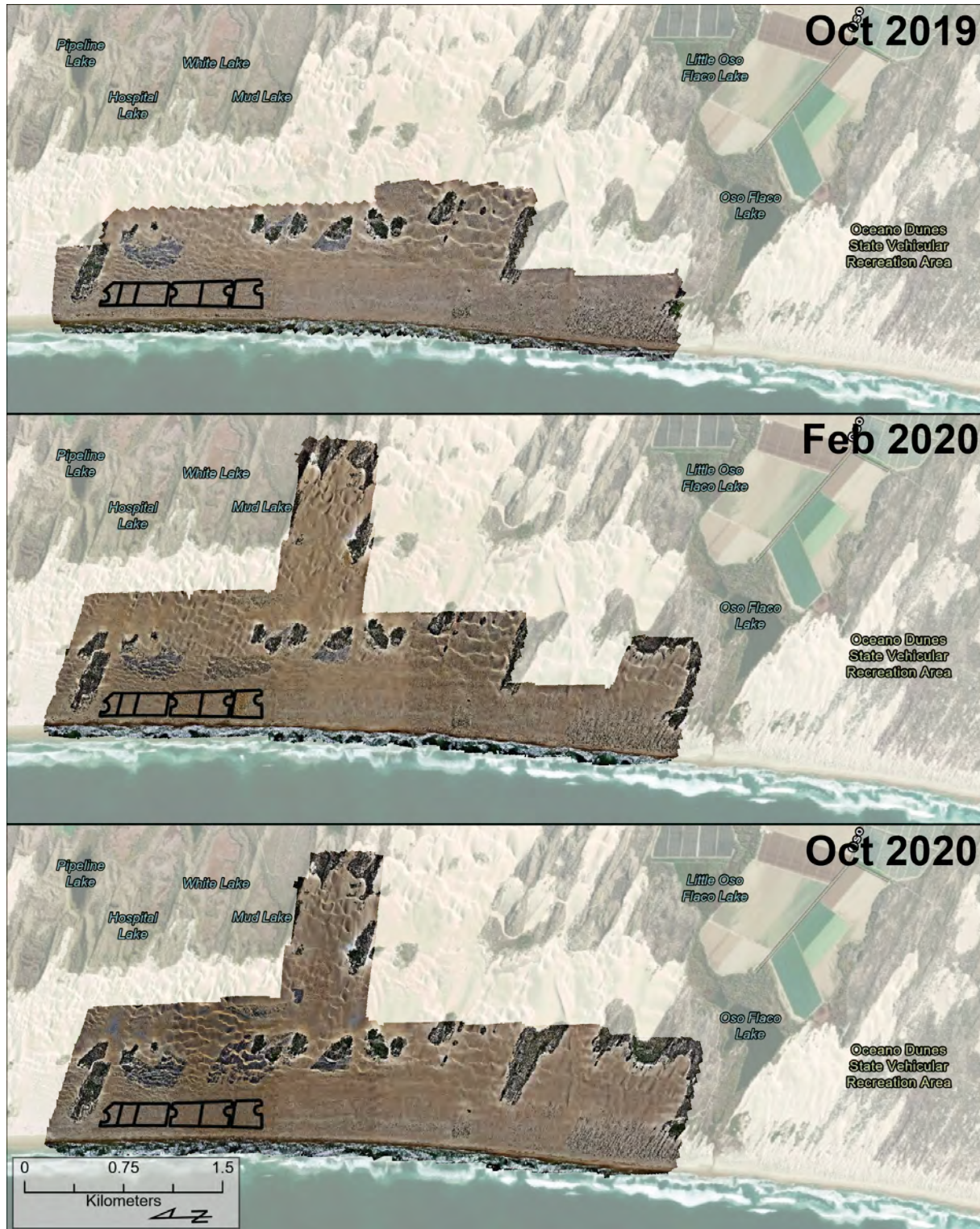
Multi-spectral imagery:
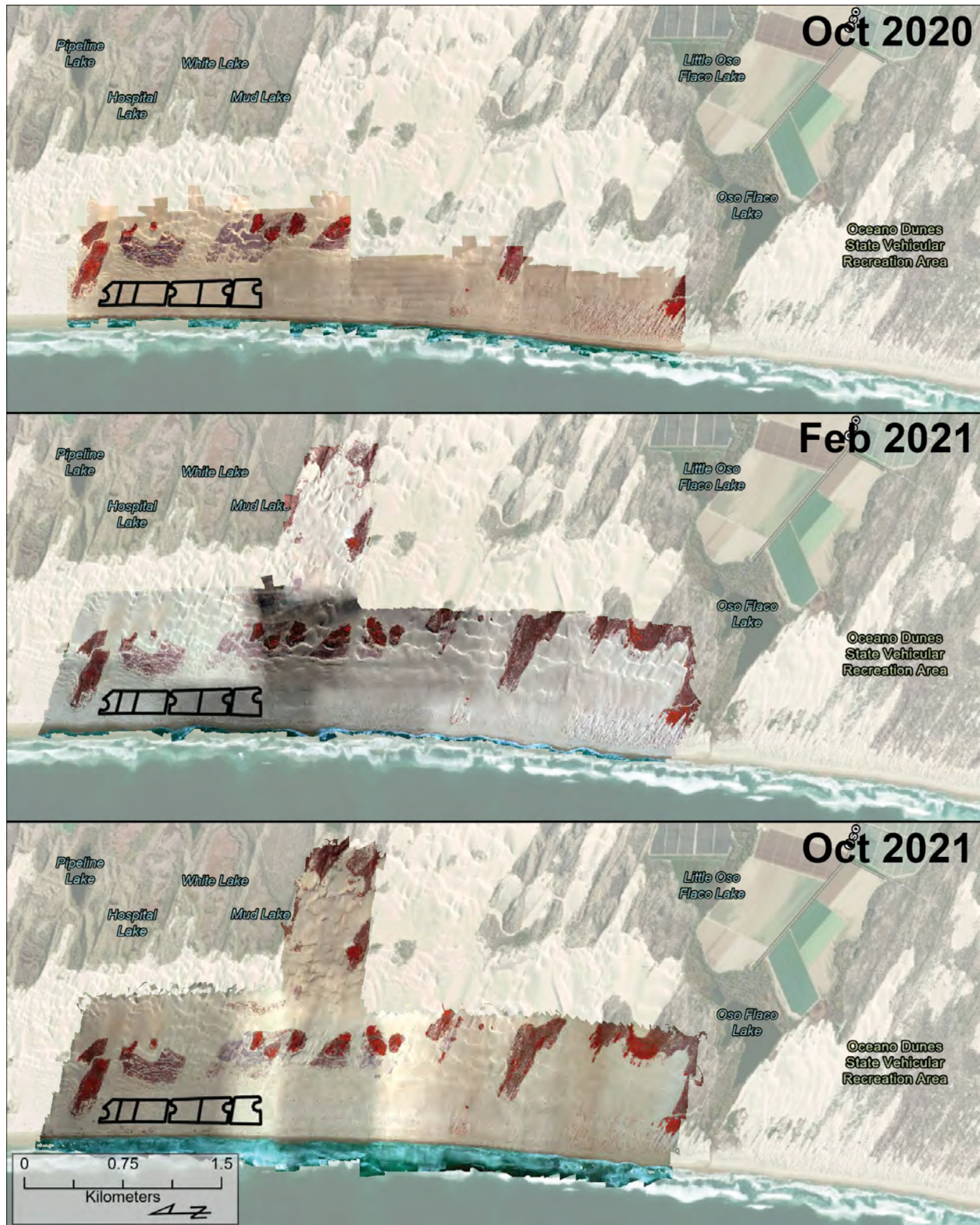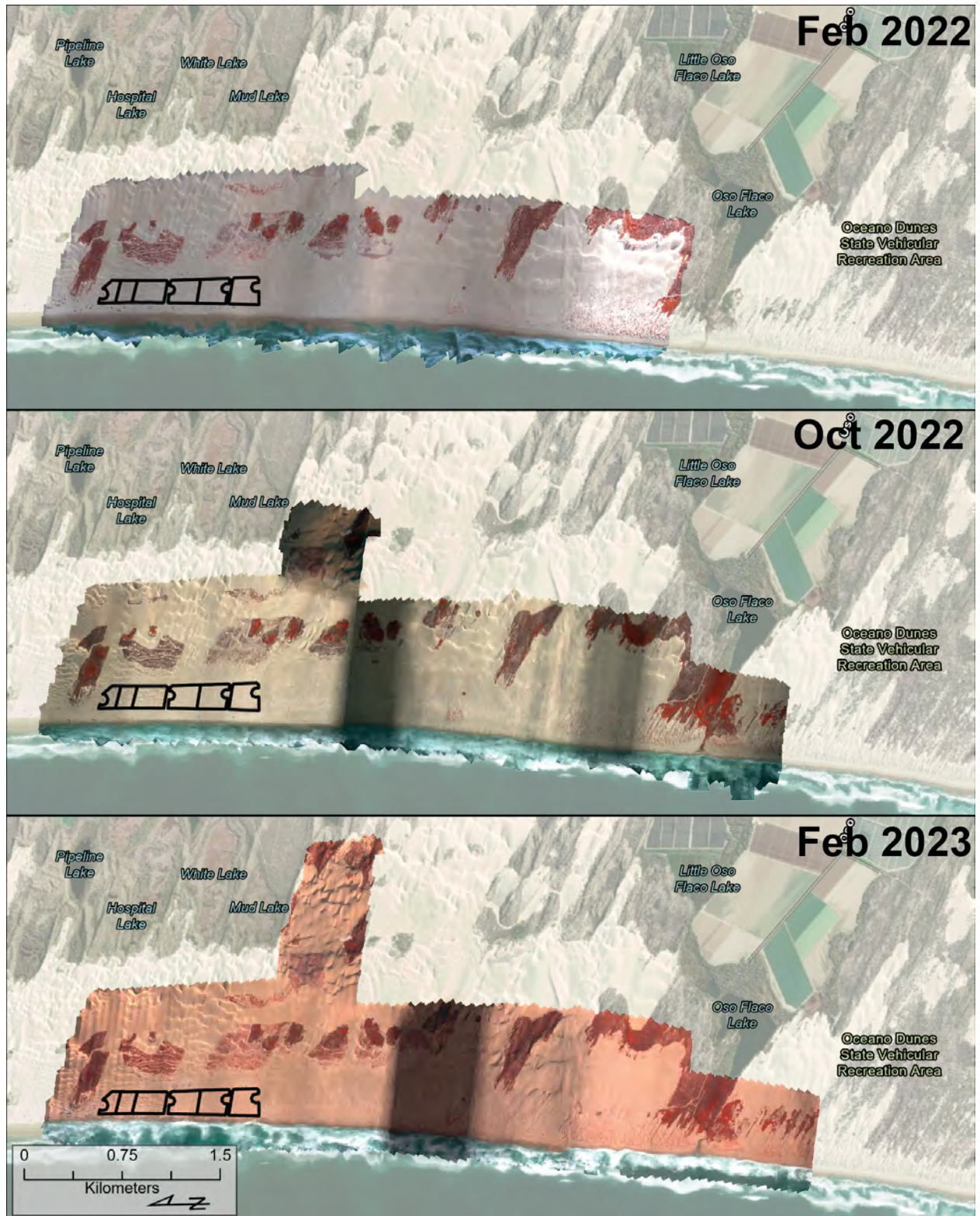
THIS PAGE WAS INTENTIONALLY LEFT BLANK.

March 8, 2024

Memo: <u>SAG Review of UCSB Report " Foredune Restoration UAS Survey Report" (UCSB 2022-2023 ODSVRA)</u>

From: Scientific Advisory Group (SAG)

To: Jon O'Brien, California Department of Parks and Recreation

Cc: Ronnie Glick, California Department of Parks and Recreation

This is a very complete and informative summary of the foredune restoration project implemented at the Oceano Dunes State Recreational Vehicle Area (ODSRVA). The report presents three forms of data that describe the evolution of the experimental dune development complex: vegetation cover changes, geomorphic changes, and volumetric changes. Relevant photographs, graphs, and tables explaining and interpreting the data are incorporated into the report. It is an important contribution to understanding the development of foredune systems in this region, and provides good descriptions of the data collection technologies, strategies, and interpretation.

Members of the SAG, excluding Dr. Walker (because of a conflict of interest), provided reviews of this report. The comments received are conveyed below, with reference to section and page number.

List of Acronyms, page 1:

- Uncrewed Aerial Platform – UAS should be 'System' rather than 'Platform' to be consistent with the acronym

Executive Summary, page 2:

- Provide a brief statement about the purpose of the project. Some of the language at the beginning of point 5 on page 6 of the Introduction would serve well.
- Page 3. With respect to sediment budgets, please indicate that these are annual budgets (presumably) and the beginning/end times (e.g., Jan 1 through Dec 31 or otherwise). Also be very clear to distinguish between an annual budget total versus the long-term accumulation (or removal) of sediment volume from a treatment area. In other words, an area can experience a negative budget in one year but still have a positive overall volume contribution over the three years.
- Page 3. With respect to plant cover, the same comment as with sediment budgets. The phrasing is very unclear because the first sentence in the bullet point (3) states that plant cover continues to increase in all treatment plots but the next sentence indicates that plant cover declined notably this past year. Both can't be true unless you are referring to different time intervals (i.e., annual trend versus long-term).

- Page 3. In reference to the PI-SWERL campaign of 2022, the outcome is now well known so a summary sentence could be inserted here (recognizing that this report was submitted a long time ago).
- It would help to have the dates for the study in the summary, as terms like "over this past year" are unclear and could be more specific.
- Question: can a good success versus a poor success be defined yet or does that require evolution to play out a bit longer? (see additional comment below about use of the term 'success')
-

Section 1: Introduction
- Page 4, Footnote 1. The explanation of DTM vs DEM is useful, but it is not clear as to whether the vegetation was also removed from the DTM (to produce a DEM) prior to change detection of sand volume. All that is stated here is that buildings and vehicles were removed. This is also pertinent to Point 4 for GCD maps because the description indicates that DTMs were used for elevation differences when, in fact, it would be the DEM that should be used. Some clarification would be useful in this section so that the reader does not become confused as to whether a DTM or a DEM was used for change detection.
- Page 4, last paragraph. There is no need to insert "or 'success'" into this sentence after performance because 'success' is a value judgement with positive implications. This report deals with performance assessment, full stop.
- Point 3, page 5: Substitute the word 'enhance' for 'initiate' in the first sentence. Sedimentation can occur without plant cover, which is not a necessary condition for the 'initiation' of sedimentation.
- Point 5, page 6: as a "main impetus", this criterion should be referenced at the very beginning of the introduction.

Section 2: Methods:

- Figure 1, page 7: The caption fails to make clear that the coverage is indicated by the shaded area. Thus, the reader makes the assumption that the coverage is restricted to the zones outlined in black (A and B). Also, the choice of shading is unfortunate because it looks like the vegetation areas to the north. Can you not put a boundary line around the covered area or select a different color?
- Table 1, page 9: Is "treatment response" the same as "growing season"? If not, where are these data from the first growing season? Please clarify the difference between "growing season" (i.e., an annual seasonal time period roughly from March through October when plants grow) and "treatment response" (i.e., roughly a year-long period that includes the plant growth period as well as the geomorphic response for that year extending over Christmas period), or something to that effect.

- Figure 2, page 10: Delete last sentence from figure caption – it is a commentary that does not apply to this figure directly.
- Figure 3, page 11: there is no readily detectable difference between the NDVI and the thresholded views
- Table 2, page 12: Delete last sentence from figure caption—there is no "NA" in the table of values.

Section 3: Results
- 3.1, page 12. Please put Figures 4 and 5 in this section instead of in the next one.
- 3.2 page 13. Neither the Western Snowy Plover exclosure nor the Oso Flaco Lake area are shown on Figure 6.
- 3.2 page 14, second paragraph: …to allow for species-level identification…
- Figure 7, page 18: Caption says that these are "changes in percent cover" but actually they are just "percent cover" (or perhaps temporal trends in percent cover). In other words, they are not a 'delta' quantity.
- Page 22, last paragraph: The discussion of the influence of the transportation corridor on drift development in area 6 is recognized as "not technically reflect(ing) the effectiveness of the restoration treatment itself." One wonders whether the statistics for change in each of the treatment areas should be based on an internal area (smaller than the fence lines) and not consider a buffer zone inside the treatment boundaries of say, 5 meters or so, in order to eliminate these 'boundary' effects. It is increasingly evident from the trips to the ODSVRA that there is a transition from the conditions outside the fences to inside the fences. This will reduce the total area within each of the treatment areas, but by eliminating the buffer strips from consideration, you may get a more representative picture of the actual treatment responses. This would also reduce the impact of large erosional events by waves and high tides at the upwind margin.
- 3.3 page 22: Last sentence: what does "between plots" mean?
- Figure 9, page 23: It is striking how different the conditions are in the backdune area behind treatment areas 4, 5, and 6 relative to what goes on within the treatment areas. There is substantial erosion. Is this stimulated by the fence or a consequence of the enhanced roughness and turbulence shed from the dunes? It is also interesting that when you look at these change images, you get the impression that there is overall erosion (more pink than blue) within the treatments and yet the tabular data indicate that there has been net accretion everywhere. Puzzling? Is there any need for the color index to extend from -2.7 m to +2.7 m when most of the data represented in these graphs show changes of less than 1 m?
- 3.3, last paragraph, page 26-27: "The trend of this cycle is predominantly neutral to slightly negative in treatment plots 4-6. In plot 6, the trend has become

increasingly negative." Clarify if you are referring to the inland dunes behind these treatment plots.

- Table 4, page 25: dark horizontal lines separating data from each treatment would be helpful here in seeing patterns.
- Page 27, middle paragraph: The following sentence is confusing: "Since installation of the treatments in Feb. 2020, only foredune plots 4,5 (greatest overall), and 6 have experienced net gains in sand volume, while plots 1 through 3 have seen net deficits." This is counter to the data presented in Table 4, unless you are referring specifically to the beach rather than the foredune treatments. Please clarify.
- Clarify that the Western Snowy Plover exclosure is no longer seasonal. Clarify other references to "seasonal nesting exclosure" throughout the document.

Section 4 Discussion

- 4.1 page 27, 2nd paragraph. It's not clear how to interpret the fact that plots 4, 5 and 6 have had net gains in sand volume, while plots 1-3 have net deficits (of volume) yet plots 2-6 have maintained net positive sediment budgets. Can this be clarified, i.e., how can 2 and 3 be in net deficit, but have net positive budgets?
- 4.1 page 27, 2nd paragraph and Figure 12, page 28: Similar to the point above, it is difficult to tell if the paper includes the beach area and landward dune in the discussion of overall volumetric changes.
- Page 28 (last paragraph) and Page 29 (first paragraph). The explanations about the downwind (inland) zones as being decoupled from the foredunes seems very speculative. Yes, there is OHV traffic, but this does not explain the erosional strip along the fence line. Also, the notion that there is a flow separation zone behind the treatment areas with dunes seems counter to there being a strip of erosion. Ordinarily one would find sediment accretion in a flow separation zone, especially in the zone immediately behind the dunes. This is consistent with your description of a downwind 'sheltering' effect. And yet, there is erosion here, rather significant in the case of treatment areas 4, 5, and 6 where the dunes are the largest (Figures 9 and 10). In short, these two paragraphs are quite general descriptions of what one might generally expect, but they are contrary to what is observed. In contrast, the first paragraph on Page 30 indicates that deflation hollows are expected in the lee of dunes, and this seems to be what is being observed behind treatment areas 4, 5, and 6, likely to enhanced wake turbulence rather than a 'sheltering' effect.
- 4.1 page 30. Last paragraph of section. Is "seasonal bird nesting exclosure" the same as Western Snowy Plover exclosure? Please standardize terminology.
- Figure 14, page 32. The figure caption mentions 'erosional streets' and this term is used elsewhere in the report. Are you certain that there is actual erosion along these linear features or are they simply transport corridors?

Section 5 Summary and Conclusions

- Somewhere, a discussion of the difference between Treatments 2 and 3 would be useful. What difference does it seem to make if there is sterile ryegrass seed in addition to the native seed? Do we see the ryegrass persisting in the vegetation? What purpose do we think it serves, as it DOES seem to make a discernable difference.
- Given that the implications for long term development and sustainability of the foredune remains uncertain, will these measurements continue indefinitely?
- Section 5, page 33: "Supply to the beach was variable, but net positive as all beach plots recorded net deposition." Figure 12 shows some plots have significant beach area erosion, please clarify.

Appendix A:

- The scale of these images is such that you can't see anything within the restoration site. What purpose do these images serve?
- General Comment – these images are only useful in showing the UAS coverage areas from year to year, and don't show any detail regarding the foredune restoration area, which is the subject of the report. It seems that there is one report topic that deals with the changes in the foredune restoration area and another report topic that deals with UAS survey campaigns. Perhaps in future it would make sense to generate two separate reports, one that covers the technical details of the UAS campaigns, and a second that focuses specifically on the foredune restoration area (as a dust mitigation tool). It may also make sense, at some later date. to provide a summary report on what the expanded coverage of the UAS campaigns reveals about broader conditions in the ODSVRA.

THIS PAGE WAS INTENTIONALLY LEFT BLANK.

ODSVRA Dust Control Program Draft 2024 ARWP

ATTACHMENT 04B

UCSB 2023-2024 ODSVRA Foredune Restoration UAS Survey Report

- UCSB 2023-2024 ODSVRA Foredune Restoration UAS Survey Report (UCSB Report)

- SAG Review of UCSB Report "2023-2024 ODSVRA Foredune Restoration UAS Monitoring Report"

THIS PAGE WAS INTENTIONALLY LEFT BLANK.

2023-2024 ODSVRA
Foredune Restoration UAS Monitoring Report

Prepared by: Zach Hilgendorf[1,2], Ian Walker[1], and Madison Heffentrager[1]

[1] Department of Geography, University of California, Santa Barbara
[2] Department of Geography and Anthropology, University of Wisconsin-Eau Claire

Revised July 2024

List of Acronyms:

California Department of Parks and Recreation – CDPR

Desert Research Institute – DRI

Digital Terrain Model – DTM Foredune

Restoration Area - FRA Geomorphic

Change Detection – GCD Ground

Sampling Distance – GSD Light

Detection and Ranging - LIDAR Near

Infrared – NIR

Normalized Difference Vegetation Index – NDVI

Oceano Dunes State Vehicular Recreation Area –

ODSVRA Off-Highway Vehicles – OHV

Particulate Matter – PM

Particulate Matter Reduction Plan - PMRP

Portable In-Situ Wind Erosion Laboratory – PI-SWERL

Post-Processing Kinematic - PPK

Red-Edge – RE

Red-Green-Blue Spectral Bands – RGB

San Luis Obispo Air Pollution Control District – SLO-APCD

Scientific Advisory Group – SAG

Structure-from-Motion – SfM

Stipulated Order of Abatement - SOA

Treatment Plot - TP

Uncrewed Aerial System – UAS

University of California Santa Barbara – UCSB

EXECUTIVE SUMMARY

A foredune restoration project was established in Feb. 2020 at ODSVRA as a nature-based solution to mitigate PM_{10} dust emissions from a highly emissive 48-acre site by promoting sand deposition and dune development. The foredune restoration area (FRA) consists of six treatment plots (TP), including (north-south): TP1) a control plot only textured by a sheepsfoot roller; TP2) sheepsfoot texture and broadcast native seeds; TP3) sheepsfoot texture and broadcast native plant and sterile rye grass seeds; TP4) low-density straw planting circles with nodes of juvenile native plants; TP5) high-density straw planting circles with nodes of juvenile native plants; TP6) complete straw cover with high density of juvenile plants.

An uncrewed aerial system (UAS) with high resolution cameras has been flown biannually (October and February) since Oct. 2019 to monitor and detect geomorphic and vegetation changes in the FRA and adjoining beach and back dune areas. To date, 10 flights have been conducted and resulting datasets include: georeferenced orthomosaics, plant cover maps, digital elevation maps (DTMs), topographic change maps, and sand volumetric change estimates. These datasets are used to examine patterns and volumes of sediment erosion/deposition across the site and changes in vegetation through time. In turn, these results are used to identify and interpret the performance of the treatments based on indicators of dune development, sediment budget response, vegetation trends, and dust mitigation potential. This report provides results from four years of development from Oct. 2019 to Feb. 2024.

Sand supply to the beach, which feeds aeolian transport into the FRA and subsequent dune development, has been highly variable through time, as expected, due to seasonal to interannual changes in wave energy, beach erosion/rebuilding, and movement of rip current embayments. Generally, though variable, beach sediment budgets trended from positive from the pre-restoration baseline interval (Oct. 2019 to Feb. 2020) to negative by Feb. 2023, then back to positive values most recently (Oct. 2023 to Feb. 2024). Net changes over the period of study within the beach units indicate erosion in the northern three plots (TP1-3) and deposition in the southern three plots (TP4-6).

Despite notable fluctuations in sand supply to the beach, the treatment plots have maintained net depositional responses, albeit with small deviations over the years. Deviations include neutral (+/- 0.001 $m^3\,m^{-2}\,mo^{-1}$) to negative sediment budgets in Feb. to Oct. 2020, Feb. to Oct. 2023, and Oct. 2023 to Feb. 2024. Meanwhile, net change of the TP1 control site has remained neutral while the neighboring TP2 showed the lowest rates of accumulation of the treatment plots, indicating notable sediment bypassing and longer-term declines in sand inputs from beach erosion. Comparable recent beach erosion occurred at TP3, yet this treatment exhibited the

second highest net positive sediment budget and significant dune development. TP4 and TP5 showed moderate amounts of sand accumulation (fourth and third highest, respectively), while TP6 accumulated the greatest net amount of sand, although the majority of this deposition was confined to the seaward edge of the plot and downwind of a drift fence along the northern margin. TP6 was the only plot that did not exhibit a negative sediment budget interval, while TP3 and TP5 only experienced one negative change interval (Feb. 2023 to Oct. 2023).

Plant cover generally increased since implementation for all treatment plots except the TP1 control site, which continues to show limited cover. TP6, the most intensive treatment, showed the greatest net increase in plant cover (+11.68%) to Feb. 2024, followed by TP3 (+6.95%), TP5 (+6.18%), TP4 (+4.85%), and TP2 (+3.10%). Peak observed historical cover at the FRA site and in the broader foredune zone (~400 m inland) in the OHV riding area, respectively, were about 3% and 6% in 1966[3]. Since Oct. 2023, a distinct decrease in plant cover in all treatment plots has occurred with TP6 experiencing the largest declines (-7.70%) followed by TP5 (-3.50%), then TP3 (-3.40%). The cause of this recent decline is unclear, but the patterns are widespread (vs. localized) and could relate to unusually wet and stormy winters since 2022. Some species, namely Abronia latifolia, have shown rapid establishment and growth, and played leading roles in dune development.

In terms of FRA treatment performance, following four full wind and plant growth seasons, the plots continue to evolve on different trajectories as a function of initial treatments and variability in sand supply, plant cover, and changing roughness. Relative rankings of treatment performance have not changed significantly since Oct. 2022, with TP3 as a top performer, followed by TP5, due to continued positive sediment budgets, greatest amounts of dune development and extension, maintenance of aeolian activity, continued increases in plant cover, and greatest potential for reducing dust emissions. TP2 maintains the lowest performance due to modest amounts of accretion and dune development, low plant cover, and correspondingly low dust emissions control potential. The most intensive treatment (TP6) slid recently to second lowest performance due to continued declines in sediment budget, limited dune development, and marked declines in vegetation cover. Monitoring will continue as the treatments evolve to detect further responses indicative of success or concern for adaptive management and for longer-term sustainability of the FRA as a dust control mitigation.

1. Introduction

The purpose of this project is to contribute to reduced dust emissions in the ODSVRA and downwind through the implementation of a nature-based foredune restoration area (FRA) on a formerly highly emissive site. To monitor and assess the performance of the FRA dust emissions mitigation project at the ODSVRA, a team from UC Santa Barbara, in collaboration with CDPR, have been conducting UAS flights biannually since Oct. 2019. The UAS imagery datasets have been used to create the following data products:

1. Ten (10) visual (RGB) georeferenced aerial orthomosaic images of the FRA at ~1.5 cm resolution,

2. Eight (8) multispectral (RGB-RE-NIR-Pan) georeferenced orthomosaic images of the FRA at ~3.0-7.5 cm resolution collected concurrently with the RGB datasets since Oct. 2020,

3. Eight (8) NDVI orthomosaics used to assess vegetation cover in the FRA at ~3.0-7.5 cm resolution derived from the multispectral orthomosaic datasets

4. Eight (8) georeferenced, orthorectified maps of vegetation cover derived from RGB and NDVI imagery used to track changes in plant cover within the FRA,

5. Ten (10) three-dimensional point clouds of surface topography within the FRA at a decimated resolution of 10 cm,

6. Ten (10) three-dimensional digital elevation models (DTMs) of topography within the FRA at 10 cm pixel resolution,

7. Nine (9) topographic change maps derived from statistically significant pixels of erosion and deposition between DTM intervals used to assess site geomorphic and sediment volume changes.

Data collected during the UAS flights allows for high resolution, three-dimensional DTM surfaces to be constructed and compared through time to quantify sand volume changes and dune dynamics. Given the low-lying, prostrate nature of the vegetation, separation of the vegetation from the surface is difficult without introducing artifacts in the point cloud. Other data collected allow for examination of the growth of vegetation and the development of dune forms within the FRA. This report details the methods used for data collection, processing, as well as initial baseline conditions collected prior to the implementation of the FRA (Oct. 2019) through to Feb. 2024, or 4 full years following the treatment installations in Feb. 2020.

The performance of the restoration treatments at ODSVRA are assessed using 5 indicators, developed in consultation with SAG and CDPR, that track the geomorphic, sediment transport,

vegetation characteristics and responses within the treatment plots (Walker et al. 2023)[1]. These indicators characterize the re-establishment of dynamic ecological and geomorphic conditions required to improve dune ecosystem form and function. The first indicator is establishment and maintenance of a positive sediment budget (i.e., gains in sediment volume through time). This is particularly important during the initial stages of foredune development in which small incipient nebkha (mounds of windblown sand trapped in vegetation) establish and related downwind shadow dunes grow. Eventually, as nebkha and shadow dunes grow and coalesce they will alter the wind field and sand transport patterns and promote localized reductions in surface shear stress, saltation, and promote deposition. In short, to build dunes, the treatment plots need to act as a sink (store) of sediment.

The second indicator is to maintain aeolian activity within the treatments, namely sand transport (saltation), migrating ripples, and open sand surfaces. Saltation, and related erosion and deposition patterns, are critical for dune development and maintenance, and aeolian activity is a key ecological disturbance process required by psammophytic (sand loving) plants for their success.

The third indicator is to increase and/or maintain foredune plant cover. Most coastal dunes owe their form and function to plants. So, to re-establish a new foredune ecosystem it is imperative that plants establish and survive to enhance sedimentation and promote ecological feedbacks and conditions needed to maintain dunes. Eventually, however, plant cover density should plateau at an amount that is in balance with dune form/position, aeolian activity, soil nutrients, and regional climate conditions. Typically, dune systems with natural plant communities in central and southern California have modest vegetation cover (rarely exceeding 30-40%) given regional climatic conditions. As ecosystem re-establishment occurs, it is also anticipated that species richness would improve and plant cover would reach a sustainable amount comparable to the nearby reference sites at Oso Flaco Lake. Targets for species richness and plant cover have not yet been defined in consultation with SAG and CDPR.

The fourth indicator is enhanced dune development. The establishment, growth, and maintenance of foredunes and related dune forms (e.g., nebkha, blowouts, parabolic dunes, etc.) is a key target for restoration performance. Important interactions and feedback mechanisms exist between wind flow, sand transport, vegetation cover, and dune development that are required to build and maintain natural foredunes. As the system develops and evolves, the variety of dune forms is expected to change and organize to a form that reflects plant cover, aeolian activity, and regional climate controls. Natural foredunes in this region are not

---

[1] Walker, I. J., Hilgendorf, Z., Gillies, J. A., Turner, C. M., Furtak-Cole, E., & Nikolich, G. (2023). Assessing performance of a "nature-based" foredune restoration project, Oceano Dunes, California, USA. Earth Surface Processes and Landforms, 48(1), 143-162.

characterized by a uniform foredune ridge with high plant cover, as is common farther north in California and Oregon. Rather, a more hummocky, discontinuous form with active sand surfaces is the preferred ecosystem form in this climatic setting[2].

The fifth indicator is a reduction in dust emissivity. The main impetus for the FRA project at ODSVRA was to implement a sustainable, nature-based dust mitigation solution that had both onsite and downwind impacts. As dune terrain and vegetation roughness increase, it is expected that surface shear stress patterns that drive saltation and dust emissions within the FRA, and downwind, would be reduced as would surface emissivity.

This report provides new results from the 2023-2024 season in the context of past observations, interprets these findings to understand the ongoing evolution of the restoration treatments, and assesses the implications of observed responses for relative performance of the restoration treatments to date.

2. Methods

UAS platforms and SfM photogrammetry have experienced widespread and rapid advancements in the last decade[3,4]. SfM photogrammetry refers to the reconstruction of a three-dimensional landscape from highly overlapped (≥70% frontal and side overlap) images. UAS-SfM datasets are used to detect change in a wide variety of landscapes and ecosystems, including coastal dunes[5]. The quality and resulting data products are dependent on the sensors used, methods for georectification, and, in the case of UAS platforms, flight altitude, shutter speed, and stability[6]. Advantages for using UAS datasets for monitoring and detecting change include the relative ease and low cost of data collection, compared to aerial LIDAR, and the high accuracy (mm-cm resolution) of the resulting maps and elevation point clouds.

A fixed-wing, fully autonomous WingtraOne UAS platform was used at the ODSVRA from Oct. 2019 to Feb. 2024 to monitor and characterize changes in sediment volumes, geomorphic

---

[2] Hesp, P.A., & Walker, I. J. (2022). 7.21 Coastal Dunes. Treatise on Geomorphology, 2nd edition, ed. J. F. Shroder, Volume 7, Pages 540-591. Elsevier. https://doi.org/10.1016/B978-0-12-818234-5.00220-0

[3] Anderson, K., Westoby, M. J., & James, M. R. (2019). Low-budget topographic surveying comes of age: Structure from motion photogrammetry in geography and the geosciences. Progress in Physical Geography: Earth and Environment, 43(2), 163–173. https://doi.org/10.1177/0309133319837454.

[4] James, M. R., Chandler, J. H., Eltner, A., Fraser, C., Miller, P. E., Mills, J. P., Noble, T., Robson, S., & Lane, S. N. (2019). Guidelines on the use of structure-from-motion photogrammetry in geomorphic research. Earth Surface Processes and Landforms, 44(10), 2081–2084. https://doi.org/10.1002/esp.4637.

[5] Hilgendorf, Z., Marvin, M. C., Turner, C. M., & Walker, I. J. (2021). Assessing geomorphic change in restored coastal dune ecosystems using a multi-platform aerial approach. Remote Sensing, 13(3), 354.

[6] Singh, K. K., & A. E. Frazier. (2018). A meta-analysis and review of unmanned aircraft system (UAS) imagery for terrestrial applications. International Journal of Remote Sensing, 39(15–16), 5078–5098. https://doi.org/10.1080/01431161.2017.1420941

responses, and vegetation cover within and beyond the restoration treatments (Figure 1). The UAS is typically flown at altitudes over 100 m above ground level and is equipped with on board, survey-grade GPS with PPK correction capabilities. During data collection, a GPS base station is operated in static collection mode and these occupation datasets are used to refine UAS photo point locations to within millimeters of their real-world location. Ten collection campaigns have been flown (Table 1) with 8 multispectral datasets collected concurrently since Oct. 2020.

Two RGB camera sensors have been used: a Sony RX1RII 42 MP full-frame sensor (Oct. 2019 through Feb. 2023) and a Sony RGB61 61 MP full-frame sensor (Oct. 2023 through present). The Sony RGB61 sensor covers a larger footprint with each picture, resulting in fewer images taken for the same area covered. This results in lower data volume and faster flight time for the same high resolution data product. Both sensors produce high resolution (<2 cm) orthomosaic imagery that, in turn, is used with SfM to create three-dimensional point clouds of the underlying surface. Point clouds between campaigns are aligned to one another using static features in the landscape (e.g., structures, roads, etc.). Point cloud datasets are also used to produce the gridded (rasterized) DTMs. The raster surface is gridded to 0.1 m/pixel and is assigned an elevation value by averaging all points within that 0.1 m^2 cell. DTMs are then compared between campaigns to quantify volumetric changes (Table 1).

Successive DTMs are imported into a GIS and the Geomorphic Change Detection (GCD) toolset (Figure 2), developed by Riverscapes Consortium, is used to calculate volumes of change between collocated raster grid cells. This method applies a spatial statistical filter to remove surface changes that fall below a threshold uncertainty value with 95% confidence[7,8]. This threshold is determined by developing an uncertainty budget that includes the accuracy of the GPS station, the calculated uncertainty of the point cloud, and the root mean square error from the alignment of each point cloud with static features in the landscape. The uncertainty between two surveys is additive and pixels that exceed the minimum level of detection threshold (typically ~5 cm) are included. As such, repeat DTMs derived from the UAS imagery (Figure 2) are compared through time. Pixels of statistically significant elevation change are used to create topographic (elevation) change maps for estimating volumetric changes (between significant pixels) and interpreting corresponding geomorphic changes. Results can also be partitioned into specified units to monitor plot-based change through time, such as between the foredune restoration treatment plots themselves, as well as their adjoined beach and landward dune components (Figure 1).

[7] Wheaton, J. M., Brasington, J., Darby, S. E., & Sear, D. A. (2009). Accounting for uncertainty in DEMs from repeat topographic surveys: improved sediment budgets. Earth Surface Processes and Landforms, 35(2), 136-156. https://doi.org/10.1002/esp.1886.

[8] Hilgendorf, Z., Marvin, M. C., Turner, C. M., & Walker, I. J. (2021). Assessing Geomorphic Change in Restored Coastal Dune Ecosystems Using a Multi-Platform Aerial Approach. Remote Sensing, 13(3), 354. https://doi.org/10.3390/rs13030354.
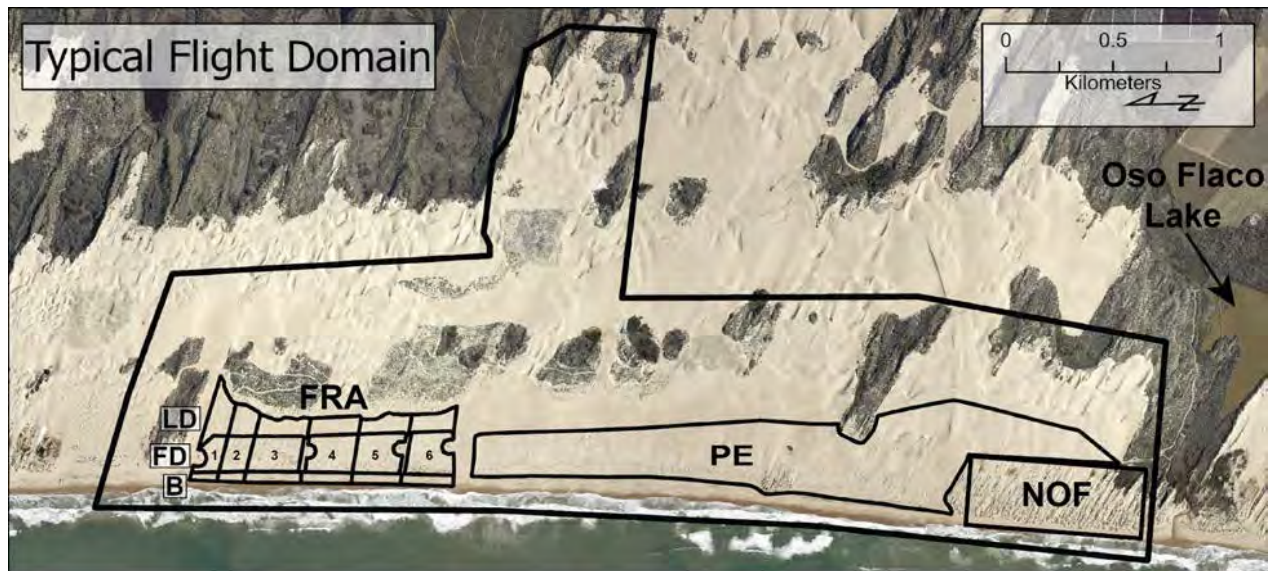
Figure 1. Map showing the typical extent of the UAS surveys (North oriented to the left). The foredune restoration area (FRA) and foredune (FD) treatment plots (1-6) are shown with adjoining beach (B) and landward dune (LD) polygons for examining volumetric exchanges with the FRA. The Western Snowy Plover exclosure (PE, as of Feb. 2024) and North Oso Flaco (NOF) reference site are also shown. The underlying orthomosaic is from 27 Jan. 2023 (NOAA, 2023)[9].

Two multispectral sensors were used to date: a Micasense RedEdge-MX (Oct. 2020 - Feb. 2022) and a Micasense RedEdge-P (Oct. 2022 to present). The RedEdge-MX has a 5-band sensor that captures visual (RGB), red edge (RE), and near-infrared (NIR) bands. This sensor was replaced with the RedEdge-P, which contains the same five bands, but has an additional panchromatic (Pan) band that is used to improve the resolution of the dataset from ~7 to ~3.5 cm/pix. From these bands, a normalized difference vegetation index (NDVI) is used to help identify vegetation on the surface (differentiated from sand or straw) to quantify plant cover across the FRA (Figure 3). NDVI is calculated using a ratio of the difference in reflectance values of NIR light (reflected strongly by plants) and red (R) light (absorbed by plants), using the following equation:

$$NDVI = (NIR - R) / (NIR + R)$$

where NIR is near-infrared light reflectance and R is visible red light reflectance. NDVI values range from -1 to +1. Areas with dense vegetation will typically have positive values (~+0.3 to 0.8) while water surfaces or fog (that absorb both bands) tend to have low positive to slightly negative values. Soil surfaces also tend to be characterized by low positive NDVI values (~+ 0.1 to 0.2), depending on color and moisture content. The output histograms of NDVI values for each survey were examined and a threshold value was set to identify pixels with high index values

---

[9] National Geodetic Survey, 2024: 2023 NOAA NGS Aerial Imagery for Situational Awareness: Central California, https://www.fisheries.noaa.gov/inport/item/69185.

(representative of vegetation) (Figure 3). Currently, vegetation cover datasets derived from the UAS surveys do not identify plant species, only pixels that have plant cover.
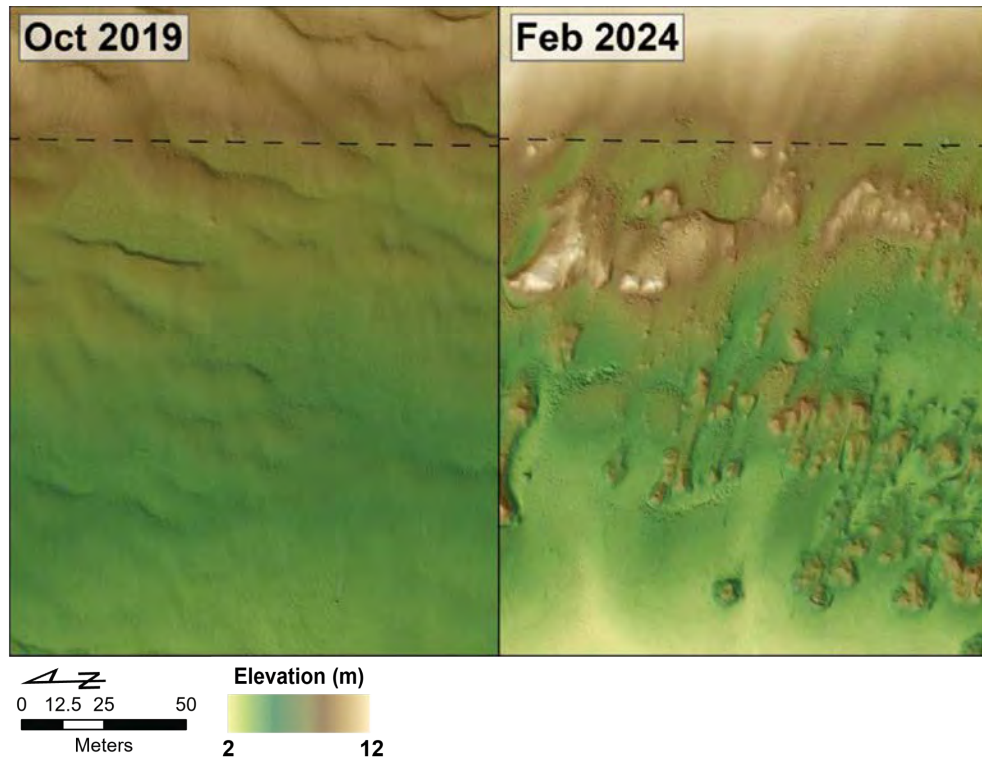
Figure 2. Example DTMs from the Oct. 2019 and Feb. 2024 collection campaigns from TP3. The development from unvegetated transverse dunes to coalesced, vegetated nebkha ridges is evident in the Feb. 2024 DTM. Dashed line represents the landward extent of the treatment plot.

Table 1. Specifications for the RGB and multispectral UAS campaigns. Multispectral sensors were only used after installation of the vegetation treatments in Feb. 2020. GSD is the distance between the center of adjacent pixels and describes the cell size (pixel resolution) of each pixel in centimeters. Total uncertainty values are the calculated vertical uncertainty for datasets used in DTM development and volumetric change detection mapping. As the multispectral datasets were not used for this purpose, no uncertainty value is shown.

UAS Survey Campaign	Survey Date	Sensor Payload	Average Altitude (m)	GSD (cm/pix)	Total Uncertainty (m)
1. Baseline pre- restoration survey	1-2 Oct. 2019	Sony RX1RII	114	1.45	0.038
2. Initial treatment installations	10-11 Feb. 2020	Sony RX1RII	123	1.56	0.033
3. First post-treatment survey and growing season	13-15 Oct. 2020	Sony RX1RII	121	1.54	0.037
	16 Oct. 2020	Micasense RedEdge-MX	113	7.53	—
4. End of first year of geomorphic response and vegetation growth	17-18 Feb. 2021	Sony RX1RII	120	1.52	0.030
	18-21 Feb. 2021	Micasense RedEdge-MX	118	7.89	—
5. Second growing season	4-5 Oct. 2021	Sony RX1RII	121	1.54	0.025
	5-7 Oct. 2021	Micasense RedEdge-MX	119	7.82	—
6. End of second year of geomorphic response and vegetation growth	23-25 Feb. 2022	Sony RX1RII	112	1.42	0.043
	25-26 Feb. 2022	Micasense RedEdge-MX	116	7.71	—
7. Third growing season	17-18 Oct. 2022	Sony RX1RII	125	1.66	0.026
	19-21 Oct. 2022	Micasense RedEdge-P	111	3.67	—
8. End of third year of geomorphic response and vegetation growth	23 Feb. 2023	Sony RX1RII	121	1.59	0.034
	20-21 Feb. 2023	Micasense RedEdge-P	120	3.97	—
9. Fourth growing season	9 Oct. 2023	Sony RGB61	108	1.65	0.049
	10-13 Oct. 2023	Micasense RedEdge-P	135	4.42	—
10. End of fourth year of geomorphic response and vegetation growth	23 Feb. 2024	Sony RGB61	116	1.78	0.071
	21-23 Feb. 2024	Micasense RedEdge-P	133	4.38	—
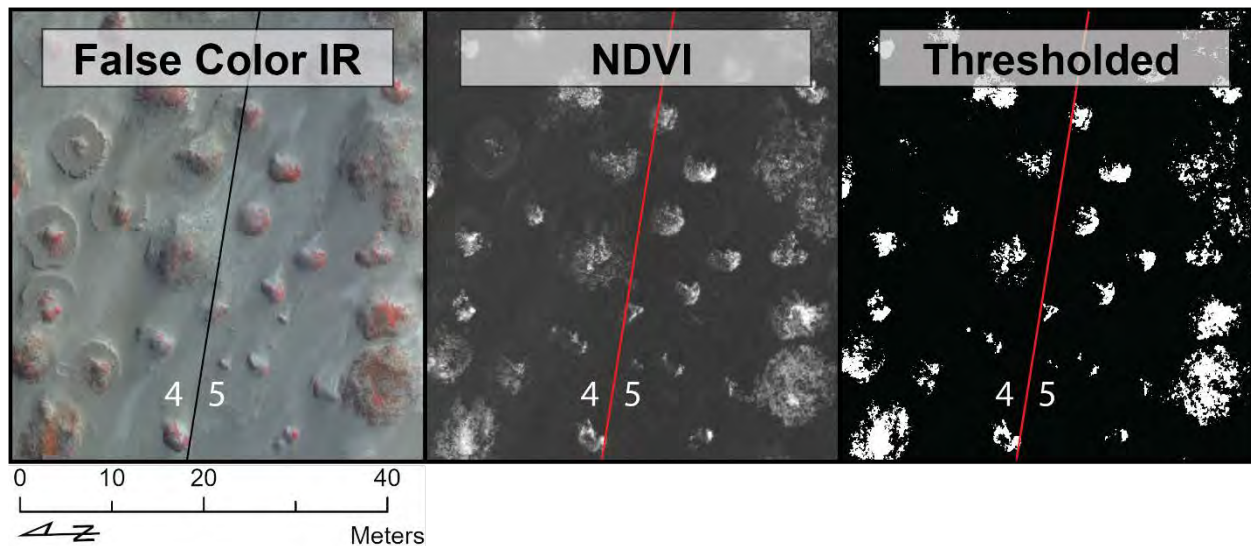
Figure 3. Example of the false color IR output (shows vegetation as red pixels), NDVI output (vegetation as lighter grayscale colors), and thresholded NDVI (vegetation as white pixels) used to extract distinct vegetation pixels within the treatment plots. This location is along the boundary of the low density planting node (TP4) and high density node (TP5) treatment plots.

3. Results

3.1 UAS visible (RGB) imagery and orthophoto mosaics

Figure 1 shows the typical extent of the UAS visual (RGB) orthophoto campaigns. Figure 4 and Appendix A show all biannual UAS RGB orthophoto mosaics of the FRA back to Oct. 2019. These images are used to interpret geomorphic responses within the treatment plots, such as aeolian sand transport corridors (ripples), deflation surfaces (coarse lag deposits), and dune development.

Survey extents have varied slightly through time due to logistical constraints and modifications suggested by SAG and CDPR. The Feb. 2020 campaign included collection of an eastward extending panhandle swath to monitor the rate of change of the landward dunes, and another eastward extent immediately north of Oso Flaco Lake and landward of more established foredunes. The Oct. 2020 campaign included the area between the southern landward extent and the eastern extent, south of the panhandle. The Feb. 2022 campaign included a flight south of Oso Flaco Lake to better understand how those dunes were developing. These changes were made, on advice of SAG and CDPR, to monitor restoration efforts and dune responses landward of the established foredune to the south, as an analog to compare against the FRA to the north. In Feb. 2023 there was a smaller flight extent with the RGB sensor given challenging weather conditions and prioritization of the multispectral sensor, which was flown first and covered the

entire domain. Oct. 2023 saw the addition of a deeper landward extent behind the Western Snowy Plover exclosure through the north Oso Flaco reference area, but this extension was not maintained during the Feb. 2024 collection, which was limited due to inclement weather and prioritization of the multispectral data collection, although the RGB flight did fully cover the FRA. To date, the UAS surveys cover four full plant growth and dune development seasons since implementation of the treatment plots in Feb. 2020.

Figure 4. Visible (RGB) orthophoto mosaics of the FRA from the earliest (Oct. 2019) and latest (Feb. 2024) UAS surveys. Numbers represent the treatment plot (TP) types: TP1) Sheepsfoot texturing (control site), TP2) native seeds, TP3) native seeds + sterile ryegrass seed, TP4) low density straw planting nodes, TP5) high density planting nodes, and TP6) broadcast straw, randomly planted seedlings, and broadcast seed. Notable aeolian activity, nebkha development, and streamlined shadow dune accretion is widespread in all treatments except within the control plot (TP1).

3.2 UAS multispectral imagery and plant cover estimation

To enhance the detection and monitoring of vegetation at the landscape scale in restoration treatment areas, multispectral imagery has been collected since Oct. 2020 (Figure 5). The initial survey focused primarily on the seaward extent of the ODSVRA, including the FRA, seasonal plover exclosure, and established foredunes near Oso Flaco Lake. The Feb. 2021 survey covered a

larger extent to match that of the RGB surveys and this coincident survey strategy has been followed since (Figure 1), with minor variations related to logistics. Multispectral sensors are calibrated pre- and post-flight with a calibration panel so that, while the orthomosaics in Figure 5 may appear to have variable contrast, individual pixels are properly scaled and the extracted indices are accurate.

NDVI values were calculated for all multispectral surveys to detect and map vegetation and its changes through time. Percent plant cover (normalized by total area of each treatment plot) has generally increased through time in all plots except for the control site (TP1) (Figure 6, Table 2). TP6 shows the greatest plant cover change (from 2.5% in Oct. 2020 to 11.7% by Feb. 2024), followed by TP3 (2.7 to 7.0%), TP5 (1.7 to 6.2%), TP4 (0.9 to 4.9%), and TP2 (0.4 to 3.1%). Negligible (<1.0%) plant cover has been observed in the TP1 control site to date.

For context, plant cover observed in historical aerial imagery back to 1939 within the broader ODSVRA was approximately 25% in 1939 with a peak at 37% in 2012 and slight decline to 35% by 2020, before implementation of the FRA. This coverage includes extensive back dune forests and restoration sites, however. Within the foredune zone of the OHV riding area, plant cover was low (2.6 %) in 1939, rose to a peak of 5.3 % in 1966, but steadily declined to ~1% from 1985 to 1998. These lower values reflect the influence of decades of vehicular and other recreation activities at ODSVRA prior to the earliest aerial photography. Within the FRA area specifically, the maximum observed vegetation cover was 3.30% in 1939 then declined to negligible cover by 1985[10]. Since then, plant cover in the FRA remained negligible until after implementation of the restoration treatments in 2020. In contrast, at the nearby South Oso Flaco reference site, plant cover was 26% in 1939, decreased to a low of 24% in 1949, increased to a peak of 66% in 2012, and remained >60% by 2020. At North Oso flaco, foredune plant cover was extremely low (<1%) in the 1930s, but increased notably after 1985 to over 24% by 2012. Plant cover estimates in these reference sites partly reflect the influence of invasive species in these areas. Following restoration in the FRA, plant cover has increased to an average of 6.55% across all treatment plots by Feb. 2024 (Table 2), which remains well below historic coverage ranges of the nearby reference sites.

Superimposed on the general increasing trends in plant cover, Figure 6 also shows seasonal declines (February), then increases (October) in vegetation bracketing the plant growth season. Most treatments also showed a notable decline in plant cover in the most recent monitoring interval (Oct. 2023 - Feb. 2024).

---

[10] Swet, N., Hilgendorf, Z., & Walker, IJ. (2022). UCSB Historical Vegetation Cover Change Analysis (1930-2020) within the Oceano Dunes SVRA. Technical report to the Oceano Dunes Scientific Advisory Group (SAG) and the State of California Parks and Recreation Department Off-Highway Vehicle Division. February 2022.

Table 2. Vegetation cover (%) in each treatment plot (TP1-6) as shown in Figure 6.

	TP1	TP2	TP3	TP4	TP5	TP6
10-11 Feb. 2020	0.00	0.00	0.00	0.00	0.00	0.00
16 Oct. 2020	0.02	0.41	2.66	0.87	1.65	2.54
18-21 Feb. 2021	0.03	0.42	2.15	0.95	1.85	3.28
5-7 Oct. 2021	0.14	1.85	4.87	1.93	3.63	3.54
25-26 Feb. 2022	0.08	1.74	4.55	2.24	4.64	11.35
19-21 Oct. 2022	0.26	3.45	11.47	6.03	9.57	14.82
20-21 Feb. 2023	0.12	2.68	8.93	5.52	9.66	14.83
10-13 Oct. 2023	0.73	3.83	10.36	7.55	9.68	19.36
21-23 Feb. 2024	0.42	3.10	6.95	4.85	6.18	11.68

3.3 Topographic Differencing and Volumetric Change Trends

The topographic difference maps (Figures 7-8) show areas and quantities of significant elevation change that are used to calculate volumes of sediment erosion or deposition between surveys in cubic meters (m^3) or normalized by area ($m^3 \, m^{-2}$), which is effectively an average depth of change (m) over the entire treatment plot (or adjoining unit) areas. Data are also normalized by month to allow comparison of change through time (Table 3), given the difference between the Feb. to Oct. (~8 months) and the Oct. to Feb. (~4 months) intervals. The raster grid from which the volume estimates are determined remains fixed in positioning and size (0.10 m x 0.10 m) across all surveys. Pixels of statistically insignificant change, as determined by a two-tailed T test at a 95% confidence interval in the GCD package (see section 2), are not shown in the change detection maps and are not used to calculate sediment volumes.

Figures 7-9 and Table 3 provide topographic change maps and related values and time series of normalized volumetric changes within the treatment areas and their adjoined geomorphic units between Oct. 2019 and Feb. 2024. Geomorphic units include each of the foredune treatment areas (FD), an adjoining beach area (B) and landward backdune areas (LD)(Figure 1). The first interval (Oct. 2019 to Feb. 2020) provides baseline reference conditions prior to implementation of the restoration treatments. The remaining intervals show responses of the treatment plots for the following four wind, plant growth, and dune development seasons through to Feb. 2024.

One key control on the volumetric and geomorphic responses in the treatments is the amount of sand that enters the upwind beach from the nearshore, which effectively provides supply for aeolian delivery to the treatment plots. Beach units fronting the plots saw variable trends of positive (depositional) and negative (erosional) change in sediment volumes that relate to

seasonal variations (e.g., winter storm erosion signals) and migration of rip current embayments. Generally, the beach units show a declining, albeit highly variable, trend in sand volumes from positive values in the initial Oct. 2019 to Feb. 2020 baseline interval to negative values by Feb. 2023. More recently, the beach units fronting all treatment plots, except TP6, have shown distinct positive trends and values of sedimentation between Oct. 2023 and Feb. 2024. Net change values since the baseline survey (Table 3) suggest beach erosion has dominated fronting the northern plots (TP1-3) while deposition prevails at the southern plots (TP4-6).

Figure 5. Multispectral false-color (G+B+NIR) UAS orthomosaics captured from a Micasense RedEdge-MX 5-band sensor (R, G, B, RE, NIR) in Oct. 2020 and a Micasense RedEdge-P 6-band sensor (R, G, B, Pan, RE, NIR) in Feb. 2024, used to map vegetation cover. Contrast differences are only visual and do not impact the indices calculated from the values of compared bands. Locations of the FRA treatment plots are outlined.
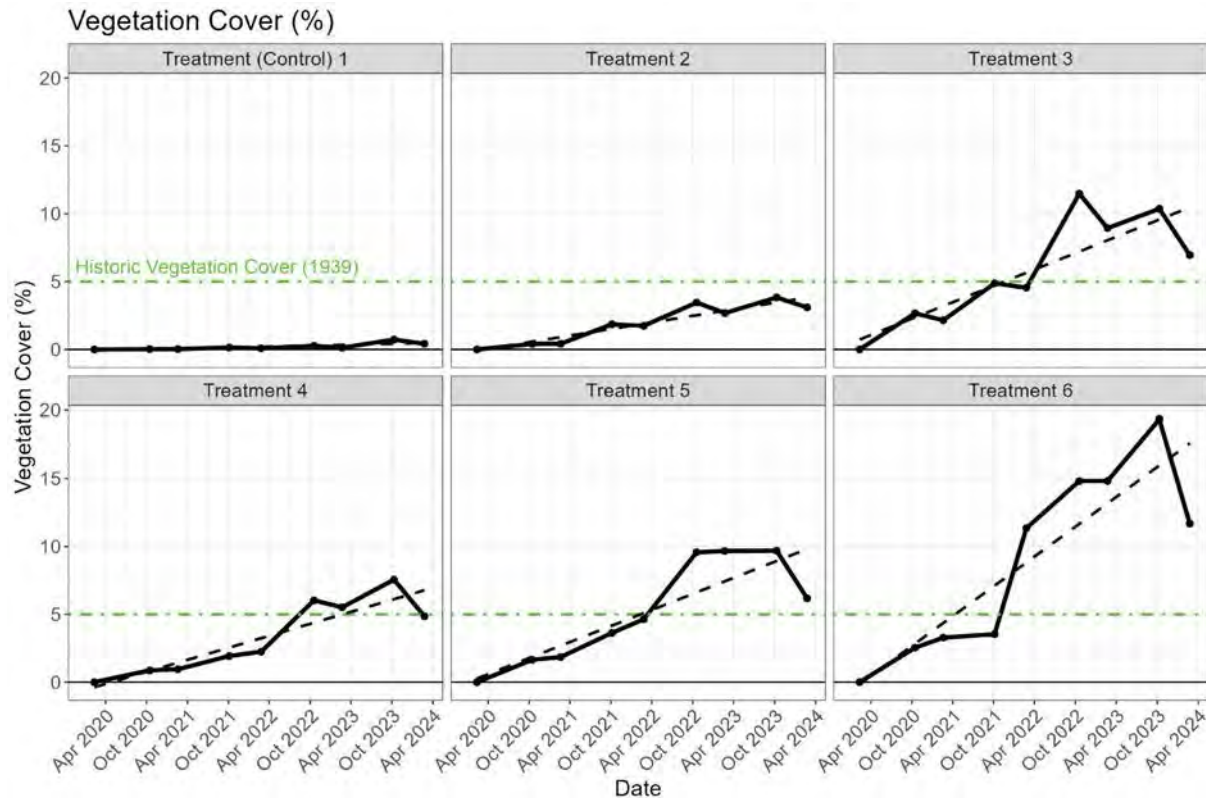
Figure 6. Plant cover (%) by treatment plot through time derived from the multispectral UAS surveys from Feb. 2020 (treatment implementation) through to Feb. 2024. Seasonal fluctuations are evident in most treatments due to declining cover before (Feb.) and increasing cover after (Oct.) the plant growth season. Linear regression fits (black, dashed line) show general trends of increasing vegetation cover, while the green dash-dot line is the peak extent of historic vegetation cover in 1966 (5.3%) within the foredune zone of the OHV riding area in 1966 prior to establishment of the ODSVRA (Swet et al. 2022). Corresponding values shown in Table 2.

In general, net deposition has occurred across all foredune restoration treatment plots, with some deviations, over the monitoring period. The current status of the plots, however, is near neutral to slightly positive accretion (Figure 9, Table 3). Most plots saw distinct negative (erosional) responses from Feb. to Oct. 2023 (except for T6), but trends shifted to positive in all but one treatment (T6) in the most recent interval. TP1 and TP2 continue to show some of the lowest rates of accumulation, reflective of significant recent beach erosion and consistent sediment bypassing due to limited vegetation establishment and nebkha dune development. TP3, despite exhibiting negative net change in both the beach and landward dunes units, shows the second highest net accumulation of sand. TP4 and TP5 experienced comparatively moderate change, as the fourth and third (respectively) highest accumulating plots. TP6 is the only plot that has not exhibited a negative change interval through time and recorded the greatest net deposition, although this is focused largely on the seaward and northern edges of the plots, where fences play a role in capturing sand. Since Oct. 2022, all treatment plots have shown

negative (declining) trends in normalized sediment volumes.

Figure 7. Topographic change maps with corresponding pixels of significant area-normalized volumetric changes (reds = erosion, blues = deposition) for each survey interval between Oct. 2019 and Feb. 2022 overlain on the UAS photomosaics for the second time step in each interval. Restoration treatment areas are outlined and progress from TP1 (control) on the left to TP6 on the right (as indicated in Figures 1 and 4). Intervening OHV transportation corridors, between TP3 and 4, and 5 and 6, are not included in the analysis.

Figure 8. Topographic change maps with corresponding pixels of significant area-normalized volumetric changes (reds = erosion, blues = deposition) for each survey interval between Feb. 2022 and Feb. 2024 overlain on the UAS photomosaics for the second time step in each interval. Restoration treatment areas are outlined and progress from TP1 (control) on the left to TP6 on the right (as indicated in Figures 1 and 4). Intervening OHV transportation corridors, between TP3 and 4, and 5 and 6, are not included in the analysis.

Table 3. Normalized surface volumetric changes for the foredune treatment plots (FD, bold values) and adjoining beach (B) and landward dune (LD) zones. Blue cells indicate sand accumulation, red cells show erosion. Uncertainty values associated with individual measurement campaigns are provided in Table 1.

		Normalized Volumetric Change by Total Area ($m^3\, m^{-2}\, mo^{-1}$) x 100									
Treatment Plot	Geomorphic unit	10/2019 - 2/2020	2/2020 - 10/2020	10/2020 - 2/2021	2/2021 - 10/2021	10/2021 - 2/2022	2/2022 - 10/2022	10/2022 - 2/2023	2/2023 - 10/2023	10/2023 - 2/2024	Net Change (10/2019 - 2/2024)
TP1 (control)	B	1.7	-0.2	-1.1	-0.5	1.5	-0.7	-9.0	0.6	1.6	-0.4
	FD	0.1	0.1	0.4	0.9	0.8	0.4	-0.7	-1.6	0.0	0.0
	LD	-0.1	0.2	0.6	-0.3	0.0	-0.1	0.2	0.0	-0.4	-0.1
TP2	B	1.1	0.6	0.1	0.2	0.0	-0.5	-8.5	-0.6	0.1	-0.6
	FD	0.1	-0.2	0.5	0.3	0.8	0.3	0.6	-0.6	0.0	0.1
	LD	0.2	0.6	0.5	-0.2	-0.3	0.3	0.9	-0.1	0.1	0.1
TP3	B	2.0	0.5	0.4	-0.5	1.6	-1.8	-6.6	0.6	3.6	0.0
	FD	0.3	0.1	0.6	0.7	0.7	1.6	1.0	-0.5	0.0	0.5
	LD	0.2	-0.5	0.7	-0.1	0.4	-0.9	0.4	-1.0	-0.1	-0.3
TP4	B	3.6	1.2	-0.7	-0.3	1.1	-1.5	-1.2	0.6	4.5	0.6
	FD	0.4	-0.2	0.2	0.4	0.4	1.2	0.8	-0.6	0.1	0.3
	LD	0.1	-1.3	0.0	-1.4	0.0	-0.9	0.1	-1.2	0.0	-0.8
TP5	B	3.4	-0.1	0.6	-0.2	1.4	-0.3	-2.0	0.6	3.0	0.6
	FD	0.2	0.1	0.1	0.3	0.3	1.1	0.8	-0.1	0.1	0.4
	LD	-0.1	-1.8	0.1	-1.4	0.0	-2.2	-0.5	-1.7	-0.1	-1.2
TP6	B	1.6	2.3	-1.4	-1.0	0.6	-0.9	-0.1	0.9	-2.0	0.1
	FD	0.2	0.2	0.3	1.1	0.4	1.7	0.8	0.4	0.1	0.7
	LD	-0.1	-2.1	-0.3	-2.2	-0.4	-2.9	-0.9	-1.8	0.0	-1.7
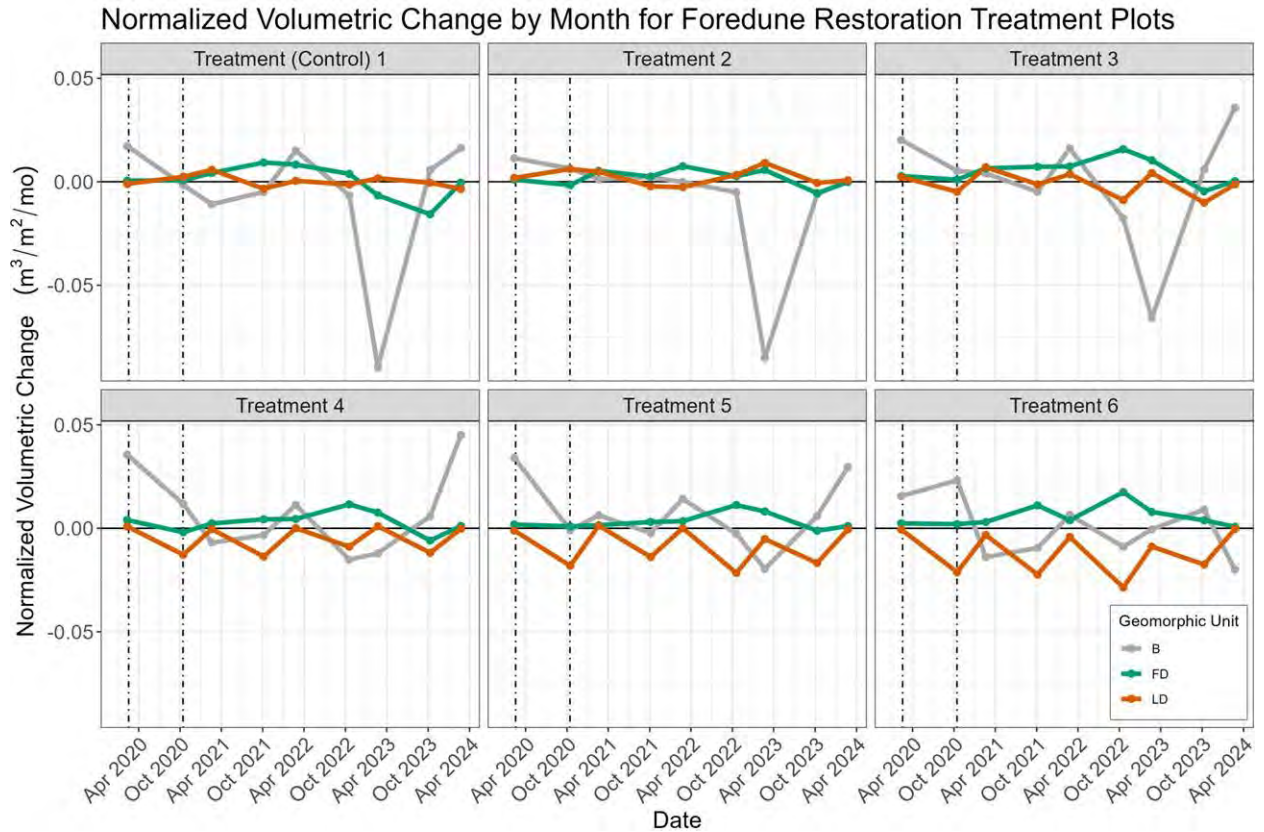
Figure 9. Time series of normalized volumetric changes derived from successive survey intervals for each foredune restoration treatment plot (FD), adjacent beach (B), and landward dune (LD) units. Each point represents net results of volumetric change for the preceding interval (e.g., first point represents net change between Oct. 2019 and Feb. 2020, etc.). Dashed lines delimit the COVID-19 closure period (March 2020 through Oct. 2020).

The foredune plots vary notably in their sedimentation responses to vegetation establishment and/or surface treatments. TP1 (control) and TP2 (native seed) were the least altered by treatment interventions and maintained similar change patterns across all intervals. Sand transport in these plots generated low-lying (0.4-0.6 m), slowly migrating semi-continuous transverse and barchanoid dune ridges and protodunes. Negligible plant cover established in TP1 except for a very few plants near the seaward edge of the plot, first observed in Oct. 2022. Some shadow dunes were present in the landward half of these plots, but these were not associated with vegetation (i.e., nebkha), but rather with nodes of cemented sand and anthropogenic debris[11]. TP2 exhibited a developing nebkha cluster in the center of the plot, but this has not expanded notably by Feb. 2024. TP1 and TP2 recorded the smallest net changes in sand volume over the monitoring period (Table 3).

---

[11] Hilgendorf, Z. Walker, I.J., Swet, N., and Heffentrager, M.(2023). UCSB 2022-2023 ODSVRA Foredune Restoration Survey Report. Research report to the Oceano Dunes Scientific Advisory Group (SAG) and the State of California Department of Parks and Recreation. 44 p.

TP3 (native seed with sterile rye grass seed) has developed significant nebkha, predominantly with Abronia latifolia, and these dunes have started to coalesce to form discontinuous ridges over 2 m tall, which are the tallest dunes across all of the treatment plots. The latest two intervals (since Feb. 2023) showed negative and neutral volumetric changes, respectively, within TP3. The Feb. 2023 to Oct. 2023 interval recorded the only negative budget for TP3, since the installation of the treatment plots. TP3 has shown among the greatest and most consistent positive volumetric changes across the sites and the second largest depositional interval (Feb. to Oct. 2022, 0.122 m^3 m^{-2}) and second greatest net deposition (Oct. 2019 to Feb. 2023, 0.247 m^3 m^{-2}) to date (Table 3).

TP4 and TP5 (low and high density straw planting nodes) suffered localized erosion between planting nodes during early intervals. These 'erosional streets' persist, although nebkha are growing and slowly coalescing in both plots[14]. TP4 and TP5 experienced the fourth and third highest net positive deposition amounts, respectively, to date (Table 3). Nebkha dunes in TP5 are larger than in the neighboring TP4 and closer in height to the larger dunes in TP3, with some dunes over 1.5 m tall. In the most recent Feb. 2024 surveys, however, dunes in TP4 had grown notably, particularly along the seaward half of the plot. Nebkha coalescence was observed in both treatments along the seaward half of the plot by Oct. 2023.

TP6 (broadcast straw + native seeds + plant seedlings) had the most intensive treatment with the highest planting density and complete surface straw cover on installation. Although it maintains the highest plant coverage (Figure 6, Table 2), greatest depositional volumes, and highest net positive sediment budget (Table 3), large nebkha are not developing in this plot, compared to TP3-5. A notable portion of the accretion in TP6 is associated with the sand fence on the northern border with the transportation corridor, which has promoted significant drift development in the treatment plot. This influences the net accretion values, but does not reflect the effects of the restoration treatment itself. The same fence-drift pattern is also observed on the north fence line of TP4.

4. Discussion

Most coastal dunes owe their form and function to the presence of vegetation. In turn, sand loving (psammophytic) plants require the conditions and disturbance processes offered by aeolian processes for their success[12,13] (Hesp & Martinez, 2007; Pickart, Wiedemann & Pickart,

---

[12] Hesp, PA, and Martinez, M. (2007) Disturbance in coastal dune ecosystems. In: Johnson EA and Miyanishi K (eds.) Plant Disturbance Ecology: The Process and the Response, pp. 217–247. Elsevier.

[13] Wiedemann, A, and Pickart, A. (2007). Temperate Zone Coastal Dunes. Ch. 4 in Martinez, M. and Psuty, N. *Coastal Dunes: Ecology and Conservation. Ecological Studies 171*, 53-66. Elsevier.

2007). These interactions are particularly important to recognize when designing and assessing foredune restoration projects. In addition, variability in sand inputs from the upwind beach, variations in other supply- and transport-limiting factors can also influence treatment responses and resulting dune evolution. At ODSVRA, sand volume and resulting geomorphic changes within the treatment plots show seasonal and interannual responses related to variations in factors that limit either the supply of sand to, or transport capacity of, aeolian transport, including: a) surface moisture, which acts as a supply-limiting factor that is highest in wetter winter months, b) the frequency of transporting winds, a transport-limiting factor that is highest in the April-June wind season, c) sand supply to the beach, a supply-limiting factor that varies on seasonal to interannual scales, and d) the extent and type of treatment modifications, such as vegetation establishment and straw cover, which can act as both a supply- and/or transport-limiting factor on seasonal to interannual scales. The following sections interpret these interactions and responses within the FRA treatment plots with respect to sand volume and geomorphic changes, vegetation cover, and dune development. Following this, an assessment of performance of the treatments based on identified indicators is provided.

4.1 Geomorphic and Sand Volume Change Trends

Absolute volumes of sand inputs to the beach, foredune, and landward dune units at each treatment site over the total monitoring period (Figure 10) indicate relatively small changes in TP1 and TP2 in contrast to very large changes in T5 and T6, which reflects an observed north-south gradient in sand supply to the beach as well as an increasing trend in wind strength. In addition, notable erosion is evident in the landward units behind TP4, TP5 and TP6, which reflects lower sediment bypassing and an erosional wake effect that is not as pronounced in the more northern treatment plots. Seasonal to interannual variations are also evident at many locations, reflecting winter beach erosion and/or movement of rip cell embayments that reduce beach width, or spring/summer bar welding on to the upper beach and increased aeolian activity (see also erosion/deposition patterns and trends in Figures 7-9). Figure 9 also shows that, despite high variability in beach sand volumes and a general net erosional trend, the foredune treatment plots have maintained a net positive sediment budget response, indicative of continued accretion in developing vegetated dunes. Significant declines in beach sediment during the winter 2023 season (Oct. 2022 to Feb. 2023) were not mirrored in the adjoined foredune treatment plots, although most showed a continued or increasing negative trend in sand volume in the following interval (to Oct. 2023). This lagged response, on the order of months, reflects an expected delay between sand volume changes on the beach and resulting responses of aeolian delivery into the treatment plots. The most recent Oct. 2023 to Feb. 2024 interval showed some of the smallest volumetric changes, overall, speculatively attributed to wetter conditions (limiting transport) and weaker winds (observed at the monitoring stations, not presented in this report).
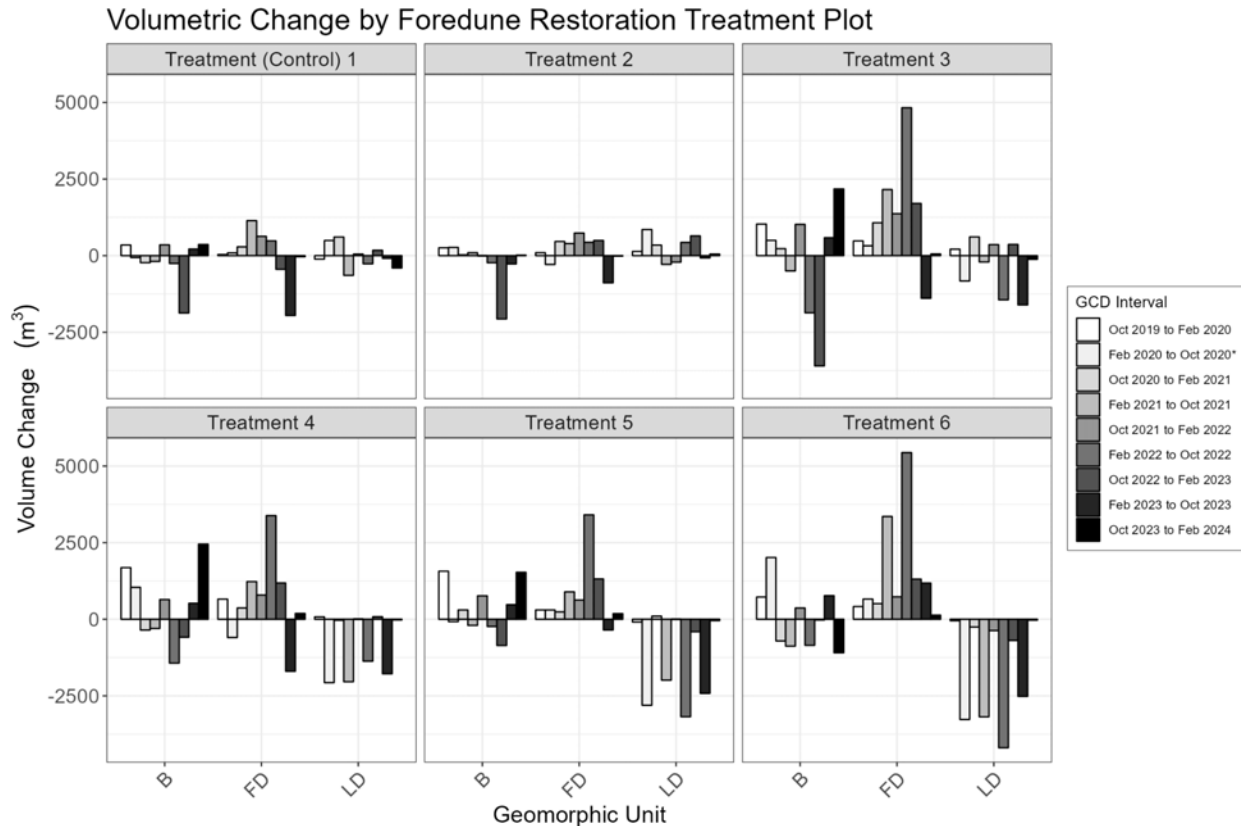
Figure 10. Bar graph of observed volumetric changes (m³) within the beach (B), foredune restoration plots (FD), and landward dunes (LD), for each treatment, across each topographic change interval. Asterisk in the legend indicates the Feb. 2020 to Oct. 2020 COVID-19 closure period that occurred between Mar. and Oct. of 2020.

Changes in the landward dune units (LD) behind the FRA are somewhat decoupled from those within the upwind treatments and beach plots due to the continued influence of OHV traffic. These units also differentially experience landscape scale secondary flow patterns generated by larger dunes outside of the FRA (e.g., Pavilion Hill or larger barchanoid and transverse dunes)(Figure 1) as well as evolving vegetation and dune roughness effects that modulate surface shear stress and sand transport patterns within and beyond the treatment plots. Areas downwind of TP3-6 show seasonally alternating (peak-valley) trends in their sediment budgets, whereas areas downwind of TP1-2 do not show this trend. This could also relate to the greater and seasonally varying influence of plant growth/roughness, sand accretion, and dune development within TP3-6 compared to TP1-2. For instance, this seasonal pattern is evident in the LD unit downwind of TP3, which alternated between positive budgets in fall/winter (Oct. to Feb.) and negative budgets during the wind and plant growth season (Feb. to Oct.) when more sediment accreted in the upwind treatment plot. The longer-term trend of this cycle is predominantly negative in the LD units behind TP4-6 (Table 3), which have developed increasingly larger dunes and more extensive plant cover.

The influence of regional scale seasonal to interannual climatic variability events, such as El Niño seasons, are not easily discernible in foredune treatment responses. Generally, El Niño seasons bring increased chance of elevated erosional water levels in coastal California[14]. The El Niño event of 2023-24 was one of the five strongest on record[15] and peaked in Nov. 2023 through Jan. 2024. This event did not directly correlate, however, with significant beach erosion at ODSVRA. Rather, notable beach erosion occurred in the preceding winter (2022-2023) during a season of pronounced coastal storms and atmospheric river events.

4.2 Vegetation Change and Dune Development

Since implementation, all restoration treatment plots (TP2-6) have shown an increase in plant cover (Figure 6). TP6 and TP3, respectively, experienced the fastest rates of vegetation establishment, while the TP1 control site and TP2 have shown negligible to slow rates of plant cover to values that remain below the historical average. Interestingly, all plots showed a notable decrease in plant cover in the most recent interval (Oct. 2023 to Feb. 2024).

The patterns of vegetation change in this most recent interval are shown in Figure 11. While all plots recorded decreases in plant cover, TP6 experienced the greatest loss (-7.70%), followed by TP5 (-3.50%), then TP3 (-3.40%). The vegetation change map shows that declines in plant cover were widespread and relatively evenly distributed across all plots, as opposed to localized impacts along the seaward edge that could relate to high water event impacts (e.g., erosion, seawater inundation), for example. Although the specific cause of this decline is unknown, some combination of relatively wet winters, lower wind conditions (which reduce burial and inhibit the growth of many coastal plants[16]), and saltwater inundation from recent winter storms could be at play. It is unclear if this downturn reflects a plateau response in the plant community, or simply just natural variability as the ecosystem continues to develop. Regardless, continued monitoring is recommended to track progress in plant cover and, in conjunction with CDPR vegetation transect monitoring, to identify if there are particular species responses behind this recent decline in vegetation.

Corresponding dune development continues to differ distinctly across the treatment plots. At the TP1 control site, protodunes and transverse/barchanoid ridges continue to migrate through the

---

[14] Barnard, P.L., Short, A.D., Harley, M.D., Splinter, K.D., Vitousek, S., Turner, I.L., Allan, J., Banno, M., Bryan, K.R., Doria, A., Hansen, J.E., Kato, S., Kuriyama, Y., Randall-Goodwin, E., Ruggiero, P., Walker, I.J., & Heathfield, D.K. (2015). Coastal vulnerability across the Pacific dominated by El Niño/Southern Oscillation. Nature Geoscience 8, 801–807. https://doi.org/10.1038/ngeo2539.

[15] [12] World Meteorological Organization (WMO), 05 March 2024. "El Niño weakens but impacts continue." https://wmo.int/news/media-centre/el-nino-weakens-impacts-continue.

[16] Tobias, M.M.(2015). California foredune plant biogeomorphology. Physical Geography, 36(1), pp.19-33.

plot, ranging in height from 0.3 m near the seaward edge to 1.3 m at the landward edge, with limited nebkha development near the seaward edge of the plot. Combined with a net neutral sediment budget, this indicates appreciable sand bypassing through the control plot due to limited vegetation cover.
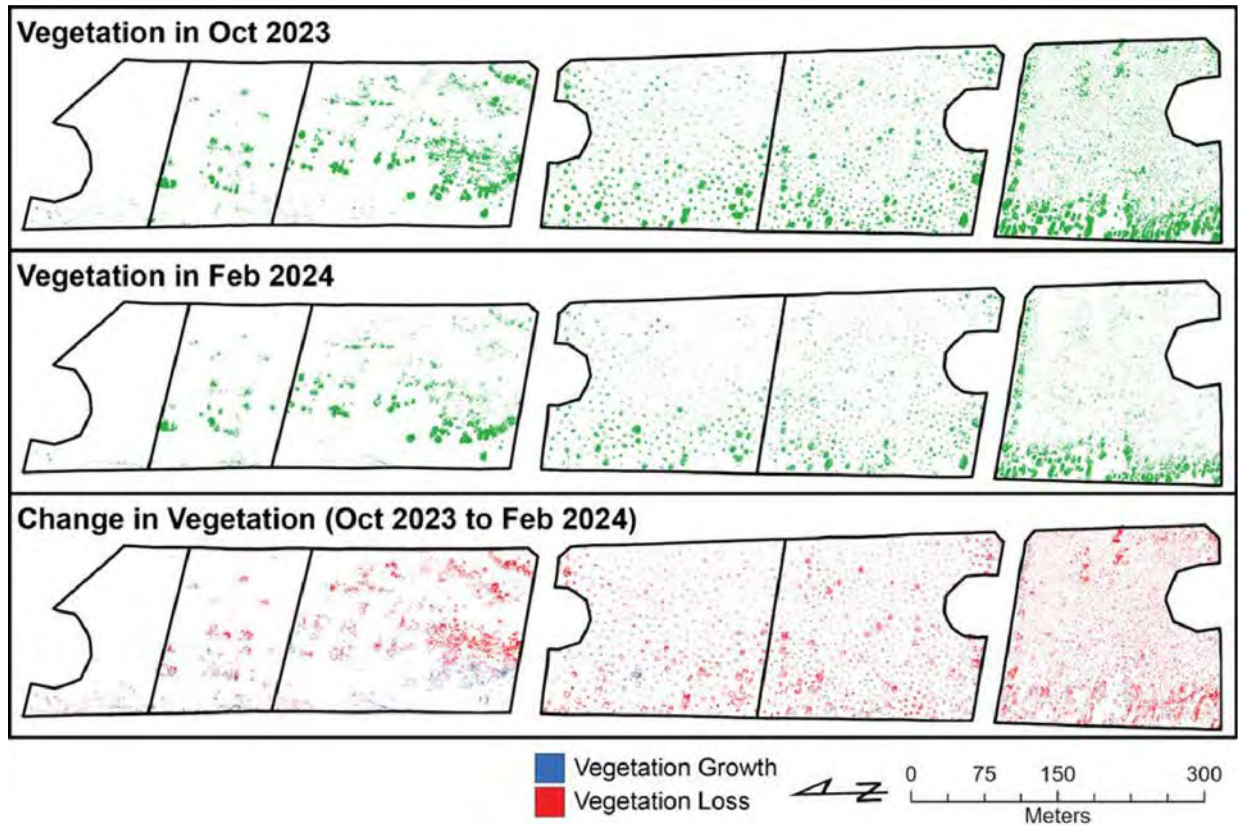
Figure 11. Change in vegetation between Oct. 2023 and Feb. 2024. Green represents pixels with vegetation in the top two panels (Oct. 2023 and Feb. 2024). The bottom panel shows where vegetation expanded (blue) or was lost (red) from Oct. 2023 to Feb. 2024.

A similar pattern of migrating dune ridges was observed in TP2 and TP3, but with vegetated nebkha near the center of TP2 (>2 m high) and much larger (>3 m) coalesced nebkha ridges in TP3. These nebkha are formed predominantly with Abronia latifolia. Until Oct. 2023, TP2 and TP4 were the only sites with developed nebkha to show net erosion (volumetric loss) in response to wind erosion following installation. In TP4, this related to the development of erosional streets between the lower density straw planting circles.

Widespread nebkha development was observed in TP4-6. In TP4 and TP5 nebkha developed mostly on the planting circles and now reach heights > 2 m. TP5 has a greater number of larger nebkha distributed more broadly across the plot due to the closer spacing of the planting nodes, whereas nebkha in TP4 are generally confined to the seaward half of the plot. TP6 began as the

roughest of all the plots (full straw cover, many randomly distributed plants), but only the seaward edge and northern fence line of the plot have shown appreciable dune development, while the size and development of nebkha in the central portion of the plot remains limited.

Feedbacks between dune roughness, secondary flow patterns, surface shear stress, and sand transport will continue to evolve and influence dune development[17]. While beyond the scope of this report, ongoing work comparing wind data from the meteorological stations at the eastern edge of the plots, nebkha development, and geomorphic change suggests that TP3, TP5, and TP6 have the greatest impact on the wind fields. Variations in roughness patterns between these plots has resulted in notably different dune development pathways (Figure 12). TP5 has formed elongated nebkha chains with some coalescence, partly in response to the initial (random) arrangement of the straw planting circles. TP3 has developed laterally coalesced nebkha ridges at multiple locations to form some of the largest dunes within the FRA. Additional observations in TP2 and TP6 confirm two distinct developmental pathways. First, nebkha in TP2 and TP6 tend to 'clump' (wind-normal coalescence) and widen to produce discontinuous flow-transverse nebkha ridges. This lateral extension of nebkha is key to the development of a shore-parallel foredune ridge and the discontinuous morphology of foredune ridges in central and southern California is the preferred form, given the controls of regional climate and native dune plant communities[2]. Second, nehbkha in TP4 and TP5 primarily exhibit 'chaining' (wind-aligned extension) that connects downwind nebkha via shadow dune extension. This pattern is partly driven by initial positioning of the planting zones and intervening erosional streets, but this type of morphological organization (long streamlined nebkha ridges with erosional deflation troughs) is also observed in the North Oso Flaco reference site (see Figure 1).

---

[17] Walker, I. J., & Hesp, P. A. (2013). 11.07 Fundamentals of Aeolian Sediment Transport: Airflow Over Dunes. Treatise on Geomorphology, ed. J. F. Shroder, 109–133. Elsevier
https://linkinghub.elsevier.com/retrieve/pii/B9780123747396003006

Figure 12. Examples of two distinct dune evolution responses emerging in the treatment plots. Nebkha chaining (example from TP5) involves wind-aligned extension of nebkha and shadow dunes to form long, linear ridges that do not exhibit substantial wind-normal coalescence with proximal nebkha. Nebkha clumping (example from TP3) refers to lateral coalescence of nebkha that produces discontinuous wind-normal dune ridges with some wind-aligned shadow dune extension that facilitates wider nebkha organization with a broader tail.

4.3 Performance Assessment of Restoration Treatments

The foredune restoration project at ODSVRA was designed to re-establish a foredune ecosystem with dust emissions mitigation benefits using a 'nature-based' approach with an assortment of treatment types of increasing levels of intervention. As the project is subject to adaptive management, it is important to recurrently evaluate the relative performance of the treatments for forming self-sustaining dunes and reducing dust emissions. In response, we developed, in consultation with SAG and APCD, a series of indicators of performance that would be monitored and assessed each year. The outcome is a cumulative score whereby lower total values indicate higher overall performance. Indicators and relative performance assessment evaluation (Figure 13) are discussed below and explained further in Walker et al. (2023)[1].
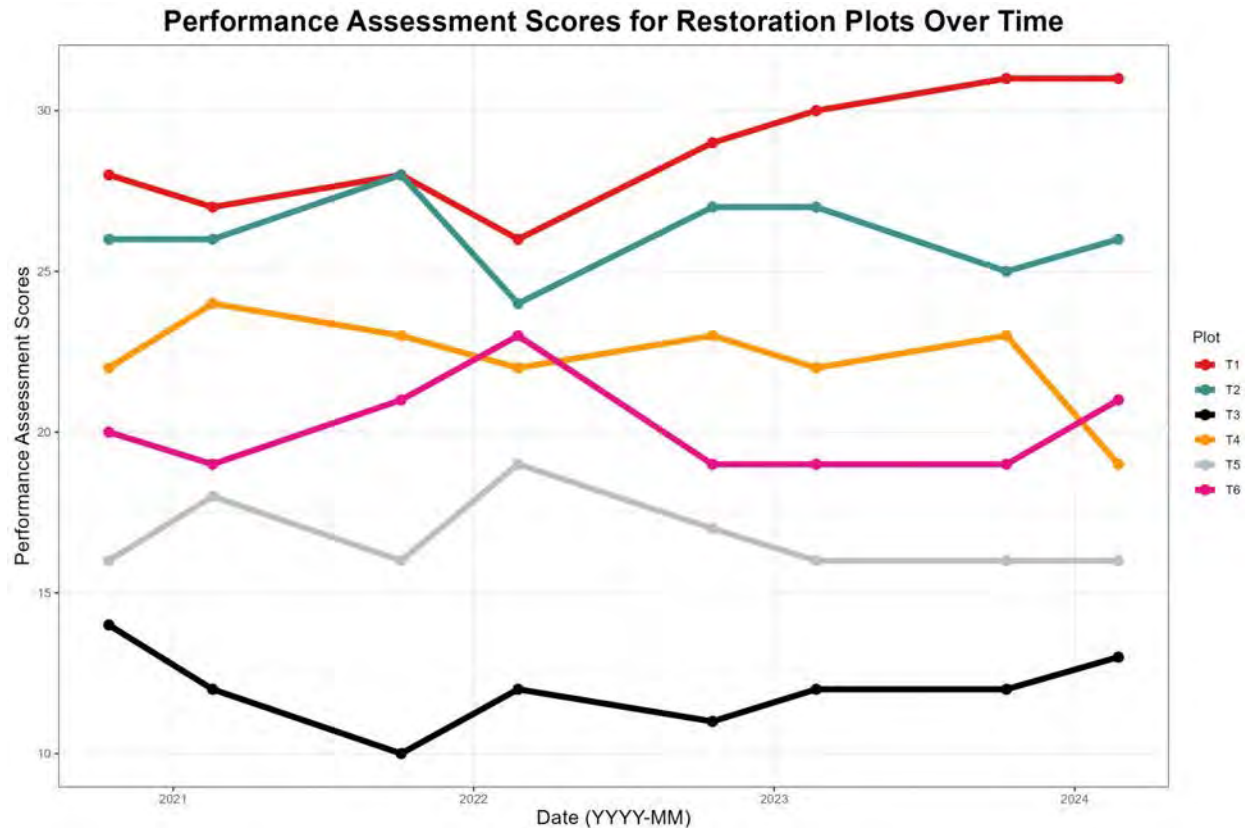
Figure 13. Performance assessment trends of restoration treatment plots since installation in Feb. 2020. Performance scores are derived based on relatively ranked scores (1 = best performer, 6 = poorest performer) across 5 different indicators, including: 1) positive sediment budget, 2) aeolian activity, 3) plant cover, 4) dune development, and 5) dust emissions mitigation potential. Lower cumulative scores indicate more effective performance. See text and Walker et al. (2023)[1] for further description.

Figure 13 shows the trajectories of cumulative treatment plot performance since installation in Feb. 2020. Generally, the rankings have not changed significantly since Oct. 2022, with the exception of a recent switch between TP4 and TP6. Overall, TP3 has maintained the highest performance ranking (lowest scores) since installation, followed by TP5. TP2 maintains the poorest performance, whereas TP4 and TP6 have alternated twice through time for third and fourth in the total performance ranking. The recent switch in ranking for TP4 over TP6 relates to a negative trend in sediment budget (though still positive), limited nebkha development, and greatest declines in vegetation cover in TP6. Specific summaries for each of the assessment criteria are as follows:

1. All foredune treatment plots continue to show net positive sediment budgets. Even though the last two intervals have exhibited mostly negative (Feb. 2023 to Oct. 2023) or neutral (Oct. 2023 to Feb. 2024) budgets, the net change remains positive across all plots and greater than that of the TP1 control plot (minimal/neutral). TP6 exhibits the highest net positive change,

followed by TP3, yet most of the response in TP6 is limited to sand fence accretion along the northern margin and development of nebkha along the seaward edge.

2. Aeolian processes remain active in all treatments shown by rippled sand transport corridors, continued dune development, coalescence and migration, and persistence of erosional deflation surfaces with coarse lag deposits on all sites. Some interdune erosional responses are expected during early stages of dune development (e.g., erosional corridors between developing nebkha) and do not necessarily reflect poor performance. Maintenance of aeolian processes is required to provide needed ecological disturbance required for plant growth and dune development.

3. Plant cover shows a net positive trend in all treatment plots. Increases in the TP1 control site have been negligible until recently and, although very small, are restricted to the seaward edge of the plot. Appreciable declines in plant cover were observed in all treatments since Oct. 2023. This was most pronounced in TP6, with smaller declines in TP3-TP5, and little change in TP2. The pattern of vegetation decline is widespread (vs. localized) in all plots and the cause remains uncertain, but could relate partly to recent unusually wet and stormy winter conditions. On average, plant cover across the FRA (excluding TP1) is 6.55% with a current maximum of 11.68% in TP6 and a minimum of 3.10% in TP2. Some species, namely Abronia latifolia, have shown rapid establishment and growth, promoting appreciable dune development. Recent changes in the trajectory of plant community development reinforce that more time is required to assess broader foredune ecosystem re-establishment and sustainability.

4. Dune development continues in all treatment plots. The largest (>2 m) nebkha have developed in TP3 and TP5, smaller (1.0-1.5 m) nebkha in TP2 and TP4, and multiple smaller nebkha in TP6. This past year (2023-2024) also saw increased development of nebkha along the seaward edge of most treatment plots. Appreciable transverse, unvegetated dune migration and sand bypassing continues within the TP1 control plot, yet it is important to maintain a control site that is also not subject to OHV activity for reference. Two distinct patterns of dune evolution have emerged - nebkha clumping (with lateral extension) and chaining (with downwind elongation) - both of which are important indicators of the next stages of foredune evolution at the site. As dune evolution continues in the presence of vegetation, continued accretion, geomorphic and ecological diversity, and dust mitigation benefits are expected.

5. Potential for treatments to reduce dust emissions is increasing as indicated by qualitative observations of increasing dune development, net increases in sediment accretion and vegetation cover, and recent PI-SWERL testing by DRI in the FRA in Summer 2022. Collectively, these observations suggest that the FRA, and other exclosed areas experiencing dune

development and increasing plant cover (e.g., the Western Snowy Plover exclosure) have lower dust emissivity than neighboring open riding areas. More quantitative assessment of FRA treatments on flow dynamics and shear stress patterns is recommended to better identify related aerodynamic processes within, and dust emissions mitigation benefits downwind, of the restoration treatments.

5. Summary and Conclusions

To monitor and assess the performance of the foredune restoration dust mitigation project at the ODSVRA, biannual UAS surveys of the FRA have been conducted from Oct. 2019 through to Feb. 2024. Primary data products, gathered with a WingtraOne fixed-wing UAS platform, include:

1. Ten (10) high resolution (~1.5 cm) visual (RGB) aerial orthomosaic images encompassing ongoing foredune restoration efforts and sites of landward interest between Pavilion Hill and Oso Flaco Lake,

2. Eight (8) high resolution (~3.0-7.5 cm) multispectral (RGB-RE-NIR-Pan) orthomosaic images collected concurrently with the RGB datasets since Oct. 2020,

3. Eight (8) high resolution (~3.0-7.5 cm) NDVI orthomosaics derived from the multispectral orthomosaic datasets used to assess vegetation extent and change,

4. Ten (10) high resolution (10 cm) three-dimensional point clouds and rasterized DTMs of surface topography used to assess site geomorphic and sediment volume changes, and

5. Nine (9) topographic change maps of statistically significant locations of erosion and deposition derived by comparison between DTM intervals.

Prior to implementation of the FRA in Feb. 2020, there was negligible vegetation present at the site and site geomorphology was primarily driven by: i) aeolian processes moving sand landward by saltation and low transverse dune migration, and ii) the impacts of vehicle activity and camping. From the baseline (pre-restoration) surveys (Oct. 2019 to Feb. 2020), supply to the beach was variable, but net positive and deposition within the FRA generally was low to negligible over the barren sand surfaces. Following implementation of restoration treatments, sand accretion, plant growth, and resulting dune development has continued steadily within the treatment plots, with some (TP2-TP6) featuring larger nebkha dunes (exceeding 2 m in TP3, TP5) and appreciable vegetation cover (~3-12%) to date. During this past year (2023-2024), low winds and significant precipitation might partly explain observed decreases in plant growth and low to neutral rates of accretion, although this is speculative. Despite a strong El Niño event during 2023-24, widespread erosion of the beach was not recorded in the recent change detection results, although some overwash and localized erosion along the leading edge of the plots was

observed.

Following four full wind and plant growth seasons, the restoration plots continue to evolve on different trajectories as a function of initial treatments and variability in other controlling factors such as sand supply to the beach, plant cover, and roughness effects. The relative rankings of treatment performance has not changed significantly since Oct. 2022. Overall, TP3 has maintained the highest performance since installation, followed by TP5, due largely to continued positive sediment budgets, greatest amounts of dune development and extension, consistent maintenance of aeolian activity, continued increases in plant cover, all with collective impacts for providing the greatest potential reductions in dust emissions. Next to the TP1 control plot, which received no vegetation treatment intervention, TP2 maintains the lowest performance due to modest amounts of accretion and dune development, low rates of plant cover increase, and correspondingly lower relative dust emissions reduction potential. The most intensive treatment (TP6) slid recently to second lowest performance due to continued declines in sediment budget, limited dune development, and marked declines in vegetation cover. Monitoring will continue as the treatments evolve to detect further responses indicative of success or concern for adaptive management and for longer-term sustainability of the FRA as a dust control mitigation.

Appendix A: Biannual RGB orthomosaics of the FRA from Oct. 2019 to Feb. 2024.

Oct 2020

Feb 2021

Oct 2023

Feb 2024
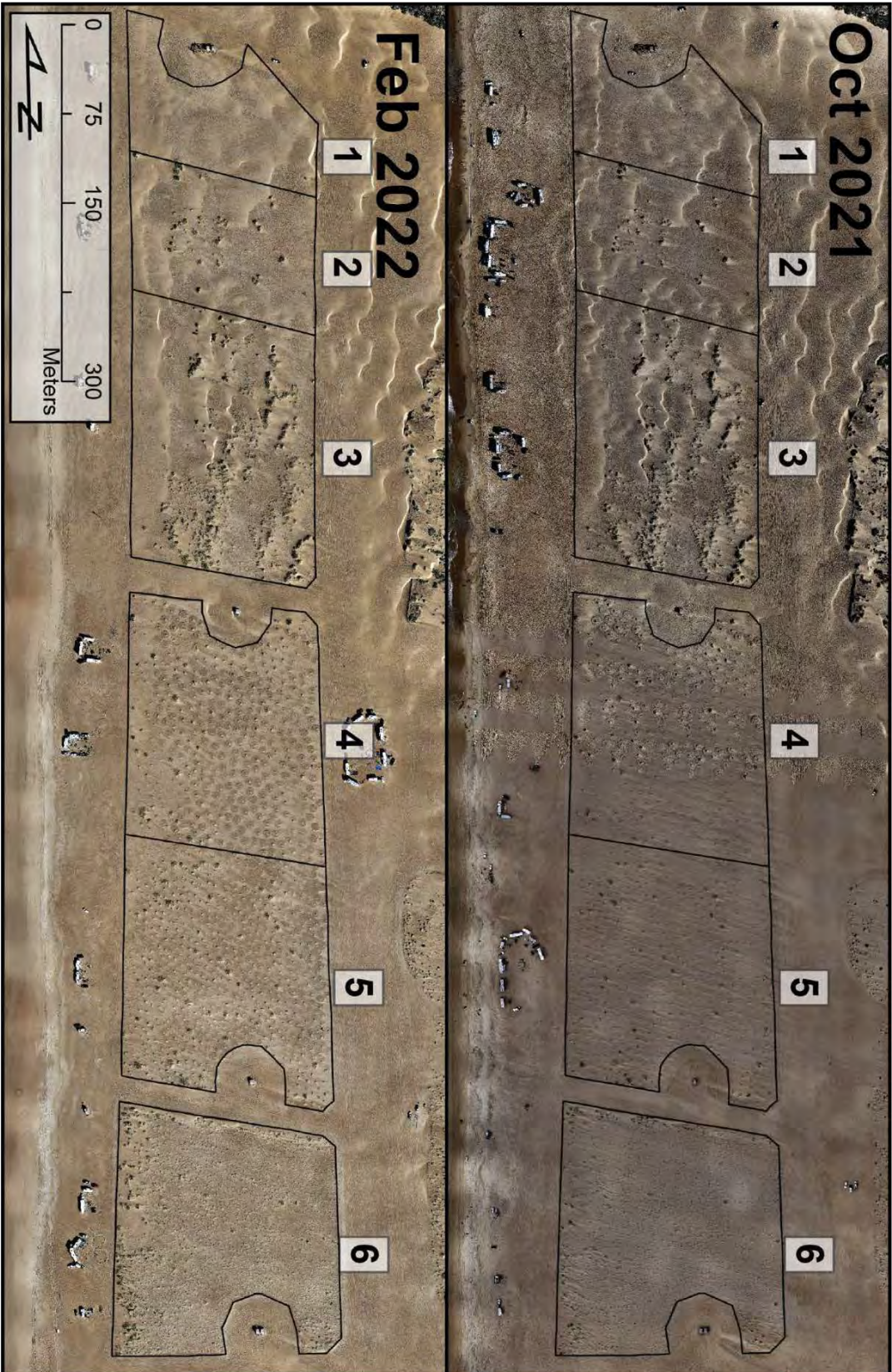
THIS PAGE WAS INTENTIONALLY LEFT BLANK.

July 3, 2024

Memo: <u>SAG Review of UCSB Report - "2023-2024 ODSVRA Foredune Restoration UAS Monitoring Report"</u>

From: Scientific Advisory Group[1]

To: Jon O'Brien, California Department of Parks and Recreation

Cc: Ronnie Glick, California Department of Parks and Recreation

The Scientific Advisory Group (SAG) received a copy of the University of California, Santa Barbara (UCSB) report *"2023-2024 ODSVRA Foredune Restoration UAS Monitoring Report"* on June 19, 2024. SAG members have had the opportunity to review the document and this memo provides feedback on the UCSB report. Line item comments and editorial suggestions have been inserted into a PDF copy of the report forwarded with this memo.

The UCSB report offers a thorough analysis of the performance of the nature-based foredune restoration project at the Oceano Dunes State Recreational Vehicle Area (ODSVRA). The report provides insightful descriptions of data collection technologies and methodologies and incorporates relevant photographs, graphs, and tables to elucidate data interpretation. Previous concerns raised by SAG regarding the 2022-2023 UCSB report have been addressed. The UCSB report effectively tracks dune development in the project area over the past four years compared to a pre-restoration baseline survey and is an important contribution to understanding the development of foredune systems in this region.

As the foredune restoration area moves toward an equilibrium state of adjustment following initial treatments in 2019, SAG suggests revisiting the performance assessment criteria. While the current criteria, developed in collaboration with SAG, evaluate performance based on changes from prior states (e.g., sediment volume capture), it may be beneficial to consider how these criteria will apply once the treatment areas evolve to an equilibrium condition.

Respectfully,

The Scientific Advisory Group

Bernard Bauer (Chair), Carla Scheidlinger (Vice-Chair), Mike Bush, Jack Gillies, Jenny Hand, Leah Mathews

---

[1] SAG member Dr. Ian Walker recused himself from SAG review of this document due to potential conflict of interest.

2023-2024 ODSVRA
Foredune Restoration UAS Monitoring Report

Prepared by: Zach Hilgendorf[1,2], Ian Walker[1], and Madison Heffentrager[1]

[1] Department of Geography, University of California, Santa Barbara
[2] Department of Geography and Anthropology, University of Wisconsin-Eau Claire
June 2024

List of Acronyms:

California Department of Parks and Recreation – CDPR
Desert Research Institute – DRI
Digital Elevation Model – DEM
Foredune Restoration Area - FRA
Geomorphic Change Detection – GCD
Ground Sampling Distance – GSD
Light Detection and Ranging - LIDAR
Near Infrared – NIR
Normalized Difference Vegetation Index – NDVI
Oceano Dunes State Vehicular Recreation Area – ODSVRA
Off-Highway Vehicles – OHV
Particulate Matter – PM
Particulate Matter Reduction Plan - PMRP
Portable In-Situ Wind Erosion Laboratory – PI-SWERL
Post-Processing Kinematic - PPK
Red-Edge – RE
Red-Green-Blue Spectral Bands – RGB
San Luis Obispo Air Pollution Control District – SLO-APCD
Scientific Advisory Group – SAG
Structure-from-Motion – SfM
Stipulated Order of Abatement - SOA
Treatment Plot - TP
Uncrewed Aerial System – UAS
University of California Santa Barbara – UCSB

EXECUTIVE SUMMARY

A foredune restoration project was established in Feb. 2020 at ODSVRA as a nature-based solution to mitigate PM_{10} dust emissions from a highly emissive 48-acre site by promoting sand deposition and dune development. The foredune restoration area (FRA) consists of six treatment plots (TP), including (north-south): TP1) a control plot only textured by a sheepsfoot roller; TP2) sheepsfoot texture and broadcast native seeds; TP3) sheepsfoot texture and broadcast native plant and sterile rye grass seeds; TP4) low-density straw planting circles with nodes of juvenile native plants; TP5) high-density straw planting circles with nodes of juvenile native plants; TP6) complete straw cover with high density of juvenile plants.

An uncrewed aerial system (UAS) with high resolution cameras has been flown biannually (October and February) since Oct. 2019 to monitor and detect geomorphic and vegetation changes in the FRA and adjoining beach and back dune areas. To date, 10 flights have been conducted and resulting datasets include: georeferenced orthomosaics, plant cover maps, digital elevation maps (DEMs), topographic change maps, and sand volumetric change estimates. These datasets are used to examine patterns and volumes of sediment erosion/deposition across the site and changes in vegetation over [1] time. In turn, these results are used to identify and interpret the performance of the treatments based on indicators of dune development, sediment budget response, vegetation trends, and dust mitigation potential. This report provides results from four years of development from Oct. 2019 to Feb. 2024.

Sand supply to the beach, which feeds aeolian transport into the FRA and subsequent dune development, has been highly variable over time, as expected, due to seasonal to interannual changes in wave energy, beach erosion/rebuilding, and movement of rip current embayments. Generally, though variable, beach sediment budgets trended from positive from the pre-restoration baseline interval (Oct. 2019 to Feb. 2020) to negative by Feb. 2023, then back to positive values most recently (Oct. 2023 to Feb. 2024). Net changes over the period of study within the beach units indicate erosion in the northern three plots (TP1-3) and deposition in the southern three plots (TP4-6).

Despite notable fluctuations in ~~beach supply,~~[3] the treatment plots [2]~~have~~ maintained net depositional responses, albeit with small deviations over the years. Deviations include neutral (+/- 0.001 $m^3m^{-2}mo^{-1}$) to negative sediment budgets in Feb. to Oct. 2020, Feb. to Oct. 2023, and Oct. 2023 to Feb. 2024. Meanwhile, net change of the TP1 control site [4]~~as~~ remained neutral while the neighboring TP2 showed the lowest rates of accumulation of the treatment plots,

Number: 1   Author: SAG   Subject: Comment on Text   Date: 7/1/2024 10:52:07 AM
Suggest using "through" time and "over" or "across" space when writing about space and time.

Number: 2   Author: SAG   Subject: Cross-Out   Date: 6/20/2024 2:38:25 PM

Number: 3   Author: SAG   Subject: Inserted Text   Date: 6/20/2024 2:37:21 PM
sand supply to beach

Number: 4   Author: SAG   Subject: Cross-Out   Date: 6/20/2024 2:38:52 PM

indicating [1] notable sediment bypassing and long[2]er-term declines in sand inputs from beach erosion. Comparable recent beach erosion occurred at TP3, yet this treatment exhibited the second highest net positive sediment budget and significant dune development. TP4 and TP5 showed moderate amounts of sand accumulation (fourth and third highest, respectively), while TP6 accumulated the greatest net amount of sand, although the majority of this deposition was confined to the seaward edge of the plot and downwind of a drift fence along the northern margin. TP6 was the only plot that did not exhibit a negative sediment budget interval, while TP3 and TP5 only experienced one negative change interval (Feb. 2023 to Oct. 2023).

Plant cover [3] has generally increased since implementation for all treatment plots except the TP1 control site, which continues to show limited cover. T[4]6, the most intensive treatment, showed the greatest net increase in plant cover (+11.68%) to Feb. 2024, followed by TP3 (+6.95%), TP5 (+6.18%), TP4 (+4.85%), and TP2 (+3.10%). Peak observed historical cover at the FRA site and in the broader foredune zone (~400 m inland) in the OHV riding area, respectively, were about 3% and 6% in 1966[3]. Since Oct. 2023, a distinct decrease in plant cover in all treatment plots [5] has occurred with TP6 experiencing the largest declines (-7.70%) followed by TP5 (-3.50%), then TP3 (-3.40%). The cause of this recent decline is unclear, but the patterns are widespread (vs. localized) and could relate to unusually wet and stormy winters since 2022. Some species, namely *Abronia latifolia*, have shown rapid establishment and growth, and played leading roles in dune development.

In terms of FRA treatment performance, following four full wind and plant growth seasons, the plots continue to evolve on different trajectories as a function of initial treatments and variability in sand supply, plant cover, and changing roughness. Relative rankings of treatment performance have not changed significantly since Oct. 2022, which[6] TP3 as a top performer, followed by TP5, due to continued positive sediment budgets, greatest amounts of dune development and extension, maintenance of aeolian activity, continued increases in plant cover, and greatest potential for reducing dust emissions. TP2 maintains the lowest performance due to modest amounts of accretion and dune development, low plant cover, and correspondingly low dust emissions control potential. The most intensive treatment (TP6) slid recently to second lowest performance due to continued declines in sediment budget, limited dune development, and marked declines in vegetation cover. Monitoring will continue as the treatments evolve to detect further responses indicative of success or concern for adaptive management and for long[7]er-term sustainability of the FRA as a dust control mitigation.

Number: 1   Author: SAG   Subject: Cross-Out   Date: 6/20/2024 2:39:11 PM

Number: 2   Author: SAG   Subject: Cross-Out   Date: 6/20/2024 2:39:17 PM

Number: 3   Author: SAG   Subject: Cross-Out   Date: 6/20/2024 2:40:11 PM

Number: 4   Author: SAG   Subject: Comment on Text   Date: 6/26/2024 1:15:29 PM
These percent increases are relative to what time period? This would help clear up the last part of this paragraph when discussing cover decline.

Number: 5   Author: SAG   Subject: Cross-Out   Date: 6/20/2024 2:40:41 PM

Number: 6   Author: SAG   Subject: Inserted Text   Date: 6/20/2024 2:41:46 PM
with

Number: 7   Author: SAG   Subject: Cross-Out   Date: 6/20/2024 2:42:43 PM

1. Introduction:

The purpose of this project is to contribute to reduced dust emissions in the ODSVRA and downwind through the implementation of a nature-based foredune restoration area (FRA) on a formerly highly emissive site. To monitor and assess the performance of the FRA dust emissions mitigation project at the ODSVRA, a team from UC Santa Barbara, in collaboration with CDPR, have been conducting UAS flights biannually since Oct. 2019. The UAS imagery datasets have been used to create the following data products:

1. Ten (10) visual (RGB) georeferenced aerial orthomosaic images of the FRA at ~1.5 cm resolution,
2. Eight (8) multispectral (RGB-RE-NIR-Pan) georeferenced orthomosaic images of the FRA at ~3.0-7.5 cm resolution collected concurrently with the RGB datasets since Oct. 2020,
3. Eight (8) NDVI orthomosaics used to assess vegetation cover in the FRA at ~3.0-7.5 cm resolution derived from the multispectral orthomosaic datasets
4. Eight (8) georeferenced, orthorectified maps of vegetation cover derived from RGB and NDVI imagery used to track changes in plant cover within the FRA,
5. Ten (10) three-dimensional point clouds of surface topography within the FRA at a decimated resolution of 10 cm,
6. Ten (10) three-dimensional digital elevation models (DEMs) of topography within the FRA at 10 cm pixel resolution,
7. Nine (9) topographic change maps derived from statistically significant pixels of erosion and deposition between DEM intervals used to assess site geomorphic and sediment volume changes.

Data collected during the UAS flights allows for high resolution, three-dimensional [1] DEM surfaces to be constructed and compared over time to quantify sand volume changes and dune dynamics. Given the low-lying, prostrate nature of the vegetation, separation of the vegetation from the surface is difficult without introducing artifacts in the point cloud. Other data collected allow for examination of the growth of vegetation and the development of dune forms within the FRA. This report details the methods used for data collection, processing, as well as initial baseline conditions collected prior to the implementation of the FRA (Oct. 2019) through to Feb. 2024, or 4 full years following the treatment installations in Feb. 2020.

The performance of the restoration treatments at ODSVRA are assessed using 5 indicators, developed in consultation with SAG and CDPR, that track the geomorphic, sediment transport,

Number: 1   Author: SAG   Subject: Comment on Text   Date: 7/3/2024 11:12:55 AM

All references to DTMs in last year's report have been changed to DEMs in this year's report.

Is there any significance to this change or simply a lapse use of terminology? If DTMs is the preferred acronym, then a word search needs to be done (with replacement), an entry for DTM needs to be made in the list of acronyms, and a footnote should be added to explain the difference between DEM and DTM (which might be useful in any case).

vegetation characteristics and responses within the treatment plots (Walker et al. 2023)[1]. These indicators characterize the re-establishment of dynamic ecological and geomorphic conditions required to improve dune ecosystem form and function. The first indicator is establishment and maintenance of a <u>positive sediment budget</u> (i.e., gains in sediment volume over time). This is particularly important during the initial stages of foredune development in which small incipient nebkha (mounds of windblown sand trapped in vegetation) establish and related downwind shadow dunes grow. Eventually, as nebkha and shadow dunes grow and coalesce they will alter the wind field and sand transport patterns and promote localized reductions in surface shear stress, saltation, and promote deposition. In short, to build dunes, the treatment plots need to act as a sink (store) of sediment.

The second indicator is to <u>maintain aeolian activity</u> within the treatments, namely sand transport (saltation), migrating ripples, and open sand surfaces. Saltation, and related erosion and deposition patterns, are critical for dune development/maintenance and aeolian activity is a key ecological disturbance process <mark>needed by</mark> psammophytic (sand loving) plants for their success.

The third indicator is to ~~increase~~ and/or maintain <u>foredune plant cover</u>. Most coastal dunes owe their form and function to plants. So, to re-establish a new foredune ecosystem it is imperative that plants establish and survive to enhance sedimentation and promote ecological feedbacks and conditions needed to maintain dunes. Eventually, however, plant cover density should plateau at an amount that is in balance with dune form/position, aeolian activity, soil nutrients, and regional climate conditions. Typically, dune systems with natural plant communities in central and southern California have modest vegetation cover (rarely exceeding 30-40%) given regional climatic conditions. As ecosystem re-establishment occurs, it is also anticipated that species richness would improve.

The fourth indicator is <u>enhanced dune development</u>. The establishment, growth, and maintenance of foredunes and related dune forms (e.g., nebkha, blowouts, parabolic dunes, etc.) is a key target for restoration performance. Important interactions and feedback mechanisms exist between wind flow, sand transport, vegetation cover, and dune development that are required to build and maintain natural foredunes. As the system develops and evolves, the variety of dune forms is expected to change and organize to a form that reflects plant cover, aeolian activity, and regional climate controls. Natural foredunes in this region are not characterized by a uniform foredune ridge with high plant cover, as is common ~~further~~ north in

---

[1] Walker, I. J., Hilgendorf, Z., Gillies, J. A., Turner, C. M., Furtak-Cole, E., & Nikolich, G. (2023). Assessing performance of a "nature-based" foredune restoration project, Oceano Dunes, California, USA. *Earth Surface Processes and Landforms*, 48(1), 143-162.

Number: 1	Author: SAG	Subject: Comment on Text	Date: 6/26/2024 12:42:33 PM

or tolerated by?

Number: 2	Author: SAG	Subject: Inserted Text	Date: 6/20/2024 2:46:13 PM

optimize???

Number: 3	Author: SAG	Subject: Inserted Text	Date: 6/20/2024 2:47:19 PM

farther not further

California and Oregon. Rather, a more hummocky, discontinuous form with active sand surfaces is the preferred ecosystem form.

The fifth indicator is a reduction in dust emissivity. The main impetus for the FRA project at ODSVRA was to implement a sustainable, nature-based dust mitigation solution that had both onsite and downwind impacts. As dune terrain and vegetation roughness increase, it is expected that surface shear stress patterns that drive saltation and dust emissions within the FRA, and downwind, would be reduced as would surface emissivity.

This report provides new results from the 2023-2024 season in the context of past observations, interprets these findings to understand the ongoing evolution of the restoration treatments, and assesses the implications of observed responses for relative performance of the restoration treatments to date.

2. Methods:

UAS platforms and SfM photogrammetry have experienced widespread and rapid advancements in the last decade[2,3]. SfM photogrammetry refers to the reconstruction of a three-dimensional landscape from highly overlapped (≥70% frontal and side overlap) images. UAS-SfM datasets are used to detect change in a wide variety of landscapes and ecosystems, including coastal dunes[4]. The quality and resulting data products are dependent on the sensors used, methods for georectification, and, in the case of UAS platforms, flight altitude, shutter speed, and stability[5]. Advantages for using UAS datasets for monitoring and detecting change include the relative ease and low cost of data collection, compared to aerial LIDAR, and the high accuracy (mm-cm resolution) of the resulting maps and elevation point clouds.

A fixed-wing, fully autonomous WingtraOne UAS platform was used at the ODSVRA from Oct. 2019 to Feb. 2024 to monitor and characterize changes in sediment volumes, geomorphic responses, and vegetation cover within and beyond the restoration treatments (Figure 1). The

---

[2]Anderson, K., Westoby, M. J., & James, M. R. (2019). Low-budget topographic surveying comes of age: Structure from motion photogrammetry in geography and the geosciences. *Progress in Physical Geography: Earth and Environment, 43(2)*, 163–173. https://doi.org/10.1177/0309133319837454

[3] James, M. R., Chandler, J. H., Eltner, A., Fraser, C., Miller, P. E., Mills, J. P., Noble, T., Robson, S., & Lane, S. N. (2019). Guidelines on the use of structure-from-motion photogrammetry in geomorphic research. *Earth Surface Processes and Landforms,* 44(10), 2081–2084. https://doi.org/10.1002/esp.4637

[4] Hilgendorf, Z., Marvin, M. C., Turner, C. M., & Walker, I. J. (2021). Assessing geomorphic change in restored coastal dune ecosystems using a multi-platform aerial approach. Remote Sensing, 13(3), 354.

[5] Singh, K. K., & A. E. Frazier. (2018). A meta-analysis and review of unmanned aircraft system (UAS) imagery for terrestrial applications. *International Journal of Remote Sensing,* 39(15–16), 5078–5098. https://doi.org/10.1080/01431161.2017.1420941

UAS is typically flown at altitudes over 100 m above ground level and is equipped with on board, survey-grade GPS with PPK correction capabilities. During data collection, a GPS base station is operated in static collection mode and these occupation datasets are used to refine UAS photo point locations to within millimeters of their real-world location. Ten collection campaigns have been flown (Table 1) with 8 multispectral datasets collected concurrently since Oct. 2020.

Two RGB camera sensors have been used: a Sony RX1RII 42 MP full-frame sensor (Oct. 2019 through Feb. 2023) and a Sony RGB61 61 MP full-frame sensor (Oct. 2023 through present). The Sony RGB61 sensor covers a larger footprint with each picture, resulting in less images taken for the same area covered. This results in lower data volume and faster flight time for the same high resolution data product. Both sensors produce high resolution (<2 cm) orthomosaic imagery that, in turn, is used with SfM to create three-dimensional point clouds of the underlying surface. Point clouds between campaigns are aligned to one another using static features in the landscape (e.g., structures, roads, etc.). Point cloud datasets are also used to produce the gridded (rasterized) DEMs. The raster surface is gridded to 0.1 m/pixel and is assigned an elevation value by averaging all points within that 0.1 m^2 cell. DEMs are then compared between campaigns to quantify volumetric changes (Table 1).

Successive DEMs are imported into a GIS and the Geomorphic Change Detection (GCD) toolset (Figure 2), developed by Riverscapes Consortium, is used to calculate volumes of change between collocated raster grid cells. This method applies a spatial statistical filter to remove surface changes that fall below a threshold uncertainty value with 95% confidence[6,7]. This threshold is determined by developing an uncertainty budget that includes the accuracy of the GPS station, the calculated uncertainty of the point cloud, and the root mean square error from the alignment of each point cloud with static features in the landscape. The uncertainty between two surveys is propagated and pixels that exceed the minimum level of detection threshold (typically ~5 cm) are included. As such, repeat DEMs derived from the UAS imagery (Figure 2) are compared through time and pixels of statistically significant elevation change are used to create topographic (elevation) change maps for estimating volumetric changes (between significant pixels) and interpreting corresponding geomorphic changes. Results can also be subset by specified units to monitor plot-based change over time, such as between the

[6] Wheaton, J. M., Brasington, J., Darby, S. E., & Sear, D. A. (2009). Accounting for uncertainty in DEMs from repeat topographic surveys: improved sediment budgets. *Earth Surface Processes and Landforms*, 35(2), 136-156. https://doi.org/10.1002/esp.1886

[7] Hilgendorf, Z., Marvin, M. C., Turner, C. M., & Walker, I. J. (2021). Assessing Geomorphic Change in Restored Coastal Dune Ecosystems Using a Multi-Platform Aerial Approach. *Remote Sensing*, 13(3), 354. https://doi.org/10.3390/rs13030354

Number: 1   Author: SAG   Subject: Inserted Text   Date: 6/20/2024 2:57:01 PM
fewer

Number: 2   Author: SAG   Subject: Comment on Text   Date: 6/20/2024 2:59:04 PM
some additional clarification would be useful to let the reader understand what 'propogation' means in this context

Number: 3   Author: SAG   Subject: Sticky Note   Date: 6/20/2024 3:00:02 PM
end one sentence after time, and begin the next sentence with Pixels of statistically.....

Number: 4   Author: SAG   Subject: Comment on Text   Date: 6/20/2024 3:00:39 PM
is 'subset' a legitimate verb? is there a better word?

foredune restoration treatment plots themselves, as well as their adjoined beach and landward dune components (Figure 1).
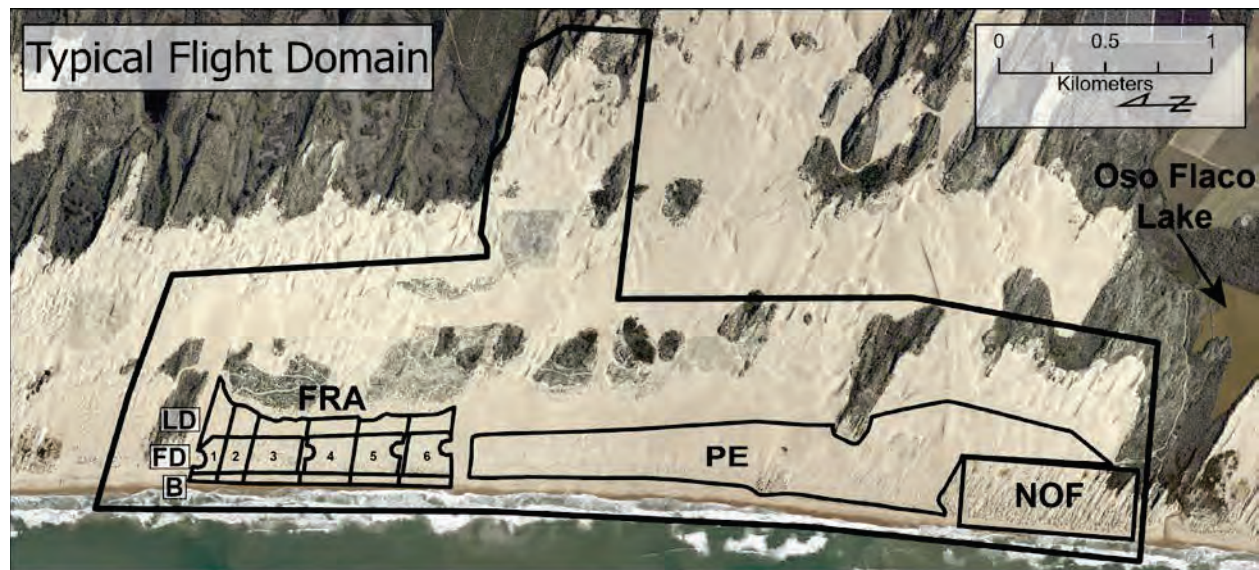
Figure 1. Map showing the typical extent of the UAS surveys (North oriented to the left). The foredune restoration area (FRA) and treatment plots (1-6) are shown with adjoining beach (B) and landward dune (LD) polygons for examining volumetric exchanges with the FRA. The Western Snowy Plover exclosure (PE, as of Feb. 2024) and North Oso Flaco (NOF) reference site are also shown. The underlying orthomosaic is from 27 Jan. 2023 (NOAA, 2023)[8].

Two multispectral sensors ~~have been~~ used to date: a Micasense RedEdge-MX (Oct. 2020 through Feb. 2022) and a Micasense RedEdge-P (Oct. 2022 through present). The RedEdge-MX features a 5-band sensor payload that captures visual (RGB), red edge (RE), and near-infrared (NIR) bands. This sensor was eventually replaced by the RedEdge-P, which contains the same five bands, but has an additional panchromatic (Pan) band that is used to improve the resolution of the dataset from ~7 to ~3.5 cm/pix. From these bands, a normalized difference vegetation index (NDVI) is used to help identify vegetation on the surface (differentiated from sand or straw) to quantify plant cover across the FRA (Figure 3).

NDVI is calculated using a ratio of the difference in reflectance values of NIR light (reflected strongly by plants) and red (R) light (absorbed by plants), using the following equation:

$$NDVI = (NIR - R) / (NIR + R)$$

where NIR is near-infrared light reflectance and R is visible red light reflectance. NDVI values ranging from -1 to +1. Areas with dense vegetation will typically have positive values (~+0.3 to

---

[8] National Geodetic Survey, 2024: 2023 NOAA NGS Aerial Imagery for Situational Awareness: Central California, https://www.fisheries.noaa.gov/inport/item/69185.

Number: 1   Author: SAG   Subject: Comment on Text   Date: 7/1/2024 12:52:46 PM
"FD" appears in the image but is not defined in the caption.

Not sure if this is critical at this juncture, but how exactly were the LD polygons identified given that they are all different sizes and shapes?

Number: 2   Author: SAG   Subject: Inserted Text   Date: 6/20/2024 3:03:24 PM
were

Number: 3   Author: SAG   Subject: Comment on Text   Date: 7/1/2024 2:13:54 PM
*range

0.8) while water surfaces or fog (that absorb both bands) tend to have low positive to slightly negative values. Soil surfaces also tend to be characterized by low positive NDVI values (~+ 0.1 to 0.2), depending on color and moisture content. The output histograms of NDVI values for each survey were examined and a threshold value was set to identify pixels with high index values (representative of vegetation) (Figure 3). Currently, vegetation cover datasets derived from the UAS surveys do not identify plant species, only pixels that have plant cover.

Table 1. Specifications for the RGB and multispectral UAS campaigns. Multispectral sensors were only used after installation of the vegetation treatments in Feb. 2020. GSD is the distance between the center of adjacent pixels and describes the cell size of each pixel in centimeters (i.e., pixel resolution). Total Uncertainty values are the calculated vertical uncertainty for datasets used in DEM development and volumetric change detection mapping. As the multispectral datasets were not used for this purpose, no uncertainty value is shown.

UAS Survey Campaign	Survey Date	Sensor Payload	Average Altitude (m)	GSD (cm/pix)	Total Uncertainty (m)
1. Baseline pre-restoration survey	1-2 Oct. 2019	Sony RX1RII	114	1.45	0.038
2. Initial treatment installations	10-11 Feb. 2020	Sony RX1RII	123	1.56	0.033
3. First post-treatment survey and growing season	13-15 Oct. 2020	Sony RX1RII	121	1.54	0.037
	16 Oct. 2020	Micasense RedEdge-MX	113	7.53	—
4. End of first year of geomorphic response and vegetation growth	17-18 Feb. 2021	Sony RX1RII	120	1.52	0.030
	18-21 Feb. 2021	Micasense RedEdge-MX	118	7.89	—
5. Second growing season	4-5 Oct. 2021	Sony RX1RII	121	1.54	0.025
	5-7 Oct. 2021	Micasense RedEdge-MX	119	7.82	—
6. End of second year of geomorphic response and vegetation growth	23-25 Feb. 2022	Sony RX1RII	112	1.42	0.043
	25-26 Feb. 2022	Micasense RedEdge-MX	116	7.71	—
7. Third growing season	17-18 Oct. 2022	Sony RX1RII	125	1.66	0.026
	19-21 Oct. 2022	Micasense RedEdge-P	111	3.67	—
8. End of third year of geomorphic response and vegetation growth	23 Feb. 2023	Sony RX1RII	121	1.59	0.034
	20-21 Feb. 2023	Micasense RedEdge-P	120	3.97	—
9. Fourth growing season	9 Oct. 2023	Sony RGB61	108	1.65	0.049
	10-13 Oct. 2023	Micasense RedEdge-P	135	4.42	—
10. End of fourth year of geomorphic response and vegetation growth	23 Feb. 2024	Sony RGB61	116	1.78	[1]0.071
	21-23 Feb. 2024	Micasense RedEdge-P	133	4.38	—

Number: 1   Author: SAG   Subject: Comment on Text   Date: 6/20/2024 3:07:38 PM
Why was the uncertainty so much greater in this campaign compared to previous years?
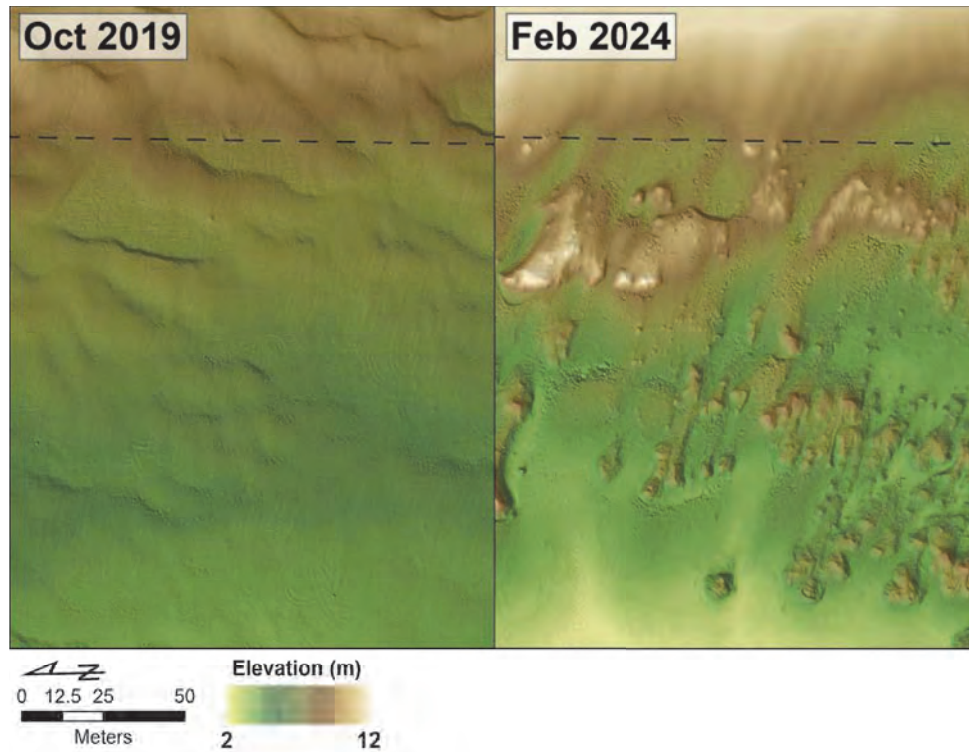
Figure 2. Example DEMs from the Oct. 2019 and Feb. 2024 collection campaigns from TP3. The development from unvegetated transverse dunes to coalesced, vegetated nebkha ridges is evident in the Feb. 2024 DEM. Dashed line represents the landward extent of the treatment plot.
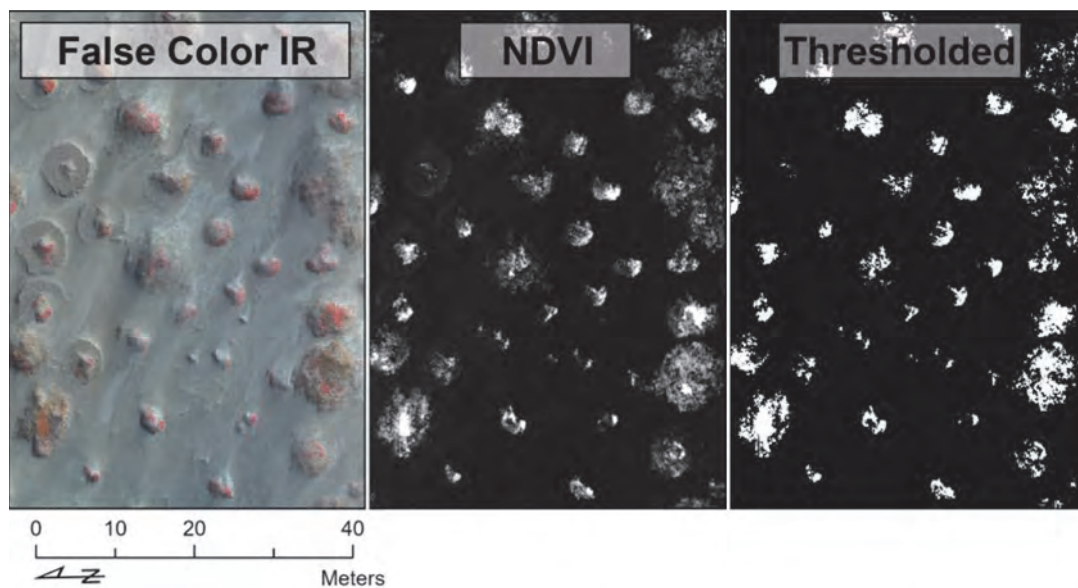
Figure 3. Example of the false color IR output (shows vegetation as red pixels), NDVI output (vegetation as lighter grayscale colors), and thresholded NDVI (vegetation as white pixels) used to extract distinct vegetation pixels within the treatment plots. This location is along the boundary of the low density planting node (TP4) and high density node (TP5) treatment plots.

Number: 1   Author: SAG   Subject: Comment on Text   Date: 7/3/2024 11:16:37 AM
Are we seeing low density nodes, or high density nodes, or both?

Is it possible to draw in the boundary?

3. Results:

3.1. UAS visible (RGB) imagery and orthophoto mosaics

Figure 1 shows the typical extent of the ten UAS visual (RGB) orthophoto campaigns. Figure 4 and Appendix A show the UAS RGB orthophoto mosaics of the FRA. These images are used to interpret geomorphic responses within the treatment plots, such as aeolian sand transport corridors (ripples), deflation surfaces (coarse lag deposits), and dune development.

Figure 4. Visible (RGB) orthophoto mosaics of the FRA from the earliest (Oct. 2019) and latest (Feb. 2024) UAS surveys. Numbers represent the following treatments: 1) Sheepsfoot texturing (control site), 2) native seeds, 3) native seeds + sterile ryegrass seed, 4) low density straw planting nodes, 5) high density planting nodes, and 6) broadcast straw, randomly planted seedlings, and broadcast seed. Notable aeolian activity, nebkha development, and streamlined shadow dune accretion is widespread in all treatments except within the control plot (#1).

Survey extents have varied slightly over time due to logistical constraints and modifications suggested by SAG and CDPR. The Feb. 2020 campaign included collection of an eastward extending panhandle swath to monitor the rate of change of the landward dunes, and another eastward extent immediately north of Oso Flaco Lake and landward of more established

Number: 1   Author: SAG   Subject: Sticky Note Date: 7/3/2024 11:17:48 AM
Are (1) and (TP1) the same? Switch in labelling?

foredunes. The Oct. 2020 campaign included the area between the southern landward extent and the eastern extent, south of the panhandle. The Feb. 2022 campaign included a flight south of Oso Flaco Lake to better understand how those dunes were developing. These changes were made, on advice of SAG and CDPR, to monitor restoration efforts and dune responses landward of the established foredune to the south, as an analog to compare against the FRA to the north. In Feb. 2023 there was a smaller flight extent with the RGB sensor given challenging weather conditions and prioritization of the multispectral sensor, which was flown first and covered the entire domain. Oct. 2023 saw the addition of a deeper landward extent behind the Western Snowy Plover exclosure through the north Oso Flaco reference area, but this extension was not maintained during the Feb. 2024 collection, which was limited due to inclement weather and prioritization of the multispectral data collection, although the RGB flight did fully cover the FRA. To date, the UAS surveys cover four full plant growth and dune development seasons since implementation of the treatment plots in Feb. 2020.

3.2. UAS multispectral imagery and plant cover estimation

To enhance the detection and monitoring of vegetation at the landscape scale in restoration treatment areas, multispectral imagery has been collected since Oct. 2020 (Figure 5). The initial survey focused primarily on the seaward extent of the ODSVRA, including the FRA, seasonal plover exclosure, and established foredunes near Oso Flaco Lake. The Feb. 2021 survey covered a larger extent to match that of the RGB surveys and this incident survey strategy has been followed since (Figure 1), with minor variations related to logistics. Multispectral sensors are calibrated pre- and post-flight with a calibration panel so that, while the orthomosaics in Figure 5 may appear to have variable contrast, individual pixels are properly scaled and the extracted indices are accurate.

NDVI values were calculated for all multispectral surveys to detect and map vegetation and its changes over time. Percent plant cover (normalized by total area of each treatment plot) has generally increased over time in all plots except for the control site (TP1) (Figure 6, Table 2). TP6 shows the highest plant cover change (from 2.5% in Oct. 2020 to 11.7% by Feb. 2024), followed by TP3 (2.7 to 7.0%), TP5 (1.7 to 6.2%), TP4 (0.9 to 4.9%), and TP2 (0.4 to 3.1%). Negligible (<1.0%) plant cover has been observed in the TP1 control site to date. For context, historic plant cover in the FRA derived from aerial imagery back to 1939 reached a maximum of 30% in 1949 and then declined to negligible cover by 1985[9]. Since 1985, there was no detectable increase in plant cover at the FRA until after implementation of the restoration treatments in

[9] Swet, N., Hilgendorf, Z., & Walker, IJ. (2022). UCSB Historical Vegetation Cover Change Analysis (1930-2020) within the Oceano Dunes SVRA. Technical report to the Oceano Dunes Scientific Advisory Group (SAG) and the State of California Parks and Recreation Department Off-Highway Vehicle Division. February 2022. 86p.

Number: 1   Author: SAG   Subject: Cross-Out   Date: 6/20/2024 3:12:28 PM

Number: 2   Author: SAG   Subject: Cross-Out   Date: 6/20/2024 3:13:05 PM

Number: 3   Author: SAG   Subject: Cross-Out   Date: 6/20/2024 3:13:03 PM

Number: 4   Author: SAG   Subject: Inserted Text   Date: 6/20/2024 3:14:28 PM
greatest

Number: 5   Author: SAG   Subject: Comment on Text   Date: 6/20/2024 3:22:39 PM
Somewhere above you suggest that 30-40% plant cover is maximum for this area (with the implicit notion that this might be 'normal' under ideal conditions), but here you suggest that it would be less than 4% based on photo evidence going back at least 75 years. This is a bit confusing for the reader. What exactly is the normative target for plant cover? Also, I seem to recall that the 1939 image analysis likely under-estimated veg cover.

A critic might say that if the 1939 'norm' was only 3.3%, why would anyone think that greater than 5% is 'natural' and a good thing?

Number: 6   Author: SAG   Subject: Cross-Out   Date: 6/20/2024 3:24:46 PM

2020. Following restoration, plant cover has increased to an average of 6.55% across the entire FRA by Feb. 2024 (Table 2).

Superimposed on the general increasing trends in plant cover, Figure 6 also shows seasonal declines (February), then increases (October) in vegetation bracketing the plant growth season. Most treatments also showed a notable decline in plant cover in the most recent monitoring interval (Oct. 2023 - Feb. 2024).

Figure 5. Multispectral false-color (G+B+NIR) UAS orthomosaics captured from a Micasense RedEdge-MX 5-band sensor (R, G, B, RE, NIR) in Oct. 2020 and a Micasense RedEdge-P 6-band sensor (R, G, B, Pan, RE, NIR) in Feb. 2024, used to map vegetation cover. Contrast differences are only visual and do not impact the indices calculated from the values of compared bands.
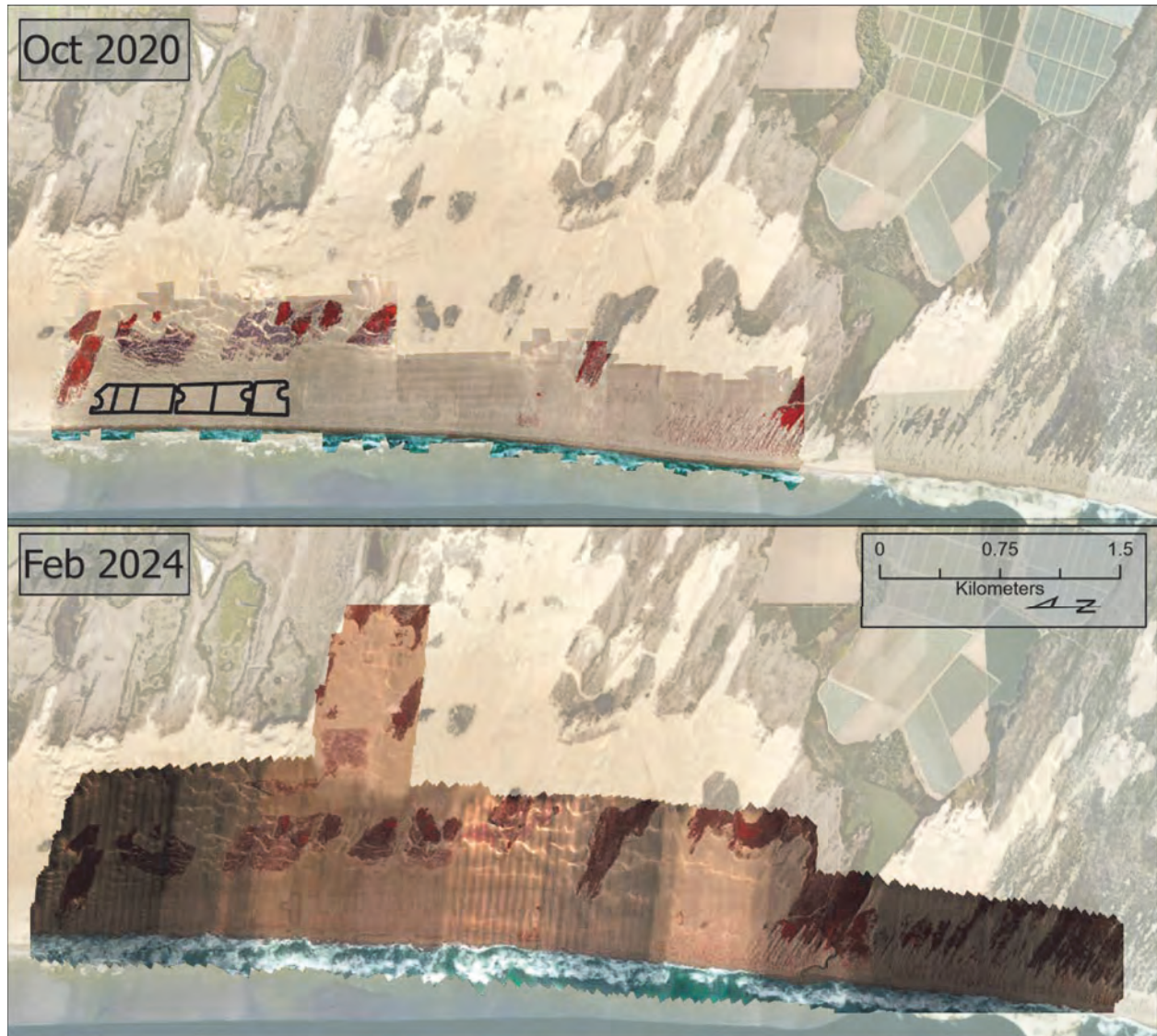
Number: 1 Author: SAG Subject: Comment on Text Date: 7/3/2024 11:20:10 AM
The location of the foredune project and treatments should be in this lower image. .
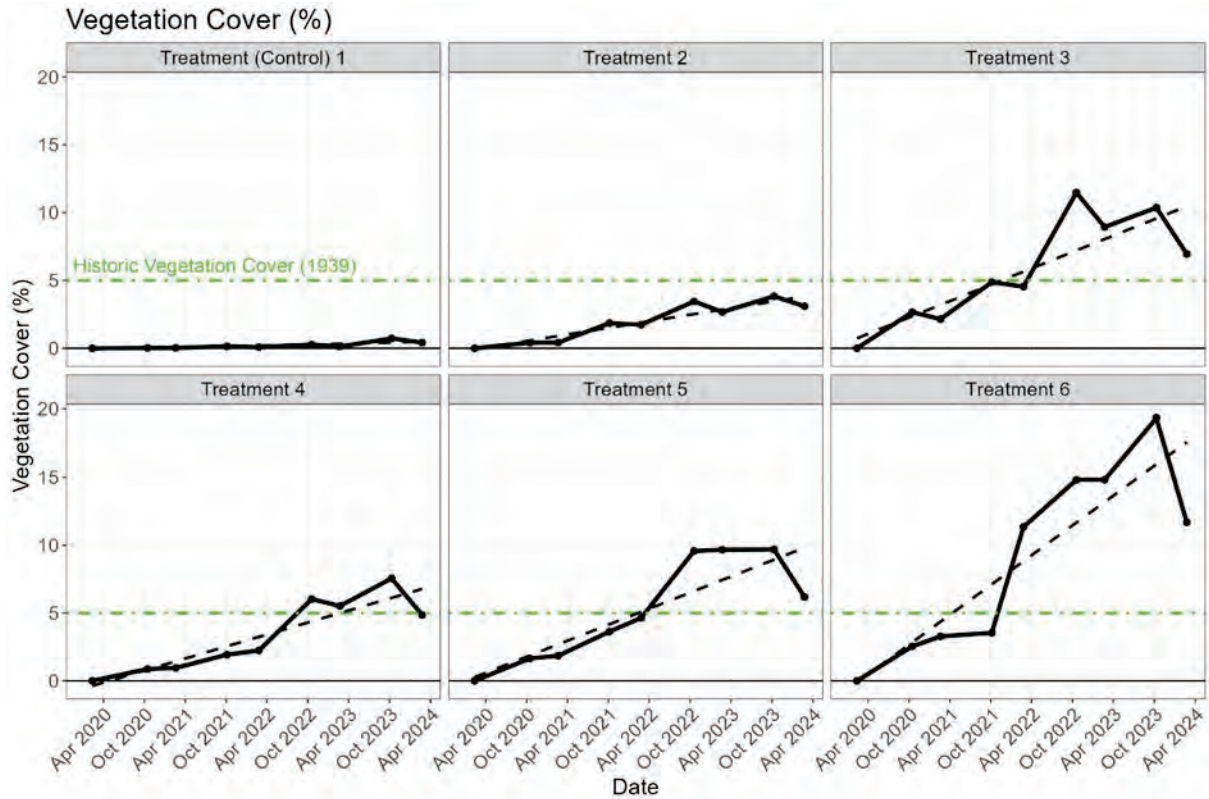
Figure 6. Plant cover (%) by treatment plot over time derived from the multispectral UAS surveys from Feb. 2020 (treatment implementation) through to Feb. 2024. Seasonal fluctuations are evident in most treatments due to declining cover before (Feb.) and increasing cover after (Oct.) the plant growth season. Linear regression fits (black, dashed line) show general trends of increasing vegetation cover, while the [1] green dash-dot line is the 'pre-disturbance' extent of historic vegetation cover in 1939. Corresponding values shown in Table 2.

Table 2. Vegetation cover percentage (%) per treatment plot (TP1-6) as shown in Figure 6.

	TP1	TP2	TP3	TP4	TP5	TP6
10-11 Feb. 2020	0.00	0.00	0.00	0.00	0.00	0.00
16 Oct. 2020	0.02	0.41	2.66	0.87	1.65	2.54
18-21 Feb. 2021	0.03	0.42	2.15	0.95	1.85	3.28
5-7 Oct. 2021	0.14	1.85	4.87	1.93	3.63	3.54
25-26 Feb. 2022	0.08	1.74	4.55	2.24	4.64	11.35
19-21 Oct. 2022	0.26	3.45	11.47	6.03	9.57	14.82
20-21 Feb. 2023	0.12	2.68	8.93	5.52	9.66	14.83
10-13 Oct. 2023	0.73	3.83	10.36	7.55	9.68	19.36
21-23 Feb. 2024	0.42	3.10	6.95	4.85	6.18	11.68

Number: 1   Author: SAG   Subject: Comment on Text   Date: 6/20/2024 3:26:06 PM
in the paragraphs above, you say that the maximum was 3.3% in 1949 but this green dashed line is at 5%.

3.3. Topographic Differencing and Volumetric Change Trends

The topographic difference maps (Figures 7-8) show areas and quantities of significant elevation change that are used to calculate volumes of sediment erosion or deposition between surveys in cubic meters (m^3) or normalized by area (m^3 m^{-2}), which is effectively an average depth of change (m) over the entire treatment plot (or adjoining unit) areas. Data are also normalized by month to allow comparison of change over time, given the difference between the Feb. to Oct. (~8 months) and the Oct. to Feb. (~4 months) intervals. The raster grid from which the volume estimates are determined remains fixed in positioning and size (0.10 m x 0.10 m) across all surveys. Pixels of insignificant change are not shown in the change detection maps and are not used to calculate sediment volumes.

Figures 7-9 and Table 3 provide topographic change maps and related values and time series of normalized volumetric changes within the treatment areas and their adjoined geomorphic units between Oct. 2019 and Feb. 2024. Geomorphic units include each of the foredune treatment areas (FD), an adjoining beach area (B) and landward backdune areas (LB)(Figure 1). The first interval (Oct. 2019 to Feb. 2020) provides baseline reference conditions prior to implementation of the restoration treatments. The remaining intervals show responses of the treatment plots for the following four wind, plant growth, and dune development seasons through to Feb. 2024.

One key control on the volumetric and geomorphic responses in the treatments is the amount of sand that enters the upwind beach, which effectively provides supply for aeolian delivery to the treatment plots. Beach units fronting the plots saw variable trends of positive (depositional) and negative (erosional) change in sediment volumes that relate to seasonal variations (e.g., winter storm erosion signals) and migration of rip current embayments. Generally, the beach units show a declining, albeit highly variable, trend in sand volumes from positive values in the initial Oct. 2019 to Feb. 2020 baseline interval to negative values by Feb. 2023. More recently, all treatment plots, except TP6, have shown distinct positive trends and values of sedimentation between Oct. 2023 and Feb. 2024. Net change values since the baseline survey (Table 3) suggest beach erosion has dominated fronting the northern plots (TP1-3) while deposition prevails at the southern plots (TP4-6).

Number: 1   Author: SAG   Subject: Inserted Text   Date: 6/24/2024 12:37:42 PM

(Table 3)

Number: 2   Author: SAG   Subject: Comment on Text   Date: 6/20/2024 4:12:17 PM

add the quantity (i.e., less than 1 cm of elevation change) to remind the reader what 'insignificant' means

---

Number: 3   Author: SAG   Subject: Comment on Text   Date: 6/24/2024 12:41:17 PM

Figures 7 and 8 are not 'normalized', so be clear on which figures present which data format.

Number: 4   Author: SAG   Subject: Sticky Note   Date: 6/20/2024 4:17:51 PM

conditions plural?

Number: 5   Author: SAG   Subject: Inserted Text   Date: 6/20/2024 4:18:52 PM

from the nearshore

Number: 6   Author: SAG   Subject: Comment on Text   Date: 6/24/2024 12:41:47 PM

are you referring to the beach fronting the treatment plots or to the treatment plots directly?

Number: 7   Author: SAG   Subject: Cross-Out   Date: 6/24/2024 12:42:01 PM

Number: 8   Author: SAG   Subject: Cross-Out   Date: 6/20/2024 4:19:48 PM

Figure 7. Topographic change maps with corresponding pixels of significant elevation change (reds = erosion, blues = deposition) for each survey interval between Oct. 2019 and Feb. 2022 overlain on the UAS photomosaics for the second time step in each interval. Restoration treatment areas are outlined and progress from TP1 (control) on the left to TP6 on the right. Intervening OHV transportation corridors, between TP3 and 4, and 5 and 6, are not included in the analysis.

Figure 8. Topographic change maps with corresponding pixels of significant elevation change (reds = erosion, blues = deposition) for each survey interval between Feb. 2022 and Feb. 2024 overlain on the UAS photomosaics for the second time step in each interval. Restoration treatment areas are outlined and progress from TP1 (control) on the left to TP6 on the right. Intervening OHV transportation corridors, between TP3 and 4, and 5 and 6, are not included in the analysis.

Table 3. *Normalized surface volumetric changes for the foredune treatment plots (FD, bold values) and adjoining beach (B) and landward dune (LD) zones. Blue cells indicate sand accumulation, red cells show erosion. Uncertainty values associated with individual measurement campaigns are provided in Table 1.*

		Normalized Volumetric Change by Total Area (m^3 m^{-2}mo^{-1})									
Treatment Plot	Geomorphic unit	Oct. 2019 – Feb. 2020	Feb. 2020 – Oct. 2020	Oct. 2020 – Feb. 2021	Feb. 2021 – Oct. 2021	Oct. 2021 – Feb. 2022	Feb. 2022 – Oct. 2022	Oct. 2022 – Feb. 2023	Feb. 2023 – Oct. 2023	Oct. 2023 – Feb. 2024	*Net Change (Oct. 2019 – Feb. 2024)*
TP1 (control)	B	0.017	-0.002	-0.011	-0.005	0.015	-0.007	-0.090	0.006	0.016	-0.004
	FD	**0.001**	**0.001**	**0.004**	**0.009**	**0.008**	**0.004**	**-0.007**	**-0.016**	**0.000**	**0.000**
	LD	-0.001	0.002	0.006	-0.003	0.000	-0.001	0.002	0.000	-0.004	-0.001
TP2	B	0.011	0.006	0.001	0.002	0.000	-0.005	-0.085	-0.006	0.001	-0.006
	FD	**0.001**	**-0.002**	**0.005**	**0.003**	**0.008**	**0.003**	**0.006**	**-0.006**	**0.000**	**0.001**
	LD	0.002	0.006	0.005	-0.002	-0.003	0.003	0.009	-0.001	0.001	0.001
TP3	B	0.020	0.005	0.004	-0.005	0.016	-0.018	-0.066	0.006	0.036	0.000
	FD	**0.003**	**0.001**	**0.006**	**0.007**	**0.007**	**0.016**	**0.010**	**-0.005**	**0.000**	**0.005**
	LD	0.002	-0.005	0.007	-0.001	0.004	-0.009	0.004	-0.010	-0.001	-0.003
TP4	B	0.036	0.012	-0.007	-0.003	0.011	-0.015	-0.012	0.006	0.045	0.006
	FD	**0.004**	**-0.002**	**0.002**	**0.004**	**0.004**	**0.012**	**0.008**	**-0.006**	**0.001**	**0.003**
	LD	0.001	-0.013	0.000	-0.014	0.000	-0.009	0.001	-0.012	0.000	-0.008
TP5	B	0.034	-0.001	0.006	-0.002	0.014	-0.003	-0.020	0.006	0.030	0.006
	FD	**0.002**	**0.001**	**0.001**	**0.003**	**0.003**	**0.011**	**0.008**	**-0.001**	**0.001**	**0.004**
	LD	-0.001	-0.018	0.001	-0.014	0.000	-0.022	-0.005	-0.017	-0.001	-0.012
TP6	B	0.016	0.023	-0.014	-0.010	0.006	-0.009	-0.001	0.009	-0.020	0.001
	FD	**0.002**	**0.002**	**0.003**	**0.011**	**0.004**	**0.017**	**0.008**	**0.004**	**0.001**	**0.007**
	LD	-0.001	-0.021	-0.003	-0.022	-0.004	-0.029	-0.009	-0.018	0.000	-0.01

18

Number: 1   Author: SAG   Subject: Comment on Text   Date: 7/3/2024 11:22:07 AM

Table 3 shows values with three decimal places that suggests resolution to millimeter precision. If resolution of sensors on the UAS are <2 cm, should any related values calculated from these measurements have 3 decimal places of precision when units are identified as meters?

Number: 2   Author: SAG   Subject: Sticky Note Date: 6/24/2024 12:54:16 PM

Although these values use correct SI units (meters), there are a lot of zeros in the table. It could be simplified and made more pleasing to the eye by multiplying the values by 100. This would turn them into centimeters of change and you could note this in the table heading as "x 100" and in the caption by mentioning the equivalency to cm (as is done in the body of the report).   Just a suggestion to ponder.
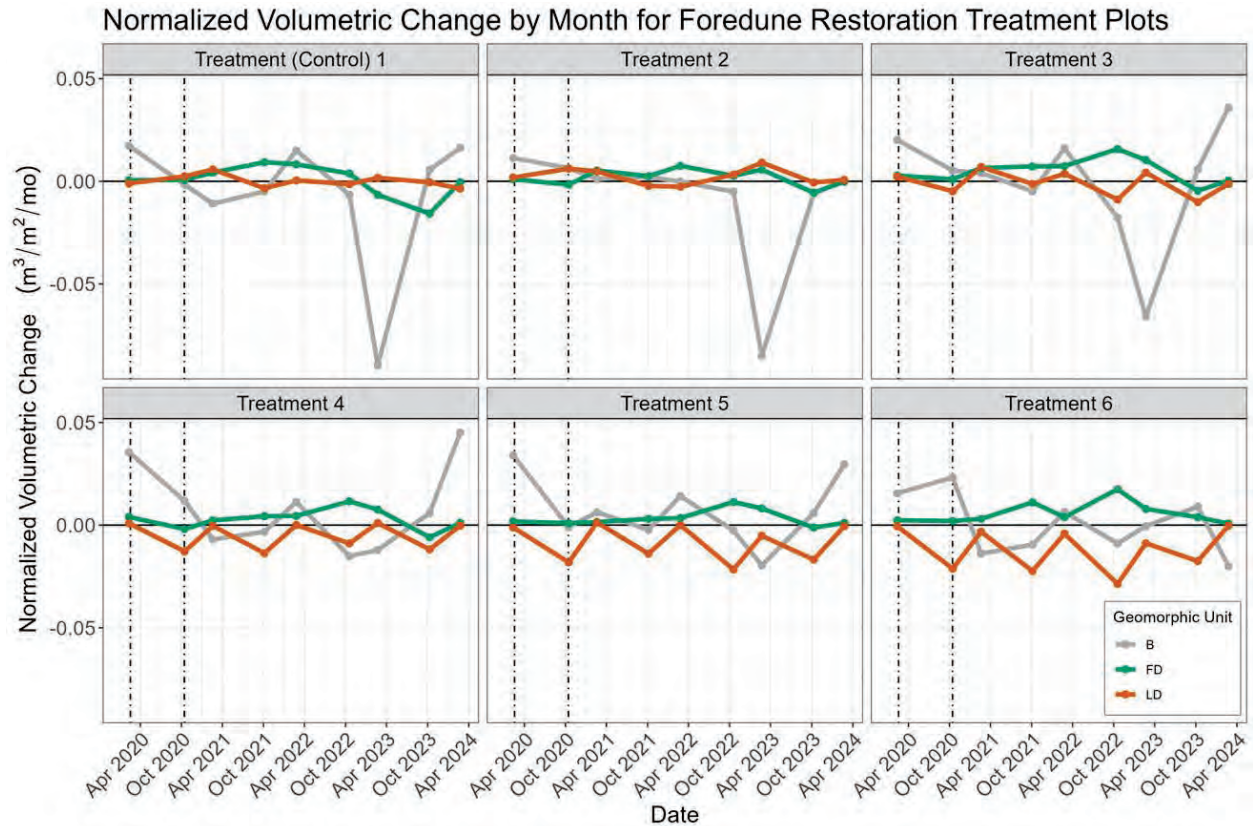
Figure 9. Time series of normalized volumetric changes derived from successive survey intervals for each foredune restoration treatment plot (FD), adjacent beach (B), and landward dune (LD) units. Each point represents net results of volumetric change for the preceding interval (e.g., first point represents net change between Oct. 2019 and Feb. 2020, etc.). Dashed lines delimit the COVID-19 closure period (March 2020 through Oct. 2020).

In general, net deposition has occurred across all foredune restoration treatment plots, with some deviations, over the monitoring period. The current status of the plots, however, is near neutral to slightly positive accretion (Figure 9, Table 3). Most plots saw distinct negative (erosional) responses from Feb. to Oct. 2023 (except for T6), but trends shifted to positive in all but one treatment (T6) in the most recent interval. TP1 and TP2 continue to show some of the lowest rates of accumulation, reflective of significant recent beach erosion and consistent sediment bypassing due to limited vegetation establishment and nebkha dune development. TP3, despite exhibiting negative net change in both the beach and landward dunes units, shows the second highest net accumulation of sand. TP4 and [1] experienced comparatively moderate change, as the fourth and third (respectively) highest accumulating plots. TP6 recorded the greatest net deposition, but this has been focused largely on the seaward and northern edges of the plots, where fences have played a role in capturing sand. [2] P6 is the only plot that has not exhibited a negative change interval, although its overall trend since Oct. 2022 has been negative, like most of the other plots.

19

Number: 1   Author: SAG   Subject: Comment on Text   Date: 7/1/2024 3:05:43 PM
TP5

Number: 2   Author: SAG   Subject: Comment on Text   Date: 6/26/2024 12:46:46 PM
This sentence is unclear and appears to contradict itself. How can it have no negative change intervals yet have an overall negative trend?

The foredune plots vary notably in their sedimentation responses to vegetation establishment and/or surface treatments. TP1 (control) and TP2 (native seed) were the least altered by treatment interventions and maintained similar change patterns across all intervals. Sand transport in these plots generated low-lying (0.4-0.6 m), slowly migrating semi-continuous transverse and barchanoid dune ridges and protodunes. Negligible plant cover established in TP1 except for a very few plants near the seaward edge of the plot, first observed in Oct. 2022. Some shadow dunes were present in the landward half of these plots, but these were not associated with vegetation (i.e., nebkha), but rather with nodes of cemented sand and anthropogenic debris[10]. TP2 exhibited a developing nebkha cluster in the center of the plot, but this has not expanded notably by Feb. 2024. TP1 and TP2 recorded the smallest net changes in sand volume over the monitoring period (Table 3).

TP3 (native seed with sterile rye grass seed) has developed significant nebkha, predominantly with *Abronia latifolia*, and these dunes have started to coalesce to form discontinuous ridges over 2 m tall, which are the tallest dunes across all of the treatment plots. The latest two intervals (since Feb. 2023) showed negative and neutral volumetric changes, respectively, within TP3. The Feb. 2023 to Oct. 2023 interval recorded the only negative budget for TP3, since the installation of the treatment plots. TP3 has shown among the greatest and most consistent positive volumetric changes across the sites and the second largest depositional interval (Feb. to Oct. 2022, 0.122 $m^3 m^{-2}$) and second greatest net deposition (Oct. 2019 to Feb. 2023, 0.247 $m^3 m^{-2}$) to date (Table 3).

TP4 and TP5 (low and high density straw planting nodes) suffered localized erosion between planting nodes during early intervals. These 'erosional streets' persist, although nebkha are growing and slowly coalescing in both plots[14]. TP4 and TP5 experienced the fourth and third highest net positive deposition amounts, respectively, to date (Table 3). Nebkha dunes in TP5 are larger than in the neighboring TP4 and closer in height to the larger dunes in TP3, with some dunes over 1.5 m tall. In the most recent Feb. 2024 surveys, however, dunes in TP4 had grown notably, particularly along the seaward half of the plot. Nebkha coalescence was observed in both treatments along the seaward half of the plot by Oct. 2023.

TP6 (broadcast straw + native seeds + plant seedlings) had the most intensive treatment with the highest planting density and complete surface straw cover on installation. Although it maintains the highest plant coverage (Figure 6, Table 2), greatest depositional volumes, and

---

[10] For more discussion, see Hilgendorf, Z. Walker, I.J., Swet, N., and Heffentrager, M.(2023). UCSB 2022-2023 ODSVRA Foredune Restoration Survey Report. Research report to the Oceano Dunes Scientific Advisory Group (SAG) and the State of California Department of Parks and Recreation. 44 p.

highest net positive sediment budget (Table 3), large nebkha are not developing in this plot, compared to TP3-5. A notable portion of the accretion in TP6 is associated with the sand fence on the northern border with the transportation corridor, which has promoted significant drift development in the treatment plot. [1]This influences the net accretion values, but does not reflect the effects of the restoration treatment itself. The same fence-drift pattern is also observed on the north fence line of TP4.

4. Discussion:

Most coastal dunes owe their form and function to the presence of vegetation. In turn, [2]sand loving (psammophytic) plants require the conditions and disturbance processes offered by aeolian processes for their success. These interactions are particularly important to recognize when designing and assessing foredune restoration projects. In addition, variability in sand inputs from the upwind beach, variations in other supply- and transport-limiting factors can also influence treatment responses and resulting dune evolution. At ODSVRA, sand volume and resulting geomorphic changes within the treatment plots show seasonal and interannual responses related to variations in surface moisture ([3]supply-limiting, highest in wetter winter months), the frequency of transporting winds (transport-limiting, highest in the April-June wind season), sand supply to the beach (supply-limiting, seasonal to interannual), and the extent and type of treatment modifications, such as vegetation establishment and straw cover (supply- and/or transport-limiting, seasonal to interannual). The following sections interpret these interactions and responses within the FRA treatment plots with respect to sand volume and geomorphic changes, vegetation cover and dune development, [4]then an assessment of performance of the treatments based on identified indicators.

4.1. Geomorphic and Sand Volume Change Trends

Absolute volumes of sand inputs to the beach, foredune, and landward dune units at each treatment site over the total monitoring period (Figure 10) [5]highlight the general north-south gradient in increasing sand supply to the beach. In addition, seasonal to interannual variations are evident at many locations, reflecting winter beach erosion and/or movement of rip cell embayments that reduce beach width, or spring/summer bar welding on to the upper beach and increased aeolian activity (see also erosion/deposition patterns and trends in Figures 7-9). Figure 9 also shows that, despite high variability in beach sand volumes and a general net erosional trend, the foredune treatment plots have maintained a net positive sediment budget response, indicative of continued accretion in developing vegetated dunes. Significant declines in beach sediment during the winter 2023 season (Oct. 2022 to Feb. 2023 interval) were not

Number: 1   Author: SAG   Subject: Comment on Text   Date: 7/3/2024 11:26:28 AM

Is there a way to separate out this effect?

Some time ago it was suggested to use a 'buffer' zone inside the fence lines (of say, 5 m) to cancel out this effect and to use only the inner area for change calculations. It might be useful to undertake such an analysis for TP6 to assess how much difference this might make to the overall results (and hence the performance ratings).

Number: 2   Author: SAG   Subject: Comment on Text   Date: 6/26/2024 12:50:51 PM

Does it appear that these species would not survive in the absence of blowing sand? Or is it simply that they can grow in active dunes where nothing else can?

Number: 3   Author: SAG   Subject: Comment on Text   Date: 6/26/2024 12:51:19 PM

It is not clear what this, and the following, parenthetic phrase is referring to. You propose two limiting factors: supply and transport. Perhaps these should be defined in context. Supply = there might not be enough of something? Transport = sand cannot move due to lack of wind?

Number: 4   Author: SAG   Subject: Comment on Text   Date: 6/24/2024 12:59:52 PM

not a complete sentence

Number: 5   Author: SAG   Subject: Comment on Text   Date: 6/24/2024 1:06:47 PM

this doesn't really pop out of Figure 10...what does pop out in terms of a N-S trend is the relatively small changes in T1 and T2 and very large changes in T5 and T6, especially the erosion of the landward units in T4, T5 and T6 (i.e., sediment is not by-passing the treated areas in the southern treatments, in contrast to T1 and T2). This likely has more to do with the vegetation cover rather than sediment supply from the beach (which makes things noisy!).

mirrored in the adjoined foredune treatment plots, although most exhibited a continued or increasing negative trend in sand volume in the following interval (to October 2023). This lagged response, on the order of months, reflects an expected delay between sand volume changes on the beach and resulting responses of aeolian delivery into the treatment plots. The most recent Oct. 2023 to Feb. 2024 interval showed some of the smallest volumetric change values, overall, which could be attributed to wetter conditions (limiting transport) and weaker winds (observed at the meteorological stations in each of the plots, not presented in this report).
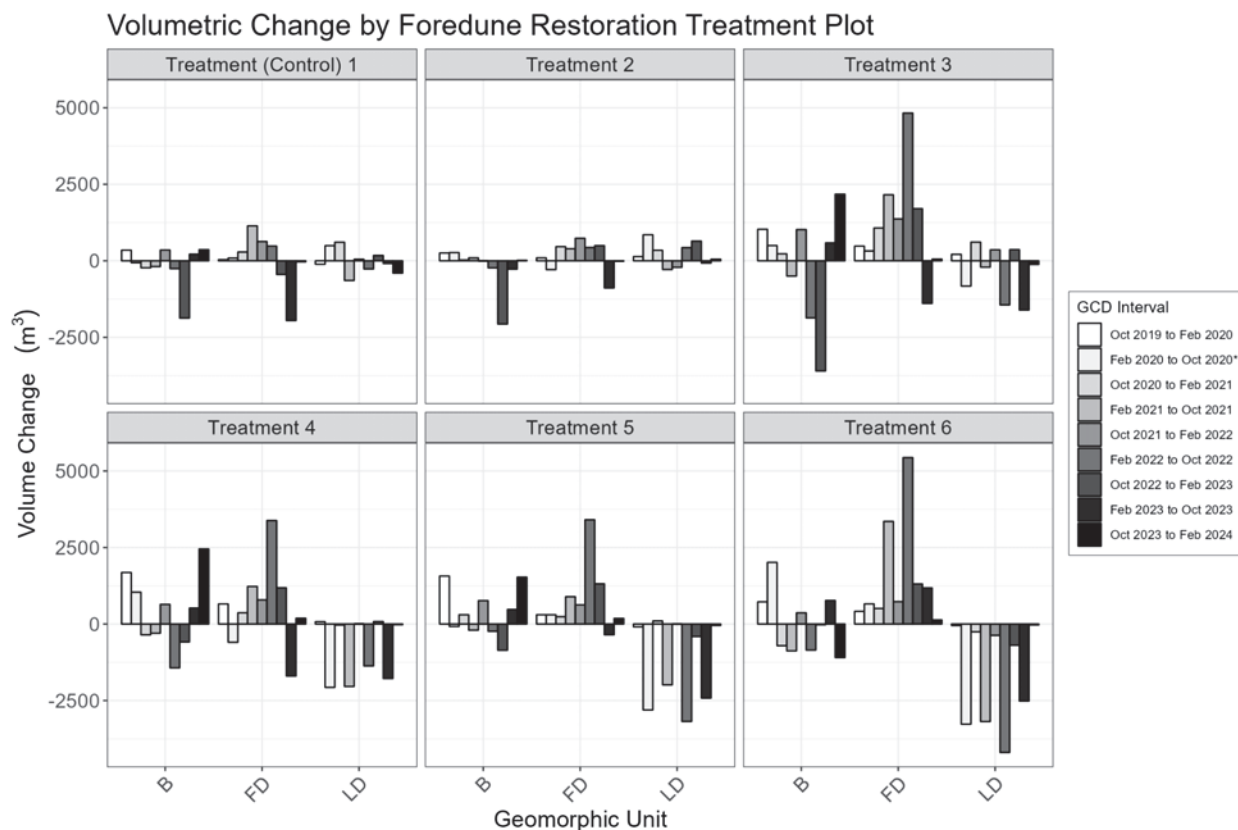
Figure 10. Bar graph of observed volumetric changes (m³) within the beach (B), foredune restoration plots (FD), and landward dunes (LD), for each treatment, across each topographic change interval. Asterisk in the legend indicates the Feb. 2020 to Oct. 2020 COVID-19 closure period that occurred between Mar. and Oct. of 2020.

Changes in the landward dune units (LD) behind the treatment plots are somewhat decoupled from those within the upwind foredune treatment and beach plots due to the continued influence of OHV traffic. These units also differentially experience landscape scale secondary flow patterns generated by larger dunes outside of the FRA (e.g., Pavilion Hill or larger barchanoid and transverse dunes)(Figure 1) as well as evolving vegetation and dune roughness effects that modulate surface shear stress and sand transport patterns within and beyond the

treatment plots. Areas downwind of TP3-6 show seasonally alternating (peak-valley) trends in their sediment budgets, whereas areas downwind of TP1-2 do not show this trend. This could also relate to the greater and seasonally varying influence of plant growth/roughness, sand accretion, and dune development within TP3-6 compared to TP1-2. For instance, this seasonal pattern is evident in the LD unit downwind of TP3, which alternated between positive budgets in fall/winter (Oct. to Feb.) and negative budgets during the wind and plant growth season (Feb. to Oct.) when more sediment accreted in the upwind treatment plot. The longer term trend of this cycle is predominantly negative in the LD units behind TP4-6 (Table 3), which have developed increasingly larger dunes and more extensive plant cover.

The influence of regional scale seasonal to interannual climatic variability events, such as El Niño seasons, are not easily discernible in foredune treatment responses. Generally, El Niño seasons bring increased chance of elevated erosional water levels in coastal California[11]. The El Niño event of 2023-24 was one of the five strongest on record[12] and peaked in Nov. 2023 through Jan. 2024. This event did not directly correlate, however, with significant beach erosion at ODSVRA. Rather, notable beach erosion occurred in the preceding winter (2022-2023) during a season of pronounced coastal storms and atmospheric river events.

4.2. Vegetation Change and Dune Development

Since implementation, all restoration treatment plots (TP2-6) have shown an increase in plant cover (Figure 6). TP6 and TP3, respectively, experienced the fastest rates of vegetation establishment, while the TP1 control site and TP2 have shown negligible to slow rates of plant cover to values that remain below the historical average. Interestingly, all plots showed a notable decrease in plant cover in the most recent interval (Oct. 2023 to Feb. 2024).

The patterns of vegetation change in this most recent interval are shown in Figure 11. While all plots recorded decreases in plant cover, TP6 experienced the greatest loss (-7.7%), followed by TP5 (-3.5%), then TP3 (-3.4%). The vegetation change map shows that declines in plant cover were widespread and relatively evenly distributed across all plots, as opposed to localized impacts along the seaward edge that could relate to high water event impacts (e.g., erosion, seawater inundation), for example. Although the specific cause of this decline is unknown, some combination of relatively wet winters, lower wind conditions (which reduce burial and inhibit

[11] Barnard, P.L., Short, A.D., Harley, M.D., Splinter, K.D., Vitousek, S., Turner, I.L., Allan, J., Banno, M., Bryan, K.R., Doria, A., Hansen, J.E., Kato, S., Kuriyama, Y., Randall-Goodwin, E., Ruggiero, P., Walker, I.J., & Heathfield, D.K. (2015). Coastal vulnerability across the Pacific dominated by El Niño/Southern Oscillation. *Nature Geoscience* 8, 801–807. https://doi.org/10.1038/ngeo2539

[12] World Meteorological Organization (WMO), 05 March 2024. *"El Niño weakens but impacts continue."* https://wmo.int/news/media-centre/el-nino-weakens-impacts-continue

the growth of many coastal plants[13]), and saltwater inundation from recent winter storms could be at play. It is unclear if this downturn reflects a plateau response in the plant community, or simply just natural variability as the ecosystem continues to develop. Regardless, continued monitoring is recommended to track progress in plant cover and, in conjunction with CDPR vegetation transect monitoring, to identify if there are particular species responses behind this recent decline in vegetation.

Figure 11. Change in vegetation between Oct. 2023 and Feb. 2024. Green represents pixels with vegetation in the top two panels (Oct. 2023 and Feb. 2024). The bottom panel shows where vegetation expanded (blue) or was lost (red) from Oct. 2023 to Feb. 2024.

Corresponding dune development continues to differ distinctly across the treatment plots. At the TP1 control site, protodunes and transverse/barchanoid ridges continue to migrate through the plot, ranging in height from 0.3 m near the seaward edge to 1.3 m at the landward edge, with limited nebkha development near the seaward edge of the plot. Combined with a net neutral sediment budget, this indicates appreciable sand bypassing through the control plot due to limited vegetation cover.

---

[13] Tobias, M.M.(2015). California foredune plant biogeomorphology. *Physical Geography*, 36(1), pp.19-33.

A similar pattern of migrating dune ridges was observed in TP2 and TP3, but with vegetated nebkha near the center of TP2 (>2 m high) and much larger (>3 m) coalesced nebkha ridges in TP3. These nebkha are formed predominantly with *Abronia latifolia*. Until Oct. 2023, TP2 and TP4 were the only sites with developed nebkha to show net erosion (volumetric loss) in response to wind erosion following installation. In TP4, this related to the development of erosional streets between the lower density straw planting circles.

Widespread nebkha development was observed in TP4-6. In TP4 and TP5 nebkha developed mostly on the planting circles and now reach heights > 2 m. TP5 has a greater number of larger nebkha distributed more broadly across the plot due to the closer spacing of the planting nodes, whereas nebkha in TP4 are generally confined to the seaward half of the plot. TP6 began as the roughest of all the plots (full straw cover, many randomly distributed plants), but only the seaward edge and northern fenceline of the plot have shown appreciable dune development, while the size and development of nebkha in the central portion of the plot remains limited.

Feedbacks between dune roughness, secondary flow patterns, surface shear stress, and sand transport will continue to evolve and influence dune development[14]. While beyond the scope of this report, ongoing work comparing wind data from the meteorological stations at the eastern edge of the plots, nebkha development, and geomorphic change suggests that TP3, TP5, and TP6 have the greatest impact on the wind fields. Variations roughness patterns between these plots has resulted in significantly different dune development pathways (Figure 12). TP5 has formed elongated nebkha chains with some coalescence, partly in response to the initial (random) arrangement of the straw planting circles. TP3 has developed laterally coalesced nebkha ridges at multiple locations to form some of the largest dunes within the FRA. Additional observations in TP2 and TP6 confirm two distinct developmental pathways. First, nebkha in TP2 and TP6 tend to 'clump' (wind-normal coalescence) and widen to produce discontinuous flow-transverse nebkha ridges. This lateral extension of nebkha is key to the development of a shore-parallel foredune ridge and the discontinuous morphology of foredune ridges in central and southern California is the preferred form, given the controls of regional climate and native dune plant communities. Second, nehbkha in TP4 and TP5 primarily exhibit 'chaining' (wind-aligned extension) that connects downwind nebkha via shadow dune extension. This pattern is partly driven by initial positioning of the planting zones and intervening erosional streets, but this type of morphological organization (long streamlined nebkha ridges with erosional deflation troughs) is also observed in the North Oso Flaco reference site (see Figure 1).

---

[14] Walker, I. J., & Hesp, P. A. (2013). 11.07 Fundamentals of Aeolian Sediment Transport: Airflow Over Dunes. *Treatise on Geomorphology*, ed. J. F. Shroder, 109–133. Elsevier
https://linkinghub.elsevier.com/retrieve/pii/B9780123747396003006

Number: 1   Author: SAG   Subject: Inserted Text   Date: 6/24/2024 1:22:13 PM

in

Number: 2   Author: SAG   Subject: Comment on Text   Date: 7/1/2024 10:46:38 AM

Suggest deleting "significantly". How do you demonstrate significance?
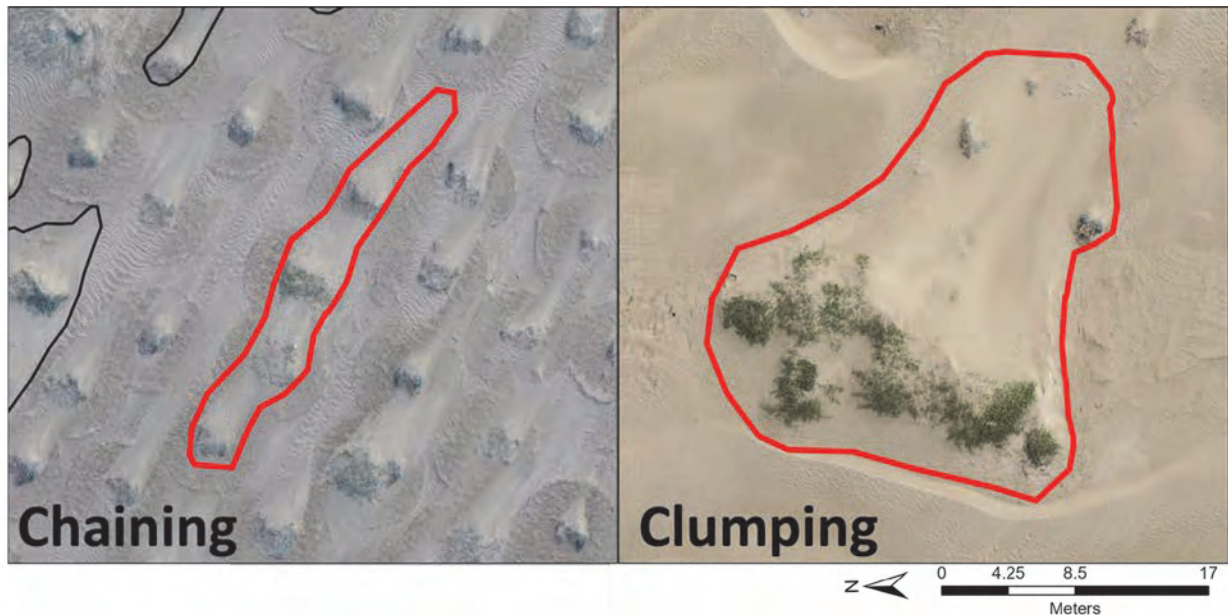
Figure 12. Examples of two distinct dune evolution responses emerging in the treatment plots. Nebkha chaining (example from TP5) involves wind-aligned extension of nebkha and shadow dunes to form long, linear ridges that do not exhibit substantial wind-normal coalescence with proximal nebkha. Nebkha clumping (example from TP3) refers to lateral coalescence of nebkha that produces discontinuous wind-normal dune ridges with some wind-aligned shadow dune extension that facilitates wider nebkha organization with a broader tail.

4.3. Performance Assessment of Restoration Treatments

The foredune restoration project at ODSVRA was designed to re-establish a foredune ecosystem with dust emissions mitigation benefits using a 'nature-based' approach with an assortment of treatment types of increasing levels of intervention. As the project is subject to adaptive management, it is important to recurrently evaluate the relative performance of the treatments for forming self-sustaining dunes and reducing dust emissions. In response, we developed, in consultation with SAG and APCD, a series of indicators of performance that would be monitored and assessed each year. The outcome is a cumulative score whereby lower total values indicate higher overall performance. Indicators and relative performance assessment evaluation (Figure 13) are discussed below and explained further in [1]Walker et al. (2023).

Number: 1   Author: SAG   Subject: Comment on Text   Date: 7/3/2024 11:27:58 AM
Only reference listed to not get a footnote. Stylistic point.
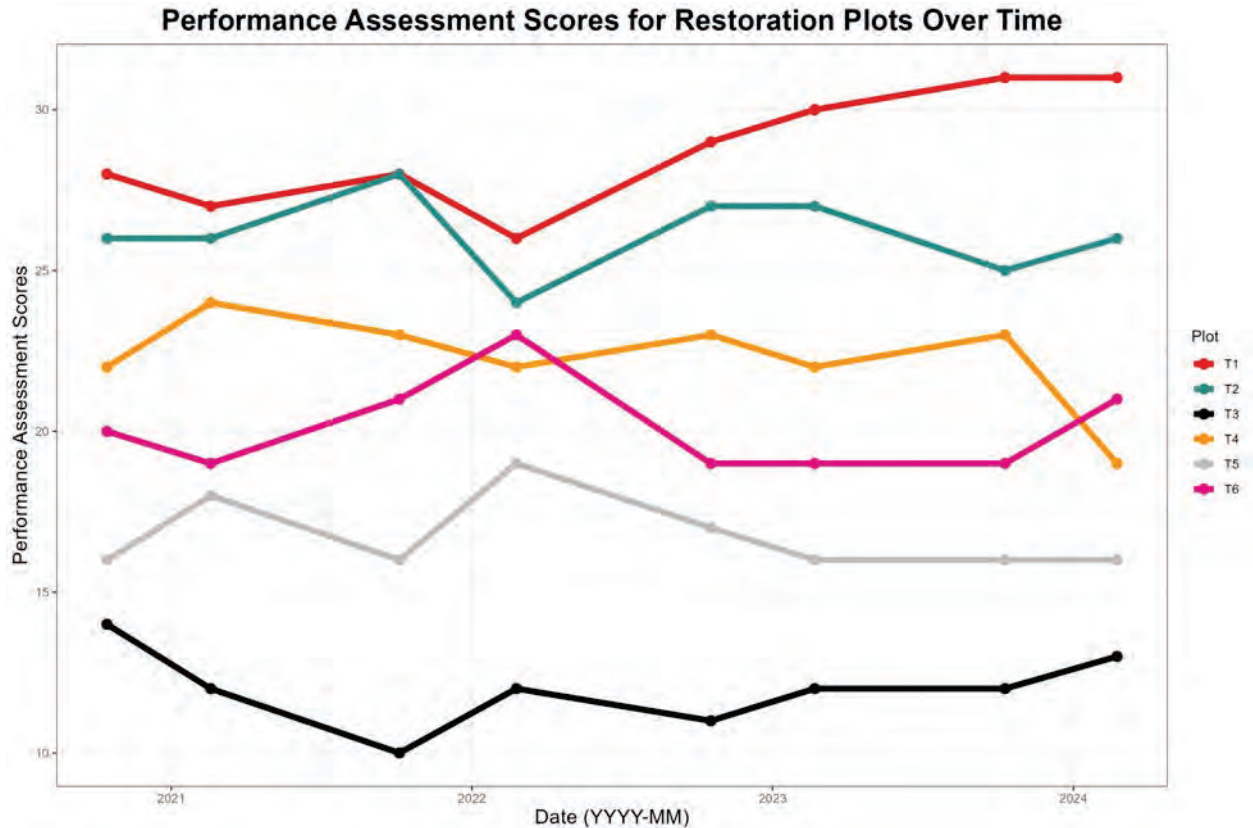
Figure 13. Performance assessment trends of restoration treatment plots since installation in Feb. 2020. Performance scores are derived based on relatively ranked scores (1 = best performer, 6 = poorest performer) across 5 different indicators, including: 1) positive sediment budget, 2) aeolian activity, 3) plant cover, 4) dune development, and 5) dust emissions mitigation potential. Lower cumulative scores indicate more effective performance. See text and Walker et al. (2023) for further description.

Figure 13 shows the trajectories of cumulative treatment plot performance since installation in Feb. 2020. Generally, the rankings have not changed significantly since Oct. 2022, with the exception of a recent switch between TP4 and TP6. Overall, TP3 has maintained the highest performance ranking (lowest scores) since installation, followed by TP5. TP2 maintains the poorest performance, whereas TP4 and TP6 have alternated twice over time for third and fourth in the total performance ranking. The recent switch in ranking for TP4 over TP6 relates to a negative trend in sediment budget (though still positive), limited nebkha development, and greatest declines in vegetation cover in TP6. Specific summaries for each of the assessment criteria are as follows:

1. **All foredune treatment plots continue to show net positive sediment budgets**. Even though the last two intervals have exhibited mostly negative (Feb. 2023 to Oct. 2023) or neutral (Oct. 2023 to Feb. 2024) budgets, the net change remains positive across all plots

and greater than that of the TP1 control plot (minimal/neutral). TP6 exhibits the highest net positive change, followed by TP3, yet most of the response in TP6 is limited to sand fence accretion along the northern margin and development of nebkha along the seaward edge.

2. **<u>Aeolian processes remain active in all treatments</u>** shown by rippled sand transport corridors, continued dune development, coalescence and migration, and persistence of erosional deflation surfaces with coarse lag deposits on all sites. [1]<mark>rosional responses are expected during dune development and do not necessarily reflect poor performance.</mark> Maintenance of aeolian processes is required to provide needed ecological disturbance required for plant growth and dune development.

3. **<u>Plant cover shows a net positive trend in all treatment plots</u>**. Increases in the TP1 control site have been negligible until recently and, although very small, are restricted to the seaward edge of the plot. Appreciable declines in plant cover were observed in all treatments since Oct. 2023. This was most pronounced in TP6, with smaller declines in TP3-TP5, and little change in TP2. The pattern of vegetation decline is widespread (vs. localized) in all plots and the cause remains uncertain, but could relate partly to recent unusually wet and stormy winter conditions. On average, plant cover across the FRA (excluding TP1) is 6.55% with a current maximum of 11.68% in TP6 and a minimum of 3.10% in TP2. Some species, namely *Abronia latifolia*, have shown rapid establishment and growth, promoting appreciable dune development. Recent changes in the trajectory of plant community development reinforce that more time is required to assess broader foredune ecosystem re-establishment and sustainability.

4. **<u>Dune development continues in all treatment plots</u>**. The largest (>2 m) nebkha have developed in TP3 and TP5, smaller (1.0-1.5 m) nebkha in TP2 and TP4, and multiple smaller nebkha in TP6. This past year (2023-2024) also saw increased development of nebkha along the seaward edge of most treatment plots. Appreciable transverse, unvegetated dune migration and sand bypassing continues within the TP1 control plot, yet it is important to maintain a control site that is also not subject to OHV activity for reference. Two distinct patterns of dune evolution have emerged - nebkha clumping (with lateral extension) and chaining (with downwind elongation) - both of which are important indicators of the next stages of foredune evolution at the site. As dune evolution continues in the presence of vegetation, continued accretion, geomorphic and ecological diversity, and dust mitigation benefits are expected.

5. **<u>Potential for treatments to reduce dust emissions is increasing</u>** as indicated by qualitative observations of increasing dune development, net increases in sediment accretion and

Number: 1   Author: SAG   Subject: Comment on Text   Date: 6/24/2024 1:35:47 PM

this is an interesting statement given that the rankings are influenced by whether the treatment area is accumulating sediment (in criterion 1).

vegetation cover, and recent PI-SWERL testing by DRI in the FRA in Summer 2022. Collectively, these observations suggest that the FRA, and other exclosed areas experiencing dune development and increasing plant cover (e.g., the Western Snowy Plover exclosure) have lower dust emissivity than neighboring open riding areas. More quantitative assessment of FRA treatments on flow dynamics and shear stress patterns is recommended to better identify related aerodynamic processes within, and dust emissions mitigation benefits downwind, of the restoration treatments.

5. Summary and Conclusions:

To monitor and assess the performance of the foredune restoration dust mitigation project at the ODSVRA, biannual UAS surveys of the FRA have been conducted from Oct. 2019 through to Feb. 2024. Primary data products, gathered with a WingtraOne fixed-wing UAS platform, include:

1. Ten (10) high resolution (~1.5 cm) visual (RGB) aerial orthomosaic images encompassing ongoing foredune restoration efforts and sites of landward interest between Pavilion Hill and Oso Flaco Lake,
2. Eight (8) high resolution (~3.0-7.5 cm) multispectral (RGB-RE-NIR-Pan) orthomosaic images collected concurrently with the RGB datasets since Oct. 2020,
3. Eight (8) high resolution (~3.0-7.5 cm) NDVI orthomosaics derived from the multispectral orthomosaic datasets used to assess vegetation extent and change,
4. Ten (10) high resolution (10 cm) three-dimensional point clouds and rasterized DEMs of surface topography used to assess site geomorphic and sediment volume changes, and
5. Nine (9) topographic change maps of statistically significant locations of erosion and deposition derived by comparison between DEM intervals.

Prior to implementation of the FRA in Feb. 2020, there was negligible vegetation present at the site and change was primarily driven by: i) aeolian processes moving sand landward by saltation and low transverse dune migration, and ii) the impacts of vehicle activity and camping. From the baseline (pre-restoration) surveys (Oct. 2019 to Feb. 2020), supply to the beach was variable, but net positive and deposition within the FRA generally was low to negligible over the barren sand surfaces. Following this, sand accretion, plant growth, and resulting dune development has continued steadily within the treatment plots, with some (TP2-6) featuring larger nebkha dunes (exceeding 2 m in TP3, TP5) and appreciable vegetation cover (~3-12%) to date. During this past year (2023-2024), low winds and significant precipitation might partly explain observed decreases in plant growth and low to neutral rates of accretion. Despite a strong El Niño event during 2023-24, widespread erosion of the beach was not recorded in the recent change

Number: 1   Author: SAG   Subject: Comment on Text   Date: 6/26/2024 12:59:33 PM
change from to to what?

Number: 2   Author: SAG   Subject: Comment on Text   Date: 7/1/2024 3:53:47 PM
foredune restoration

Number: 3   Author: SAG   Subject: Comment on Text   Date: 6/26/2024 1:00:36 PM
There is continued reference to significant precipitation being harmful to plant growth. What aversion to water do these species have? Do we see similar growth suppression in the back dunes? Is it possibly cooler temperatures or fewer days of sun instead of more water?

detection results, although some overwash and localized erosion along the leading edge of the plots was observed.

Following four full wind and plant growth seasons, the restoration plots continue to evolve on different trajectories as a function of initial treatments and variability in other controlling factors such as sand supply to the beach, plant cover, and roughness effects. The relative rankings of treatment performance has not changed significantly since Oct. 2022. Overall, TP3 has maintained the highest performance since installation, followed by TP5, due largely to continued positive sediment budgets, greatest amounts of dune development and extension, consistent maintenance of aeolian activity, continued increases in plant cover, all with collective impacts for providing the greatest potential reductions in dust emissions. [1]P2 maintains the lowest performance due to modest amounts of accretion and dune development, low rates of plant cover increase, and correspondingly lower relative dust emissions reduction potential. The most intensive treatment (TP6) slid recently to second lowest performance due to continued declines in sediment budget, limited dune development, and marked declines in vegetation cover. Monitoring will continue as the treatments evolve to detect further responses indicative of success or concern for adaptive management and for longer-term sustainability of the FRA as a dust control mitigation.
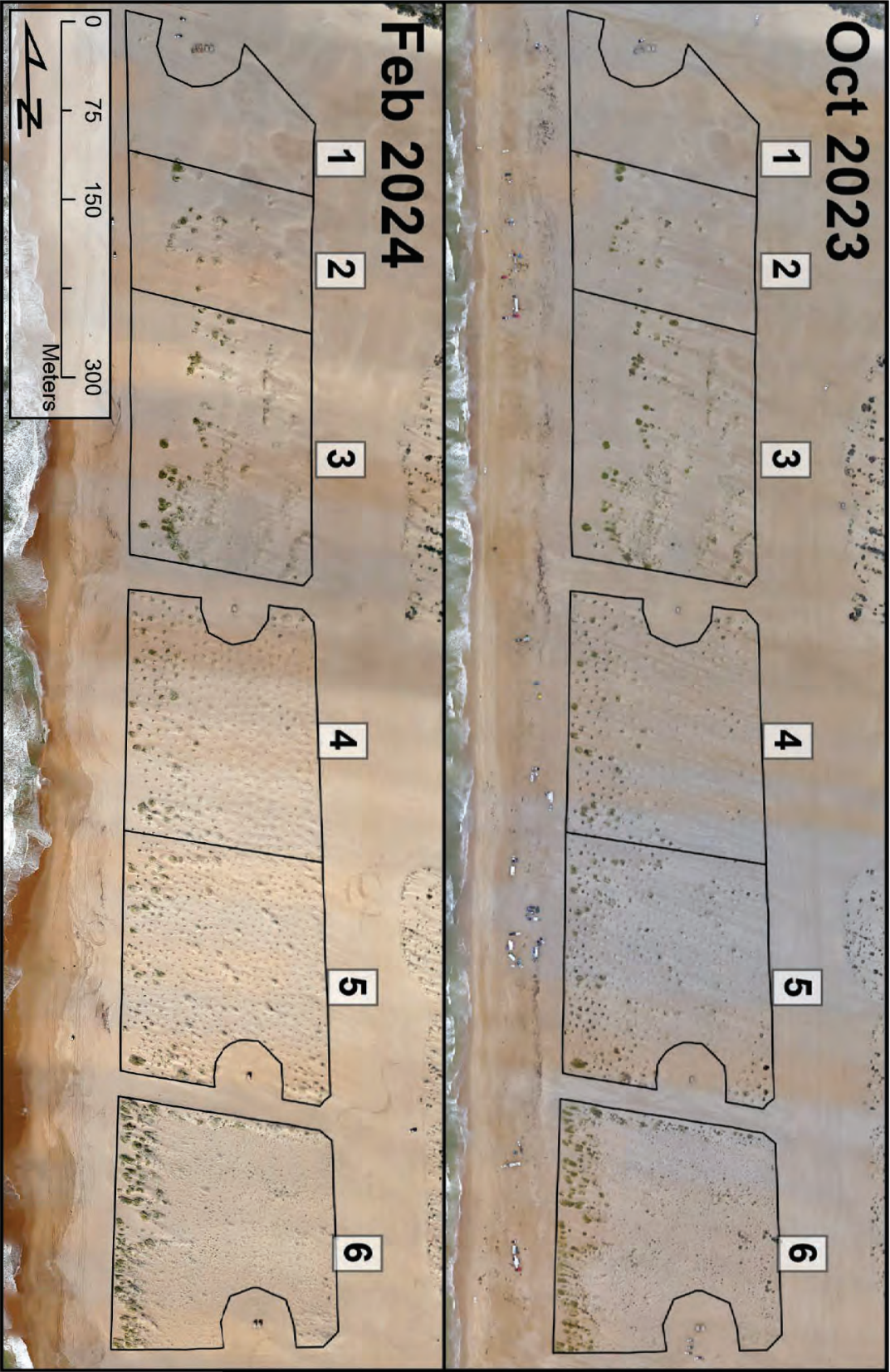
Number: 1   Author: SAG   Subject: Comment on Text   Date: 7/1/2024 3:54:29 PM
Not TP1?

Appendix A: Foredune Restoration Area RGB Orthomosaic Extent

Oct 2020

Feb 2021

1 2 3 4 5 6

1 2 3 4 5 6

0 75 150 300
Meters

Oct 2023

Feb 2024

35
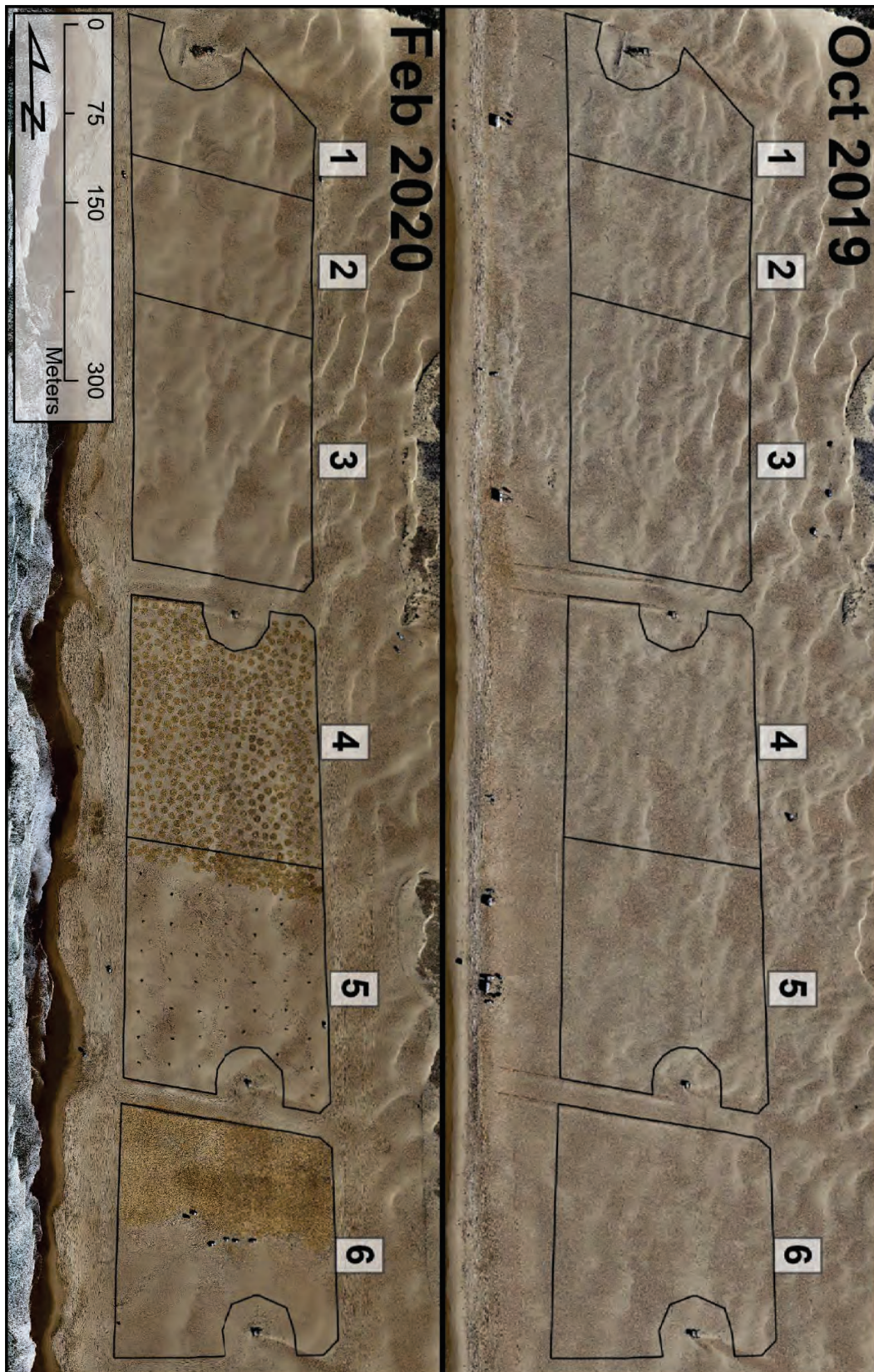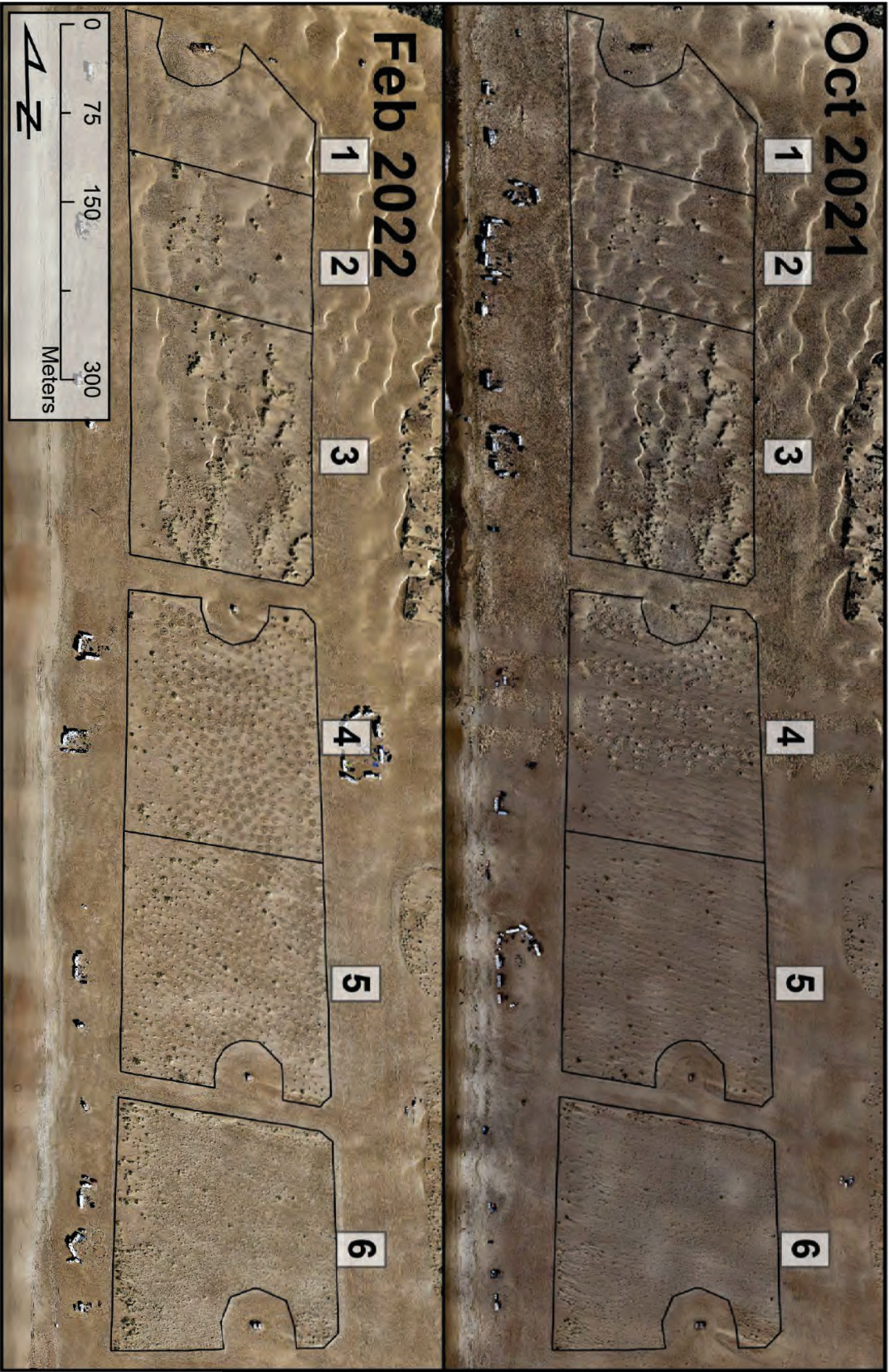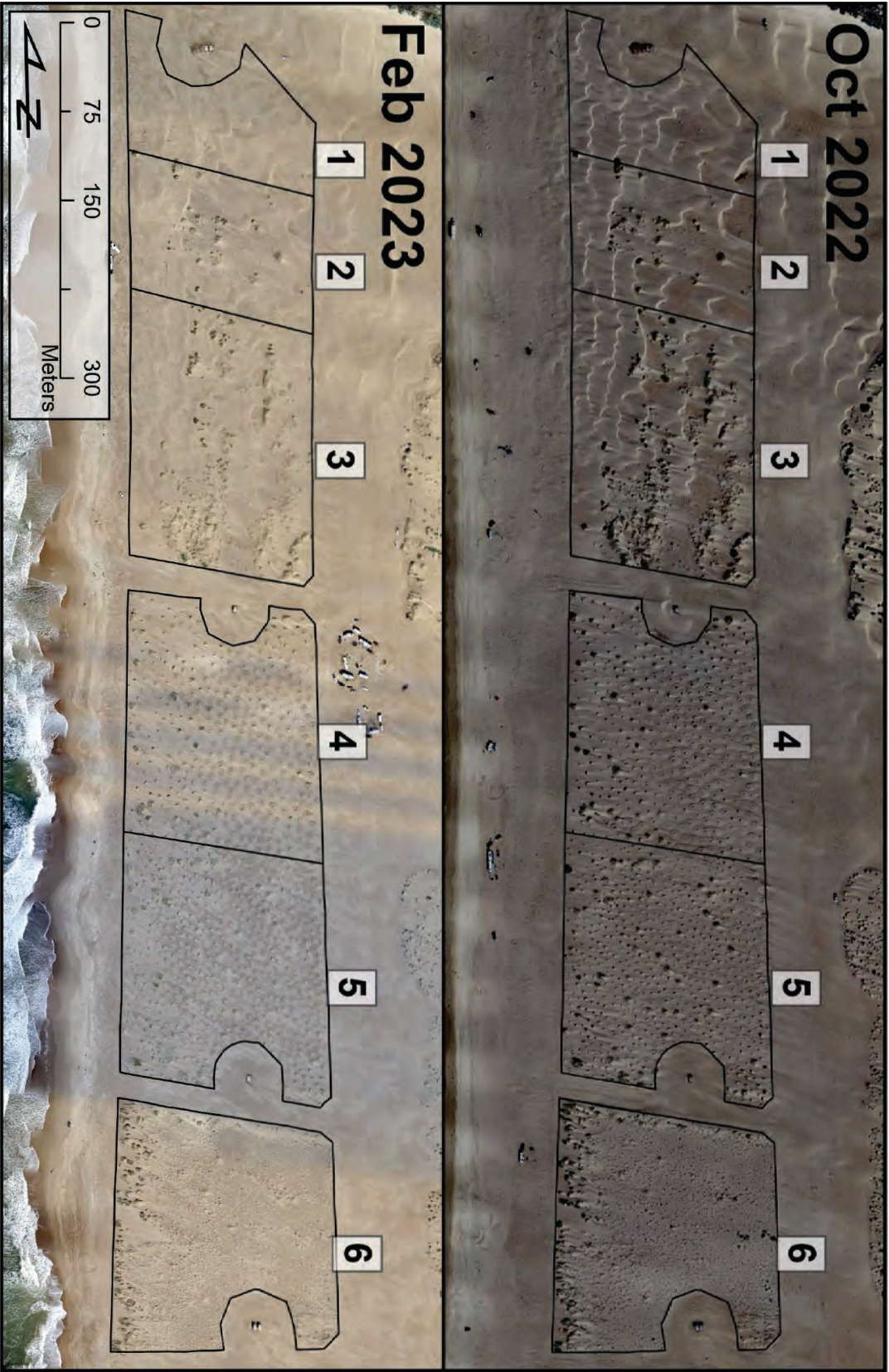
ODSVRA Dust Control Program Draft 2024 ARWP

ATTACHMENT 05

Preliminary Analysis of Time-Lapse Photo Monitoring at the Oceano Dunes Foredune Restoration Site

- Preliminary Analysis of Time-Lapse Photo Monitoring at the Oceano Dunes Foredune Restoration Site (UCSB Report)

- SAG Review of UCSB Report "Preliminary Analysis of Time-Lapse Photo Monitoring at the Oceano Dunes Foredune Restoration Site" (SAG Memo)

THIS PAGE WAS INTENTIONALLY LEFT BLANK.

Preliminary Analysis of Time-Lapse Photo Monitoring at the Oceano Dunes Foredune Restoration Site
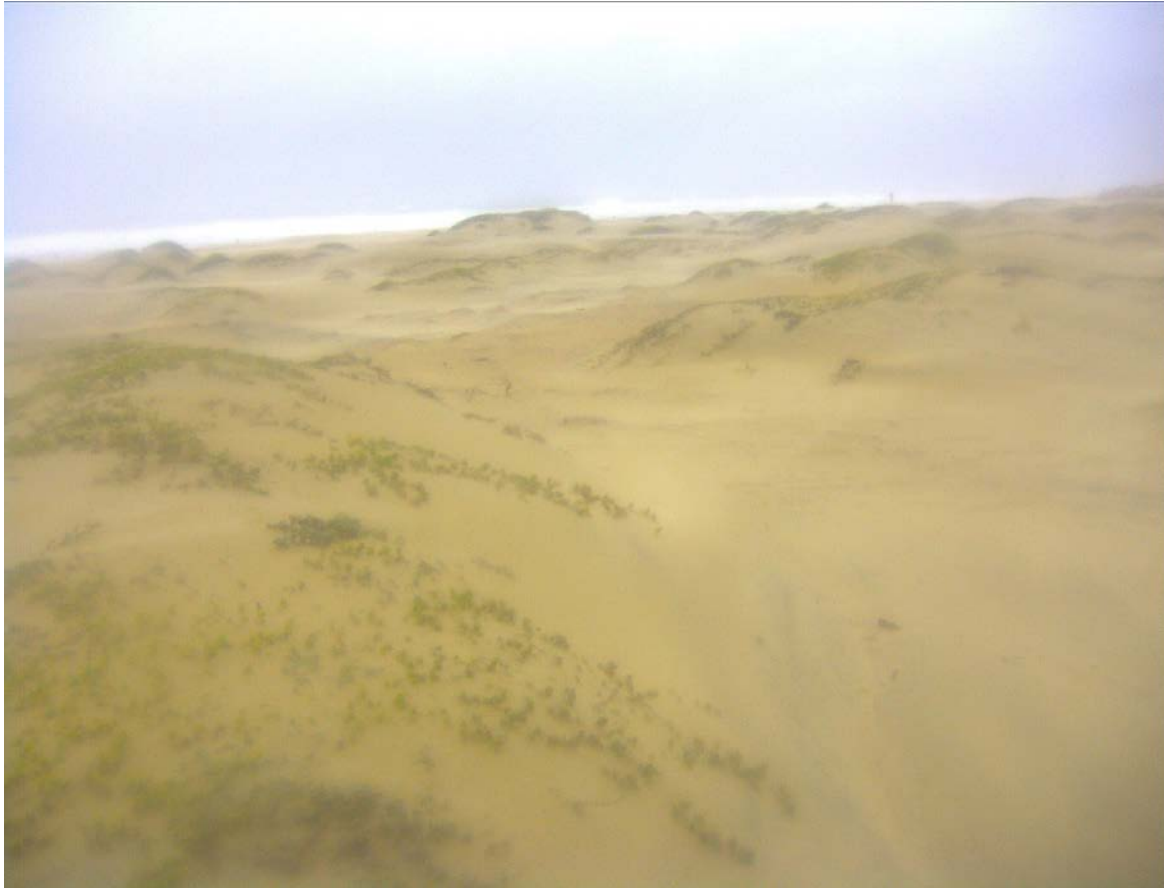
Restoration Plot 3 during a strong wind event with widespread sediment transport.

Prepared by Madison Heffentrager[1], Ian Walker[1,2], Nitzan Swet[1], and Zach Hilgendorf[1,3]

June 2023

[1] Department of Geography, University of California, Santa Barbara
[2] Member of the ODSVRA Scientific Advisory Group
[3] Department of Geography and Anthropology, University of Wisconsin-Eau Claire

INTRODUCTION

The Oceano Dunes State Vehicular Recreation Area (ODSVRA) is a popular location for recreation activity and off highway vehicle driving. However, recent monitoring and research has shown that the dunes are highly emissive of dust-sized particles (PM_{10}) which have the potential to pose a health hazard to nearby populations[1]. To mitigate this, a dune restoration strategy was implemented along the upper beach in a portion of the ODSVRA in February 2020 (Figure 1). The study site is located within an extensive Off Highway Vehicle (OHV) activity area that used to host a foredune ecosystem, and related plant cover, comparable to that further south near Oso Flaco Lake (Figure 2). The of the restoration site was designed to promote sediment deposition and dune development through implementation and evaluation of five (5) different treatment strategies (Figure 3) to promote a foredune morphology similar to nearby reference sites at Oso Flaco Lake (Figure 2)[2]. A goal of the ongoing project is to determine how the various restoration treatments respond to typical high wind and sand transport events as a means to assess their effectiveness. To date, foredune development and related plant community responses have been monitored and assessed with imagery captured from an uncrewed aerial system (UAS) and interpretation of orthomosaic images, multispectral imagery, and digital terrain models (DTMs) derived using Structure-from-Motion (SfM) photogrammetry. A more detailed description of the current goals and purposes of this project are detailed by Walker et al. (2023)[2].

Previous reports addressed the history of vegetation cover in the dunes, the design and progress of the foredune restoration project and plots, and detail erosion and deposition over time[2,3,4]. This report provides a preliminary analysis of time-lapse imagery captured from individual cameras installed at the meteorological stations on the landward edge of each restoration plot (Figure 4). From March 13, 2022, to May 31, 2023, State Parks, the Coastal San Luis Resource Conservation District (San Luis RCD), DRI, and UCSB conducted meteorological and saltation flux measurements in each of the 6 foredune treatment areas. These measurements are intended to characterize wind changes, monitor saltation activity, and relate these data to changes in vegetation cover and dune morphology through time. The measurements were conducted with a suite of instruments on a three-meter tower on a platform deployed near the eastern edge of each treatment plot, approximately 10 m west of the eastern (landward) fence line and halfway along the north-south length of each treatment area (Figure 4). Campbell Scientific CCFC cameras[5] were installed to characterize the types and frequency of formative processes within the treatment plots including sediment transport, plant growth, and dune development at a temporal scale that is much faster than the biannual UAS surveys.

[1]Gillies, J.A., Furtak-Cole, E., Nikolich, G. and Etyemezian, V., 2022. The role of off-highway vehicle activity in augmenting dust emissions at the Oceano Dunes State Vehicular Recreation Area, Oceano, CA. *Atmospheric Environment: X*, *13*, p.100146.

[2] Walker, I J., Hilgendorf, Z., Gillies, J.A., Turner, C.M., Furtak-Cole, E., Nikolich, G. (2023). Assessing performance of a nature-based foredune restoration project, Oceano Dunes, California, USA. Earth Surface Processes & Landforms, 48(1): 143-162.

[3] Swet, N., Hilgendorf, Z, & Walker, IJ. (2022). UCSB Historical Vegetation Cover Change Analysis (1930-2020) within the Oceano Dunes SVRA. Technical report to the Oceano Dunes Scientific Advisory Group (SAG) and the State of California Parks and Recreation Department Off-Highway Vehicle Division. p 86.

[4] Hilgendorf, Z & Walker, IJ. (2021). UCSB-ASU 2020-2021 ODSVRA Foredune Restoration UAS Survey Report. Technical report to the Oceano Dunes Scientific Advisory Group (SAG) and the State of California Parks and Recreation Department Off-Highway Vehicle Division. p34.

[5] https://www.campbellsci.ca/ccfc

The purpose of this report is twofold. First, it presents methods used for data collection fand related quality assessment, data compilation, and coding of distinct formative events. Second, a preliminary proof-of-concept analysis is provided from a subset of images from January 2023, almost 3 years after implementation of the foredune restoration treatments. From this, insights for further analysis, limitations, and benefits for the foredune dust mitigation project are discussed. Additional time-lapse videos of each treatment and examples of typical formative events are also available.
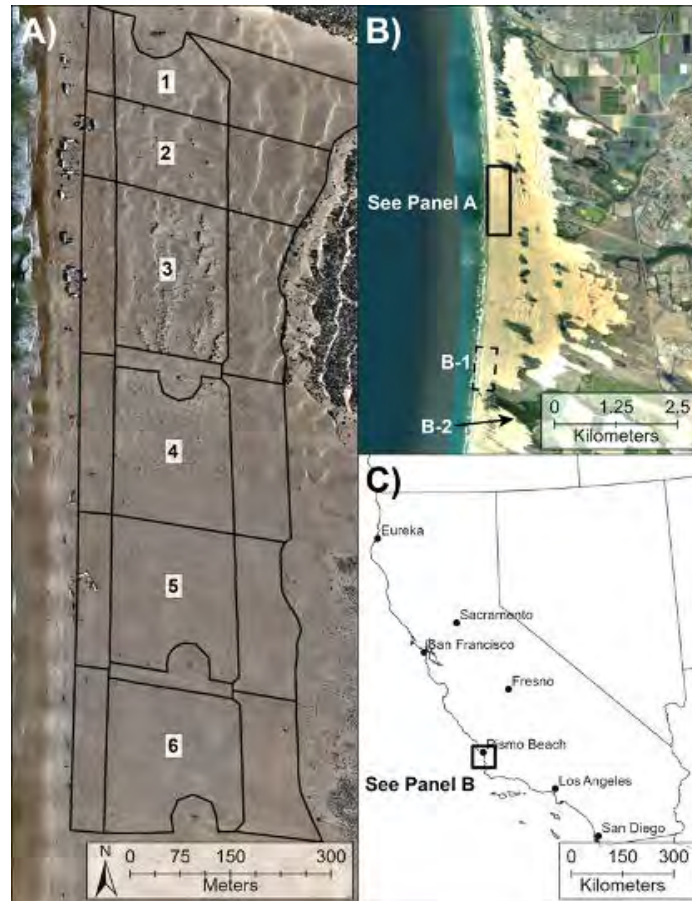
Figure 1: Location of the foredune restoration plots at ODSVRA.
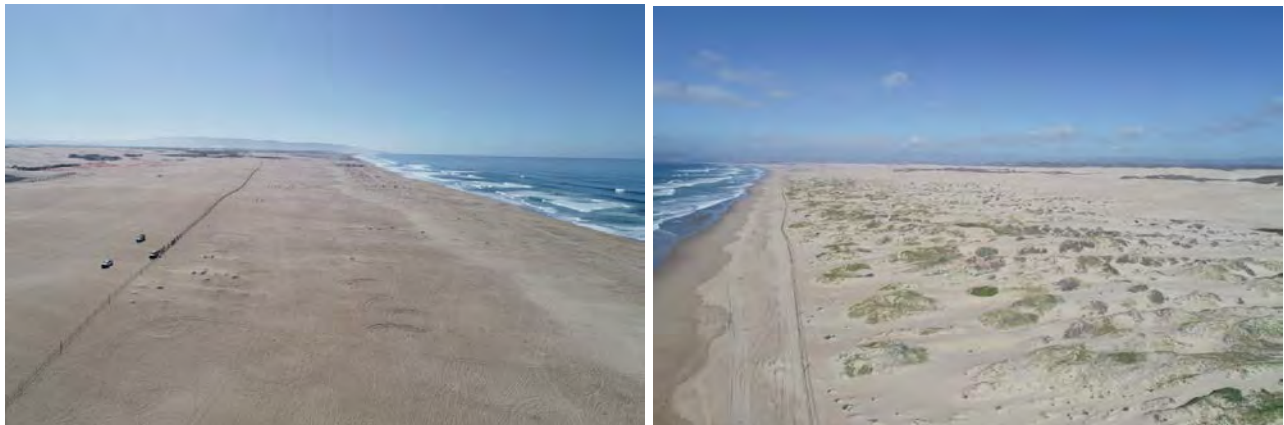
Figure 2: Oblique images of the foredune restoration site prior to fencing the treatment plots (left) compared to an established foredune reference site at Oso Flaco (right).

Figure 3: The different treatments in each of the six restoration plots. Images were taken in May 2022 (photo credit: Ian Walker).

Figure 4: Locations of the meteorological stations equipped with cameras within each restoration plot. Othomosaic is from February 2022. The northern most plot is Site 1 leading numerically in order to Site 6 as the most southern plot. Treatment types of the plots are as follows: Site 1 - Control, Site 2 -Native Seeds, Site 3- Seeds and Sterile Grass Seed, Site 4- Low Density Planting Nodes, Site 5- High Density Planting Nodes, and Site 6- Broadcast Straw and Plants and Seed.

METHODS

Imagery was collected from May 2020 to April 2023 every 30 minutes from ~16:00 - 1:30 (GMT) or 07:00 - 17:30 local time (PST) (Table 1) to capture conditions during daylight hours only. Images continue to be collected and the most recent available download is incorporated into this report. All images were manually inspected for quality and suitability by the same researcher. Poor images were deleted to clean the dataset for further processing (Figure 5). Images were deleted because of fogginess, blurriness, lens obscuration by salt/dust film, or overexposure (Figure 6). Some poor images were kept, however, if they captured other useful responses, such as changing morphology. Images were viewed within either Microsoft Photos or Mac Preview by the same researcher.

Table 1: Imagery Collection Ranges. Treatment types of the plots are as follows: Plot 1 - Control, Plot 2 -Native Seeds, Plot 3- Seeds and Sterile Grass Seed, Plot 4- Low Density Planting Nodes, Plot 5- High Density Planting Nodes, and Plot 6- Broadcast Straw and Plants and Seed.

Station	Start Date and Time (GMT)	End Date and Time (GMT)
Plot 1	5/9/20 4:22 PM	4/4/23 6:33 PM
Plot 2	5/9/20 4:30 PM	4/4/23 6:03 PM
Plot 3	5/13/20 5:30 PM	4/4/23 6:03 PM
Plot 4	5/9/20 6:30 PM	4/4/23 5:33 PM
Plot 5	5/9/20 5:30 PM	4/4/23 5:53 PM
Plot 6	5/9/20 6:00 PM	4/4/23 5:53 PM
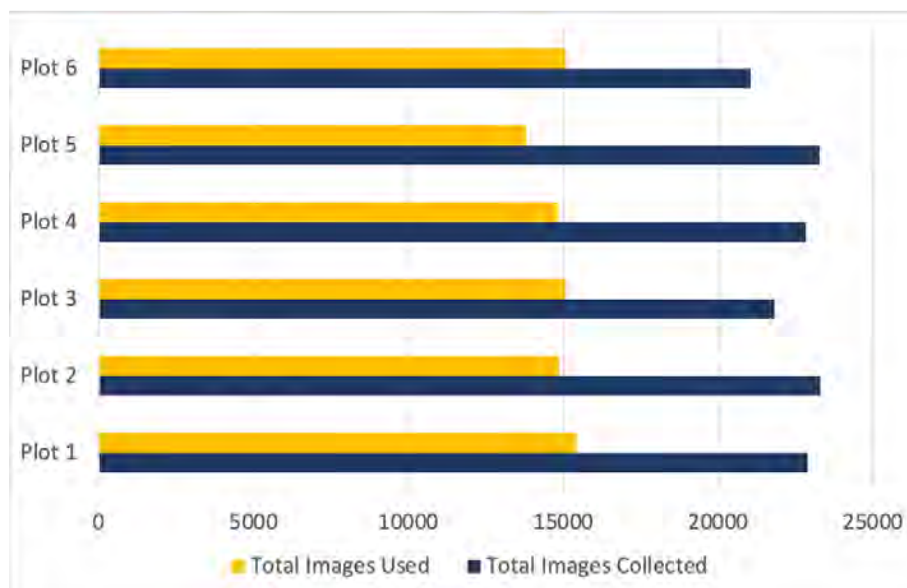
Figure 5: Total images used vs. collected. Variations in the number of total images collected result from differing collection periods (see Table 1). The number of figures used for this preliminary analysis are shown in Fig. 7. Treatment types are as follows: Plot 1 - Control, Plot 2 -Native Seeds, Plot 3- Seeds and Sterile Grass Seed, Plot 4- Low Density Planting Nodes, Plot 5- High Density Planting Nodes, and Plot 6- Broadcast Straw and Plants and Seed.
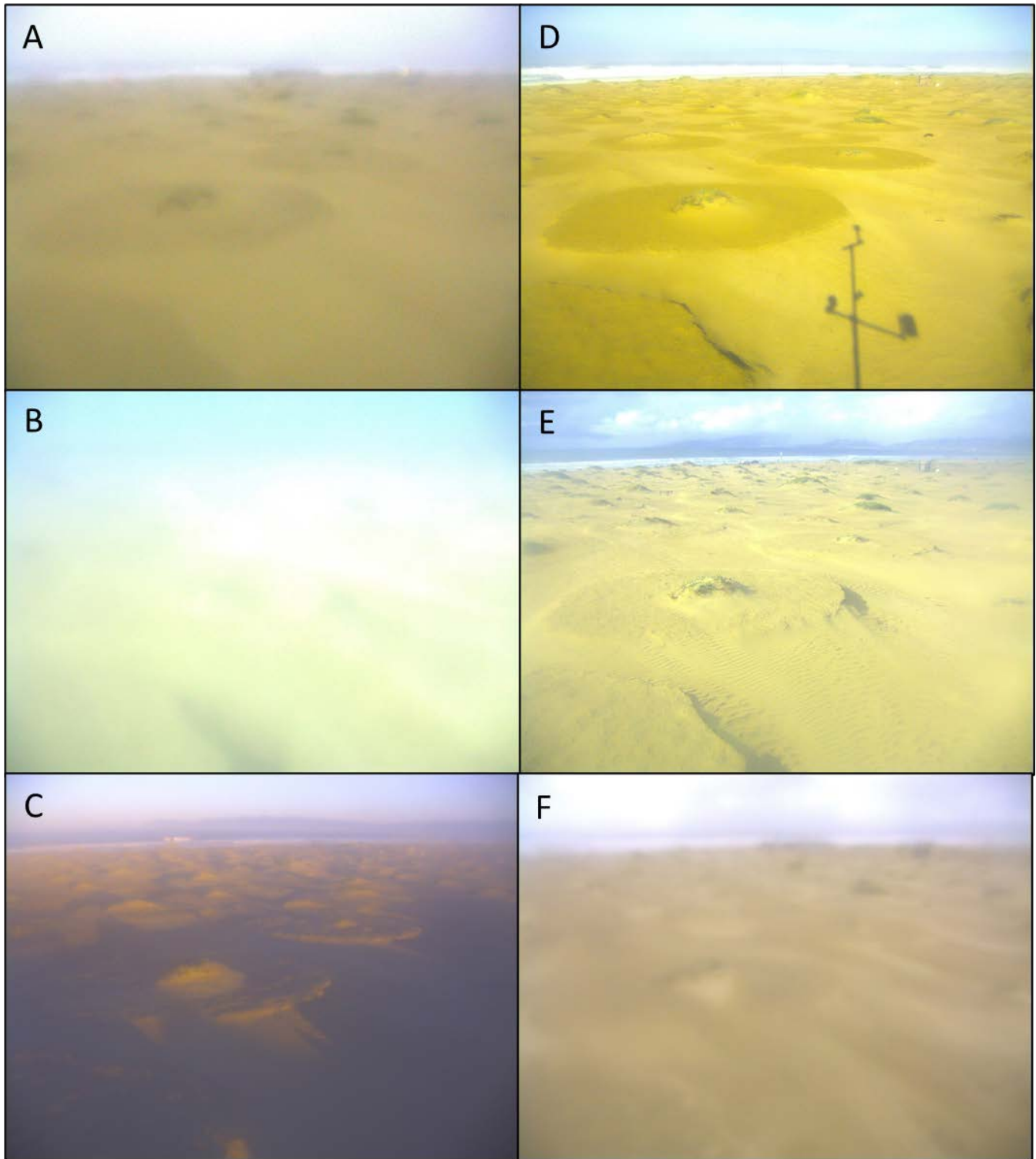
Figure 6: Examples of poor quality images showing fogginess (A), overexposure (B), and shadowing (C). D and E show good quality images. F is an example of a poorer quality image that was kept for analysis because active transport was visible between images. All are selected from January 2023 Station 4.

Images were classified based on similar methods performed by Grilliot et al. (2019)[6]. Aeolian activity

[6] Grilliot, M.J., Walker, I.J. and Bauer, B.O., 2019. The Role of Large Woody Debris in Beach-Dune Interaction. Journal of Geophysical Research: Earth Surface, 124(12), pp.2854-2876.

[6] Kalmikov, A., 2017. Wind power fundamentals. *Wind Energy Engineering*, pp. 17-24. Academic Press.

[7] Hilgendorf, Z., Walker, I.J., Pickart, A.J., & Turner, C.M., 2022. Dynamic restoration and the impact of native versus invasive vegetation on coastal foredune morphodynamics, Lanphere Dunes, California, USA. *Earth Surface Processes and Landforms*, *47*(13), pp.3083-3099.

was classified based on visible transport between the previous and following images for all images. Images were classified and tallied based on category and assigned attributes that described observable events, such as "aeolian transport" or "dune change", to generate a time chart of events and changes seen within each restoration plot (Table 2). Aeolian transport and dune change are typically directly related, and therefore coded as the same value, while meteorological conditions were coded independently (Table 2). For example, if there was trace activity of aeolian sediment transport in sunny dry conditions between two image frames, there would often be associated dune changes such as "dune migration", "dune building", "ripple movement", and/or "surface accretion". These types of conditions would result in a classification of 1,1,0 (Table 2). The classification resulted in tabular data and time series graphs that were directly compared with the timing of wind events above the sand transport threshold of approximately 6.5 m/s at 3.5 m height (see section 2.3.2.2). Corresponding wind data (speed and direction) from the same station/restoration plot were used to assess wind conditions and potential sand transport activity for each image. This assessment has not yet been cross-correlated to on-site saltation measurements.

Wind speed and associated time stamps were used to calculate a Threshold Wind Power Density (TWPD) to provide a measure of the power available for aeolian activity that could be compared to the corresponding camera imagery. TWPD was first applied by Kalmikov (2017)[6], and later by Hilgendorf et al. (2022)[7] and Walker et al. (2023)[2] for research in dune restoration. A general sand transport threshold of 6.5 m/s for the average diameter of sand grains (200 µm) was chosen to identify sand transport capable, or "high speed" wind events, while anything below this value are referred to as calm or incompetent conditions, with regards to aeolian sand transport. TWPD values were calculated in R Studio using the following equation:

$$TWPD = 0.5\, p_a\, u^3 \ \ (\text{in W/m}^2)$$

Where 0.5 is a constant, p_a is air density (1.225 kg/m^3 at 15 degrees Celsius), and u is the wind speed above the specified threshold (6.5 m/s).

TWPD values were computed for wind speeds every minute above 6.5 m/s and plotted. The wind events identified were compared to the timestamps associated with each of the station images to determine when aeolian sand transport could be visible across the plots. Sediment transport seen in the imagery was also cross compared with the wind data to determine if transport events were identified below the threshold and when sediment transport events were most visible in the imagery.

Time lapse videos were generated from the cleaned imagery to capture individual sediment transport events and various treatment plot responses. Comparison across treatment plots were made to determine how sand moved or was deposited for the same time stamps, as available. Longer videos will be produced for viewing dune building/migration over time and for long term records of dune ecosystem establishment.

Table 2: Coding key for monitoring camera image classification and analysis. Aeolian transport and associated dune changes are directly related and receive the same code. Meteorological conditions are coded independently of sediment transport and dune morphological responses.

Key	Aeolian Transport	Dune Morphological Changes	Meteorological Conditions
0	Inactive	No change	Dry, Sunny
1	Trace	Dune building, ripple formation/movement, sand accretion	Dry, Cloudy or Overcast
2	Active	Evidence of sediment erosion, sand streamers, surface deflation	Fog
3	Widespread	Widespread saltation cloud	Wet or Rain

Results from a sample subset of the larger dataset is provided below to demonstrate the concept for further analysis using the aforementioned methods. These methods can be applied monthly, seasonally, or annually to the entire dataset depending on project needs. The month of January 2023 was selected for this analysis because the restoration treatments had 3 years to develop and differences in sediment transport across the plots could be assessed. Although January is typically not the most active month for sand transport (see section 2.3.2.2, Fig. 2-9) compared to later spring months, the data were collected during a particularly stormy season, which was beneficial for capturing both abundant sand transport events, but also challenging conditions for quality image capture.

RESULTS

All useful images in the dataset to date were sorted, date/times recorded, and the dataset was quality checked. The resulting dataset contained sporadic missing dates/times for some or all of the plots, which resulted in varying image capture periods and total number of images collected across the plots (Table 1, Figure 5). For example, in Plot 3 the camera started image collection on 05/13/2020, whereas the rest of the plots started on 05/09/2020. Plot 6 had a gap in imagery from 03/17/2022 to 03/21/2022, reducing the amount of images collected for this plot. Individual days such as 11/28/2021 and 11/19/2021 also were missing in the majority of data across most plots.

The January 2023 subset of raw images did not show appreciable data gaps across the plots. The variations in the number of images shown in Figure 7 are largely due to poor image quality. There were also slight variations in timing of images across meteorological stations, ranging from 1-2 minutes off from the neighboring station. This time difference is likely not critical at the 30 minute temporal scale of the image collection, however, if exact timestamps across plots were desired for future analysis, this difference should be corrected via reference to a single station and/or a manual reset of the clocks on the data loggers.
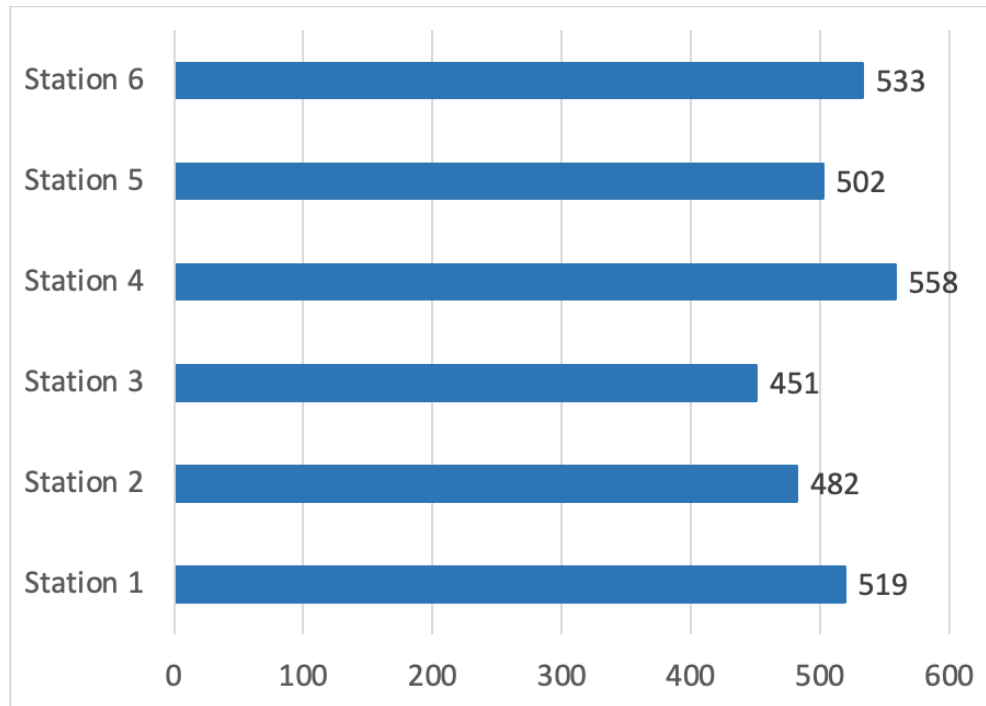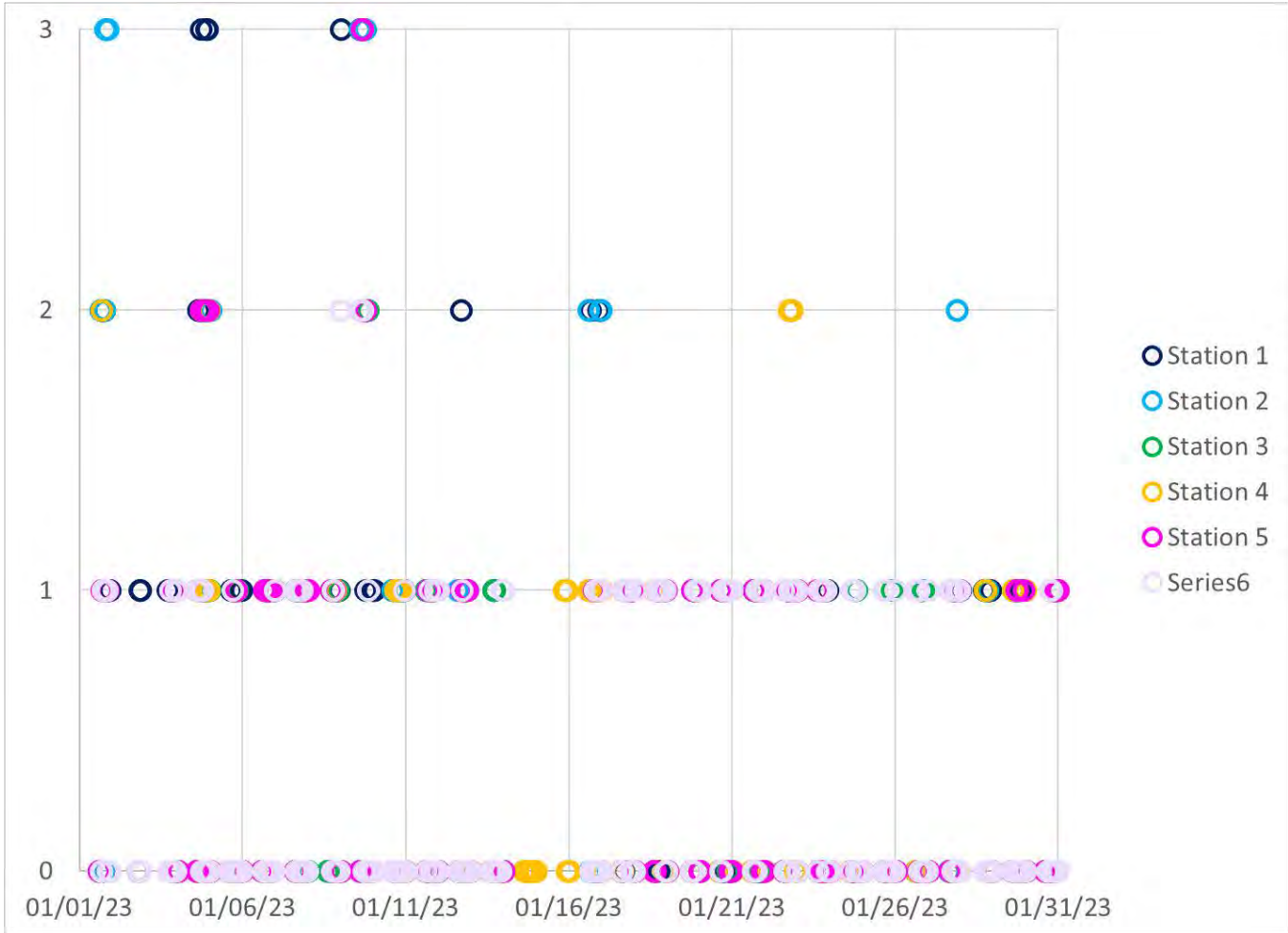
Figure 7: Number of clean images used in the January 2023 classification of aeolian activity for each of the restoration plots. Treatment types of the plots are as follows: Station 1 - Control, Station 2 -Native Seeds, Station 3- Seeds and Sterile Grass Seed, Station 4- Low Density Planting Nodes, Station 5- High Density Planting Nodes, and Station 6- Broadcast Straw and Plants and Seed.

Review of the classified images for different states of aeolian transport shows that the events of "trace" and "no transport" occurred at nearly the same times across plots (Figure 8), with some discrepancies. For example, on January 22, 2023 trace aeolian activity was identified with occurrences of active sediment transport at various times, and this varied across the restoration plots (Table 3, Time lapse videos labeled "Trace"). "Active" and "widespread" aeolian sand transport events generally varied by plot, indicating that these events were not visually detected in the imagery simultaneously across all plots (Figures 8, 10). This could relate to the influence of the various treatment types on sand transport, minor differences in the timestamp of the imagery, or variations in wind speed between the plots (discussed below and seen in Figures 11, 12).

Active transport with streamers and widespread sediment transport (codes 2 and 3) were far less common in the restoration plots with higher vegetation cover (Plots 3-6, Table 4, Figure 9). Widespread sediment transport was most observable in Plots 1 and 2 (Figure 9, Figure 10, Time lapse videos labeled "high"), given their lower or negligible plant cover. Dunes appear to block or limit sand streamers, as they were not visible directly behind the developed nebkha dunes in Plot 3. Although sediment transport was still visible across low lying interdune spaces, the amount of sediment moving through Plot 3 during a large transport event was not as noticeable (Figure 10, Time lapse videos labeled "high"). Plots 4-6 had more low-lying vegetation and less events classified as active and widespread sediment transport, perhaps due to increased plant roughness and closer spacing of the vegetation (Figures 8 and 9). Although events classified as active (2) and/or widespread (3) account for a relatively low percentage of aeolian events in each of the plots (Figure 9), they are the most easily identifiable with the largest classification confidence compared to trace events.

Figure 8: Classification of aeolian activity in each of the restoration plots prior to cross checking with the wind speeds from the meteorological stations. The y-axis represents the classification code for aeolian transport (Table 2), where 0 is inactive, 1 is trace, 2 is active, and 3 is widespread. Treatment types of the plots are as follows: Station 1 - Control, Station 2 -Native Seeds, Station 3- Seeds and Sterile Grass Seed, Station 4- Low Density Planting Nodes, Station 5- High Density Planting Nodes, and Station 6- Broadcast Straw and Plants and Seed.
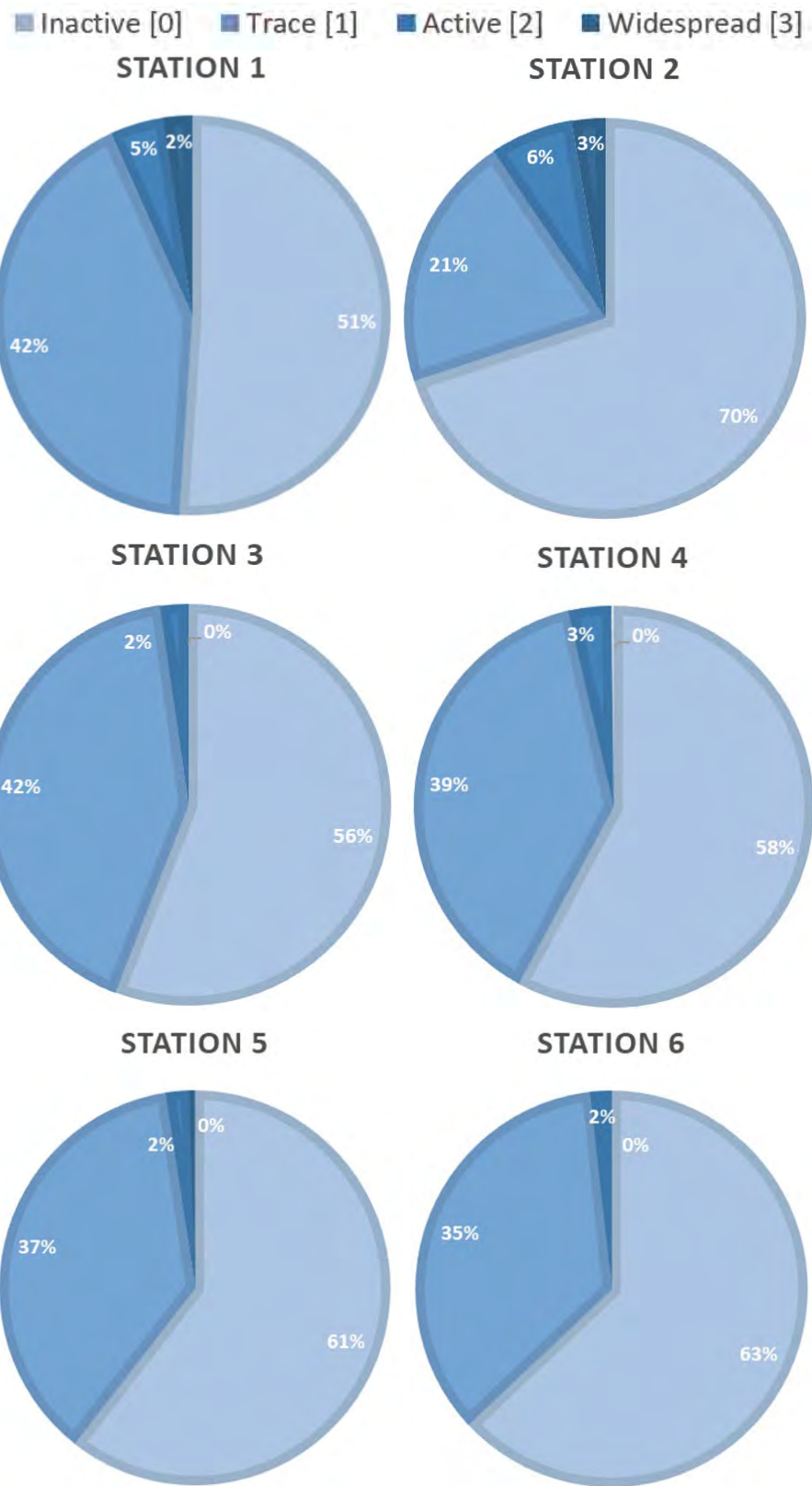
Table 3: Classification of aeolian activity on January 22nd, 2023 where 0 is Inactive, 1 is Trace, 2 is Active, and 3 is Widespread. Treatment types of the plots are as follows: Station 1 - Control, Station 2 -Native Seeds, Station 3- Seeds and Sterile Grass Seed, Station 4- Low Density Planting Nodes, Station 5- High Density Planting Nodes, and Station 6- Broadcast Straw and Plants and Seed.

Date and Time	Station 1	Date and Time2	Station 2	Date and Time3	Station 3	Date and Time4	Station 4	Date and Time5	Station 5	Date and Time6	Station 6
1/22/23 0:02	1	1/22/23 0:02	0	1/22/23 14:03	0	1/22/23 0:02	0	1/22/23 14:03	0	1/22/23 14:03	0
1/22/23 14:03	0	1/22/23 14:03	0	1/22/23 15:03	0	1/22/23 0:33	0	1/22/23 14:32	0	1/22/23 14:32	0
1/22/23 14:32	0	1/22/23 15:02	0	1/22/23 15:33	1	1/22/23 14:03	0	1/22/23 15:03	0	1/22/23 15:03	0
1/22/23 15:03	0	1/22/23 15:33	0	1/22/23 16:03	1	1/22/23 15:02	0	1/22/23 15:33	1	1/22/23 15:33	0
1/22/23 15:33	0	1/22/23 16:03	0	1/22/23 16:33	1	1/22/23 15:33	0	1/22/23 16:03	1	1/22/23 16:03	1
1/22/23 16:03	0	1/22/23 16:33	0	1/22/23 17:03	1	1/22/23 16:03	0	1/22/23 16:33	1	1/22/23 16:33	1
1/22/23 16:33	0	1/22/23 17:03	0	1/22/23 17:33	1	1/22/23 16:33	0	1/22/23 17:03	1	1/22/23 17:03	1
1/22/23 17:03	0	1/22/23 17:33	0	1/22/23 18:03	1	1/22/23 17:03	1	1/22/23 17:33	1	1/22/23 17:33	1
1/22/23 17:33	1	1/22/23 18:03	2	1/22/23 18:33	1	1/22/23 17:33	2	1/22/23 18:03	1	1/22/23 18:03	1
1/22/23 18:03	1	1/22/23 18:33	2	1/22/23 19:03	1	1/22/23 18:03	2	1/22/23 18:33	1	1/22/23 18:33	1
1/22/23 18:33	1	1/22/23 19:03	2	1/22/23 19:33	1	1/22/23 18:33	2	1/22/23 19:03	1	1/22/23 19:03	1
1/22/23 19:03	1	1/22/23 19:33	2	1/22/23 20:03	1	1/22/23 19:03	2	1/22/23 19:33	1	1/22/23 19:33	1
1/22/23 19:33	1	1/22/23 20:03	1	1/22/23 20:33	1	1/22/23 19:33	2	1/22/23 20:03	1	1/22/23 20:03	1
1/22/23 20:03	1	1/22/23 20:33	1	1/22/23 21:03	1	1/22/23 20:03	2	1/22/23 20:33	1	1/22/23 20:33	1
1/22/23 20:33	1	1/22/23 21:03	1	1/22/23 21:33	1	1/22/23 20:33	1	1/22/23 21:03	1	1/22/23 21:03	1
1/22/23 21:03	1	1/22/23 21:33	1	1/22/23 22:03	1	1/22/23 21:03	1	1/22/23 21:33	1	1/22/23 21:33	1
1/22/23 21:33	1	1/22/23 22:03	1	1/22/23 22:33	0	1/22/23 21:33	1	1/22/23 22:03	1	1/22/23 22:03	0
1/22/23 22:03	1	1/22/23 22:33	1	1/22/23 23:02	0	1/22/23 22:03	0	1/22/23 22:33	1	1/22/23 22:33	0
1/22/23 22:33	1	1/22/23 23:03	1	1/22/23 23:32	0	1/22/23 22:33	0	1/22/23 23:03	1	1/22/23 23:03	0
1/22/23 23:03	1	1/22/23 23:33	1			1/22/23 23:03	0	1/22/23 23:33	1	1/22/23 23:33	1
1/22/23 23:33	1					1/22/23 23:33	1				

Table 4: Number of aeolian activity classifications across stations, where an aeolian activity classification of 0 is Inactive, 1 is Trace, 2 is Active, and 3 is Widespread. Treatment types of the plots are as follows: Station 1 - Control, Station 2 -Native Seeds, Station 3- Seeds and Sterile Grass Seed, Station 4- Low Density Planting Nodes, Station 5- High Density Planting Nodes, and Station 6- Broadcast Straw and Plants and Seed.

Aeolian Activity Classification	Station 1	Station 2	Station 3	Station 4	Station 5	Station 6
0	265	337	252	323	304	336
1	219	100	189	215	186	188
2	23	32	10	19	10	9
3	12	13	0	1	2	0
Total Cleaned Images	519	482	451	558	502	533

11

223

STATION 1 · STATION 2 · STATION 3 · STATION 4 · STATION 5 · STATION 6

Inactive [0] · Trace [1] · Active [2] · Widespread [3]

224

225

226

Figure 9: Percentage of ranked aeolian transport events prior to cross checking with wind speed. 0 = inactive, 1 = trace sand transport, 2 = active sand transport with streamers evident, 3 = widespread. Treatment types of the plots are as follows: Station 1 - Control, Station 2 -Native Seeds, Station 3- Seeds and Sterile Grass Seed, Station 4- Low Density Planting Nodes, Station 5- High Density Planting Nodes, and Station 6- Broadcast Straw and Plants and Seed.

12
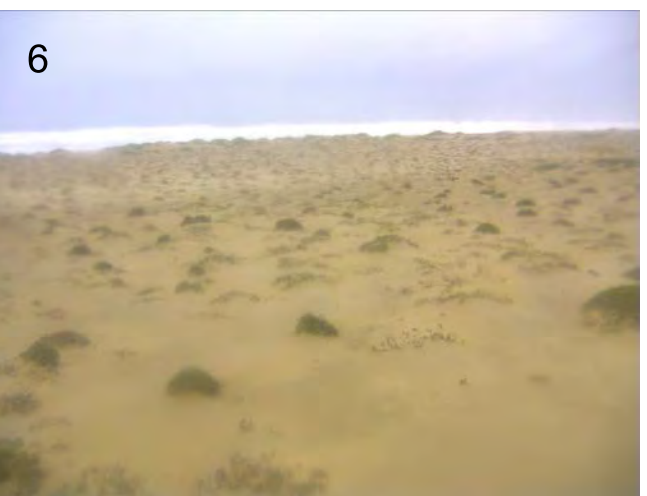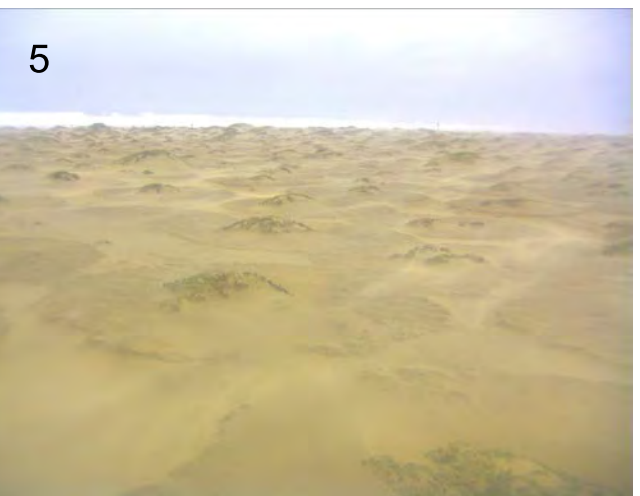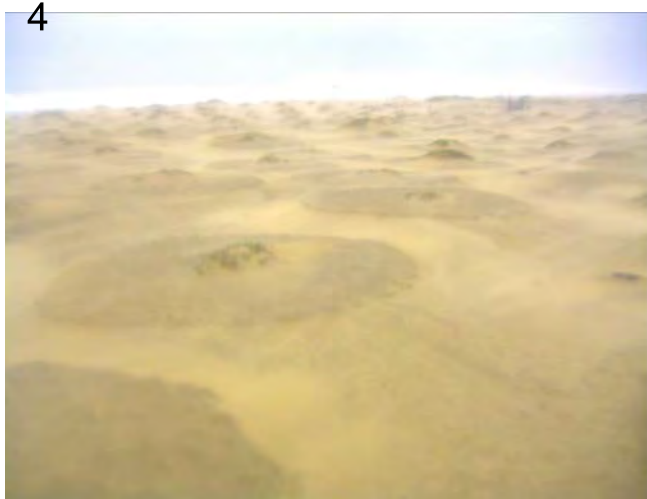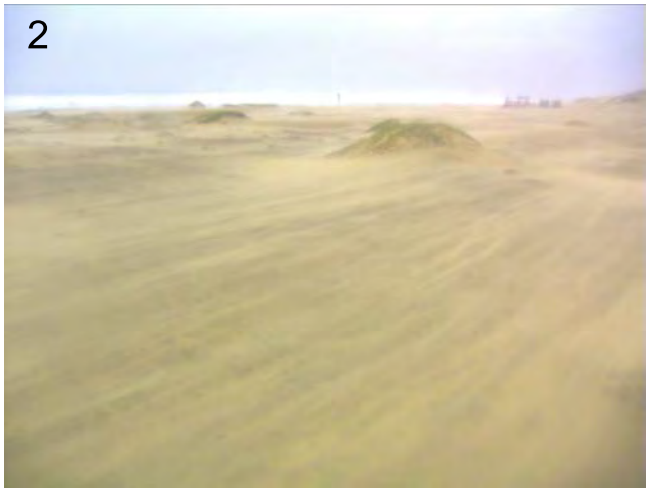
Figure 10: An active sediment transport event observed on 1/9/2023 at 15:32 GMT (8:32 PST) in foredune restoration treatment plots 1-6. Concentrated sand streamers are evident in most plots, yet widespread transport is not fully evident in all plots at this instant in time. Treatment types of the plots are as follows: Plot 1 - Control, Plot 2 -Native Seeds, Plot 3- Seeds and Sterile Grass Seed, Plot 4- Low Density Planting Nodes, Plot 5- High Density Planting Nodes, and Plot 6- Broadcast Straw and Plants and Seed.
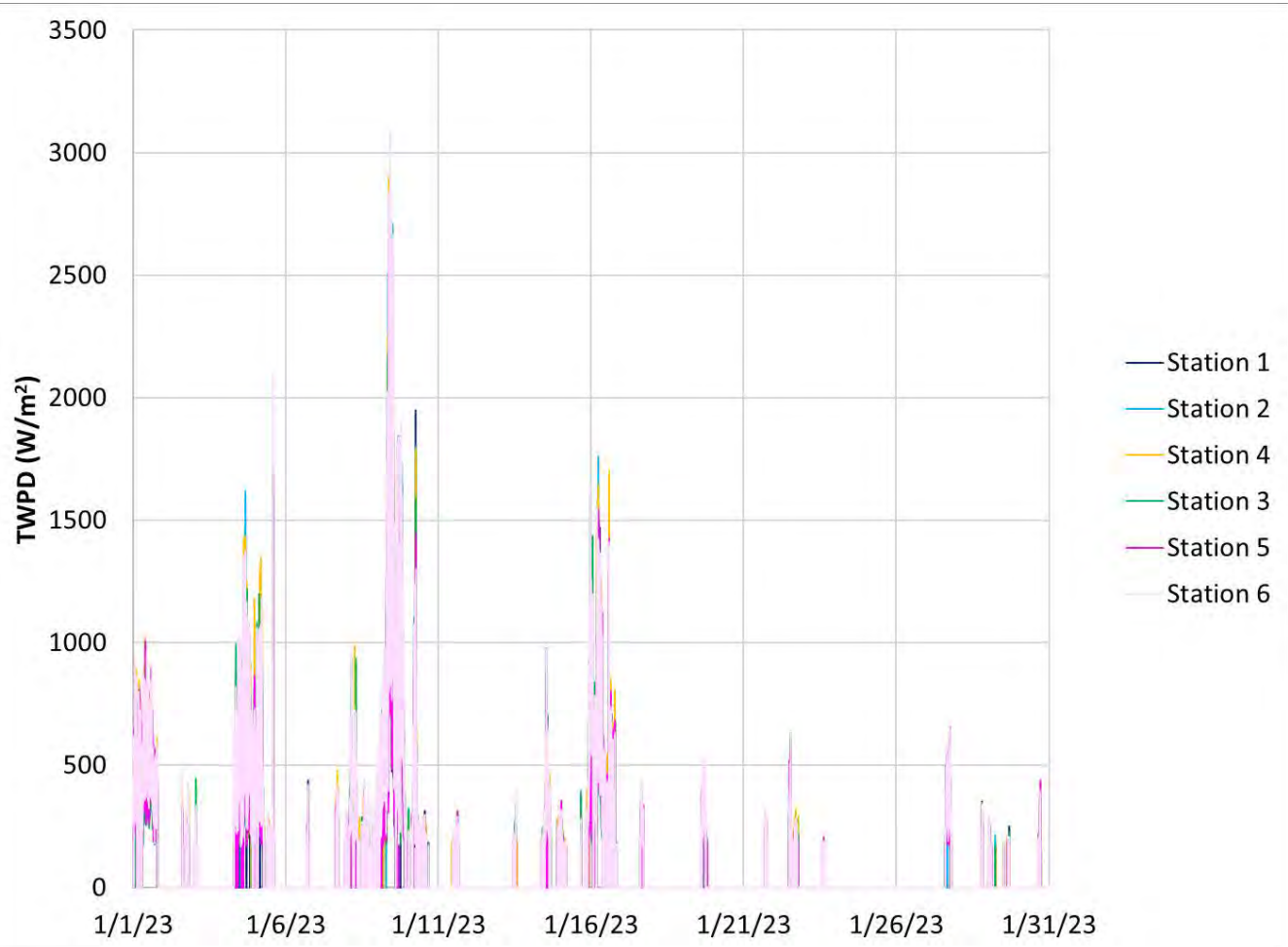
Figure 11: Threshold wind power density (TWPD) of all six restoration plots. Treatment types of the plots are as follows: Station 1 - Control, Station 2 -Native Seeds, Station 3- Seeds and Sterile Grass Seed, Station 4- Low Density Planting Nodes, Station 5- High Density Planting Nodes, and Station 6- Broadcast Straw and Plants and Seed.

Wind speed and related TWPD are mostly aligned across restoration plots, with some variability in magnitude, especially during strong wind events (Figures 11 and 12). For example, a high wind event on January 9, 2023 produced 3053 W/m^2 in restoration Plot 6 while in Plots 1 and 5 the TWPD was 2339 and 2644 W/m^2, respectively (Figure 12). Generally, this variability across stations within the minute-based measurements results partly from changes in W-E slope across the sites (increasing from N-S) and variations in treatment site roughness, but in most cases is not enough to result in visual changes in sediment transport across the surface in the imagery. This spatial variability in TWPD is also reflected in the longer-term average sand transport threshold values (see section 2.3.2.2). Regardless, these variations can have a significant impact on sand flux and, in turn, foredune formation and evolution over time.

Comparison of wind speeds, associated TWPD, and imagery was used to further verify the classification of aeolian activity events. For instance, discerning between events with trace sediment transport above the sand transport threshold vs. those influenced by surface moisture changes was difficult without reference to corresponding wind conditions. On average, 25% of all trace events were flagged as potential moisture changes with a standard deviation of ~12% (Table 5). In plot one, for example, 7 of

14

23 trace events were flagged as related to potential surface moisture changes (Table 5). However, cross-referencing the images with corresponding wind conditions revealed that some of those classified as having trace sediment transport were associated with changes in moisture content of the sand surface. For example, an appearance of dry sediments depositing over wetter sediments on January 18th 2023 was initially classified as trace aeolian activity (Time lapse video - WettoDryEx_S6_01182023). However, review of minute scale wind speed data for this event revealed that wind speeds did not exceed the transport threshold, indicating that the pattern of surface changes seen in the imagery was more likely due to gradual drying of a moist surface (showing patches of lighter colored grains) vs. deposition of fine grains by aeolian transport (Figure 13). At the time of this report, only trace aeolian activity events have been verified against wind speed conditions within the plots, but other events will be verified against their corresponding wind conditions in the future. Generally, active and widespread transport events were initially classified with higher confidence, but all types of events will be cross-referenced to corresponding wind conditions to reduce misclassification.

Table 5: Number of trace sand transport events flagged as related to potential surface moisture changes rather than trace aeolian activity for all plots. Treatment types of the plots are as follows: Plot 1 - Control, Plot 2 -Native Seeds, Plot 3- Seeds and Sterile Grass Seed, Plot 4- Low Density Planting Nodes, Plot 5- High Density Planting Nodes, and Plot 6- Broadcast Straw and Plants and Seed.

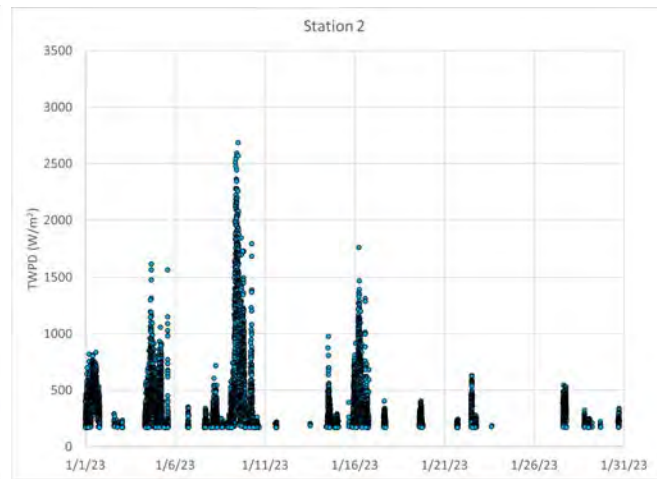| Plot	Total Trace Aeolian Events Classified	Number of Events Flagged	Percent Flagged
1	23	7	30.43%
2	13	2	15.38%
3	25	5	20.00%
4	24	3	12.50%
5	19	6	31.58%
6	23	10	43.48%

291

292

293
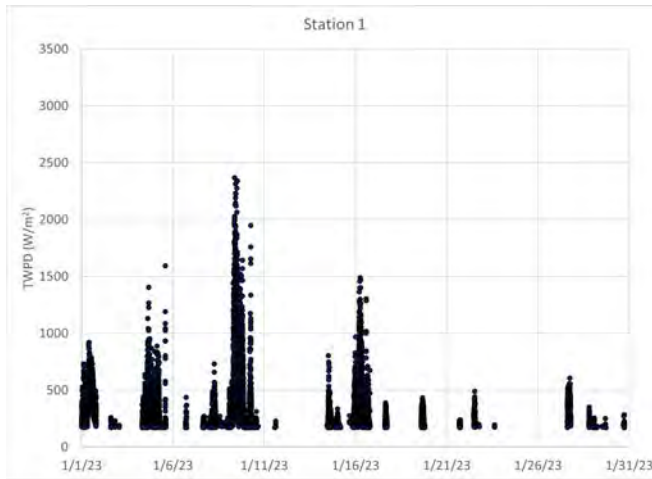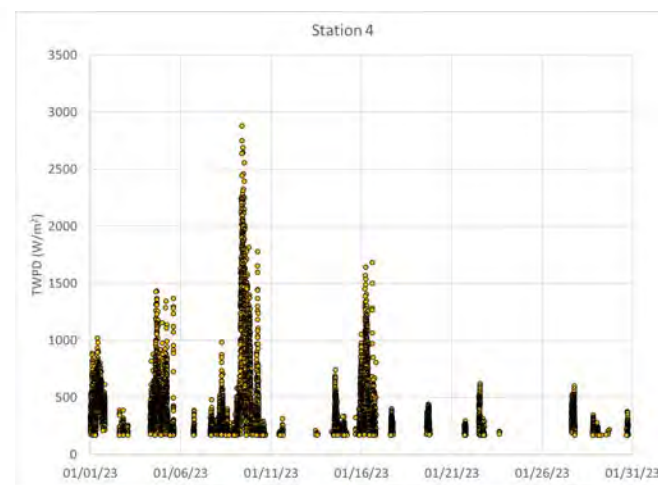
Figure 12: Thresholded Wind Power Density (TWPD) across each individual restoration plot. Treatment types of the plots are as follows: Station 1 - Control, Station 2 -Native Seeds, Station 3- Seeds and Sterile Grass Seed, Station 4- Low Density Planting Nodes, Station 5- High Density Planting Nodes, and Station 6- Broadcast Straw and Plants and Seed.

Figure 13: Wind speeds on the minute from Station 6 (Broadcast Straw and Plants and Seed) on January 18th, 2023 from 3:02 PM GMT to 11:33 PM GMT.

DISCUSSION

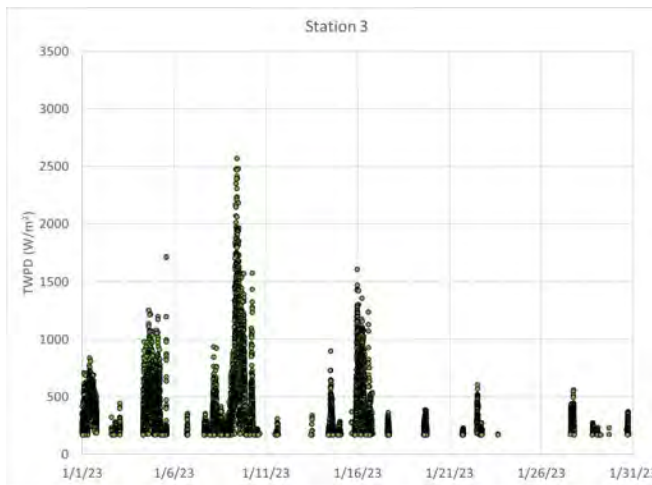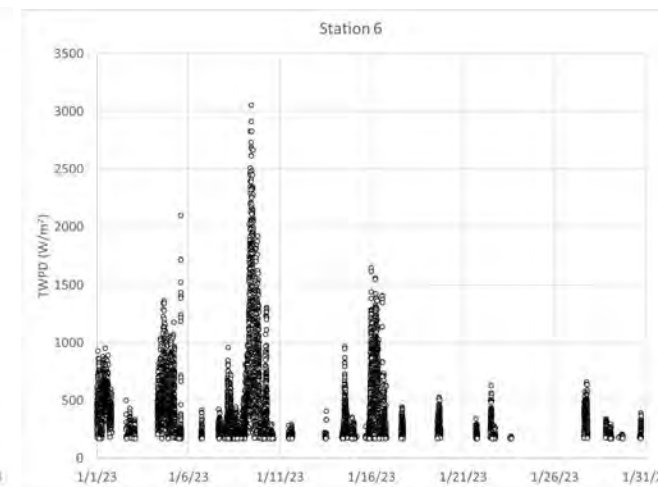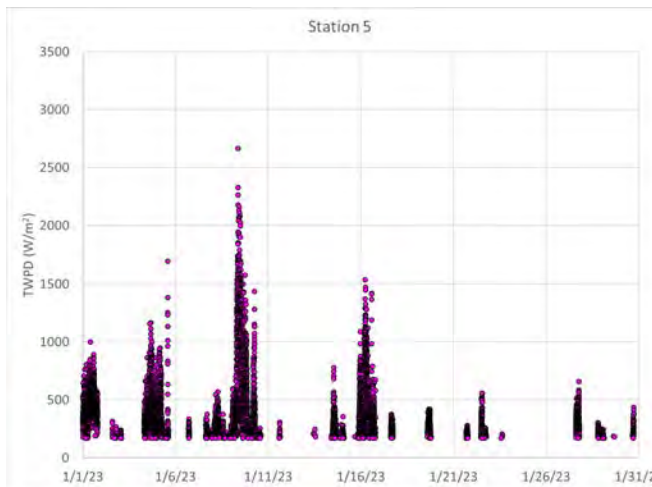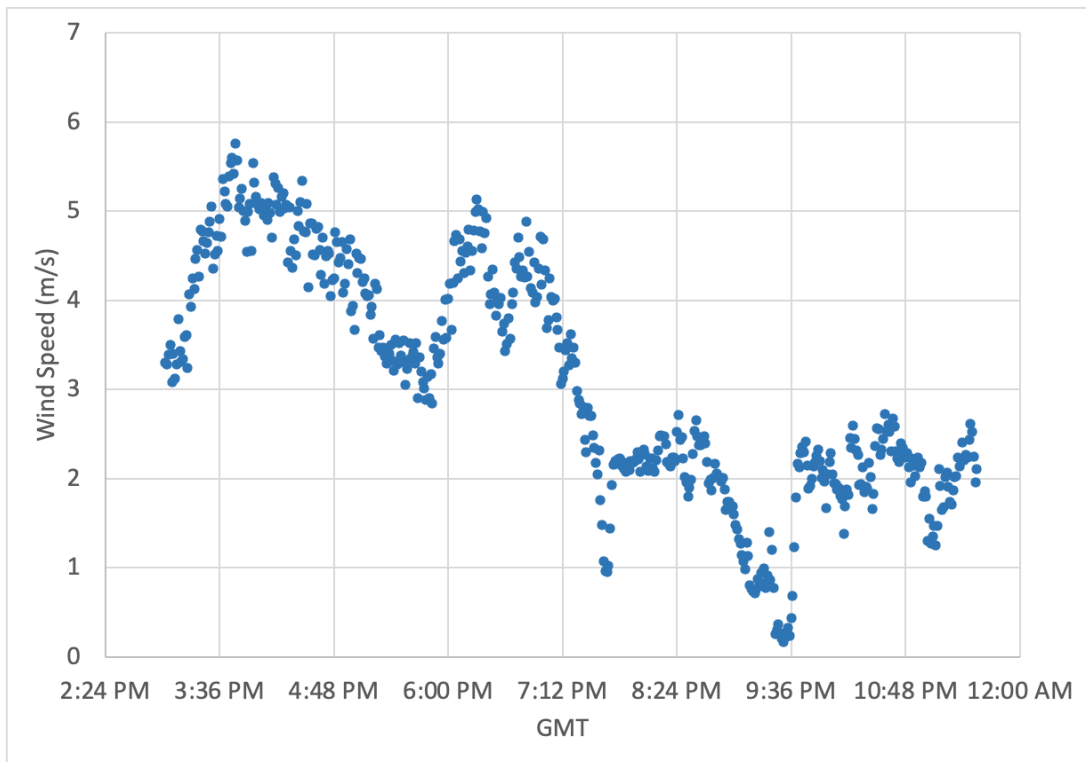This preliminary analysis indicates that the deployed camera monitoring stations provide utility for identifying the nature of aeolian activity and related sand transport events within the foredune restoration plots, despite somewhat limited resolution (5 MP or 2592 x 1944 pixels) and some challenges with obstruction of the field of view by evolving features (e.g., plant cover, nebkha dunes) within the treatment plots. This analysis provides a proof-of-concept based on a recent sub-dataset of observations (January 2023) following 3 years of treatment plot development during a particularly wet, yet active, winter season. It is expected that further analysis during earlier stages of development and drier conditions will provide appreciable results from which treatment responses over time can be assessed.

Identification and verification sand transport events

Generally, differences in the magnitude and spatial extent of various sand transport events within the treatment plots were identifiable in the monitoring camera imagery. Challenges were encountered for some types of events, and within some treatment plots, however. For instance, 'trace' sediment transport events (code 1) were difficult to verify without corresponding wind conditions and sand transport activity (Sensit sensor) data. This was particularly so in Plot 3 (native and sterile grass seed mix) due to the presence of large nebkha dunes that obscured more of the upwind fetch surface in the field of view. Similarly, in plot 4 (low density planting nodes), the upwind field of view generally did not show much variation between images, making it difficult to identify sediment transport events and

17

related deposition. In this plot, sand transport was shown more by changes in ripple movement around the straw circles than by sand streamers or saltation clouds.

Some trace sediment transport events were also originally misclassified due to changes in sand surface moisture content. For instance, sand surfaces were typically observed to become moist at night and into the morning hours. After the sun rose and the surfaces were heated and dried, they often became lighter in color (see time lapse video). In some instances, dry/light sands appeared to be transported onto a moist/dark sand surface, resulting in a trace aeolian activity classification (see time lapse video). However, a similar observation could occur as a sand surface dries (i.e., light sand streaks evident on a darker sand surface) in the absence of sand transport. Unfortunately, the monitoring stations within the plots did not include precipitation gauges or soil moisture probes, although relative humidity estimates could be used as a rough proxy for surface moisture conditions. Trace events that were flagged as those related to potential surface moisture content changes should be revisited and compared to concurrent wind speed, saltation, and relative humidity conditions across the restoration plots. Identification of uncertainty in trace aeolian events during classification is an important step to direct following efforts on where to specifically compare wind speeds for quality assurance checks.

Current Limitations and Future Directions

This proof-of-concept study involved extensive manual processing of tens of thousands of images captured from monitoring stations within each of the six restoration plots. Despite the labor intensive nature of this exercise, valuable information and data on the types and extent of sand transport events within the restoration plots vs. the control site was gleaned. Automated image analysis methods/software exist to help reduce this time sink, however, the learning/training curve required is steep and appreciable manual/human training of, for example, machine learning (artificial intelligence) software would still be required to distinguish obvious events from those less obvious (e.g. related to poor imagery, complex terrain, or requiring expert interpretation by a trained geomorphologist). Use of such methods could also result in image/event misclassification and loss of data that could be representative of formative events.

The general lack of consistency in image quality from the monitoring stations (e.g., due to changing lighting, sun angle, sea spray, dust films, precipitation/fog, etc.) also poses a major challenge for the utility of the datasets for classifying sand transport events. Such variations make training machine learning algorithms that depend on color or contrast similarities, for example, very difficult. Blurry or low quality images within the dataset are often purposefully kept for their utility in determining if there was active sediment transport either during the time of the imagery, or shortly before or after. Therefore, deleting an image based on blurriness through an automated system would result in declines in useful verification information. For these reasons, and despite time consuming processing, there is a distinct need for manual image quality assessment and image (event) classification by a trained geomorphologist.

Related, it was often noticed that sediment movement was closely followed by a clouded camera lens. This could be because wind events picked up smaller particles that clouded the view of the camera and dirtied the lens. In some instances, sediment could still be moving in a small visible corner of the field of view, so the images were kept for classification. However, if the entire field of view was blocked, the

image was deleted and could not be classified. In these instances, wind events may very likely be missed in the imagery and therefore underrepresented in the tabular classification data. Although some of the data are missed in the imagery, there are many instances where sediment transport is clearly occurring (with a clear lens). Comparison of high wind events from the meteorological station to when there is clear sediment transport and when there is a high wind event and no imagery data will provide a better insight to how many high wind events are not seen due to this problem. Additionally, wind speed and direction are calculated on a 24 hr clock, but the camera does not capture images during the night time. The wind does not stop blowing at night, and it is likely that some high wind events are captured in the wind data but are not seen in the imagery if they occur at night.

The field of view of the monitoring cameras was found to be generally wide enough to capture sediment transport events within the treatment plots. At times it was wished that the camera had a view from the center of the boundary of the restoration plot looking north. This would have provided a more profile view of sediment transport and dune migration, rather than having the camera facing toward the shore and oncoming sediment transport and migrating dunes. However, the current view point from the camera provided good resolution of small-scale sediment movement and captured streamers across the landscape that may not have been possible with the other suggested orientation. Another limitation of the camera orientation is the limited visibility of the treatment plot when dunes reach a certain height (Figure 9). When the dune gets too tall, it inhibits the view of sediment transport across the majority of the treatment plot.

The time interval of the imagery provides a rich dataset that is beneficial to the project goals. Cameras capturing imagery at the short temporal scale provides the opportunity to view how long sand transport events last, roughly. These ground based observations can be directly related to the meteorological and sand transport activity data from the corresponding stations. Therefore, wind speed and direction (and resultant variables) can be directly compared to observed transport events. This provides the park with valuable information on when sediment transport occurs and under what site conditions, how much is visibly transporting, and how the different treatment plots respond to high wind events. The temporal scale of the image analyses is far greater than the temporal frequency of the UAS DEMs from which erosion and deposition patterns and sediment budget response values are generated (see section 2.3.3). For this reason, the image analyses provide a far richer dataset on an event basis that deepens the assessment of sediment transport and its controls within the treatment plots. These data further support which treatment plot may be best suited for future restoration at Oceano State Park and other parks or beach-dune systems undergoing restoration.

Cross-validating visible sand transport events to corresponding wind data and saltation data (from sensit probes on the monitoring stations) is an important step in event verification. This is particularly so for potentially misclassified 'trace' events related to changes in surface moisture content (e.g., localized surface drying and increased brightness under sub-threshold wind speeds < 6.5 m/s) that could be mistaken as dry sand moving and/or being deposited by wind on the surface. Validating potential sand transport events in each image with concurrent wind speed and other meteorological data will provide a more accurate representation of transport events across the treatment plots in the longer datasets since implementation. It is also important to recognize that, as the restoration treatments and exposed sand surfaces within each treatment evolve, sand transport and threshold

conditions will most likely change (e.g., in response to surface sheltering by nebkha or plants, or armouring by coarse lags). For these reasons, it is recommended that the imagery also be used to verify and update our understanding of not only sand transport threshold conditions, but also the controls and variability of these over time as the treatments evolve.

Time series analysis can be performed relatively quickly by cycling through images in iMovie to provide a useful visual understanding of sediment transport events over time. However, the images are not timestamped by default on the field dataloggers, so currently this has to be assigned manually. Depending on the temporal scale of the time series analysis (i.e., number of images in the dataset), introducing a timestamp can be time consuming. Coding or other imaging softwares can perform this task more efficiently (e.g., ffmpeg is free and has been recommended), but these methods have yet to be assessed.

Future directions also include expanding this analysis to all available data for the restoration plots (Table 1, Figure 5). For future analysis, it is recommended that the dataset is broken down into time periods or events of interest, perhaps defined by wind and/or sand transport conditions, as the density of the imagery dataset can obscure trends and event frequencies with many overlapping datapoints. The richness of the imagery and wind data is one of the most valuable assets for this type of work; however, when viewing large datasets at a time, fine details from the results may be obscured.

Next steps should also include expanding the quality checks to assess all corresponding wind speed and sand transport data with the classified transport event results as observed in the imagery. This would be beneficial for determining if classified widespread wind events align with the highest associated TWPD, for example. Likewise, classified trace wind events should be compared to the associated wind speed and sediment transport threshold. Understanding the conditions that produce trace aeolian sediment transport events and their transition to active or widespread transport would be beneficial to validate against the transport threshold model. Separately, exploring if there are high TWPD values but no images for that associated timestamp would also reveal if there are more widespread aeolian transport events than captured in the clean imagery datasets.

CONCLUSION

The purpose of this report is twofold. First, it presents the methods used for data collection, quality assessment, compilation, and coding of distinct formative events within the six restoration plots at ODSVRA. Second, a preliminary proof-of-concept analysis is provided from a subset of images from January 2023, almost three years after implementation of the foredune restoration treatments. From this, insights for further analysis, limitations, and benefits for the foredune dust mitigation project are discussed.

The time interval of the imagery (every 30 minutes during daylight hours) provides a rich dataset that is beneficial to the project goals by providing insight to how various foredune restoration treatments respond to high wind events and environmental conditions with the ultimate goal of reducing dust emissions across these restoration plots. Over 120,000 images were quality assessed from May 2020 to June 2023 spanning all six restoration plots. After manual cleaning and removal of poor images, over 80,000 images remain that have utility for aeolian activity classification. This report details results from a subset of this dataset for the month of January 2023, which contains approximately 3,000 cleaned

images.

Preliminary analysis from the photo image analysis classification and time lapse videos available indicate that trace, active, and widespread aeolian events in January 2023 generally occur around the same time stamps, but there is some variation between restoration plots. Events classified as "trace" or "no activity" occurred at nearly the same time across plots, but "active" and "widespread" events had the most variation. Similarly, the visibility of these different aeolian classifications varied across restoration plots, with active sediment transport and sand streamers less detectable in vegetated plots. Widespread activity was most visible in the plots with little to no vegetation (plots 1 and 2).

Likewise, Threshold Wind Power Density (TWPD) values generally had magnitude and timing across restoration plots, but there was variation particularly in the magnitude of these events across plots, even down to the minute scale. These variations in wind could be due to natural variability across the foredune plots as a whole and are likely influencing the variability observed in the aeolian transport classifications. Variations in TWPD may also be due to the treatment type within each restoration plot, as treatment type did appear to have an effect on aeolian classification type visible in the restoration plots.

Future directions include performing this analysis to the entire cleaned imagery dataset for all restoration plots. Classification of aeolian activity will undergo quality assurance checks to compare all wind speeds directly against the image classifications, which is especially important for trace classifications due to potential changes in moisture content identified. Additionally, high TWPD will be investigated to determine when active and widespread transport activity occurred and if values above the threshold can be identified consistently in the imagery across the entire dataset. This continued work will provide a far more thorough analysis of sediment transport events across the various restoration treatment plots, especially in the beginning stages of foredune development.

March 8, 2024

Memo: <u>SAG Review of UCSB Report "Preliminary Analysis of Time-Lapse Photo Monitoring at the Ocean Dunes Foredune Restoration Site" (06-2023 V1)</u>

From: Scientific Advisory Group (SAG)[1]

To: Jon O'Brien, California Department of Parks and Recreation

Cc: Ronnie Glick, California Department of Parks and Recreation

The SAG received a copy of the University of California, Santa Barbara (UCSB) Report "Preliminary Analysis of Time-Lapse Photo Monitoring at the Ocean Dunes Foredune Restoration Site" dated June 2023, on February 27, 2024 and members have had the opportunity to review the document. This memo provides feedback on the UCSB report.

The report focuses on how the time-lapse camera images collected at six monitoring stations on the eastern edge of the foredune restoration area (FRA) can be used to evaluate the frequency, magnitude, and duration of wind-driven saltation events at the six FRA treatment sites. For the report the available images cover the period 05/09/2020 to 04/04/2023. The total number of images captured was over 20000 for each FRA site with usable images, following a review of their quality for interpretation, being between approximately 14000 to just over 15000. As noted in the report, the images only cover daylight hours.

The stated twofold purpose of the report is to 1) present the data collection protocols, compilation process, image quality assessment, and identification of sand transport events, and 2) provide a proof-of-concept analysis based on a subset of the images from January 2023.

The quality assurance of the images selected for analysis involves a subjective review of image quality by one person based on their perception of the image with respect to: fogginess, blurriness, lens obscuration by salt/dust film on the camera lens, and overexposure. Some images that failed the screening were kept if they provided useful information such as changing dune morphology.

With respect to purpose 2, providing a proof-of-concept analysis, the report should state directly (pg. 2, line 60) what the purpose of the analysis is. What is this analysis designed to do with respect to informing the evolution or management of the FRA sites? The report goes on to present data analysis of the images and the information contained within them, but the purpose of the analysis needs to be clearly stated at the beginning of the report. In the absence of a clear purpose, the report serves mainly to provide a very limited set of results that does not instill confidence that the proof-of-concept has been achieved or demonstrated to be worthy of further pursuit. This may be reflective of the study being in too preliminary a phase of development. There is no denying that the large storehouse of images already collected over a three-year period

---

[1] Standard procedure for SAG review of UCSB reports is for Dr. Ian Walker to recuse himself from the discussions due to a potential conflict of interest. Despite being a SAG member in good standing, Dr. Walker did not participate in this review in any manner nor was UCSB consulted about any aspect of this review.

(and counting) could provide a wealth of information on sediment transport events, but this report does not provide sufficient evidence of the usefulness of the images to understand foredune evolution as a function of the different restoration approaches and how this could relate to management decision support.

The Methods section defines categories of aeolian events that are observed in the quality assured images. These are subsequently used to catalogue and tabulate the aeolian events to provide a characterization of the frequency and magnitude of the events. Additionally, time series of wind data, expressed as Wind Power Density (W m^{-2}) were presented that represent conditions where it was assumed that there was the potential for sand transport to occur based on exceedance of a sand transport WPD threshold.

The threshold wind speed for sand transport (pg. 7, line 117) is 6.5 m s^{-1} (or 168 W m^{-2}) measured at 3.5 m above ground level. The rationale for choosing this threshold should be provided when it is first introduced. It may be based on application of the Bagnold (1941) relation between particle size and threshold shear velocity or some other criterion. This should be clarified.

The introduction of the Threshold Wind Power Density term (TWPD) in the next paragraph introduces some confusion into the narrative because WPD values greater than the TWPD of 168 W m^{-2} are also termed TWPD in the report. For clarity, it is recommended that the application of the Kalmikov (2017) equation define WPD, reserving TWPD to be 168 W m^{-2}.

Figures 11 and 12 show time series data of 1-minute mean WPD that exceed TWPD for the six stations, but it is not clear what the difference between the plots is. What is the difference between TWPD (Fig. 11) and (Thresholded) TWPD (Fig. 12)? They both use TWPD on the y-axis. It is not clear how the differences in WPD among the six sites is being related to formational or evolutionary processes.

Overall, there does appear to be some potential utility to this type of time-lapse monitoring, but this has yet to be demonstrated convincingly. The images are very inexpensive to collect, but the analysis is time consuming and costly. It is recommended that the image collection effort continue for this year, perhaps with some modifications to camera placement (see below), but that a concerted analysis effort be undertaken on the existing images that were already coded to truly demonstrate proof-of-concept and overall utility of image analysis to help understand the important aspects of foredune evolution that are affecting the individual sites.

The following suggestions are provided for consideration by UCSB to potentially advance the use and utility of analysis of the collected images.

1)   Attempts should be made to overcome many of the technical challenges identified in the Discussion section of the report, not least of which would be to automate what is currently a time-intensive, manual process of classification, recognizing this would be a substantial effort. This would remove some of the subjectivity embedded in the existing process, especially if the single analyst who performed the QA/QC is not available in the future. Also, from the images presented in the report (e.g., Figure 10), there appear to be significant challenges associated with blurriness and lens contamination. This suggests it is very difficult to differentiate sediment in active

transport mode (streamers and clouds) from surface coloration effects (likely due to moisture, mineralogy, shading, and differential reflectivity).

2)   Undertake a more thorough and substantive analysis of the connection between the coded events (based on subjective interpretation of the imagery by a human operator) and the quantitative data from the meteorological towers and saltation sensors. Examining WPD is a first step, but much more can be done.

3)   Consider the temporal evolution of the different treatment areas as a dynamic control on sediment transport potential by presenting figures/graphs that show how things have changed through time. Given that the evolution of the foredune system is expected to take years, even decades, explain why the short time frames of the photo series are useful in understanding how the different treatments evolve into a foredune system over the much longer time periods

4)   Do a better job of characterizing the specific surface features of each of the six treatment areas as primary controls on sediment transport potential and near-surface boundary conditions (i.e., with respect to wind speeds above threshold). It is not sufficient to state simply that the presence of nebkha likely prevents streamers from occurring (likely true). There needs to be more detail regarding the differences between treatment areas 3 through 6 and how the surface topologies influence sediment transport potential.

5)   Begin to connect what is happening in the foredune treatment areas to conditions in other areas of the park (i.e., open sand surfaces in particular) so as to inform the overall effort of dust mitigation and PM10 concentration reductions at CDF and Mesa2. This is the ultimate objective that all research/monitoring studies in the ODSVRA should address with specificity. It would be interesting to attempt to connect the coded images showing Widespread Aeolian Activity (Code 3) with exceedance days for PM10 concentrations at CDF (given that the argument has been that most dust is generated by saltation events).

6)   Consider whether the cameras are ideally placed, with respect to position, orientation, field of view, and height. It appears from the imagery in Figure 10 that the coverage is rather 'local' and too oblique to really see what is going on more broadly in each of the treatment areas. Why not put four cameras at the top of S1 pointing in the cardinal directions, to be used as a 'control' station on transport events in the ODSVRA?

UCSB needs to consider if the limitations they have identified can be reasonably overcome to allow the collected images and the subsequent analysis to provide additional insight into the evolution of the foredunes in each treatment area. In other words, the SAG remains unconvinced that this image collection effort has yielded significantly worthwhile contributions to the dust-mitigation objective beyond what can be extracted from a combination of the UAS surveys and the meteorological towers (with saltation sensors). Nevertheless, the SAG recognizes that there is potential to do so.

Additional Suggestions

Conduct a thorough editing of the report for typos, run-on sentences, disagreements between subject and verb, and unclear references to pronouns, and lack of congruity of verbs between and among linked phrases.

Throughout the report "nebkha dune or dunes" is sometimes used. In the literature it is more conventional to use "nebka", which can be singular "one nebkha" or plural, i.e., a "field of nebkha".

Throughout: Treatment 3 is "native seeds and sterile grass seeds"

Please inform the reader in the Methods section what type of camera is being used, the data capture rate, the camera resolution, the height of observation, and the azimuth that the lens is pointing towards.

Descriptions/identification of the meteorological sensors and the Sensits should be included in the Methods section.

Editorial Issues and Comments to Adress

(The numbers on the left represent the line number in the Report.)

19 As part of suite of mitigation measures, a dune restoration strategy…

22 plant cover, comparable to that farther south near Oso Flaco Lake (Figure 2). The restoration site

25 sentence beginning "A goal…" is poorly written and doesn't make sense.

27 events as a means to assess their effectiveness. To date, foredune development and related plant

33 foredune restoration project and plots, and describe erosion and deposition through time

36-37   DRI and UCSB need acronym identification

43 [2]

58 change "fand" to "and"

59 quality assessment, data compilation, and identification of distinct formative events.65 Figure 1: [3]

82 continue to be collected and the last available data for download incorporated into this report was 4/4/2023.

83 researcher. Poor images were deleted to clean the dataset for further processing (Figure 5). [4]

101 Images were classified based on similar methods used by Grilliot et al. (2019)[6].

108[5]

115[6]

Number: 1   Author: Author   Date: Indeterminate
Their effectiveness for what?

Number: 2   Author: Author   Date: Indeterminate
define acronym CCFC

Number: 3   Author: Author   Date: Indeterminate
B-1 and B-2 are not defined in caption. Delete from image.

Number: 4   Author: Author   Date: Indeterminate
Was there any noted correlation between deleted images and periods of saltation activity?

Number: 5   Author: Author   Date: Indeterminate
Is this all done visually by the same researcher?

Number: 6   Author: Author   Date: Indeterminate
Were wind events below 6.5 m/s wind speed threshold considered if evidence of saltation was visually observed?

121 Wind speed and associated time stamps were used to calculate a Threshold Wind Power Density (TWPD) to provide a measure of the power available for aeolian activity that could be compared to the corresponding camera imagery. WPD was estimated using the relation reported by Kalmikov (2017).and later by Hilgendorf et al. (2022) and Walker et al. (2023) for research in dune restoration. A general sand transport threshold of 6.5 m/s (168 W m^{-2}) for the average diameter of sand grains (200 μm) was chosen to identify sand transport capable, or "high speed" wind events, while anything below this value are referred to as calm or incompetent conditions, with regards to aeolian sand transport. TWPD values were calculated in R Studio using the following equation:

TWPD = 0.5 p_a u^3 (in W/m^2)

where 0.5 is a constant, p_a is air density (1.225 kg/m^3 at 15 degrees Celsius), and u is the wind speed above the specified threshold (6.5 m/s). [1]

Table 2: This seems to imply that inactive situations are always dry and sunny, and all widespread transport situations occur during wet or rain?? This seems counterintuitive. If, however, the meteorological conditions do not relate to the other data, they should not be shown in this table in this form.

124 A general sand transport threshold of 6.5 m/s for the average diameter of sand grains (200 μm) [2]

132 WPD values were computed for wind speeds every minute above 6.5 m/s and plotted. [3]

152 (see section 2.3.2.2, Fig. 2-9) [4]

156 the dataset was quality checked. [5]

159-162 How are these data relevant if the analysis is done only for data from January 2023?

163 The January 2023 subset of raw images did not show appreciable data gaps among the plots.

165 also slight variations in timing of images across meteorological stations, ranging from 1-2 minutes difference between neighboring stations.

172 Figure 7: [6]

176 Review of the classified images for different states of aeolian transport shows that the events of "trace" and "no transport[7]" occurred

185 change "higher" to "denser"

188 they were not visible directly behind the nebkha in Plot 3.

190 Plot 3 during a large transport event was not as noticeable (Figure 10)[8]

217 Table 4: [9]

Number: 1   Author: Author   Date: Indeterminate
Need to identify the height of measurement.

Number: 2   Author: Author   Date: Indeterminate
Mean threshold wind speed varies among the restoration plots. Is that considered during the validation process?

Number: 3   Author: Author   Date: Indeterminate
It is not clear from this description over what interval TWPD was calculated.   This sentence suggests that TWPD is a minute-by-minute estimate of wind power, which implies that data were recorded at intervals of 1 second perhaps. OR were the wind data collected and reported as 1-minute averages, and then TWPD was calculated every hour???

Need from details here about data collection intervals and TWPD integration time.

A related question....what happens when wind/transport are intermittent---fluctuating above and below the 6.5 m/s threshold.

Number: 4   Author: Author   Date: Indeterminate
What is this referencing? Delete or add appropriate reference.

Number: 5   Author: Author   Date: Indeterminate
How?

Number: 6   Author: Author   Date: Indeterminate
This has been repeated several times in the Tables. Does it need to repeat?

Number: 7   Author: Author   Date: Indeterminate
"No transport" isn't listed in Table 2. Is this supposed to be "inactive" or are there other categories and attributes utilized in the classification of images that need to be added to Table 2?

Number: 8   Author: Author   Date: Indeterminate
Noticeable with respect to what?

Number: 9   Author: Author   Date: Indeterminate
Add that this table is for January 2023 (I presume).

227 Table 9: [1]

232 Figure 10 It is not really clear what is shown here. What does a "streamer" look like? The caption implies that streamers are not related to sand transport. What should the reader be seeing here?

242 Figure 11: [2]

249 Generally, the variability across stations within the 250 minute-based measurements results partly from changes in W-E slope across the sites (increasing from N-S) and variations in treatment site roughness, but in most cases is not enough to result in visual changes in sediment transport across the surfaces in the images. This spatial variability in WPD is also reflected in the longer-term average sand transport threshold values. Regardless, these variations can have a significant impact on sand flux and, in turn, foredune formation and evolution over time.

253 (see section 2.3.2.2) [4]

259 On average, 25% of all trace events were flagged as [5]

275 Table 5: [6]

294 Figure 12: [7]

309 [8]

313 treatment plots were identifiable in the imagery.

317 mix) due to the presence of large nebkha that

365 provide a better insight to how many high wind events are not identified due to this problem.

366 wind speed and direction were calculated on a 24 hr clock

368 events were captured in the wind data but not in the imagery if they occurred at night.

370 At times it was wished that the camera [9]

388 generated (see section 2.3.3). [10]

391 the ODSVRA

393 Sensit

404 and variability of these over time as the treatments evolve [11]

Page: 6

Number: 1   Author: Author   Date: Indeterminate

Is this for all of January 2023?

Number: 2   Author: Author   Date: Indeterminate

I'm not entirely understanding this plot. I can't tell if the colors are overlapping each other, but the graph visually looks dominated by treatment 6.

Is this the average of the TWPD listed for each day, or the highest calculated for each day?

Really difficult to see the details, and again, what is the point?

What is all the pink background? This graph is very hard to interpret.

Number: 3   Author: Author   Date: Indeterminate

This is unclear. Your initial threshold was 6.5 m/s are you presenting results that show this value has changed from your initial assumption? There is no Section 2.3.3.3.

Number: 4   Author: Author   Date: Indeterminate

Remove or add proper reference.

Number: 5   Author: Author   Date: Indeterminate

Introduce data flagging and data flagging options before the results section.

Number: 6   Author: Author   Date: Indeterminate

Suggest Percent Flagged values should not have two significant figures.

Add in this is January 2023

Number: 7   Author: Author   Date: Indeterminate

Are these WPD values above the threshold of 168 W/m2? I don't think the terminology of thresholded WPD is correct.

What are the averaging times of each dot?

Number: 8   Author: Author   Date: Indeterminate

It's not clear what is meant by an appreciable result? I think it is more clear if you phrase this something like "Further analysis of the available older data could improve our understanding of the treatment responses to transport events during earlier stages of development."

Number: 9   Author: Author   Date: Indeterminate

Please re-phrase. Maybe better to say something like "A camera orientation looking towards the north may have provided......."

Number: 10   Author: Author   Date: Indeterminate

Please refer to a specific document and remove section reference.

Number: 11   Author: Author   Date: Indeterminate

Not sure what "these" is referring to.

413 (Table 1, Figure 5). For future analysis, it is recommended that the dataset be partitioned into time

416 The richness of the imagery and wind data are one of the most valuable assets of this type of work;

417 however, when viewing large datasets at a time, fine details from the results may be obscured.[1]

424 validate against the transport threshold model.[2]

Page: 7

THIS PAGE WAS INTENTIONALLY LEFT BLANK.

ODSVRA Dust Control Program Draft 2024 ARWP

ATTACHMENT 06

Summary of Vegetation Monitoring of Restoration Sites at ODSVRA (2023)

(State Parks' ARWP Work Product)

THIS PAGE WAS INTENTIONALLY LEFT BLANK.

Summary of Vegetation Monitoring of Restoration Sites at ODSVRA

Line Intercept Transect Sampling

Methods
Line Intercept method (Line intercept: % cover = distance a+b+c+d+e+f / total transect length, where a, b, c, etc. are the intercept lengths of vegetation canopy) was used to estimate percent cover of species within each project area.

For this assessment both foredune and back dune project areas were sampled in October 2023. Reference sites for the foredune were sampled during the fall of 2021 and again during the fall of 2023 to account for any potential changes caused by storm surges or other environmental changes. For the back dune habitats, the late seral reference transects were sampled in 2021 and the early seral reference transects were sampled in 2022. Reference sites were selected in areas that had been closed to vehicular activity for at least 20 years and had not been subject to restoration plantings in the past. Within back dune habitats, early succession communities (early seral) and climax communities (late seral) can vary considerably in species composition and percent cover. For this reason, both early seral and late seral reference sites were sampled for comparison.

Within each foredune project area and reference site, a total of four transects of 30 meters each were sampled (the same transect lines were surveyed from 2020-2023). Within each back dune project area and reference site, a total of three transects of 30 meters each were sampled. In 2023, the project areas that were surveyed included the 48-Acre Foredune, planted February 2020; Eucalyptus Tree, planted January 2021; Lagrille Hill (Mid-section), planted in February 2021; and Tabletop, planted February 2021.

Starting points for the transect lines were randomly selected within each project area using GIS software. Originally, three transect lines in each project area were randomly selected from the eight cardinal and intermediate directions (i.e. N, NE, E, SE, S, SW, W, and NW). In 2022, within the 48-Acre Foredune Project Area, a fourth transect line was added in each treatment area running in the direction of the prevailing wind.

A measuring tape was run along the transect and secured with wooden stakes. It was not uncommon, for the wooden stakes to bury or become unburied by sand movement between sampling years. As a result, the stakes were re-established using the GPS unit resulting in some variability (estimated to be no more than 1-meter based on the GPS unit accuracy) in the beginning and ending points between years. As the vegetation canopy intersected the line, the species was noted on the datasheet along with the beginning and ending measurements of the canopy under "Start" and "Stop". When the canopies of two different species overlapped, each species was documented separately as two different canopies. A closed canopy for a given species was assumed until gaps in vegetation exceeded the width of 5 centimeters. All dead woody vegetation was included separately and noted as "Dead" unless it was clearly the result of seasonal dieback of a perennial plant that was still viable.

Once each 30-meter transect was surveyed, a reconnaissance level survey was conducted of the project area and any additional species observed were noted. In the reconnaissance-level survey, the entire FRA is searched for additional species by walking in belt transects of no more than 50 feet between surveyors.

Results

48-acre Foredune Project

In 2023, after the fourth growing season for the project area, Area 6-Parks Classic was the only treatment area to meet the vegetation cover of the reference site with 17.77 % cover, up from 13.8% the previous year. In comparison, the Reference Site in the North Oso Flaco Foredunes had 16.92% cover. Area 5-High Density Nodes had the second highest cover with 11.29% up from 6.4% the previous year. An increase in cover was also seen in Area 4-Low Density Nodes from 5.5% in 2022 to 7.89% in 2023. Area 2 and Area 3 both showed a decrease in cover. Area 1-Control did not show any cover on the transect lines but during the reconnaissance survey, new vegetation was documented growing on the western edge of the treatment area within debris piles deposited during storm surges the previous winter. This vegetation included both foredune specific species, which are expected to persist, and wetland specific species, which are not expected to persist. It is assumed that plant materials of these wetland species were dislodged from nearby waterways during storm events, deposited within the foredune areas and managed to persist through the summer. All of the wetland species were found with sporadic distribution along the westernmost portion of the 48 Acre Foredune, were in poor health and maintained very little cover. The foredune species observed within the storm surge debris, specifically red sand verbena (*Abronia maritima*) and sea rocket (*Cakile maritima*) appeared to be healthy and expanding in cover.

Two treatment areas, Area 6-Parks Classic and Area 4-Low density nodes, matched the species richness of the Reference Site for native species with nine (9) native species present. However, Area 4-Low Density nodes, had two wetland specific species that were only present within the storm surge debris that was deposited on the shoreline during the previous winter, including marsh jaumea (*Jaumea carnosa*) and saltgrass (*Distichlis spicata*). These species are not expected to persist in the foredune habitat into future years. When including non-native species, none of the 48 Acre Foredune areas met the species richness of the Reference Site which had 11 species present, followed by Area 6-Parks Classic, which had 10 species present. When comparing 2022 to 2023 for all observed species, species richness increased for Areas 1, 2, 3 and 4 in 2023 and remained the same for Areas 5 and 6. If the wetland specific species found in the storm surge piles and not included, species richness increased from 2022 to 2023 in Areas 1, 2, 3, and 4, decreased in Area 5 and stayed the same in Area 6 (Refer to Table 1 and Figure 1).

Table 1. Table of results from the 48 Acre Foredune Restoration Project line intercept transect sampling.

Foredune Restoration Project Vegetation Assessment (Oct 2023)							
	Area 1 Control	Area 2 Native Seed	Area 3 Native Seed & Grain Seed	Area 4 Low Density Nodes	Area 5 High Density Nodes	Area 6 Parks Classic	Reference North Oso Flaco Foredune (Oct 2023)
Age of Planting (years)	**3.5**	**3.5**	**3.5**	**3.5**	**3.5**	**3.5**	**-**
Species Richness	**8**	**5**	**7**	**10**	**9**	**10**	**11**
Transect 1	0.0%	12.5%	0.0%	5.7%	30.5%	14.2%	0.7%
Transect 2	0.0%	0.0%	12.6%	21.6%	5.7%	6.8%	42.7%
Transect 3	0.0%	0.0%	2.0%	4.3%	0.0%	44.3%	19.3%
Transect 4	0.0%	0.0%	12.3%	0.0%	9.0%	5.7%	5.0%
Mean Percent Cover	**0.00%**	**3.12%**	**6.73%**	**7.89%**	**11.29%**	**17.77%**	**16.92%**
Species	**Mean Percent Cover**						
Abronia latifolia	-	P	P	P	0.07%	P	P
Abronia maritima	P**	2.45%	5.66%	2.08%	5.90%	8.59%	9.9%
Ambrosia chamissonis	P	1.11%	0.96%	3.19%	4.73%	6.65%	4.2%
Atriplex leucopylla	-	-	-	3.06%	0.70%	P	-
*Cakile maritima	P**	P	P	0.10%	P	0.18%	1.9%
Calestegia soldanella	-	-	-	-	-	-	0.6%
Camissoniopsis cheiranthifolia	-	-	P	P	-	0.79%	0.22%
*Carpobrotus chilensis	-	-	-	-	-	-	0.3%
Distichlis spicata	P**	-	P**	P**	P**	-	-
Ericameria ericoides	-	-	-	-	-	-	p
Erigeron blochmaniae	-	-	-	-	-	-	P
Eriogonum parvifolium	-	-	-	-	-	P	-
Eriophyllum staechadifolium	-	-	-	P	P	0.93%	-
Jaumea carnosa	P**	-	P**	P**	P**	-	-
Juncus lescurii	P**	-	-	-	-	-	-
Malicothrix incana	-	-	-	P	P	P	P
Oenothera elata	-	-	-	-	-	P	-
Schoenoplectus californicus	P**	P**	-	-	-	-	-
Senecio blochmaniae	-	-	-	-	-	-	P
*Thinopyrum junceiforme	P**	-	-	-	-	-	-
Dead Vegetation	-	-	0.18%	0.01%	-	1.15%	0.81%

*Non-native species; P=Present within Project Area but not on transect line; P**=Only Present growing in storm surge debris piles from previous winter.
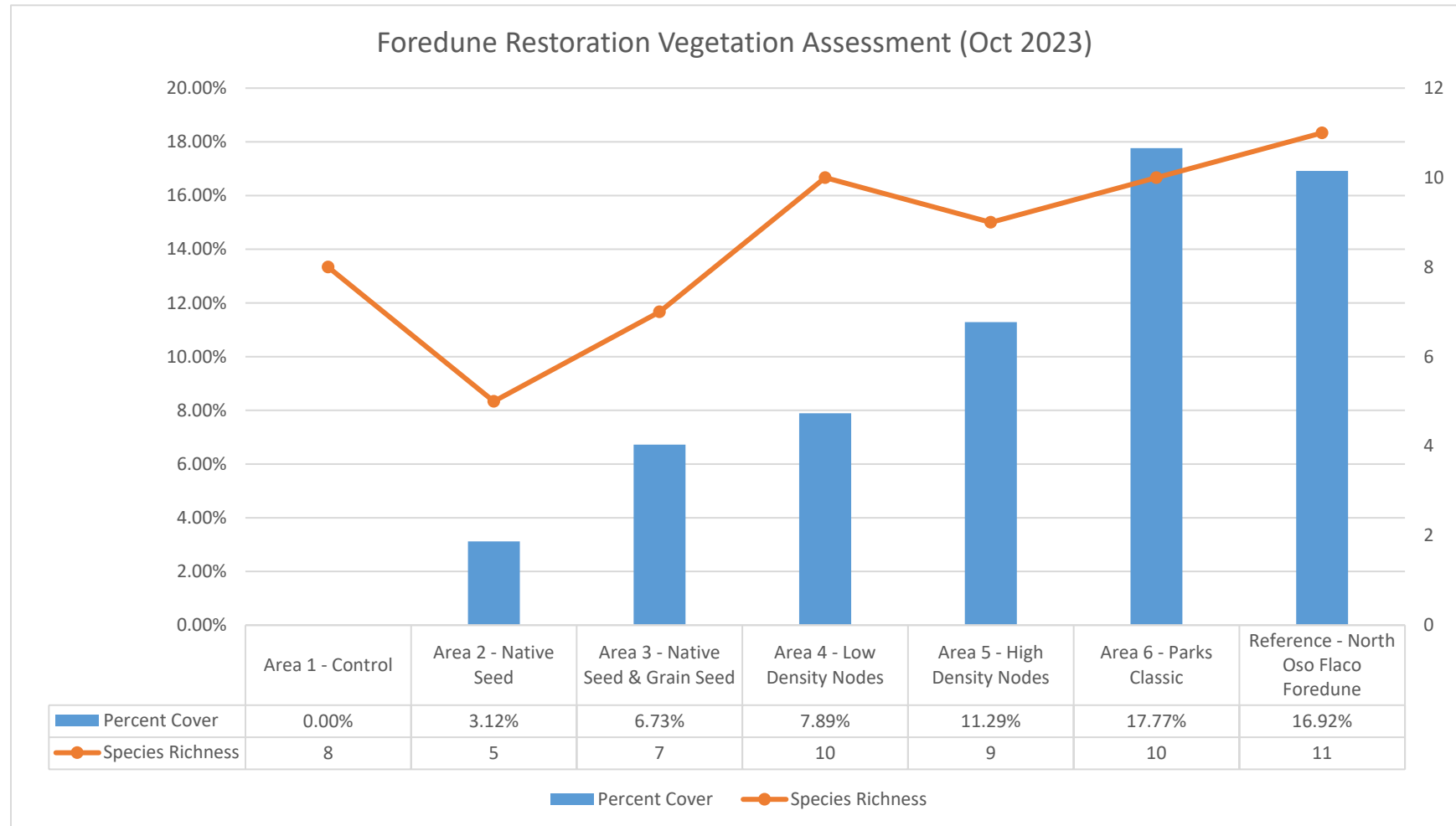
Figure 1. Vegetation composition in 48 Acre Foredune project areas compared to reference site. Four 30-meter transects were sampled in each of the Foredune areas and Reference Site.

Comparison of Line Intercept Transect Sampling Method and Results from Independent Studies

State Parks methods were designed to monitor the establishment of vegetation cover and species richness within specific project areas. Two recent and independent reports also evaluated vegetation cover within the ODSVRA using aerial imagery to analyze total vegetation cover, each using different imagery sources. Both studies were used to cross-reference the State Parks results. These reports include:

UCSB Historical Vegetation Cover Change Analysis (1930-2020) within the Oceano Dunes SVRA" (N. Swet, Z. Hilgendorf, I. Walker, December 28, 2021). Published as Attachment 07-04 in the 2022 ARWP

Hilgendorf, Z., Turner, C, Walker, I.J. UCSB-ASU 2020-2021 ODSVRA Foredune Restoration UAS Survey Report. 37p. Produced for CDPR-ODSVRA and published as Attachment 8 in the 2021 ARWP.

The methods used by Hilgendorf et al., 2021 were continued in subsequent seasons and the results from those surveys are included in Table 2.

The aerial imagery analysis of the North Oso Flaco foredune presented in (Swet et al., 2021) covered the same area as the State Parks transect monitoring reference site in North Oso Flaco and found that vegetation cover ranged from between 24.41% in 2012 and 19.05% in 2020. State Parks vegetation monitoring of the area corroborated these findings with a vegetation cover mean of 23.0% in the fall of 2021. In the fall of 2023, State Parks re-surveyed the same transect lines from 2021 and found a vegetation cover mean of 16.92% which showed a decrease of approximately 6%. This could be due to increased sand inundation, blowouts and small changes in the starting and stopping locations as the stakes are reset each year using handheld GPS devices potentially resulting in more sand and less vegetation on the transect lines. It should be noted that State Parks sampled only four (4) randomly selected 30-meter transects within the area resulting in a high degree of variation between samples (ranging from 6.2% cover to 60.1% cover in 2021 and 0.7% to 42.7% cover in 2023) and that the aerial imagery analysis looked at the entire area so some variation in the results between the two studies is expected. For the remainder of the study, (Swet et al., 2021) did not analyze project specific areas that are comparable with the State Parks transects so further analysis of their source imagery would need to be conducted to cross-reference their study with State Parks transect monitoring.

In (Hilgendorf et al., 2021) the authors did analyze vegetation cover within specific project areas but limited their analysis to the 48 Acre Foredune Project. A comparison of the two studies can be seen in Table 2 and Figures 2 and 3 below. When comparing the results from the State Parks transect monitoring with the results from (Hilgendorf et al., 2021) and their subsequent surveys, it needs to be clarified that the two studies had differing ways of defining vegetation cover and therefore variation in the results is expected. State Parks transect monitoring measured canopy cover, ignoring small gaps between leaves or stems (>5 cm), and included all parts of the vegetation canopy, not only the leaf cover, but also the woody stems, seasonally dormant plants and dead woody vegetation. (Hilgendorf et al., 2021) used 5-band multispectral imagery acquired from uncrewed aerial system (UAS) surveys and Normalized Difference Vegetation Index (NDVI) method to determine vegetation cover. NDVI looks at the differences in reflected near infrared light and red light which in turn is used to determine leaf cover. This is noteworthy because with NDVI method seasonal variations in cover are expected as seasonal changes in the leaf cover occur (i.e., NDVI does not tend to consider live woody stems or dormant vegetation that does not have photosynthesizing leaves). For example, beach primrose is a perennial herb that actively grows in the early spring but becomes dormant in the fall, leaving woody

stems with little leaf cover. With NDVI you would detect high percent cover in February and low precent cover in October but with the transect method plants would be detected in both seasons. This is significant in Treatment 6 where beach primrose is common. This is even more evident with annual species like sea rocket, which in its post season desiccated state would be counted as having cover in the transect method but not in the UAS method. This fluctuation in leaf cover may act in an opposite seasonal change for other species like red sand verbena which actively grows in the spring and summer and may have leaf yellowing in the winter. This could account for the reduction in cover in the UAS surveys in some the treatment areas from October to February and then back up in the following October. In the back dunes, seasonal changes using NDVI are very apparent in the willow thickets within the vegetation islands which drop their leaves in the winter. For these reasons, it is expected that the results of the two studies would vary, specifically when data was collected in different seasons.

In general, State Parks results follow a similar pattern as the UAS surveys with vegetation cover generally increasing over time across all treatment areas except the control (Area 1). One exception is that State Parks showed a decrease in cover in Area 3 in 2022 and again in 2023. This is consistent with the UAS surveys which showed a decreasing cover trend for Area 3 from October 2022 to February 2024. The UAS surveys also showed seasonal decreases in cover from October 2022 to February 2023 in Areas 1, 2, 3 and 4 and again in across all areas from October 2023 to February 2024. When comparing the recent October 2023 results of the UAS surveys and the Parks transect surveys, ranking order of cover was similar across treatment areas with only Area 3 showing a disparity, ranking 2nd in cover for the UAS survey and ranking 4th in cover for the Parks transect surveys. In October 2023, State Parks and the UAS surveys showed vegetation cover at similar levels as well in Area 1 (0% and 0.73%), Area 2 (3.12% and 3.83%), Area 4 (7.89% and 7.55%), Area 5 (11.29 % and 9.68%) and Area 6 (17.77% and 19.36%). Area 3 (6.73% and 10.36 %) showed the greatest difference when comparing the two methods. This inconsistency is likely a result of the State Parks method having a small sample size and a high degree of variability in cover between transects. This is apparent in the wide range of percent cover in the samples compared to the mean. For example, in 2023, Area 3 had a mean of 6.73% and a sample range of 0% to 12.6% cover.

Table 2. Vegetation cover comparison between State Parks Transect Monitoring and the UCSB/ASU UAS Surveys.

| 48 Acre Foredune	Area 1	Area 2	Area 3	Area 4	Area 5	Area 6
Feb 2020 - UCSB/ASU UAS Survey	0.00%	0.00%	0.00%	0.00%	0.00%	0.00%
Fall 2020 - State Parks Transect Monitoring	0.00%	0.10%	4.02%	0.76%	0.40%	3.57%
Oct 2020 - UCSB/ASU UAS Survey	0.02%	0.41%	2.66%	0.87%	1.65%	2.54%
Feb 2021 - UCSB/ASU UAS Survey	0.03%	0.42%	2.15%	0.95%	1.85%	3.28%
Fall 2021 - State Parks Transect Monitoring	0.00%	1.91%	12.31%	5.69%	2.14%	12.66%
Oct 2021 - UCSB/ASU UAS Survey	0.14%	1.85%	4.87%	1.93%	3.63%	3.54%
Feb 2022 - UCSB/ASU UAS Survey	0.08%	1.74%	4.55%	2.24%	4.64%	11.35%
Fall 2022 - State Parks Transect Monitoring	0.00%	5.25%	10.13%	5.14%	6.43%	13.79%
Oct 2022 - UCSB/ASU UAS Survey	0.26%	3.45%	11.47%	6.03%	9.57%	14.82%
Feb 2023 - UCSB/ASU UAS Survey	0.12%	2.68%	8.93%	5.52%	9.66%	14.83%
Fall 2023 - State Parks Transect Monitoring	0.00%	3.12	6.73%	7.89%	11.29%	17.77%
Oct 2023 – UCSB/ASU UAS Survey	0.73%	3.83%	10.36%	7.55%	9.68%	19.36%
Feb 2024 – UCSB/ASU UAS Survey	0.42%	3.10%	6.95%	4.85%	6.18%	11.68%
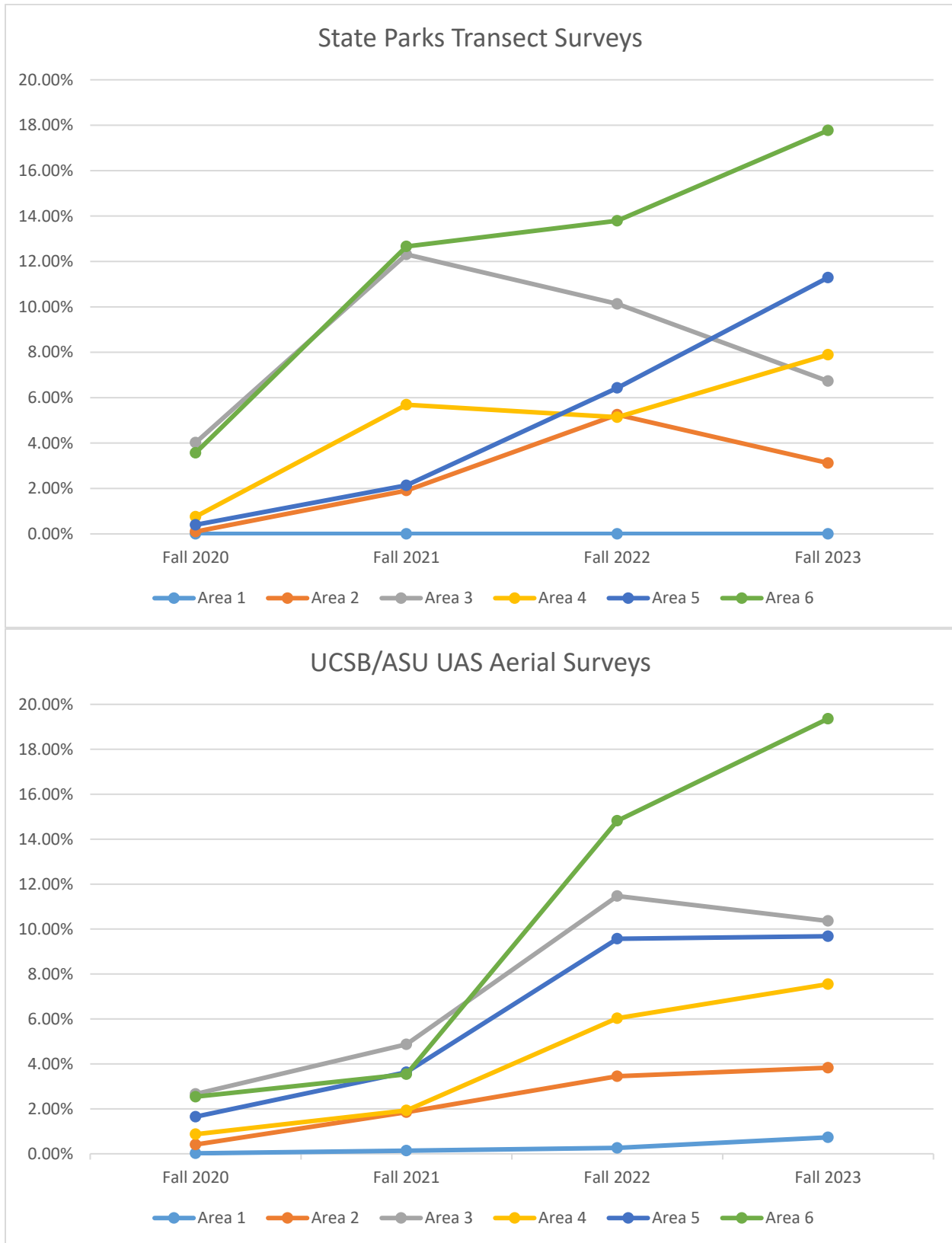
Figure 2. Vegetation cover comparison between State Parks Transect Monitoring and the UCSB/ASU UAS Surveys for Fall surveys only.
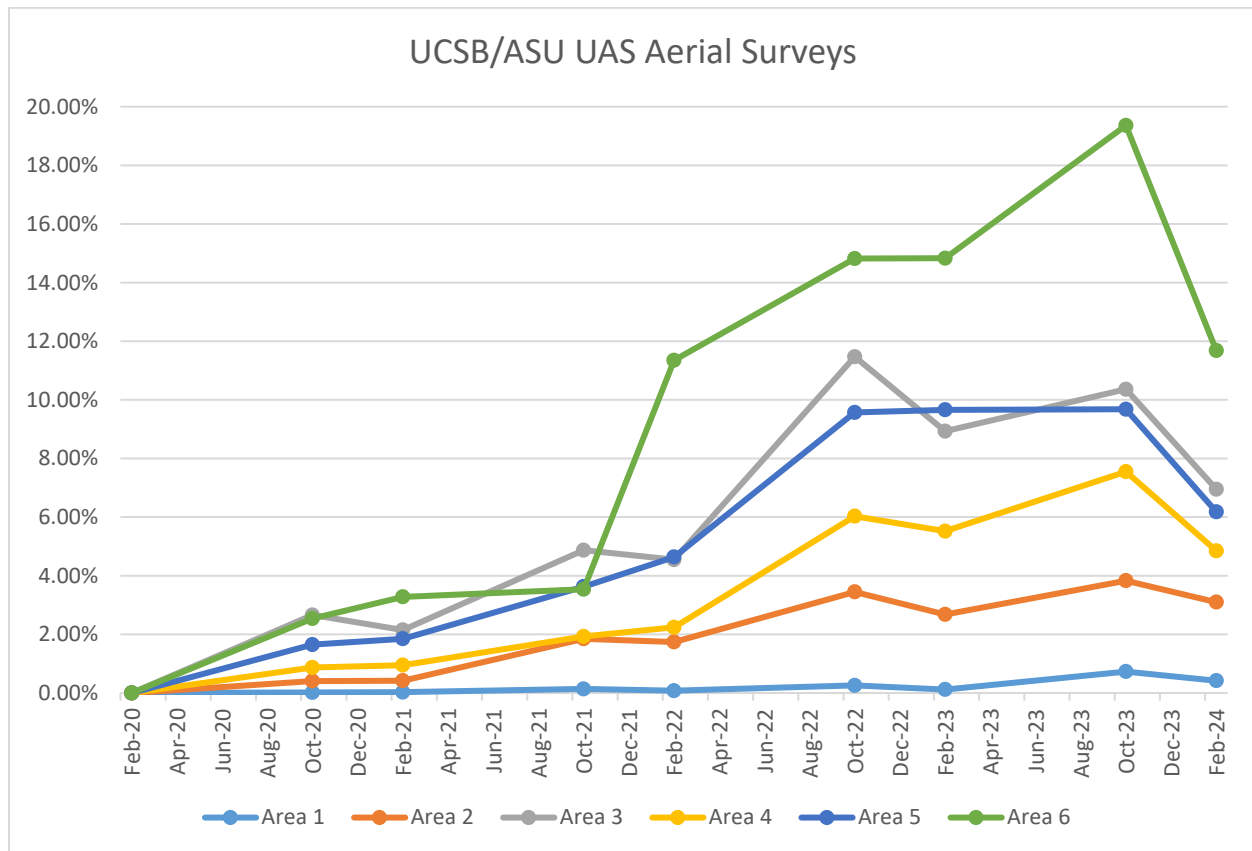
Figure 3. UCSB/ASU UAS Surveys Vegetation cover change over time including both Fall and Winter surveys.

Back Dune Projects

Each of the back dune project areas that were surveyed showed healthy levels of vegetation cover and showed similar vegetation composition compared to the early seral reference site (Refer to Table 3 and Figure 4). Of the 20 native species present within the early seral reference site, the project areas had between 10 and 12 of them and a total richness of between 14 and 19 species. The dominant species within the early seral reference site, dune bush lupine (*Lupinus chamissonis*), showed similar percent cover between the different project areas and the early seral reference site with 24.0%, 31.02% and 39.84% cover in the project areas and 29.23% cover in the early seral reference site. For overall cover, all project areas had lower percent cover than both reference sites. However, growth is anticipated to continue and percent cover is anticipated to approach the cover of the reference sites within the upcoming growing seasons.

Table 3. Table of results from the back dune restoration project line intercept transect sampling.

Back Dune Restoration Project Vegetation Assessment					
*Non-native species P=Present within project area	Eucalyptus Tree (2021-VG-03)	Lagrille Hill - Mid Section (2021-VG-02)	Tabletop (2021-VG-04)	Reference - Early Seral	Reference - Late Seral
Age of Planting (years)	2.5	2.5	2.5	-	-
Species Richness	19	14	18	22	15
Transect 1	14.2%	39.6%	0.4%	76.7%	76.3%
Transect 2	57.0%	40.7%	34.0%	63.2%	78.7%
Transect 3	62.7%	65.6%	65.2%	66.4%	76.2%
Mean Percent Cover	44.6%	48.6%	33.2%	68.8%	77.1%
Species					
Abronia umbellata	P	-	P	-	-
Achillea millefolium	0.66%	0.34%	0.13%	4.6%	p
Acmispon glaber	2.39%	7.73%	6.01%	p	3.5%
Ambrosia chamissonis	-	-	P	p	-
Baccharis pilularis	-	-	-	p	0.2%
Camissoniopsis cheiranthifolia	0.02%	1.48%	0.11%	p	-
Castilleja affinis	-	-	-	p	-
Chenopodium californicum	-	-	-	-	p
Chorizanthe eastwoodiae	-	-	-	p	-
Cirsium occidentale	-	-	-	0.4%	-
Conicosia pugioniformis	-	-	-	0.9%	0.1%
Coreopsis gigantea	P	-	-	-	
Corethrogyne filaginifolia	P	P	P	-	6.1%
Cryptantha clevelandii	-	-	-	p	-
Dudleya lanceolata	-	-	-	-	0.4%
Ehrharta calycina	-	-	-	p	p
Ericameria ericoides	P	0.06%	P	22.6%	57.9%
Erigeron blochmaniae	P	P	0.39%	1.3%	-
Eriogonum parvifolium	0.84%	0.82%	0.03%	-	0.03%

Back Dune Restoration Project Vegetation Assessment					
*Non-native species P=Present within project area	**Eucalyptus Tree (2021-VG-03)**	**Lagrille Hill - Mid Section (2021-VG-02)**	**Tabletop (2021-VG-04)**	**Reference - Early Seral**	**Reference - Late Seral**
Eriophyllum staechadifolium	P	1.92%	P	-	-
Erysimum suffrutescens	P	P	P	p	p
Heterotheca grandiflora	P	-	-	-	-
Horkelia cuneata	-	P	P	-	-
Lupinus chamissonis	39.84%	31.02%	24.00%	29.3%	-
Monardella undulata crispa	1.81%	4.26%	2.18%	p	-
Mucronea californica	P	-	P	-	-
Phacelia ramosissima	4.89%	0.66%	P	p	-
Pseudognaphalium biolettii	-	-	-	0.1%	p
Pseudognaphalium californicum	P	-	-	p	-
Pseudognaphalium ramosissimum	-	-	-	p	p
Salix lasiolepis	p	-	P	p	-
Senecio blochmaniae	0.01%	P	P	2.5%	p
Silene laciniata	-	-	-	-	p
Dead woody vegetation	-	3.32%	4.16%	12.8%	13.4%

Back Dune Restoration Project Vegetation Assessment

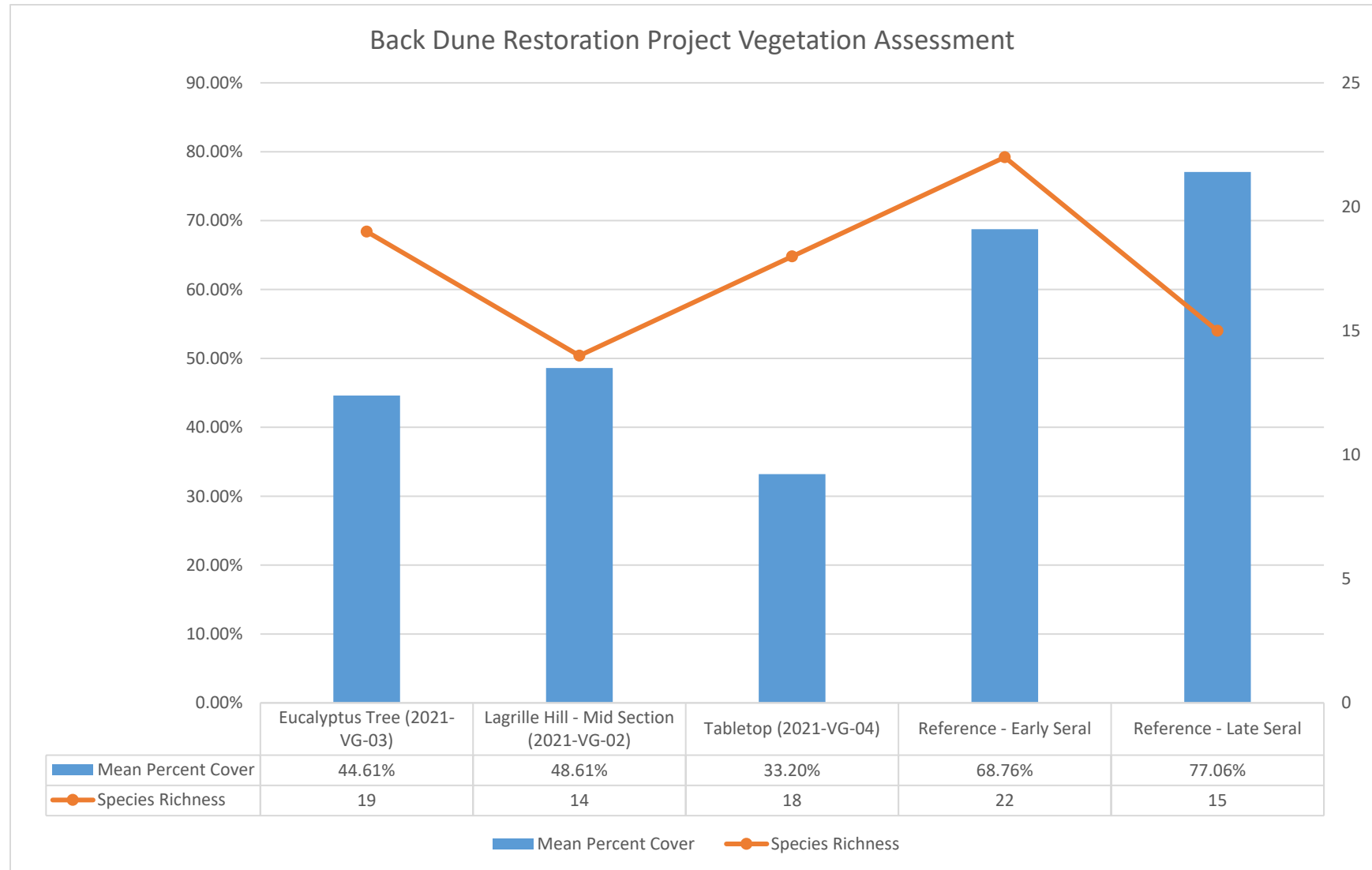|	Eucalyptus Tree (2021-VG-03)	Lagrille Hill - Mid Section (2021-VG-02)	Tabletop (2021-VG-04)	Reference - Early Seral	Reference - Late Seral
Mean Percent Cover	44.61%	48.61%	33.20%	68.76%	77.06%
Species Richness	19	14	18	22	15

Figure 4. Vegetation composition in back dune project areas compared to reference sites. Three 30-meter transects were sampled in each of the back dune areas and reference sites.

Photo Point Monitoring

On-the-ground photo point monitoring was conducted at the 48-Acre Foredune project area prior to project installation in February 2020 and following project installation in May 2020, October 2020 and during each subsequent October since. Photo point monitoring is scheduled to continue in October in future years. Photo points are located on all four corners of each treatment area. For each photo point, two photos are taken, each with one of the treatment area boundary lines on the outer edge of the photo with the interior of the treatment area centered in the photo. There is also one photo point overlooking the entire 48-Acre Foredune project from a distance. Refer to figures 5-12 for examples of 48-Acre Foredune photo points. On-the-ground photo point monitoring was also conducted throughout the back dune project areas during the Fall of 2023 and has been conducted annually since 2018. Back dune photo points are positioned to capture changes within the general areas where back dune projects are located. The number of photos for each photo point and the number of photo points varies at each location to sufficiently capture each area. In total, 41 photo points were monitored in 2023. Refer to figures 13-16 for examples of back dune photo points.

In addition to on-the-ground monitoring, drone aerial imagery photo point monitoring was conducted in May 2020, during the winter of 2020 and each winter since. Within the 48-Acre Foredune, two photo points were taken of each treatment area, one from the east and one from the west for each area. In addition, each winter, drone photo points were conducted within the back dune project areas. The number of photos for each photo point and the number of photo points varied at each location to sufficiently capture each area. Refer to figure 17-22 for example of drone photo points. Both on-the-ground and drone photo point monitoring are scheduled to continue annually.

Figure 5. Photo point of 48 Acre Foredune Area 1, west fenceline facing north. Note lack of vegetation or storm surge debris. Photo taken on October 18, 2022.

Figure 6. Photo point of 48 Acre Foredune Area 1, west fenceline facing north. Note debris from storm surge capturing sand and support plant growth. Photo taken on October 24, 2023.

Figure 7. Photo point of 48 Acre Foredune Area 4 facing south prior to planting treatment. Photo taken on February 4, 2020.

Figure 8. Photo point of 48 Acre Foredune Area 4-Low Density Nodes facing west 3.5 years after treatment. Photo taken on October 24, 2023.

Figure 9. Photo point of 48 Acre Foredune Area 5-High Density Nodes facing south prior to planting treatment. Photo taken on February 4, 2020.

Figure 10. Photo point of 48 Acre Foredune Area 5-High Density Nodes facing south 3.5 years after treatment. Photo taken on October 24, 2023.

Figure 11. Photo point of 48 Acre Foredune Area 6-Parks Classic facing west prior to planting treatment. Photo taken on February 4, 2020.

Figure 12. Photo point of 48 Acre Foredune Area 5-High Density Nodes facing west 3.5 years after treatment. Photo taken on October 24, 2023.

Figure 13. Photo point of Eucalyptus Tree facing south prior to planting treatment. Photo taken on May 19, 2020.

Figure 14. Photo point of Eucalyptus Tree facing south 2.5 years after treatment. Photo taken on October 30, 2023.

Figure 15. Photo point of Boy Scout Camp facing north prior to planting treatment. Photo taken on October 27, 2020.

Figure 16. Photo point of Boy Scout Camp facing north 1.5 years after treatment. Photo taken on October 30, 2023.

Figure 17. Drone photo point of 48 Acre Foredune Area 3-Native and Sterile Grain Seed, facing east. Image taken on May 8, 2020.

Figure 18. Drone photo point of 48 Acre Foredune Area 3-Native and Sterile Grain Seed, facing east. Image taken on February 14, 2024.

Figure 19. Drone photo point of Bigfoot restoration project area facing south. Image taken on May 8, 2020.

Figure 20. Drone photo point of Bigfoot restoration project area facing south. Image taken on February 14, 2024.

Figure 21. Drone photo point of La Grille Hill restoration project area facing northwest. Image taken on March 6, 2022.

Figure 22. Drone photo point of La Grille Hill restoration project area facing northwest. Image taken on February 14, 2024.

THIS PAGE WAS INTENTIONALLY LEFT BLANK.

ODSVRA Dust Control Program Draft 2024 ARWP

ATTACHMENT 07

Increments of Progress Toward Air Quality Objectives, ODSVRA Dust Control 2023 Update – Revised

- Increments of Progress Toward Air Quality Objectives, ODSVRA Dust Control 2023 Update – Revised (DRI Document)

- SAG Review of Desert Research Institute (DRI) "Increments of Progress Toward Air Quality Objectives, ODSVRA Dust Control 2023 Update" (SAG Memo)

THIS PAGE WAS INTENTIONALLY LEFT BLANK.

Increments of Progress Towards Air Quality Objectives - ODSVRA Dust Controls, 2023 Update -Revised

J.A. Gillies, G. Nikolich, E. Furtak-Cole

Dust controls including temporary wind fences and vegetation projects have been used within the ODSVRA to reduce the emissions of PM_{10} originating from the ODSVRA and lower the regional PM_{10} burden on the Nipomo mesa. Beginning in 2014 and continuing through 2022, a total of 412.5 acres of managed dust control areas have been established in the ODSVRA (ARWP, 2023, Attachment 1).

Here we demonstrate that the PM_{10} (hourly BAM) data measured at CDF and Mesa2 and the wind data measured 10 m above ground level (AGL) at the S1 tower show that PM_{10} measured at CDF and Mesa2 are lower now than prior to the emplacement of dust controls and that this reduction in PM_{10} scales with the increase in acres of dust control upwind of these monitoring sites. In this report we update the relation between the ratio Total PM_{10} (TPM_{10}):Total Wind Power Density (TWPD) for CDF and Mesa2 and acres of dust control from Gillies et al. (2022a) with data from April to September, 2023.

Methods

The metric used to evaluate the production of PM_{10} from the ODSVRA is the ratio of total hourly PM_{10} (TPM_{10}, $\mu g\ m^{-3}$ [measured with a Beta Attenuation Monitor or BAM]) operated by the San Luis Obispo County Air Pollution Control District, SLOAPCD and total hourly wind power density ($W\ m^{-2}$) as measured at the S1 tower within the ODSVRA, for winds that are expected to cause saltation and dust emissions during a set period of time. Here we set the period of time to be the spring-summer period from April through September, which is typically considered the windy season in the region.

The following constraints were applied for the available environmental data.

1) A wind speed filter was applied based on screening for the conditions where it was most likely that the PM_{10} reaching CDF and Mesa2 was due to the generation of dust by saltation within the ODSVRA. Winds from 248° to 326° were used to ensure, conservatively, that the air flow that reached CDF and Mesa2 had most likely travelled from the ODSVRA.
2) Wind speed that indicated the initiation of a relation with increasing PM10 at the CDF and Mesa2 sites were determined from data that relates PM_{10} to wind speed measured at each of the sites.
3) Based on searches for precipitation data for monitoring sites near the ODSVRA the number of days where precipitation was identified to occur prior to the hour of observation were identified. Hours of observation were removed from analysis if precipitation was observed less than 3 days prior.

To standardize the calculation of TWPD a lower limit of wind speed is chosen that corresponds with the lowest speed where the relation between increasing wind speed and simultaneous increase in PM_{10} is observed at a monitoring station. As for previous years a wind speed of 3.5 m s^{-1} at 10 m above ground level (AGL) (WPD= 26 $W\ m^{-2}$) for CDF and Mesa2 defines the lowest value for the range over which PM_{10} is summed at these stations to calculate TPM_{10}. TWPD is the summation of the hourly mean wind speed measured at the S1 tower for the hours identified at CDF or Mesa2 that correspond to hourly mean wind speed ≥3.5 m s^{-1} (after screening for the wind direction and precipitation criteria).

Wind power density (WPD, $W\ m^{-2}$) is defined as (e.g., Kalmikov, 2017):

$$WPD = 0.5\, \rho_a\, u^3 \qquad\qquad\qquad\qquad\qquad\qquad\qquad\qquad\qquad (1)$$

where ρ_a is air density (kg m^{-3}), and u (m s^{-1}) is wind speed at the measurement height above ground level (10 m AGL), a unit area of 1 m^2 is assumed in this application. For comparison among different locations and between different years, the height of measurement of wind speed and the lower limit of mean hourly wind speed for summation of Total Wind Power Density (TWPD) must be the same.

The importance of using a consistent lower limit of mean hourly wind speed can be demonstrated using the S1 tower wind and CDF PM10 hourly concentration data for the lower wind speed limits of 3.5 m s^{-1}, 4.0 m s^{-1}, and 4.5 m s^{-1} (Fig. 1) for each month, April through September 2022. As Fig. 1 shows, the strength of the relation between Monthly Total PM10 and Monthly Total Wind Power Density is unchanged at R^2=0.99 for all three lower limit wind speeds. The change in the lower limit does change the slope and intercept. The seasonal TPM10:TWPD (i.e., the summation of all [filtered] hours for the period April-September, 2022) value using the lower summation limits of 3.5 m s^{-1}, 4.0 m s^{-1}, and 4.5 m s^{-1} would be ,respectively, 0.161, 0.159, and 0.157. The values change slightly hence it is important to maintain consistency for the lower limit wind speed value for comparison purposes to evaluate temporal change in the ratio.
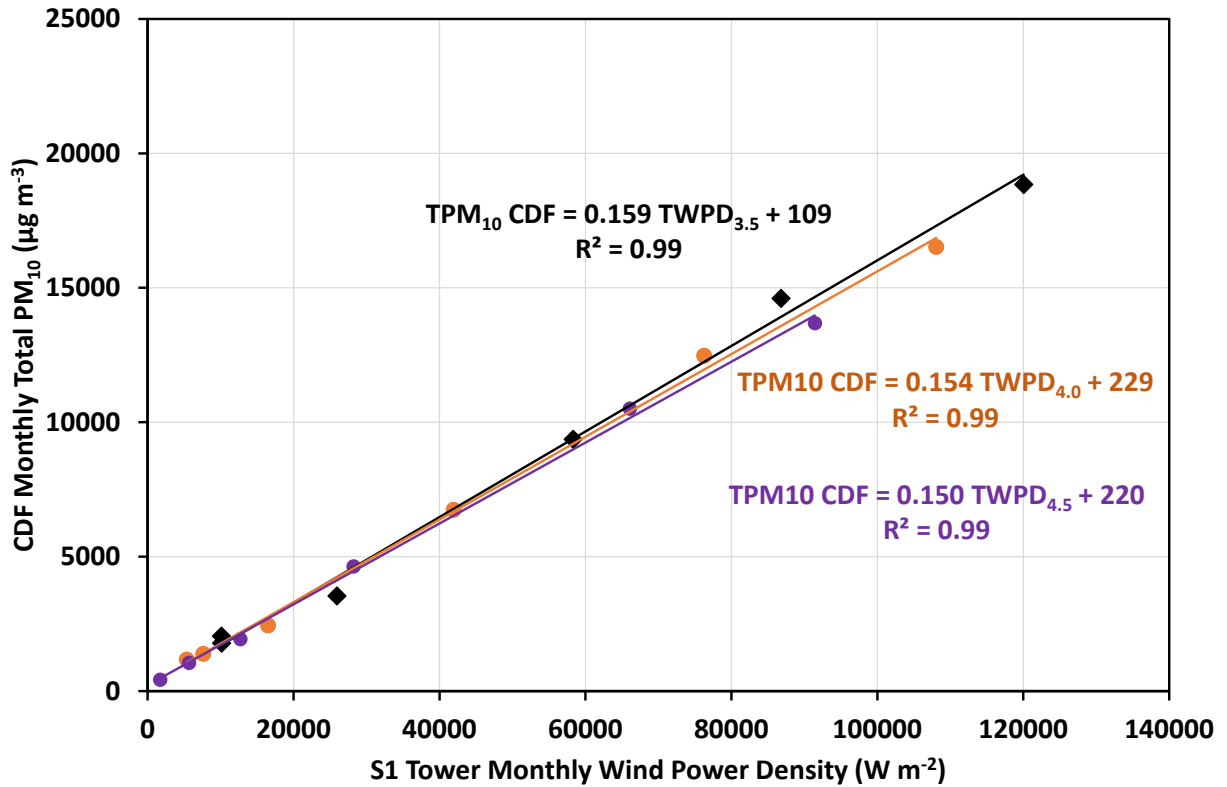

Figure 1. Relations between CDF Monthly Total PM10 and S1 Tower Monthly Total Wind Power Density (April to September 2022) as affected by the lower limit wind speed for summation (black diamonds 3.5 m s^{-1}, orange circles 4.0 m s^{-1}, purple circles 4.5 m s^{-1}).

The choice of using the lower limit of wind speed at CDF of 3.5 m s^{-1} measured at 10 m AGL is that when this hourly wind speed is observed at CDF the wind speed at the S1 tower is likely above that needed for saltation and PM10 dust emissions to be occurring within the ODSVRA (Fig. 2). Based on the available multi-year data record, saltation and dust emissions occur within the ODSVRA when the S1 tower wind speed measured at 10 m AGL is approximately 8.5 m s^{-1}. Figure 2 shows the relation between hourly wind speed at 10 m AGL at CDF and at 10 m AGL at the S1 tower for April-September 2023. In 2023 the regression derived wind speed at CDF that corresponds to 8.5 m s^{-1} at S1 is 4.1 m s^{-1}. To be consistent between years, however, the lower limit of hourly mean wind speed for summation is retained at 3.5 m s^{-1} as measured at CDF.

Results 2023

Total Wind Power Density April-September 2011-2023

To place the wind conditions into context across the available S1 tower data record, 2011-2023, TWPD for the period April-September in each year was calculated (Fig. 3). For 2023, TWPD for the period April-September is similar to, i.e., within -2 to 5.5% of the values for 2018, 2020 and 2021. In the 13-year record from 2011 to 2023, 2019 had the lowest observed and 2022 the highest observed values of TWPD.
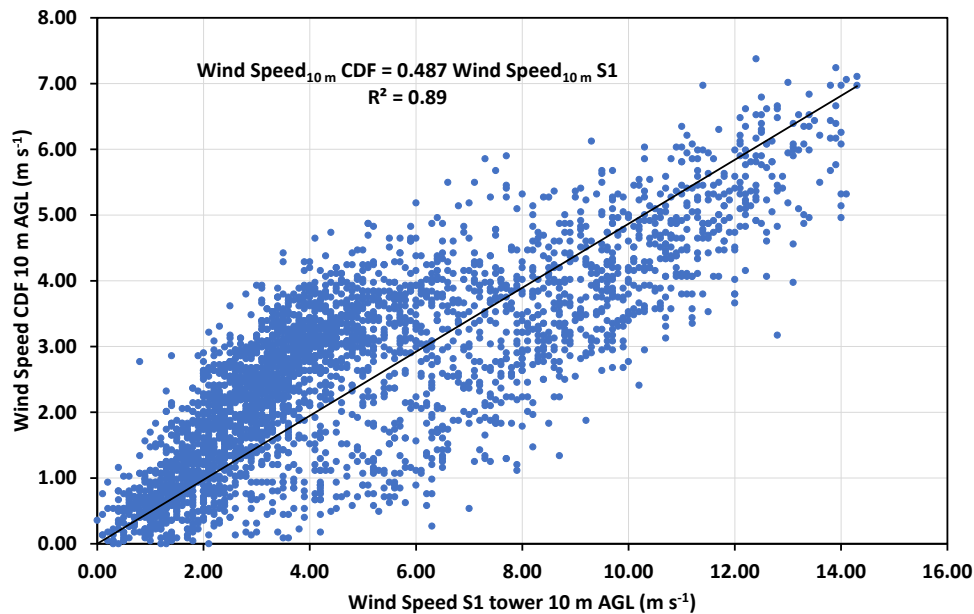

Figure 2. The correlation between mean hourly wind speed measured at 10 m AGL at CDF and S1 April through September 2023.
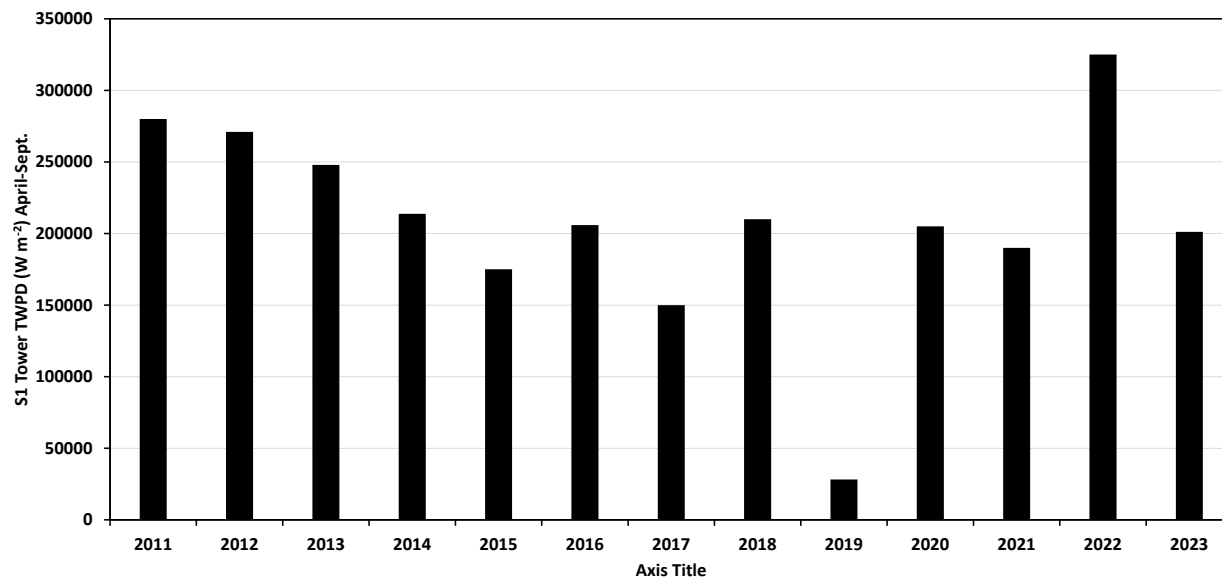
Figure 3. Total Wind Power Density (W m^{-2}) at the S1 tower for the period April-September, 2011-2023.

Total PM$_{10}$ and Total WPD April-September 2023, CDF

As shown previously (Gillies et al., 2020, 2021, 2022a) total WPD (TWPD), i.e., the summation of hourly mean wind speed for a defined period, measured at S1 correlates with total PM$_{10}$ at CDF and Mesa2 (Gillies et al., 2020, 2021, 2022b). This relation was also observed for the 2023 data (Fig. 4).

Based on the number of acres of dust control that have been established from 2013 through 2023 upwind of CDF, Fig. 5 shows that at CDF for the period April through September a downward trend in the TPM$_{10}$:TWPD ratio with increasing amounts of dust control acreage has been observed. There are, however, two years of data that have not been included. In 2019 there were few hours where the winds exceeded the lower limit of wind speed to define the summation interval (i.e., $\geq$3.5 m s^{-1} at CDF and Mesa2), which due to the paucity of higher wind speeds leads to an unstable ratio condition. The TPM$_{10}$:TWPD ratio for 2020 was also not included in the least squares regression as during April-September of that year OHV activity in the Park was restricted due to COVID19.

Figure 5 indicates that the 2023 CFD TPM$_{10}$:TWPD ratio value supports the established downward trend in this dust emission metric even though the acres of dust control remained the same in 2023. The percentage change in the TPM$_{10}$:TWPD ratio from 2022 (0.17) to 2023 (0.15), a decrease of 11%, may be reflective of natural variation in the dust emission system and the transport of PM$_{10}$ from different source areas within the ODSVRA to the receptor site. Figure 6 (top panel) shows the distribution of wind direction at CDF for April-September 2022 and 2023, which indicates that there was a shift to winds with a more frequent westerly component in 2023 compared to 2022. The distribution of wind direction at S1 tower (Fig. 6, bottom panel) is similar between 2022 and 2023, but a shift in wind direction in 2023 also favors more westerly directions in April-September, but not as great as observed at CDF. The distributions presented in Fig. 6 are for the data that have been filtered for wind

4
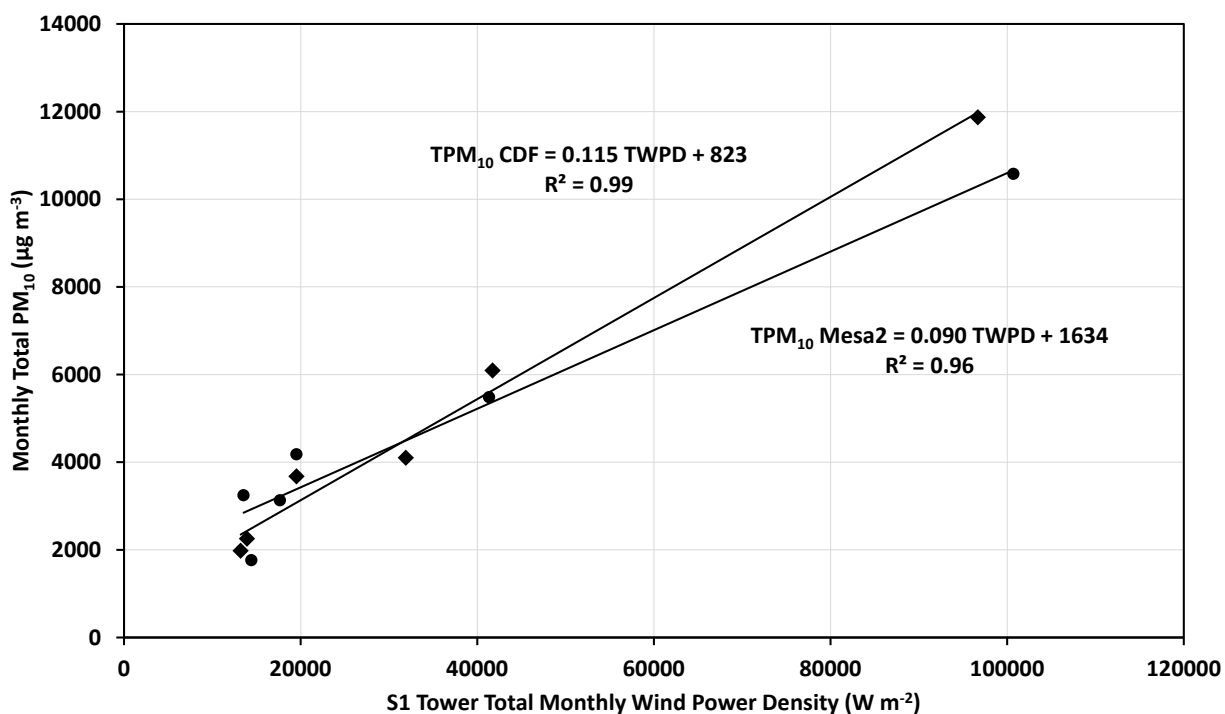
Figure 4. The relation between monthly Total PM_{10} and monthly Total Wind Power Density for all hours when the wind direction was from 248°-326° observed at CDF (diamonds) and Mesa2 (circles), wind speeds were ≥3.5 m s^{-1} (at CDF and Mesa2), and hours wherein there were <3 days since the last record of precipitation were removed.

Figure 5. The relation between TPM_{10}:TWPD ratio value measured at CDF and the acres of dust control from 2013 through to 2022 placed upwind of CDF in the directional range 270° to 325°. Data from 2019 and 2020 were excluded as discussed elsewhere. Note 2014 and 2017 data align on top of each other.
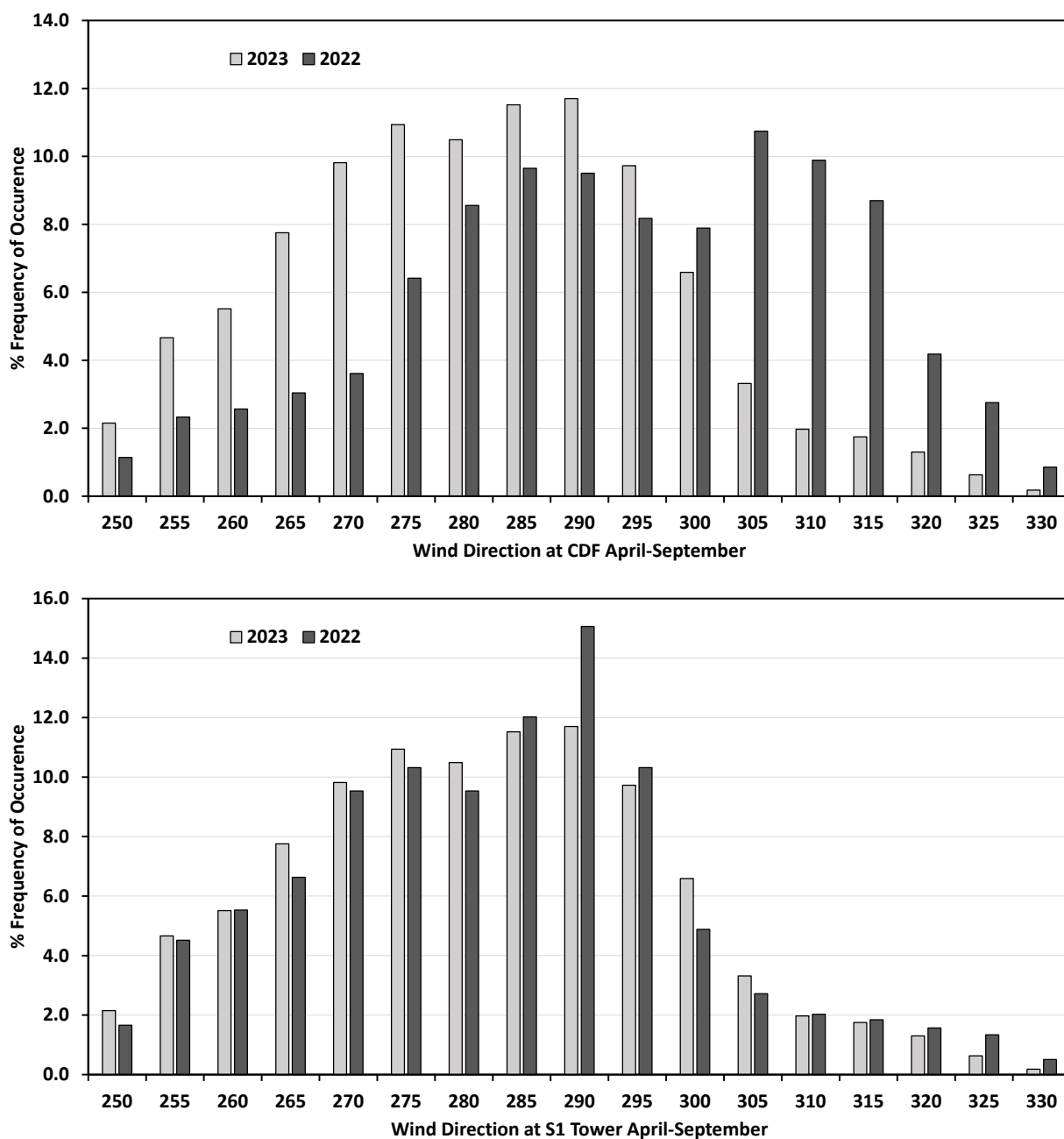
Figure 6. The distribution of wind direction at CDF and S1 tower for the period April-September 2022 and 2023, after applying the filtering criteria.

speed ($\geq$3.5 m s^{-1} at 10 m AGL), wind direction range (248°-326°), and precipitation criteria (removed days with <3 days of drying).

The continued decrease in the TPM$_{10}$:TWPD ratio in 2023 at CFD could also be due, in part, to the dust control management strategies having increased their effectiveness due to the maturation of the vegetation within the control areas and Parks maintenance practices. Larger plants and increased cover

6

should increase the degree to which the vegetation absorbs momentum and increases the area sheltered from erosive winds.

Total PM$_{10}$ and Total WPD April-September 2023, Mesa2

The ratio of TPM$_{10}$:TWPD for Mesa2 and S1 data for the period April through September for the years 2013-2023 as a function of acres of dust control upwind of Mesa2 is shown in Fig. 7. This figure shows that a downward trend in the TPM$_{10}$:TWPD ratio is observed with increasing acres of dust control for the period 2018-2022. Prior to 2018, there was no clear trend in the TPM$_{10}$:TWPD ratio data as there were few acres of dust control upwind of the Mesa2 monitoring station.

Figure 7 indicates that a downward trend in the TPM$_{10}$:TWPD ratio through time for Mesa2 is supported with the inclusion of the 2023 datum. The data for 2019 and 2020 were not included in the analysis as described above for the CDF site. In 2023 the TPM$_{10}$:TWPD ratio (0.13) was approximately 15% lower than 2022 (0.15), which is similar to the reduction observed at CDF.

Discussions and Conclusions

This analysis has demonstrated that TWPD is a robust metric for explaining the relationship between wind-driven saltation and the accompanying emission of PM$_{10}$ from the ODSVRA as measured at two key receptor sites, CDF and Mesa2. The TWPD and TPM$_{10}$ measurement-based metric indicates that the PM$_{10}$ originating from the ODSVRA has been reduced by approximately 44.5% at CDF using the 2-year (2022 and 2023) mean value of 0.16 for equivalent WPD conditions compared with the baseline year of 2013. For Mesa2, the TWPD and TPM$_{10}$ measurement-based metric indicates that the PM$_{10}$ originating from the ODSVRA has been reduced by approximately 21% using the 2-year (2022 and 2023) mean value of 0.14 for equivalent WPD conditions compared with the baseline year of 2013 (0.18) when there were few acres of dust control upwind of the Mesa2 station.

Figures 6 and 7 demonstrate that the TPM$_{10}$:TWPD ratio can be used to track the progress of the effect of dust controls on the dust emission system within the ODSVRA. It allows for quantification of the increments of progress as management efforts to limit the dust emissions are further developed to meet the SOA. It needs to be noted that the TPM$_{10}$:TWPD ratio indicates the production potential of PM$_{10}$ as a function of WPD. An increase in WPD can result in more exceedances of the State or Federal standard even in the presence of increased amounts of dust controls because the PM$_{10}$ is produced from the uncontrolled areas and it increases as a power function of wind speed, while the efficiency of the dust control does not.
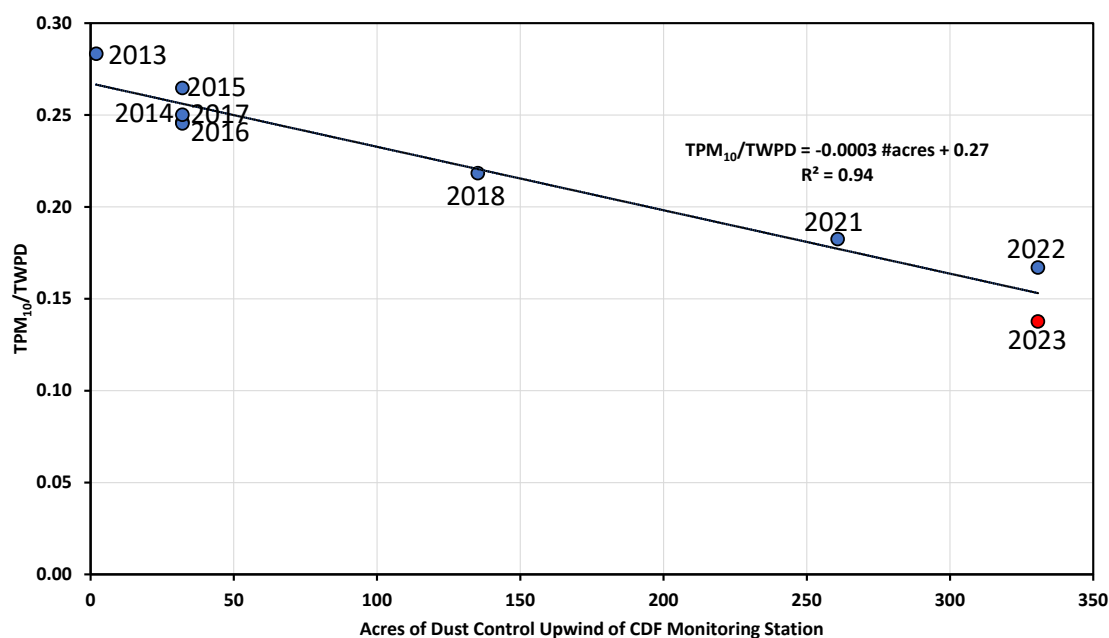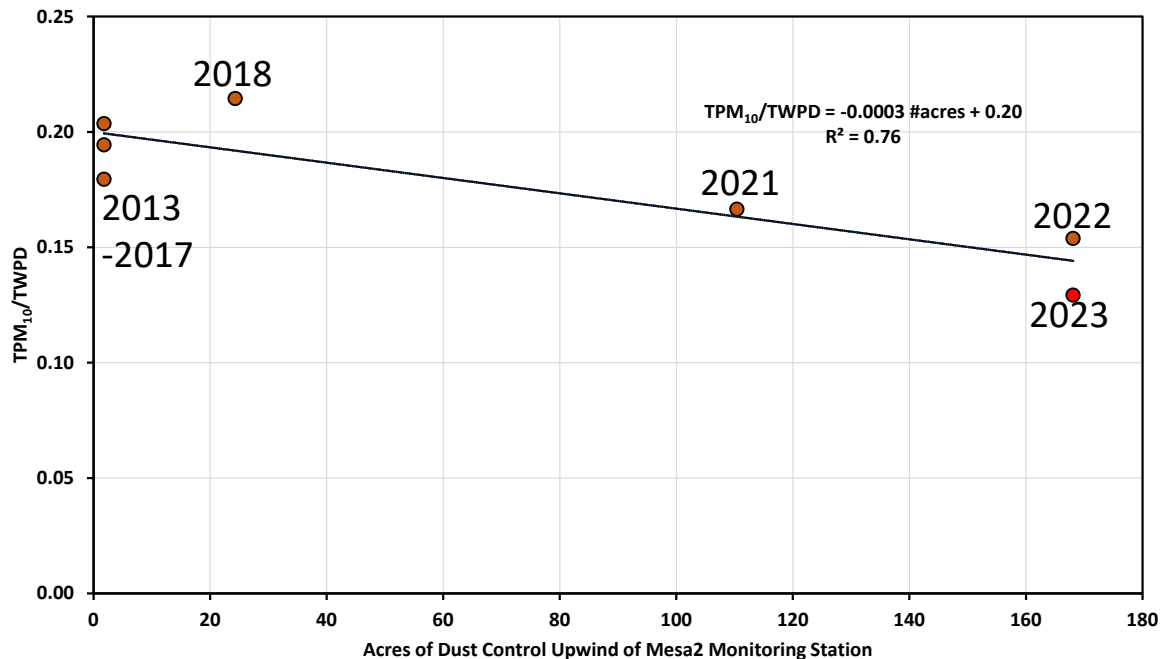
Figure 7. The relation between TPM$_{10}$:TWPD ratio value measured at Mesa2 and the acres of dust control from 2013 through to 2023 placed upwind of Mesa2 in the directional range 270° to 305°. Data from 2019 and 2020 were excluded as discussed elsewhere. Note for the 2013-2017 data points some years are aligned on top of one another.

References

Gillies, J.A., Furtak-Cole, E., Etyemezian, V. (2020). Increments of Progress Towards Air Quality Objectives - ODSVRA Dust Controls. Report prepared for California State Parks by the Desert Research Institute, December 2020.

Gillies, J.A., Furtak-Cole, E., Etyemezian, V. (2021). Increments of Progress Towards Air Quality Objectives - ODSVRA Dust Controls. Report prepared for California State Parks by the Desert Research Institute, December 2021.

Gillies, J.A., Furtak-Cole, E., Etyemezian, V. (2022a). Increments of Progress Towards Air Quality Objectives - ODSVRA Dust Controls. Report prepared for California State Parks by the Desert Research Institute, December 2022.

Gillies, J.A., E. Furtak-Cole, G. Nikolich, V. Etyemezian (2022b). The role of off highway vehicle activity in augmenting dust emissions at the Oceano Dunes State Vehicular Recreation Area, Oceano CA. *Atmospheric Environment: X*, 13, 100146, doi: 10.1016/j.aeaoa.2021.100146.

Kalmikov, A. (2017). Wind power fundamentals. In *Wind Power Engineering,* ed. T.M. Letcher. Elsevier Science Publishing Co., Inc.

January 30, 2024

Memo: <u>SAG Review of DRI Report "Increments of Progress Towards Air Quality Objectives – ODSVRA Dust Controls 2023 Update" (11-27-2023 V1)</u>

From: Scientific Advisory Group (SAG)[1]

To: Jon O'Brien, California Department of Parks and Recreation

Cc: Ronnie Glick, California Department of Parks and Recreation

The SAG received a copy of the Desert Research Institute (DRI) report (*Increments of Progress Towards Air Quality Objectives – ODSVRA Dust Controls 2023 Update*) dated November 27, 2023, and members have had the opportunity to review the document. This memo provides feedback on the DRI report.

As with the previous Increments of Progress (2022) report—original dated February 7, 2023; received and reviewed by SAG in August, 2023; revised and updated on September 5, 2023--the primary message of this 2023 update report is that the dust-mitigation efforts instituted by CDPR since 2013 continue to be effective in reducing PM_{10} concentrations at the CDF and Mesa2 monitoring stations. In particular, Figures 3 and 5 show a downward trend in the ratio of $TPM_{10}/TWPD$ as a function of increases in the total acreage under dust control measures (and therefore with time since 2013). The most convincing aspect of this assessment is the fact that TWPD has varied substantially from year-to-year, as shown in Figure 1, and yet the $TPM_{10}/TWPD$ ratio is now at its lowest value. This speaks to the **overall effectiveness of the dust control measures undertaken in the past decade.**

The report is an update of last year's Increments of Progress (2022) document with new data from 2023 added to the analysis but virtually the same document structure and narrative as before. Many of the issues that were identified in the SAG review of the 2022 document were addressed in a DRI response (September, 2023) to the SAG review (August 28, 2023), but neither the revised 2022 document nor the current (2023) document provides any of the detailed information contained within the DRI response. Thus, some important reasoning and rationale are absent in both the 2022 and 2023 progress reports. **The primary recommendation from SAG members is to include some of the narrative in the DRI response document in the 2023 (and subsequent) *Increments of Progress* reports so that they can be read as stand-alone documents without reference to prior reports and responses.**

As an example, with respect to the following sentence at the bottom of page 1—"*A lower limit of wind speed is chosen that corresponds with the lowest speed where the relation between increasing wind speed and simultaneous increase in PM_{10} is observed at a monitoring station*" we recommend that some rationale be provided for why 3.5 ms^{-1} at 10 m above ground level for

---

[1] Standard procedure for SAG review of DRI reports is for Dr. Jack Gillies to recuse himself from the discussions due to a potential conflict of interest. Despite being a SAG member in good standing, Dr. Gillies did not participate in this review in any manner nor was DRI consulted about any aspect of this review.

CDF and Mesa2 is an appropriate value for the wind speed filter used to calculate TWPD. The following paragraph (with supporting diagram) could be copied directly from the DRI response document into a footnote or appendix (or into a restructured document) with only minor editorial changes:

Using the S1 tower wind and CDF PM10 hourly concentration data TWPD and TPM10 can be calculated for the lower wind speed limits of 3.5 m s^{-1}, 4.0 m s^{-1}, and 4.5 m s^{-1} (Fig. 1) for each month, April through September 2022. As Fig. 1 shows, the strength of the relation between Monthly Total PM10 and Monthly Total Wind Power Density is unchanged at R^2=0.99 for all three lower limit wind speeds. The change in the lower limit does change the slope and intercept. Comparing TPM10 and TWPD among different months or years requires that the lower limit wind speed that sets the low end of the range of summation of the hourly values remain consistent. The seasonal TPM10:TWPD (i.e., the summation of all [filtered] hours for the period April-September, 2022) value using the lower summation limits of 3.5 m s^{-1}, 4.0 m s^{-1}, and 4.5 m s^{-1} would be ,respectively, 0.161, 0.159, and 0.157. The values change slightly, hence it is important to maintain consistency for the low end value for comparison purposes to evaluate temporal change in the ratio.
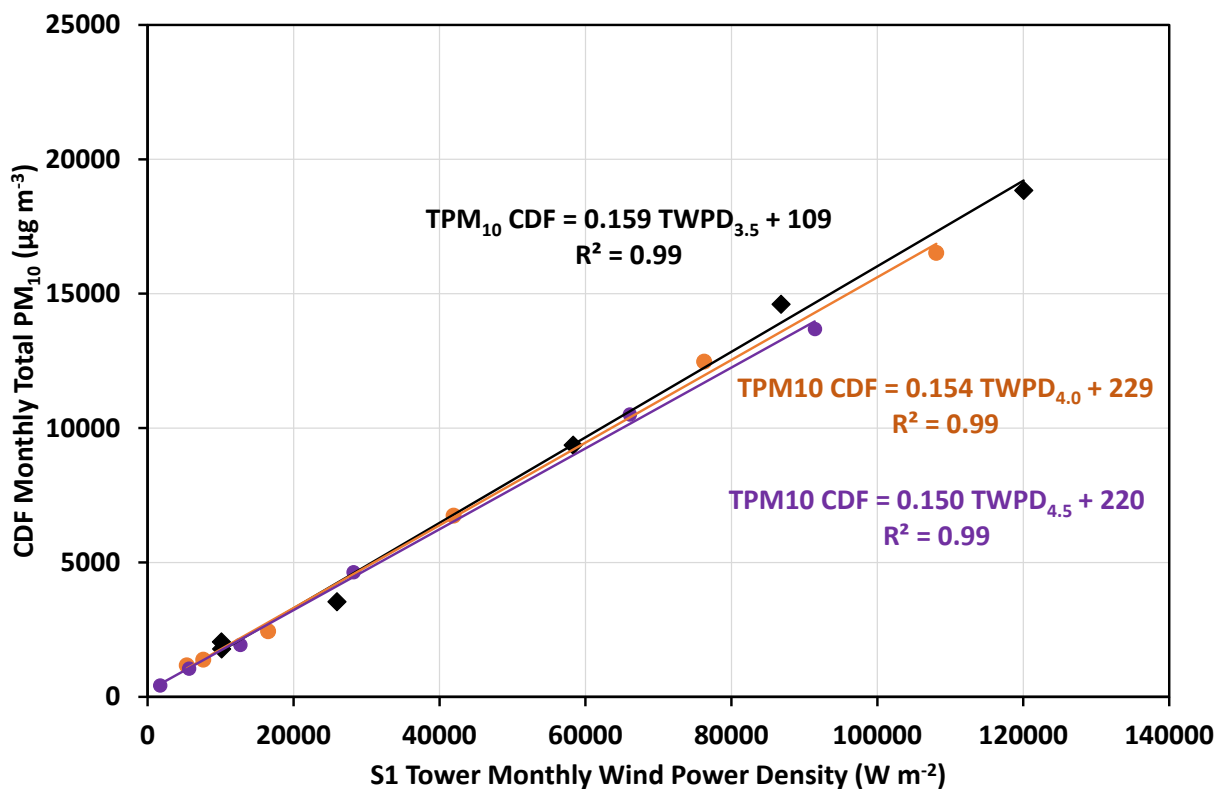

Figure 1. Relations between CDF Monthly Total PM10 and S1 Tower Monthly Total Wind Power Density (April to September, 2022) as affected by the lower limit wind speed for summation (black diamonds 3.5 m s^{-1}, orange circles 4.0 m s^{-1}, purple circles 4.5 m s^{-1}).

The key point to be made here is that it matters little to the overall interpretation of the data what the precise value of the cut-off value is for wind speed (as shown by the sensitivity analysis in Figure 1). But as noted by DRI, it is important to be consistent from year to year and use the same cut-off value for wind speed.

What should also be discussed is the physical reasoning for why 3.5 m s^{-1} is meaningful for the dust emission process. Specifically, a wind speed of 3.5 m s^{-1} measured at 10 m height at CDF is approximately equal to a wind speed of 8.5 m s^{-1} measured at 10 m height at the S1 tower, AND this is roughly when sustained saltation occurs in the ODSVRA (if we understand DRI's argument correctly). In this regard, Figure 2 and some of the language describing Figure 2 in the DRI response document could be inserted in the document to make this important point evident to the reader. As an aside, we note that the regression equation for Figure 2 (describing the relationship between CDF and S1 windspeeds) yields a CDF value of 4.1 m s^{-1} for a value of 8.5 m s^{-1} at S1. This seems to suggest that saltation at S1 may actually occur at a wind speed of about 8 m s^{-1} rather than 8.5 m s^{-1} (or alternatively, a cut off of 4.1 m s^{-1} at CDF might be more appropriate).

Additional Suggestions

The TPM$_{10}$/TWPD ratio has proven to be a robust metric by which to track the reduction in dust emissions per unit wind power (as a consequence of dust control projects since 2013). Yet, there remain outstanding questions that would benefit from a more in-depth analysis of existing data. For example, Figure 2 in the current report shows the relationship between TPM$_{10}$ and TWPD values represented on a monthly basis rather than a summation for the entire windy season (i.e., April through September). The linear fit is very good, as it was for previous reports in 2020 through 2022. However, the regression lines are different from year-to-year with different gains and offsets. Perhaps this is to be expected given that every year (and every month) can be more or less windy (and dusty). What is not clear is what the implications might be for tracking progress in dust reductions over the long term. How is one to interpret a monthly (or event based) value of the ratio relative to the annual (seasonal) value of the ratio? Could these monthly (or daily) values of the ratio provide some sense of scatter (uncertainty) in the annual values, and could they be plotted with the annual (seasonal) totals from year to year as a qualitative indication of expected variability in the ratio (in the form of box and whisker plots, perhaps)?

The data trends shown in Figures 3 and 5 suggest that without additional dust control acreage set aside for treatment in the future, the TPM$_{10}$/TWPD ratio may stabilize at a value of about 0.13 for both CDF and Mesa2. However, the regression parameters shown in Figure 2 suggest that the ratio for 2023 should be around 0.115 for CDF and 0.90 for Mesa 2. Is it possible to reconcile these differences as anything other than statistical uncertainty?

The report claims that the good correlation evident in Figure 2 (and previous versions from prior years) is an indication of 'causation.' The SAG recommends that the word 'causation' be deleted from this report, despite recognition that high wind speeds at S1 are responsible for saltation and dust emissions in the ODSVRA.

Editorial Issues

- Gillies et al., 2020, is not in the reference list.
- There are two entries for Gillies et al., 2022, which should be designated 'a' and 'b' to distinguish them.
- Figure 3 (CDF) caption states that the directional range was 270° to 325° whereas the last sentence in the prior paragraph indicates a directional range of 248° to 326° (which are the same values mentioned on page 1 where the constraints are listed). Please clarify or correct.
- Figure 5 (Mesa2) caption states that the directional range was 270° to 305° which is different from the range used for Figure 3 (CDF) and also differs from the constraint filter on page 1. Why are different directional filters applied to CDF and Mesa2, and why are they different from the constraint on page 1?
- On page 4 there is a sub-section heading entitled "Total PM_{10} and Total WPD May-September 2023, Mesa 2." The first sentence beneath (and elsewhere in the document) states that the period was April (not May) through September, which is similar to the sub-heading for CDF on page 2. Is there a typographical error or was the range different?

ODSVRA Dust Control Program Draft 2024 ARWP

ATTACHMENT 08

Updated SAG Recommendations for Establishing Emissivity Grids to be used in Modeling of Pre-Disturbance Conditions and Future Excess Emissions Reductions (SAG Memo)

THIS PAGE WAS INTENTIONALLY LEFT BLANK.

December 19, 2023

Memo: <u>Updated SAG Recommendations for Establishing Emissivity Grids to be used in Modeling of Pre-Disturbance Conditions and Future Excess Emissions Reductions</u>

From: Scientific Advisory Group (SAG)

To: Jon O'Brien, California Department of Parks and Recreation
Karl Tupper, San Luis Obispo Air Pollution Control District

Cc: Sarah Miggins, California Department of Parks and Recreation
Gary Willey, San Luis Obispo Air Pollution Control District

On June 21, 2023, the SAG forwarded a memo entitled "***SAG Recommendations for Establishing Emissivity Grids to be used in Modeling of Pre-Disturbance Conditions and Future Excess Emissions Reductions***" to the San Luis Obispo Air Pollution Control District (APCD) and to the California Department of Parks and Recreation (CDPR). In that memo, the SAG summarized their analysis of PI-SWERL (Portable In-Situ Wind ERosion Laboratory) data collected between 2013 and 2022 by personnel from the Desert Research Institute (DRI). Several recommendations were made about how to parameterize dust[1] emissions from the Oceano Dunes State Vehicular Recreation Area (ODSVRA) in a manner that addresses the requirements of the Stipulated Order of Abatement (SOA) as modified in 2022. Both APCD and CDPR reviewed the SAG proposal and provided extensive commentary and insightful suggestions on the contents of the document[2]. The SAG has considered all comments and suggestions carefully, and has made several changes to the original proposal. After extensive consultation with APCD and CDPR personnel recently, consensus has been reached regarding how best to parameterize emissivity grids for purposes of modeling the pre-disturbance[3] scenario as well as the 'current' landscape with dust mitigation treatments in place.

---

[1] "Dust" is used in this memorandum as a general term referring to PM_{10} without regard to speciation, consistent with California Air Quality Standards and Regulations. Materials sourced from terrestrial crustal non-biogenic origins (e.g., quartz, feldspar, mica, olivine, pyroxenes, amphiboles) will be referred to as "mineral dust."

[2] https://storage.googleapis.com/slocleanair-org/images/cms/upload/files/Revised%20Comments%20on%20SAG%20proposal%20on%20emissivity%20grids.pdf
https://storage.googleapis.com/slocleanair-org/images/cms/upload/files/DRI%20Comments_SAGAPCD_excess_emiss_memos_08-30-2023.pdf

[3] It is recognized that human activities, including vehicular traffic, horse riding, hiking, and camping, have been a part of the Oceano Dunes landscape for many decades, prior to establishment of ODSVRA in the 1970s. There is very limited photographic evidence of landscape configuration prior to the early 1900s when human recreational activities began to influence the natural landscape. The earliest historical aerial photography from the 1930s reflects some level of disturbance, and as such, the term 'pre-disturbance' state is somewhat of a misnomer. Nevertheless, for consistency with the language used in the SOA regarding modeling of a pre-disturbance scenario, we will continue to use the term 'pre-disturbance' (as well as 'naturally occurring' emissions'). As explained in the UCSB Vegetation Cover Analysis Report (February 2022), the 1939 imagery dataset is considered to be the best available indication of landscape configuration (i.e., vegetation cover, dune presence) prior to extensive Off-Highway Vehicle (OHV) activity within the Oceano Dunes.

In this memo, the SAG presents its findings and final recommendations for the proposed emissivity grid to be used in assessing compliance with the SOA. The bulk of the material included below repeats verbatim what was presented in the June 21, 2023 memo, but several changes have been made following suggestions from APCD and CDPR, backed up by additional data analysis. Rather than present only those findings and recommendations that were modified, SAG members felt it less confusing to deliver a comprehensive, updated document that does not require the reader to consult and cross-reference the June 21, 2023 memo. **The material presented below can be received as a stand-alone document** that prescribes the establishment of emissivity grids for purposes of modeling, as of December, 2023.

New PI-SWERL measurement campaigns will be undertaken in 2024 (and ideally beyond), and it is expected that these additional data will be integrated into the existing PI-SWERL data sets to produce updated and refined emissivity grids on an ongoing basis to meet the objectives of adaptive management. The mobile sand-dominated landscape of the ODSVRA is a dynamic one that is complex in its geologic history, contemporary geomorphology, evolving biogeography, varying meteorology and climatology, and sensitivity and responsiveness to human influences. Thus, there will always be a level of uncertainty about how effective management interventions have been (and will continue to be) in mitigating dust-related events that impact air quality in regional communities downwind of the ODSVRA. Consequently, **long-term monitoring is essential to improve our understanding of the key processes at work and, more importantly, to provide critical indicators of the relative success of dust-mitigation efforts.**

The SAG notes that the recommendations (below) for emissivity grids to be used in modeling scenarios for the pre-disturbance (1939) landscape and the 'current' (2024 and future) landscape for purposes of assessing compliance with the SOA are based on the best scientific information currently available. A balance has been struck between various constraints imposed by modeling complexity, operational/logistical requirements, and management practicality, and the SAG believes a pragmatic, optimal solution to a multi-objective problem has been achieved.

The new emissivity grids differ in substantive ways from prior approaches to quantifying dust emissions from the ODSVRA, and the revised grids have yet to be implemented in the emissions model developed and managed by the DRI. There is no way to anticipate in advance what the model results will show (i.e., compliance or non-compliance), and it should be understood that specific estimates of mass emissions (metric tons per year) from the pre-disturbance and 'current' landscape scenarios will differ from those predicted in the past (as summarized in the 2023 ARWP, for example). **Presuming that the specifics of the proposed emissivity grids, as presented below, are accepted by CDPR and APCD, the modeling results will then be used for purposes of assessing compliance within the terms of the SOA.** Prior model estimates of mass emissions will be superseded by these new model estimates, with the understanding that the earlier modeling results based on alternative emissivity grids were instrumental in guiding management decisions leading to dust-mitigation strategies and treatment implementation to date.

The SAG also recognizes that OSDRVA user groups and affected communities have polarized perspectives on how the ODSVRA should be managed and to whose primary benefit. There are legitimate concerns on all sides. In this regard, the SAG is sympathetic to all stakeholder

perspectives, but as per our SOA mandate, the SAG prioritizes scientific facts and understanding above all else. We continue to take an impartial, unbiased position on all matters before us, anticipating that our scientifically-based assessments and judgement will foster greater collaboration and help to inform all parties equally in reaching decisions about how to proceed into the future.

Respectfully,

The Scientific Advisory Group

Bernard Bauer (Chair), Carla Scheidlinger (Vice-Chair), Mike Bush, Jack Gillies, Jenny Hand, Leah Mathews, Ian Walker

OVERVIEW OF PI-SWERL MEASUREMENTS

The Portable In-Situ Wind ERosion Laboratory (PI-SWERL) and its field application at the Oceano Dunes State Vehicular Recreation Area (ODSVRA) has been described extensively in numerous publications (e.g., Mejia et al., 2019 and references therein). The Desert Research Institute (DRI) began collecting PI-SWERL data in 2011, but these early campaigns were primarily for reconnaissance purposes and to assist in the development of robust sampling protocols. Because of quality control concerns, these data will not be considered in this analysis. The first comprehensive PI-SWERL campaign directed at operational objectives was conducted in August, 2013, and the data derived from this (and subsequent) campaign(s) have been subject to strict Quality Assurance and Quality Control (QA/QC) assessments and have been used extensively in early evaluations of dust emissions from the ODSVRA. Since then, DRI personnel have conducted measurement campaigns for most years up to September, 2022 with additional measurements planned for Spring and Fall of 2024.

The majority of the PI-SWERL data are categorized as either Riding Area (RA) or Non-Riding Area (NRA), with some exceptions to be discussed later. **A total of 1516 distinct RA and NRA measurement locations have been sampled to date (Table 1). RA sampling has been prioritized over NRA sampling at a split of 984 to 532** because the riding area was identified early on as a more emissive area, and it became the focus of more intensive measurement to help guide strategic dust-mitigation efforts.

Table 1: Summary of PI-SWERL Measurements at ODSVRA

YEAR Month(s)	Riding Area	Non-Riding Area
2013_08/09	186	143
2014_09/10	45	35
2015_06/07	100	2
2015_10	165	6
2016_03	58	34
2019_05	337	124
2019_10	42	28
2022_05	51	27
2022_09	--	133
TOTAL	**984**	**532**

An additional 69 PI-SWERL measurements were taken in areas that are currently classified as 'Seasonally Exclosed', which means that riding is allowed during part of the year (October 1 through February 28) followed by a period of closure (March 1 through September 30) when riding is not allowed. These 69 measurements, taken in the vicinity of the Foredune Restoration Area (FRA), along the beach and in the riding corridors, will be treated separately at the end of this document.

A 293.3-acre area dedicated to nesting and rearing habitat for the Western Snowy Plover and the California Least Tern was permanently closed to Off-Highway Vehicle (OHV) traffic and other recreational uses in October, 2021, **but prior to that date this area was managed for seasonal exclosure.** Thus, at the time of the September, 2022 measurement campaign, the Plover Exclosure (PE), as it is referred to currently, had been closed effectively for 19 months (i.e., since March 1, 2021, given the seasonal riding restrictions). Although riding and camping were allowed from October 1, 2020 to February 28, 2021, winter storms and COVID concerns yielded extremely low visitation to the ODSVRA. Of the 133 NRA measurements taken in September, 2022 (see Table 1), 23 were taken in the footprint of the PE, with the remainder (110) taken in the FRA. However, **there were an additional 198 measurements within the footprint of the PE prior to closure, while this area was managed for seasonal riding** (2013 N=19; 2014 N=39; 2015 N=90, 2016 N=23; 2019 N=27). These 198 measurements are not included in Table 1, reflecting the fact that they are neither exclusively 'riding' nor 'non-riding.'

In total, there are 1783 (i.e., 1516 + 69 + 198) measurement locations available for development of emissivity grids, although 266 (69 + 198) of them require separate consideration because they were taken in areas that are managed for seasonal closure.

The footprint of the zones designated for riding and non-riding has evolved over time due to on-going management interventions directed at dust mitigation (summarized in the 2023 Annual Report and Work Plan as well as previous ARWPs). The majority of the land base has not changed designation, but significant acreage originally open for riding has transitioned to non-riding status, typically with sand fencing, fenced exclosures, and surface treatments (i.e., straw, surface texturing, scattered seeds, and planted vegetation). Thus, in every year since 2013 there were areas considered to be 'transitional' because they have not had sufficient opportunity to revert to naturalized conditions and may be displaying residual effects from OHV riding. As an example, the Foredune Restoration Area was fenced off in December, 2019 and, prior to that date, this zone was accessible to OHV traffic and camping activities. A total of 71 measurements were taken in this zone while it was designated as RA, and 110 measurements were taken in September, 2022, 33 months (~2.7 years) following closure and, subsequently, implementation of restoration treatments in February, 2020. The data from the FRA are included in the summary values presented in Table 1, but the FRA will be treated separately for purposes of modeling. The same situation applies to the Plover Exclosure (PE), which will also be treated separately in future modeling. As mentioned above, there is a relatively small area (34.6 acres) that is currently managed for both OHV access and Seasonal Exclosure during different times of the year, and since it is neither fully riding nor non-riding, as are other parts of the ODSVRA, it too needs to be assessed separately in the model domain.

Due to logistical challenges associated with changes in surface cover, dune movement, evolving restoration treatments, habitat protection, and inclement weather, the PI-SWERL measurements are not equally distributed over time or space. Rather, the sampling design from year-to-year addressed strategic operational needs (e.g., parameterizing the zones most likely to influence air quality or identifying priority areas for management interventions) rather than statistical requirements (e.g., quantifying uncertainty). Therefore, the sampling approach was neither (stratified) random nor regularly spaced. Repetitive sampling of the same sites is extraordinarily challenging given the dynamic terrain leading to access issues as well as location uncertainties

associated with hand-held global positioning system (GPS) units. Moreover, access to some areas is restricted during certain times of the year because of regulations regarding protected species (e.g., Snowy Plover, California Least Tern) and ecologically sensitive habitat. Nevertheless, the large number of measurements within the ODSVRA in both riding and non-riding areas ensures that statistical testing can be conducted with confidence. **When interpreting the results, it is important to appreciate that there may be sampling bias with respect to both time and space depending on how the data were clustered when assessing group differences or similarities.** The following two sections deal with the temporal and spatial elements of the PI-SWERL measurements independently.

TEMPORAL DIMENSIONS OF PI-SWERL SAMPLING

It is anticipated that there can be seasonal influences on dust emissions from the ODSVRA because of weather-related (i.e., moisture, temperature, windiness) differences between spring (wet) and fall (dry) conditions. Moisture is known to influence the potential for sediment transport on beaches and dunes, and moisture and temperature conditions greatly affect plant growth and health. In addition, the intensity of OHV traffic and camping use varies during the year. In an attempt to tease out some of these influences, the PI-SWERL measurement results from the Riding Area (RA) were disaggregated according to month/year of sampling, as represented in the box-and-whisker plots of Figure 1.

A Theil trend analysis (Wilcox, 2005) on these RA groupings resulted in no statistically significant trends (p<0.01) in emissivity over time for any of the percentiles shown in the panels in Figure 1 (see Appendix 1 for analysis results). Inordinately large dust emissions during the 2013 campaign were noted in prior documents (e.g., 2022 ARWP, Section 2.3.5.1; https://storage.googleapis.com/slocleanair-org/images/cms/upload/files/2ndDraft2022ARWP_2022914.pdf), and although not demonstrated conclusively, larger emissions could be attributed to the extended drought in California (2011-2017) with 2013 being a particularly dry year (https://weather.com/news/news/much-california-2013-was-driest-year-record-20140101). The 2013 campaign was conducted in late August, which is characteristically dry, as well as coinciding with an extended period of intense OHV use of the park. A preliminary analysis of precipitation data from the Oceano weather station (#795, operated by the San Luis Obispo County Department of Public Works) indicates that most other PI-SWERL measurement campaigns were conducted on days when there had not been any recorded precipitation for several weeks or longer prior to sampling, the only exception being the 2019 campaign conducted in May. The protocol established by the field crew was to wait at least 3 days after a moisture event (e.g., rain, fog) before resuming PI-SWERL measurements, and then only in the mid-day hours when the sand surface was dry due to solar radiation. Thus, the argument for larger emissivity during the 2013 measurement campaign because of exceptionally dry conditions is weakened by the fact that most other PI-SWERL measurements were taken during periods when the upper sand surface should have been dry even if the annual rain totals were greater than for 2013. It is noteworthy that inclusion of the 2013 data in the Theil trend analysis did not change the final result that there was no significant temporal trend overall.
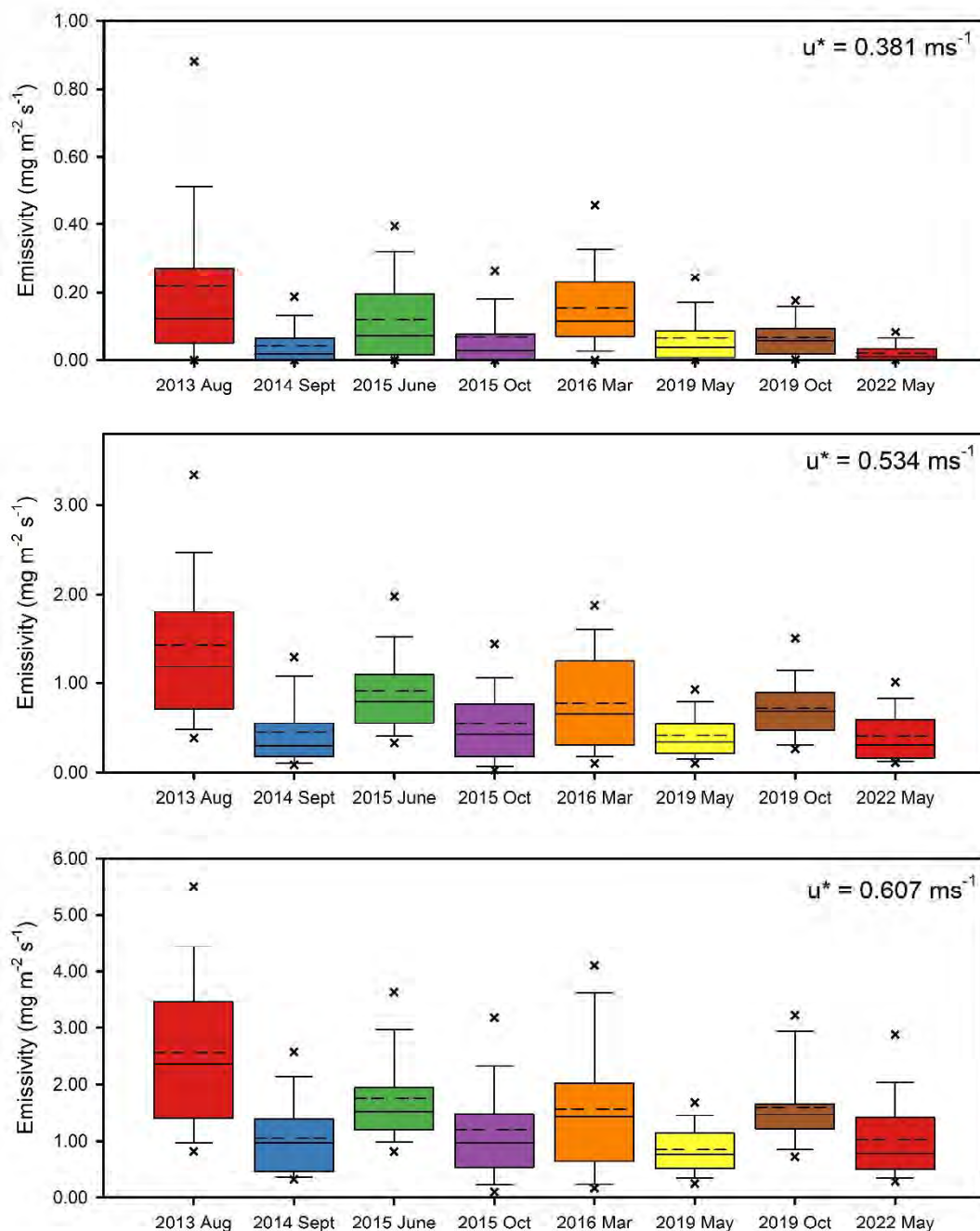
Figure 1: Box-and-whisker plots of PI-SWERL measurements made in the Riding Area (RA) for each field campaign from 2013 through 2022. The colored boxes define the range of the 25th and 75th percentiles; the whiskers correspond to the 10th and 90th percentiles; and the outer symbols (x) indicate the 5th and 95th percentiles. The median value is given by the horizontal solid line within the box, whereas the arithmetic mean (average value) is shown by the horizontal dashed line. The three panels correspond to the three RPM speeds used in the PI-SWERL device to characterize dust emissions at any single measurement location.

The clustered nature of the RA data used in Figure 1, according to measurement campaign, allows for a rigorous assessment of whether the 2013 measurements are indeed inordinate. Figure 2 shows summary results from an Analysis of Variance (ANOVA) on Ranks using Dunn's test, which is a nonparametric test that does not require equal sample sizes or assuming that all samples were drawn from normally-distributed (Gaussian) populations with equal variances. Invoking Dunn's test was necessary because none of the measurement campaigns yielded emissivity distributions that were normally distributed. The significance level for all ANOVA on Ranks tests in this report was $p < 0.01$. The results show that the August 2013 data ($n = 186$) are significantly different from most other years (indicated by red boxes), but there are two exceptions: June 2015 ($n = 100$) and October 2019 ($n = 42$), which are not statistically different from the August 2013 measurements. No precipitation was recorded for all of June, 2015, and the PI-SWERL measurements were conducted at the end of this dry period, on June 30 and July 1, 2015. Similarly, the 2019 measurements were conducted between October 8-10, following a dry period lasting approximately 6 months. In general, higher emissivity periods (August, 2013, June 2015, March 2016, and October 2019) are statistically similar to each other, but different from lower emissivity periods (September 2014, October 2015, May 2019, and May 2022). Unfortunately, the correlation to prior precipitation events is not a perfect explanator with some of the low emissivity campaigns coinciding with dry weather and vice versa.

Riding Area	Aug 2013	Sep 2014	Jun 2015	Oct 2015	Mar 2016	May 2019	Oct 2019	May 2022
Aug 2013	-							
Sept 2014	Y	-						
Jun 2015	N	Y	-					
Oct 2015	Y	N	Y	-				
Mar 2016	Y	N	N	N	-			
May 2019	Y	N	Y	Y	Y	-		
Oct 2019	N	Y	N	Y	N	Y	-	
May 2022	Y	N	Y	N	N	N	Y	-

Figure 2: Summary results from ANOVA on Ranks test to determine whether there are significant differences (P < 0.01) between measurement results from different campaigns for the Riding Area. Boxes in red with 'Y' indicate that there are significant differences between the two sets of data (column vs row) whereas boxes in green with 'N' indicate that the data sets are not statistically different. This analysis considers only the high RPM ($u_* = 0.61$ m s^{-1}) PI-SWERL data, but the other two sets of data (low and mid RPM) produced similar results.

Of additional interest for the purposes of this temporal analysis is the fact that there were two measurement campaigns in 2015 (June and October) and also in 2019 (May and October). The June 2015 campaign had greater overall emissivity than the October 2015 campaign, whereas the

opposite was true for the May 2019 and October 2019 campaigns. Thus, there is no clear seasonal signal that is consistent from year to year, with dust emissions depending on week-to-week variations in moisture conditions, which may override seasonal climatic signatures. As noted earlier, it is important to keep in mind that field campaigns in different years/seasons had different areal coverage, varying sample sizes, and did not regularly re-occupy the same locations, which makes a temporal analysis challenging. Developing a sampling framework that would allow a robust statistical analysis of ODSVRA emissivity data is a complex undertaking due to its size, temporal changes in emissivity on multiple scales, large number of potential influences (e.g., moisture, riding intensity, localized topographical variation, grain size distributions), the logistical difficulties of taking PI-SWERL measurements, and the expense of those campaigns.

Figure 3 shows box-and-whisker plots of the PI-SWERL measurement results from the Non-Riding Area (NRA) disaggregated according to year/month of sampling. As with the RA data, Theil regression demonstrated that there was no statistically significant temporal trend (Appendix 1). Relatively small emissivity values occurred in the two key areas—the Foredune Restoration Area (FRA) and the permanent Plover Exclosure (PE)--which were measured in September 2022 and clustered separately because of their 'transitional' nature. The March 2016 data (n = 34) had the largest mean and median emissivity values, which is somewhat surprising because the campaign was conducted on March 1-3 and there was significant rainfall on February 17th (0.27") and February 18th (0.24"). This suggests that a rain-free period lasting 2 weeks is sufficient to dry the sand surface and yield an emissive state. In contrast, the October 2019 data (n = 28) had the smallest mean and median emissivity (aside from the 2015 measurements with an n = 8 when the June and October data were aggregated, and ignoring the FRA and PE measurements). This is equally surprising because there was a rain-free period before the measurement campaign that lasted approximately 5 months, so the expectation would have been a much higher emissions potential. However, there is likely a spatial bias at play because most of these measurements were taken in the Oso Flaco area (where emissivity values tend to be lower than elsewhere, as discussed later). The May 2022 data for the Non-Riding Area (n = 27) show an increase in emissivity relative to the October 2019 low (n = 28), and they are also, on average, greater than the values from October 2015 (n = 8) and May 2019 (n = 124).

Figure 4 shows the results of the ANOVA on Ranks tests for the Non-Riding Area campaigns. The 2015 data set was excluded from this analysis because it comprised only 8 measurements in the Non-Riding Area. Many of the data sets from individual years are statistically different from each other. Of interest is that the August 2013 data set is different from most others with the exception of the two sampling campaigns in 2014 and 2016. The October 2019 campaign appears to be a 'swing' year, being statistically different from earlier campaigns but not different from later campaigns. Also, of note is that the May 2022 data set cannot be considered statistically different from most other years with the exception of August 2013 (much higher emissivity). Moreover, the May 2022 data for the NRA are also statistically different from both the Foredune Restoration Area and Plover Exclosure, both of which were measured later in the same year and have very low emissivity.
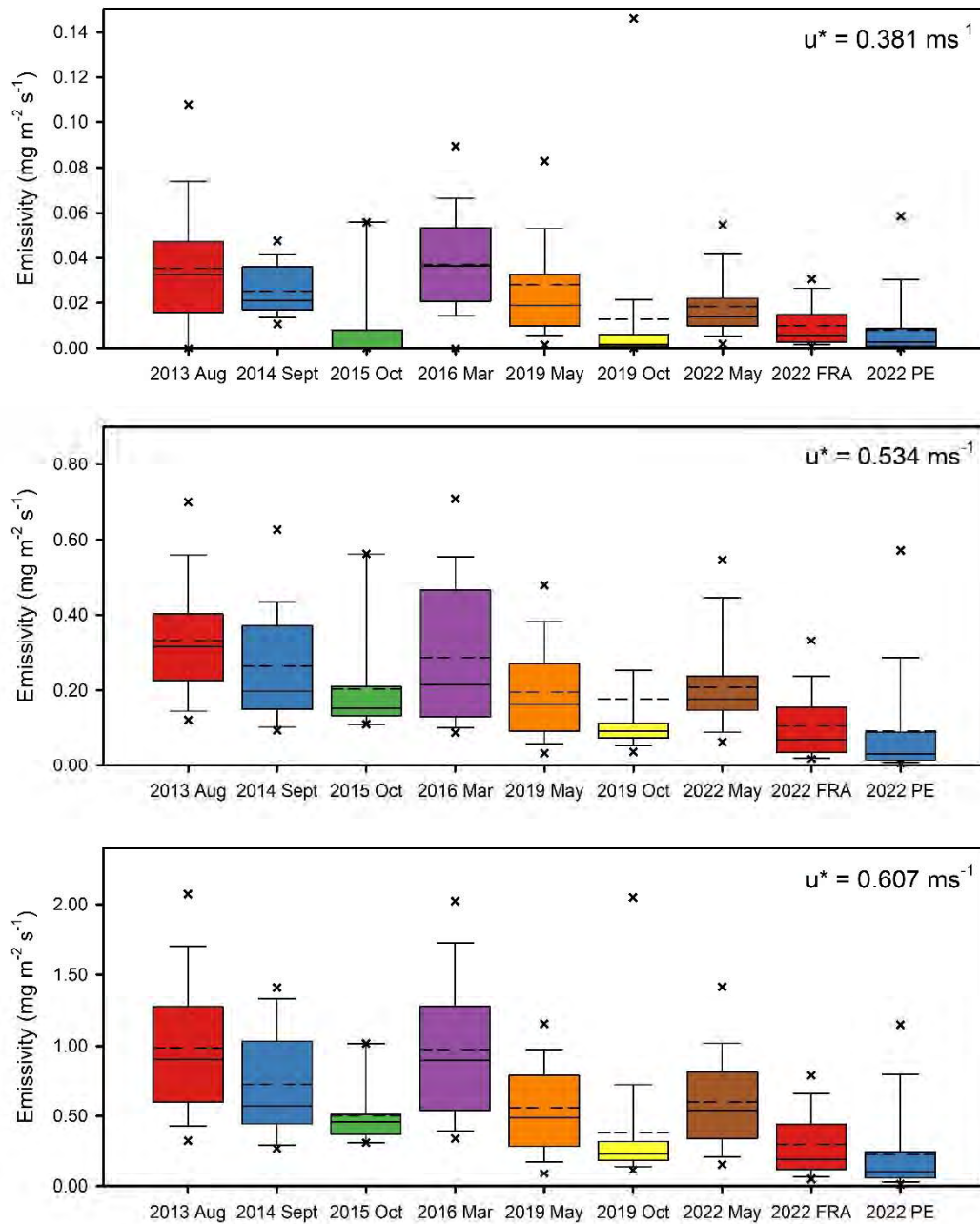
Figure 3: Box-and-whisker plots of PI-SWERL measurements made in the Non-Riding Area (NRA)from each field campaign from 2013 through 2022. The colored boxes define the range of the 25th and 75th percentiles; the whiskers correspond to the 10th and 90th percentiles; and the outer symbols (x) indicate the 5th and 95th percentiles. The median value is given by the horizontal solid line within the box, whereas the arithmetic mean (average value) is shown by the horizontal dashed line. The three panels correspond to the three RPM speeds used in the PI-SWERL device to characterize dust emissions at any single measurement location. "FRA" refers to Foredune Restoration Area; "PE" refers to Plover Exclosure.

Non-Riding Area	Aug 2013	Sep 2014	Mar 2016	May 2019	Oct 2019	May 2022	Sep 2022 FRA	Sep 2022 PE
Aug 2013	-							
Sept 2014	N	-						
Mar 2016	N	N	-					
May 2019	Y	N	Y	-				
Oct 2019	Y	y	Y	N	-			
May 2022	Y	N	N	N	N	-		
Sep 2022 FRA	Y	Y	Y	Y	N	Y	-	
Sep 2022 PE	Y	y	Y	y	N	Y	N	-

Figure 4: Summary results from ANOVA on Ranks test to determine whether there are significant differences between measurement results from different campaigns for the Non-Riding Area. Boxes in red with 'Y' indicate that there are significant differences between the two sets of data (column vs row) whereas boxes in green with 'N" indicate that the data sets are not statistically different. FRA means foredune restoration area; PE means permanent plover exclosure. This plot considers only the high RPM ($u_* = 0.61$ m s^{-1}) PI-SWERL data, but the other two sets of data (low and mid RPM) produced similar results.

This initial statistical assessment suggests that, despite notable temporal variability in the RA and NRA data, there are no statistically significant temporal trends in emissivity. Part of this outcome relates to the fact that moisture and temperature conditions are highly variable in coastal areas, yet the PI-SWERL sampling strategy does not, and logistically is unable to, control for this variability (e.g., Gillies et al., 2022). Surface moisture conditions can change hourly, daily, weekly, monthly, seasonally, and inter-annually, and it would require a significantly more intensive effort to account for sand surface moisture conditions in relation to precipitation, relative humidity, temperature, solar radiative flux, wind speed/direction, and beach groundwater changes. Moreover, there may be a co-dependency on the spatial distribution of measurements from year-to-year, which will be considered next.

SPATIAL DIMENSIONS OF PI-SWERL SAMPLING

The PI-SWERL data were imported into an open-source geographic information system (QGIS) to render a spatial view of the sampling locations. Figure 5 shows the measurement locations relative to the ODSVRA boundaries. Most areas have been sampled extensively although there are certain areas where the density of points is much greater than in others. The FRA, for

example, has a relatively large density of measurements, the majority of which (110 of 181 points) were collected in September 2022 after 33 months of closure to OHV access. The PE, in contrast, has relatively few points (n=23) post-closure given the large size of the area, and all these measurements were made in September 2022. There were an additional 198 measurements taken in the footprint of the PE area during the period when it was seasonally open for OHV riding (prior to 2021). The sampling strategy in the PE appears to have followed a longitudinal north-south transect along the middle of the preserve, with points in the north being slightly closer to the shore than points in the south where the exclosure is wider. Many of the other data points in the rest of the park follow west-east transects that run parallel with the prevailing (effective) wind direction out of the WNW.

The points in Figure 5 are color-coded to reflect the date of the measurement campaign (for RA and NRA measurements, the browns indicate older measurements taken in 2013-2015, neutral colors indicate mid-decade, and blue colors indicate recent measurements). Many points are not visible in this graphic either because the sampling was performed in tight spatial clusters or because multiple measurements in different years fall in approximately the same location (i.e., the symbols are stacked with only the most recent appearing on the map).

Figure 6 shows the same data but disaggregated according to year of the field campaign (measurements made between 2014 and 2016 are represented on one map because of the relatively small number of samples). Despite the multitude of measurements covering most of the area of the ODSVRA, it is evident that the sampling was performed unevenly, both temporally and spatially, as noted earlier. The two largest field campaigns were in 2013 (RA n=186; NRA n=143) and 2019 (RA n=379; NRA=152) with measurements spanning most of the park. The Dune Preserve to the north (also an NRA) was sampled intensely in 2013 covering most of the area and was revisited in 2019 to duplicate two of the transects. A similar sampling approach was taken to the south in the Oso Flaco NRA zone with intense sampling in 2013 and re-sampling of a west-east transect in 2019.

Measurements from 2014-2016 were focused on the central region, largely targeting the Riding Area upwind of the CDF and Mesa2 air quality monitoring stations—areas of strategic priority for dust mitigation. Measurements in 2022 also focused on the central region with focus on the FRA, PE, the SE areas, in addition to the RA. No PI-SWERL measurements were collected in 2017, 2018, and 2021. Although a set of measurements was taken in 2020, their purpose was to assess adjustments to surface emissivity during the SARS-CoV-2 pandemic closure period beginning in March, 2020 (see. Gillies et al., 2020, for detailed summary). The 2020 data are not included in this analysis (nor in Table 1) because most of the measurements were in the riding area during a period of non-riding activity. Thus, these measurements are strictly neither 'riding' nor 'non-riding' and therefore cannot be pooled accordingly, much like the measurements made in the seasonal exclosure areas, which need to be treated separately.
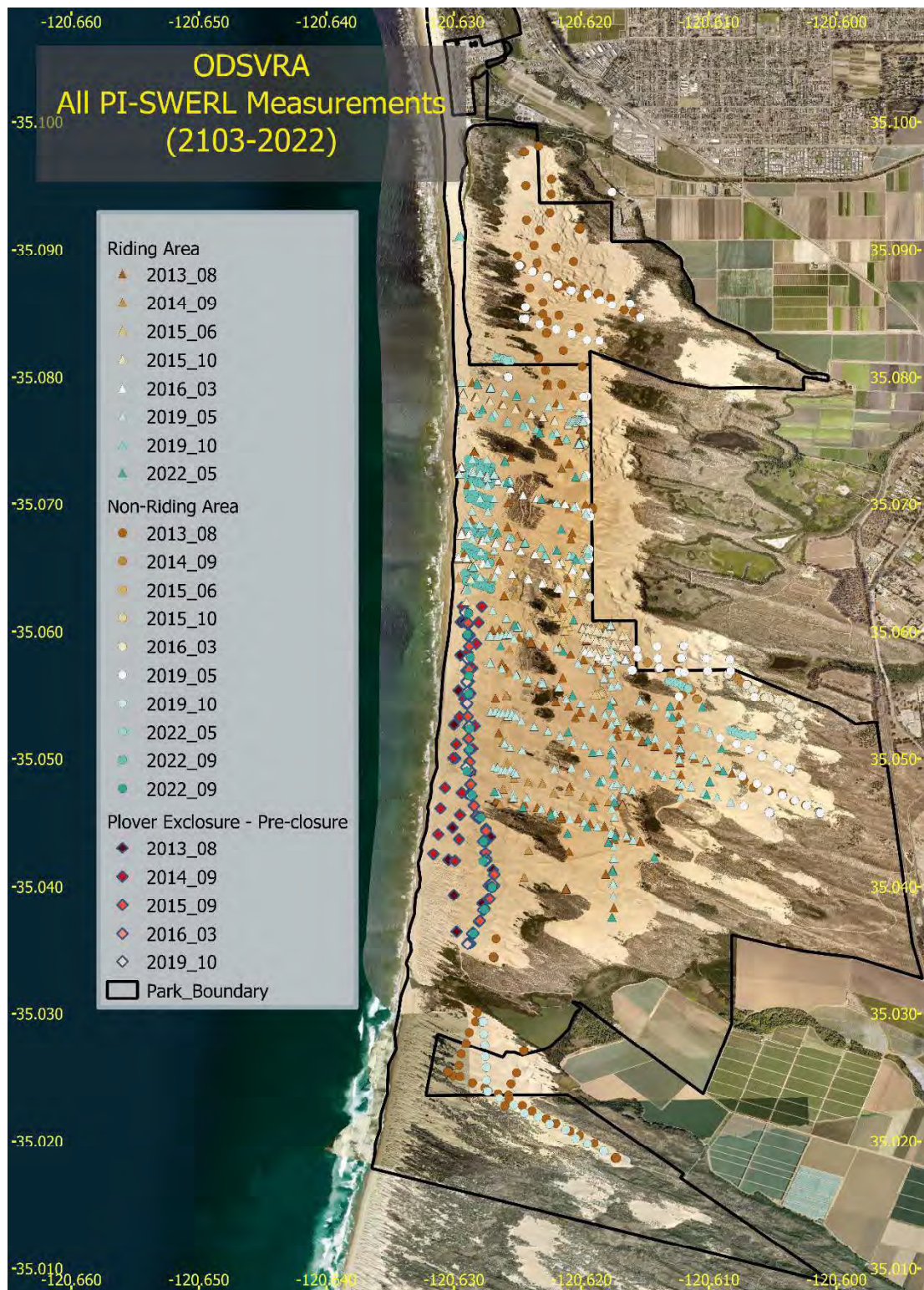
Figure 5: Location of all PI-SWERL measurements from 2013 to 2022. Triangles designate samples within the Riding Area (OHV accessible) and circles designate Non-Riding Area samples. Diamonds show samples in the Plover Exclosure area before permanent closure. Samples in the Seasonal Exclosure area around the FRA from 2022 are not shown.
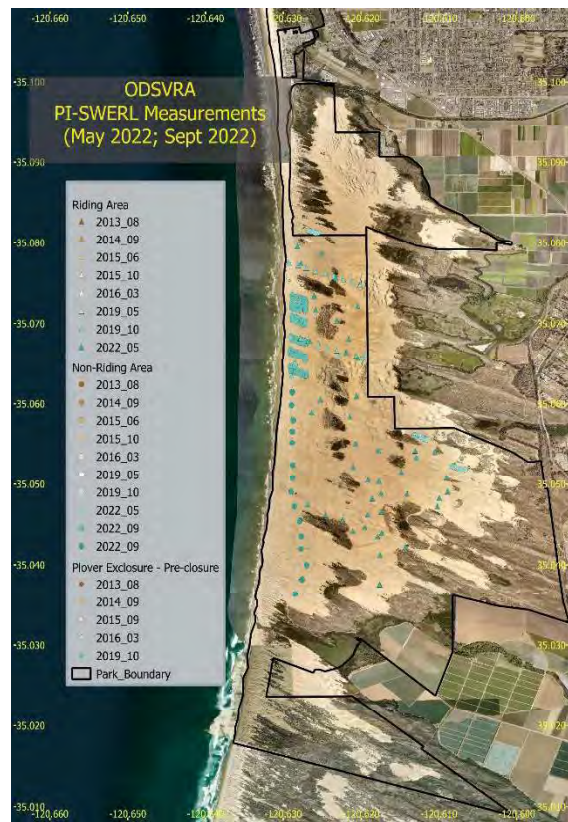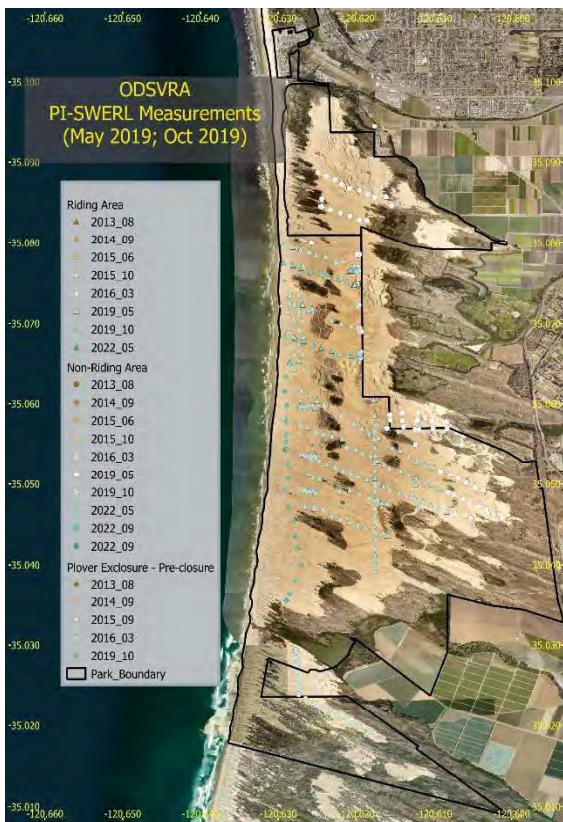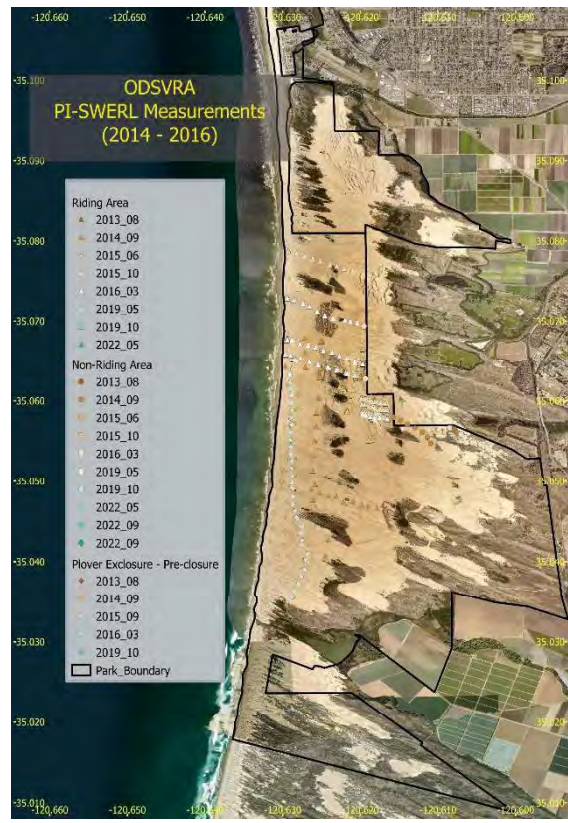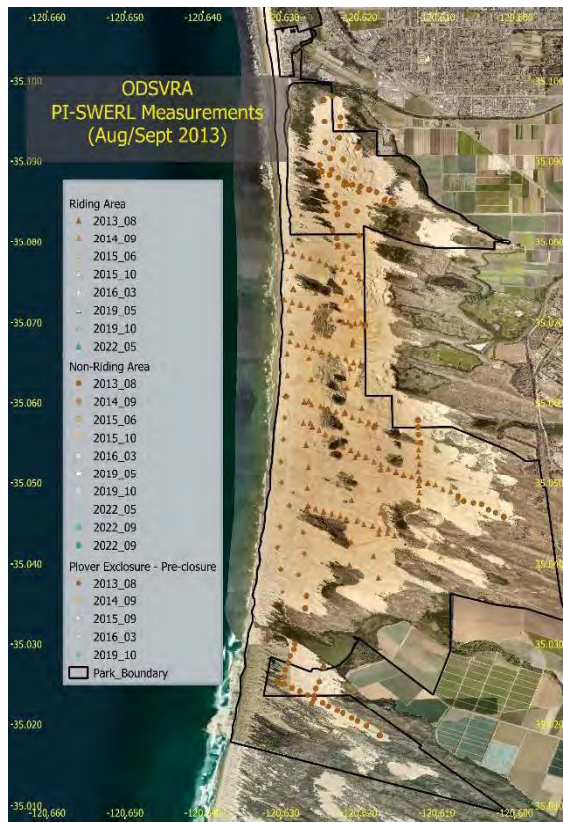
13

Figure 6: Location of PI-SWERL measurements during different field campaigns from 2013 to 2022. Triangles designate Riding Area; circles designate Non-Riding Area; diamonds designate samples in the Plover Exclosure prior to permanent closure.

As noted in the previous section, there were no discernable long-term trends in the PI-SWERL data that were statistically significant. A more in-depth assessment is hampered by the fact that the sampling design did not call for replication of measurement locations across multiple years (except for a few instances where certain transects were re-occupied in different years, e.g., 2013 and 2019). Therefore, there is an added spatial dimension to consider to the data distributions. It has been suggested, for example, that due to mean grain size increases from north to south (see Scientific Advisory Group Report, February 2023, ***Oceano Dunes: State of the Science***) there may be a corresponding decrease in dust emissions from north to south. This possibility was recognized in earlier modeling efforts by DRI, and this will now be considered for both the RA and NRA data below.

When examining the spatial distribution of the Non-Riding Area measurements, it becomes clear from Figures 5 and 6 that there are three distinct zones: (1) the Dune Preserve to the north (demarcated by N 35.0794º latitude as the southern boundary, which is marginally south of the park boundary); (2) a Southern Zone (referred to as Oso Flaco) falling immediately to the south of the Plover Exclosure; and (3) a large Central Zone that covers all the remaining area in between these lines of latitude. The PI-SWERL measurements were clustered into these three zones for statistical analysis, with the exception that the data from the Foredune Restoration Area, the Plover Exclosure, and Seasonal Exclosure Areas were kept aside and treated independently.

Figure 7 shows box-and-whisker plots for the North, Central, and South zones as well as the FRA and PE zones, retaining the year of collection as an additional variable. Visually, the emissivity values to the south are generally smaller than the north, despite considerable scatter. The data from 2013, for example, stand out as having comparatively large emissivity values relative to other years, especially in the North and South zones. In the Central zone, this difference is not quite as apparent because the data from 2016 (brown bar) have a very wide distribution despite a relatively small sample size (n=34). Approximately one third of these measurements were taken directly east of the fence that marks the riding area, whereas the remainder were taken just south of Black Lake (west of Callender) and far from the riding area. Once again, the measurements from 2015 (yellow bar) can be discounted because of small sample size (n=8).

For the purposes of testing whether there is indeed a north-south trend in emissivity, the data from each of the three zones were clustered (i.e., combining data from all years). The resulting box-and-whisker plots are shown in Figure 8. From this rendering, it becomes much clearer that **there is indeed a reduction in emissivity from north to south**. **In addition, the FRA and PE have low emissivity values in comparison to the Central and North zones**. The ANOVA on Ranks results (for the high RPM case) are shown in Figure 9, from which it is evident that the groupings are all statistically different with one exception--the FRA measurements cannot be considered to be statistically different from the PE measurements, but they are both different from the South, Central, and North zones.
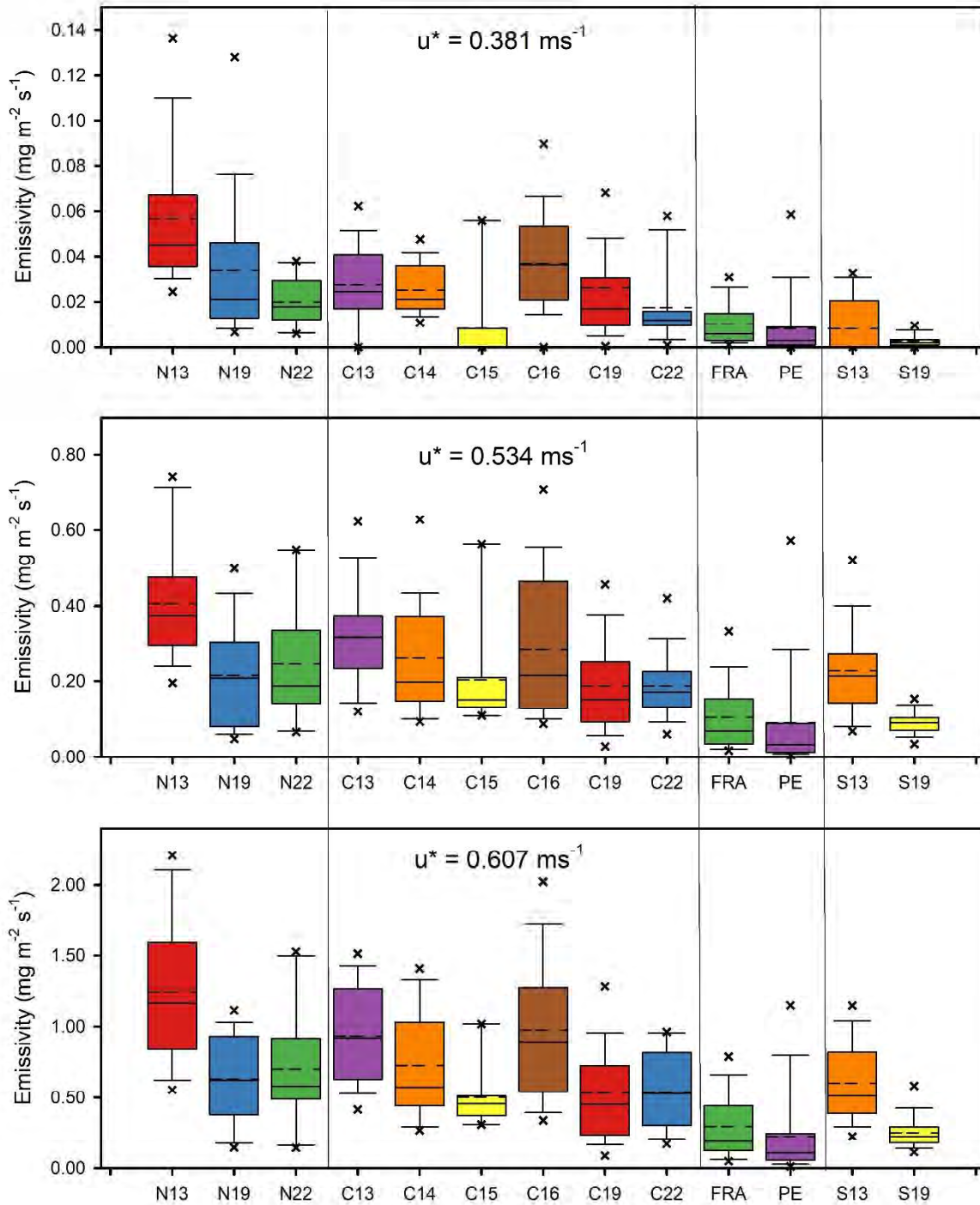
Figure 7: Box-and-whisker plots of PI-SWERL measurements made in the Non-Riding Area (NRA) from each field campaign from 2013 through 2022 disaggregated into North, Central, and South zones (delineated by vertical thin lines). Foredune Restoration Area (FRA) and Plover Exclosure (PE) are treated separately. See Figure 1 for explanation of symbols. The three panels correspond to the three RPM speeds used in the PI-SWERL device to characterize dust emissions at any single measurement location.
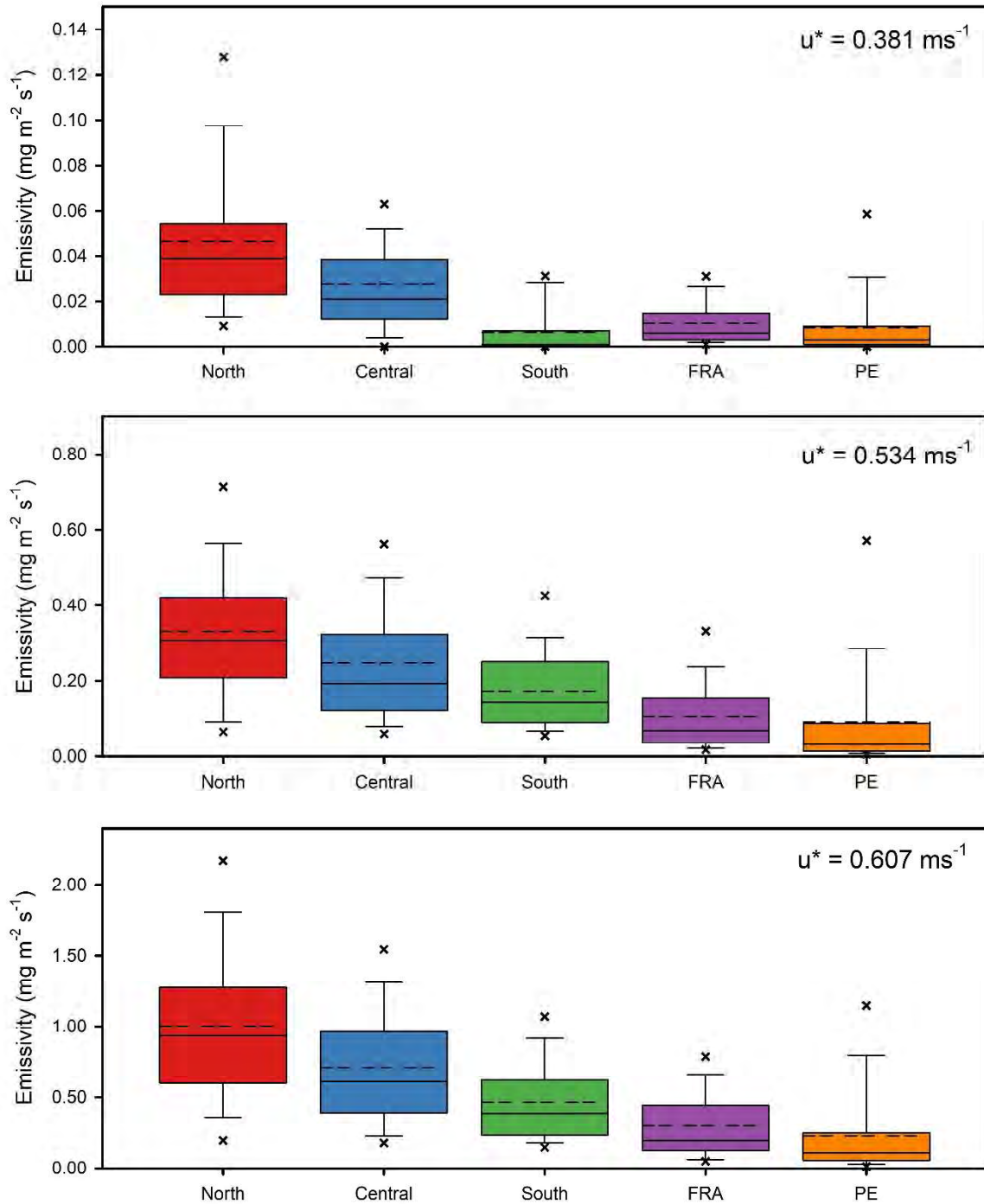
Figure 8: Box-and-whisker plots of PI-SWERL measurements made in the Non-Riding Area (NRA) aggregated into North, Central, and South zones. Foredune Restoration Area (FRA) and Plover Exclosure (PE) are treated separately. See Figure 1 for explanation of symbols. The three panels correspond to the three RPM speeds used in the PI-SWERL device to characterize dust emissions at any single measurement location.

17

Non-Riding Area	North	Central	South	FRA	PE
North	-				
Central	Y	-			
South	Y	Y	-		
FRA	Y	Y	Y	-	
PE	Y	y	y	N	-

Figure 9: Summary results from ANOVA on Ranks test to determine whether there are significant differences between measurement results for the Non-Riding Area clustered into zones in the north-south direction. Refer to Figures 7 and 8 for zones. Boxes in red with 'Y' indicate that there are significant differences between the two sets of data (column vs row) whereas boxes in green with 'N" indicate that the data sets are not statistically different. This plot considers only the high RPM ($u_* = 0.61$ m s^{-1}) PI-SWERL data, but the other two sets of data (low and mid RPM) produced similar results.

Although an analysis of potential west-east zonation was undertaken for the NRA data, the differences were not readily apparent as they were for the north-south trends. Moreover, there is considerable subjectivity with regard to placement of separation boundaries for data aggregation. Although it was anticipated that there might be a decrease in particle size from west (beach) to east (inland) due to selective transport by aeolian processes, the local variations in grain size due to topographic features (i.e., dune stoss, crest, lee), riding designations (e.g., RA, NRA, SE), vegetation patches, and treatment types lead to large variability in emissivity over distances of only tens of meters. The results of a cursory analysis of emissivity data along west-east transects appears in Appendix II, where it is demonstrated that the spatial variation in emissivity across small distances is large relative to any discernable west-east trends. As a consequence, this line of inquiry was not pursued further, and a decision was reached not to invoke west-east zonation for the NRA data.

The Riding Area data shown in Figures 5 and 6 (triangles) were all located within the Central zone because there are no North and South equivalents to the NRA data. There were no obvious break-points in the data distributions to create zones for the RA, in contrast to what was the case for the NRA, which had obvious North (Dune Preserve) and South (Oso Flaco) zones that were distinct from the Central zone. **The RA data were plotted according to latitude (Figure 10) to determine whether there was visual evidence to justify a separation. There is an apparent decrease in emissivity toward the south, which is gradual but progressive.** The resulting small R^2 values for the linear regressions through the data suggest that latitude is a weak explanatory variable given how much scatter there is at any single line of latitude. However, the scatter is skewed to much larger emissivity values in the north where the OHV use is more

intense and spatially constrained to 'corridors' than in the south. Visually, there appears to be a break in the data at about N 35.062°, which aligns roughly with the northern boundary of the PE and follows a parallel trajectory inland. The sub-region to the north of this line had characteristically larger emissivity values and large scatter than the sub-region to the south of this line of separation.
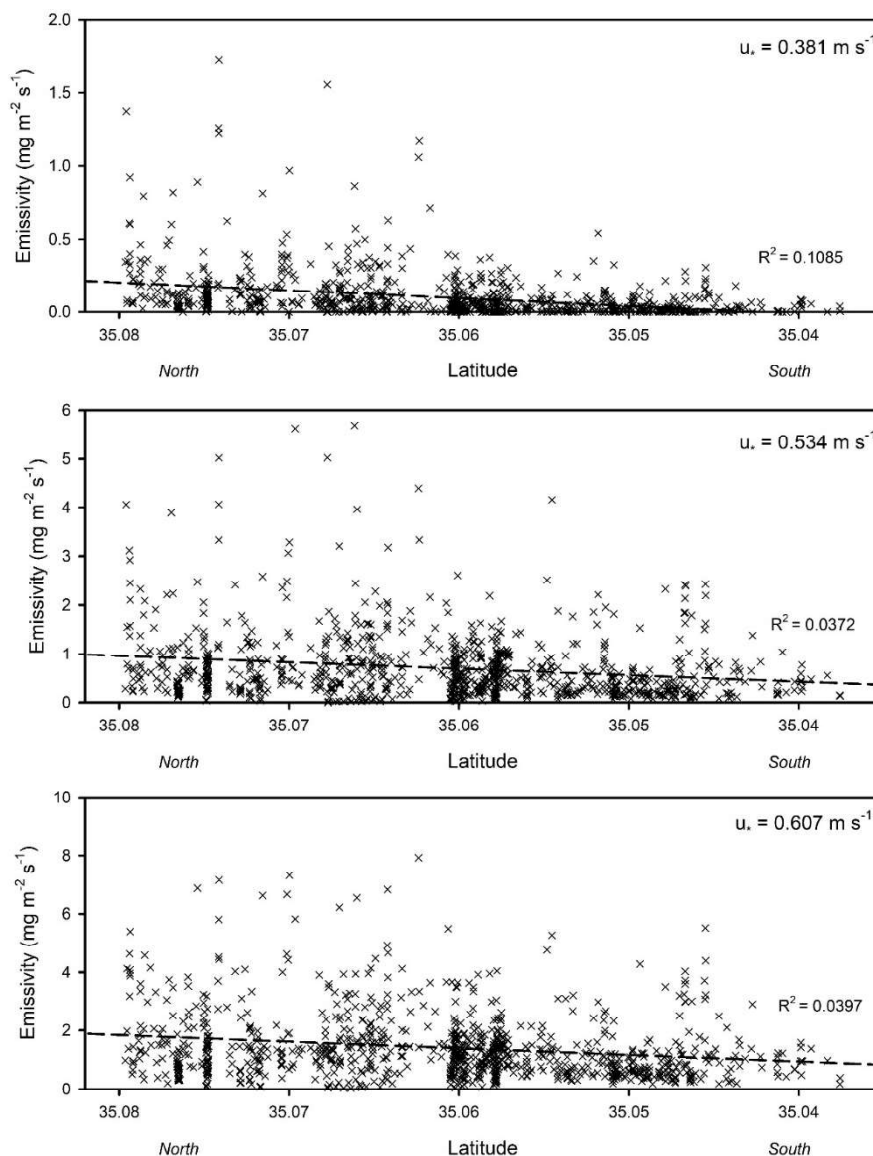
Figure 10: North-South trend in emissivity for Riding Area PI-SWERL data from 2013-2022. Dashed line is the best-fit linear regression line with R^2 values shown in each panel.

Following on the somewhat arbitrary visual cues from Figure 10, the PI-SWERL RA data were pooled into two sub-regions (Central-North and Central-South) for additional analysis. Figure 11 provides the box-and-whisker plots that graphically portray the data distributions in each zone. Although the Central-South sub-region has smaller emissivity values, there is considerable

overlap in the distributions. The Mann-Whitney Rank Sum Test was performed on the three sets of PI-SWERL data corresponding to the Lo-, Mid-, and Hi-RPM measurements to determine whether the data from the Central-North sub-region were statistically different from the Central-South sub-region. The results are provided in Table 2, and the very small p values indicate that the null hypothesis (no difference in samples) is to be rejected in each case. Thus, there is a significant difference between the paired sub-regions. An analysis of west-east trends proved less revealing, as was the case for the NRA data.
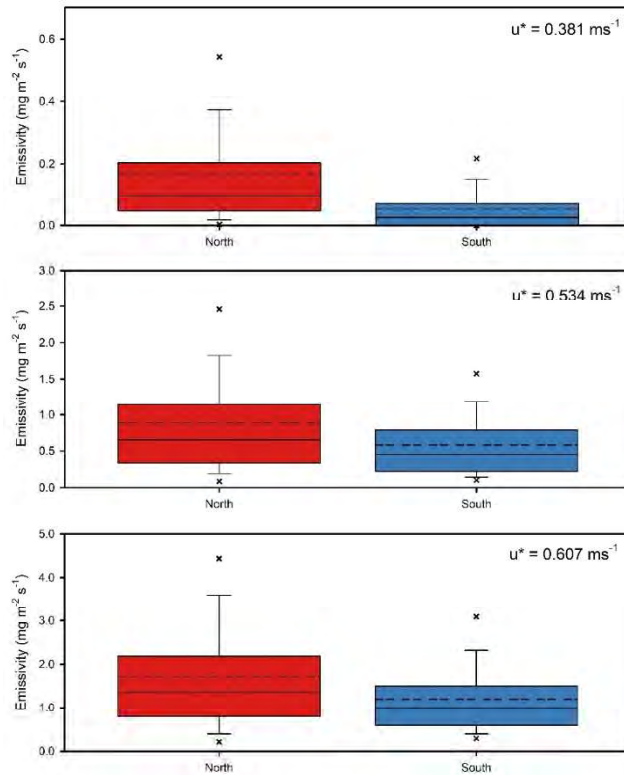
Figure 11: Box-and-whisker plots of PI-SWERL measurements made in the Riding Area (NA) aggregated into Central-North and Central-South sub-regions See Figure 1 for explanation of symbols. The three panels correspond to the three RPM speeds used in the PI-SWERL device to characterize dust emissions at any single measurement location.

Table 2: Results from Mann-Whitney Rank Sum Tests on PI-SWERL data from the Central-North (CN) and Central-South (CS) sub-regions of the Riding Area (2013-2022).

u_* (m s^{-1})	Median Emissivity (mg m^{-2} s^{-1})		U statistic	T value	p
	CN (n = 415)	CS (n = 569)			
0.381	0.098	0.026	56,062	264,422	< 0.001
0.534	0.655	0.454	89,606	229,900	< 0.001
0.607	1.360	0.996	88,582	224,646	< 0.001

Spatial Sub-Division (Zones and Sub-Regions)

The above analysis of the PI-SWERL data collected between 2013 and 2022 suggests that the **Riding Area can be subdivided in two sub-regions (Central-North and Central-South) while the Non-Riding Area can be subdivided into three zones (North, Central, and South).** Figure 12 shows these five primary areas as well as three additional areas designated as: (i) Foredune Restoration Area; (ii) Plover Exclosure; and (iii) Seasonal Exclosure (SE). The FRA and PE are now managed as non-riding areas whereas the SE precludes OHV access between March 1 and September 30 due to sensitive habitat restrictions. OHV riding is allowed in the SE area between October 1 and the end of February. Vegetated areas and transitional management zones are treated separately by overlaying cover masks on the GIS model (see later). Each of the three zones, two sub-regions, and three other areas are to be allocated different emissivity characteristics for purposes of future dust emissions modeling.

Figure 12: Proposed zonation for disaggregating the PI-SWERL measurements (2013-2022) into three zones for the Non-Riding Area (NRA North, NRA Central, NRA South, separated by purple and blue dashed lines) and two sub-regions for the Riding Area (RA Central-North, RA Central-South separated by orange dashed line). Also shown are the boundaries of the Foredune Restoration Area (FRA), the Plover Exclosure (PE), and the Seasonal Exclosure (SE) areas. The current extent of the Riding Area is mapped in a light tan color. See also Figure 17.

The following recommendations are made with regard to the zonation of the ODSVRA, based on the PI-SWERL analysis presented above:

Riding Area. The RA Central-North and RA Central-South sub-regions should be delineated **by a separation line that parallels the northern fenced boundary of the Plover Exclosure from the beach extending inland, and then following N 35.062º latitude past the eastern park boundary** (Figure 13) to the end of the modeling domain. The northern and southern boundaries of the Riding Area are the same as the boundaries for the Non-Riding Areas, as described below.
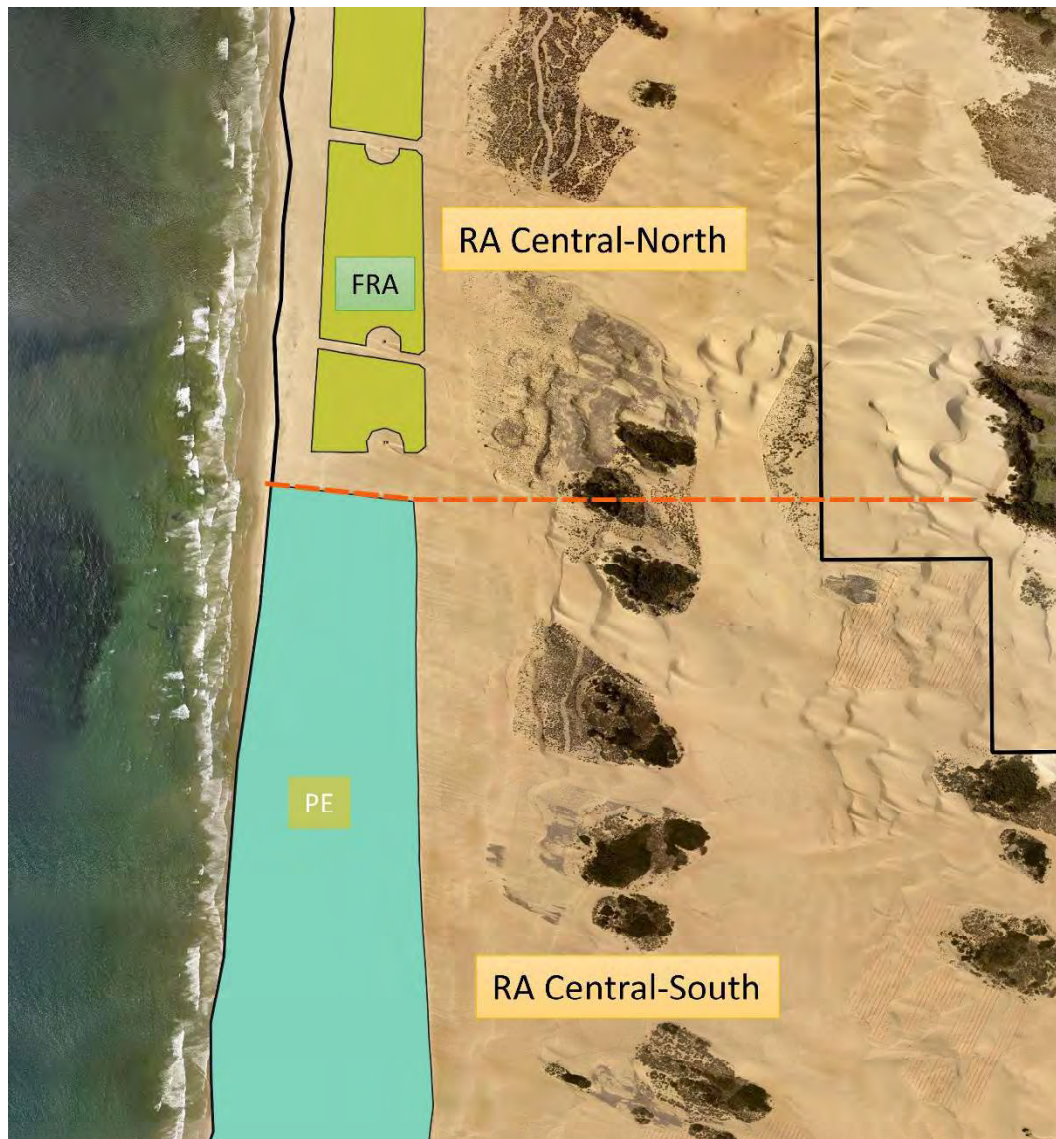

Figure 13: Proposed boundary line (orange dashed line) between the Central-North and Central-South sub-regions of the Riding Area. Refer to Figure 12 for general location. As reference points, the FRA is shown in pale green and PE is shown in teal blue.

Non-Riding Area. Three zones were identified (North, Central, South) from the statistical analysis. Figure 12 shows an overview of the recommended boundaries for these zones. A close-up of the boundary between the NRA North and NRA Central zones is shown in Figure 14, and this line also serves as the northern boundary for the Riding Area. The boundary is delineated by a fence line that trends west-east in zig-zag fashion, which then follows along the northern boundary of a sand-fencing area (converted to vegetation), and then trends eastward along N 35.0794° latitude to the eastern boundary of the ODSVRA. On the western side, the boundary follows the park fence line heading north to the mouth of Arroyo Grande Creek. There is a triangular section north of N 35.0794° latitude but south of the park boundary that is not in the ODSVRA (privately held), but for purposes of emission-dispersion modeling this sliver could be characterized by the same emissivity power relation as that for the NRA North. The open sand areas to the east of the park boundary adjacent to the NRA Central could be characterized by the emissivity power relation developed for the NRA Central zone, but this will need to be discussed in detail in the future.
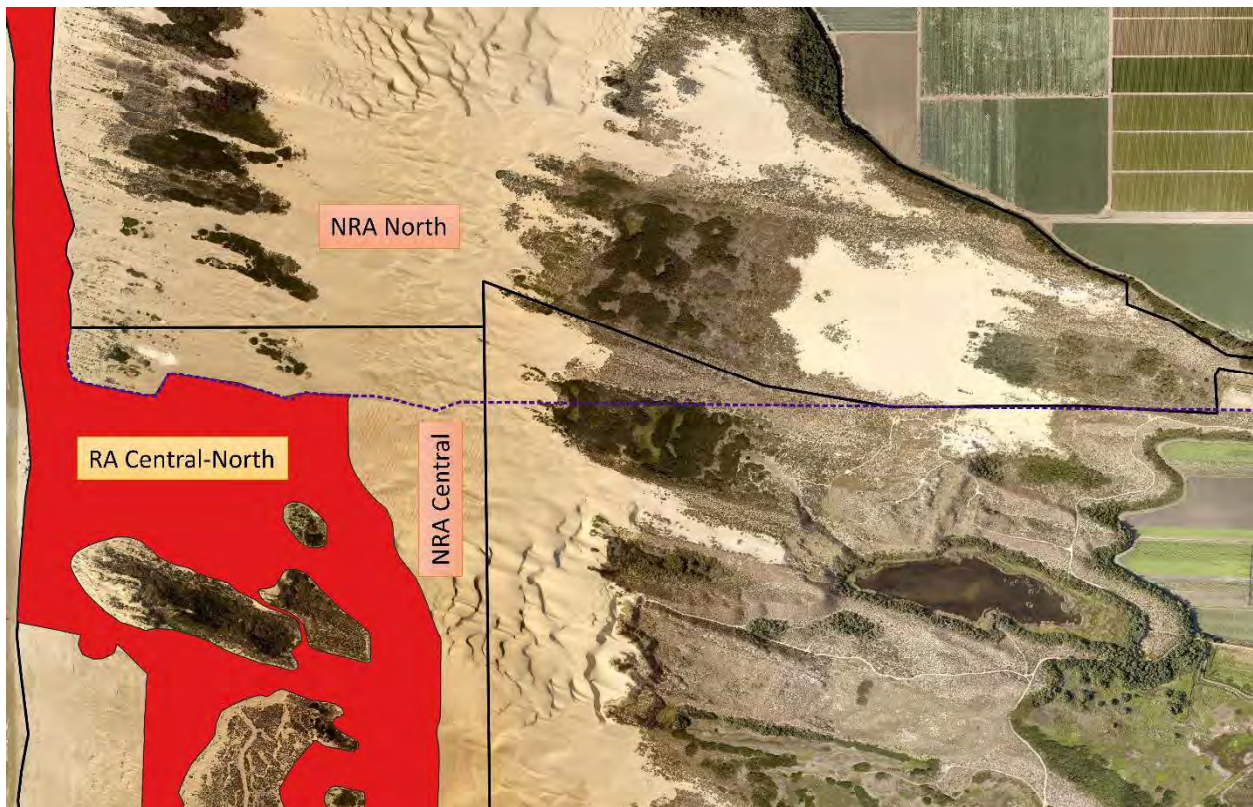
Figure 14: Proposed boundary line (purple dashed line) between the NRA North (Dune Preserve) and NRA Central zones, which also delineates the northern boundary of the Riding Area (shown in red). Refer to Figure 12 for general location.

A close-up of the southern boundary of the NRA Central zone where it borders the NRA South is shown in Figure 15. This boundary begins on the beach and follows the fence line along the southern margin of the Plover Exclosure. It then transitions to the fence line delineating the southern margin of the Riding Area (RA Central-South), and from the most southerly point of the Riding Area takes a straight line to the nearest corner of the ODSVRA boundary and continues east along the park boundary alongside private agricultural fields.

Figure 15: Proposed boundary line (dashed blue line) between NRA Central and NRA South (Oso Flaco) zones, which also delineates the southern boundary of the Riding Area (salmon red). Refer to Figure 12 for general location. Southern portion of the PE (teal) is shown for reference.

A close-up of the FRA, the northern portion of the PE, and the Seasonal Exclosure (SE) area is presented in Figure 16. Also shown are some of the vegetation islands as well as the boundary between the RA Central-North and RA Central-South. All zones are defined by GIS shapefiles managed by CDPR (T. Carmona, personal communication), and each of them will be assigned a separate emissivity relation (as described later).
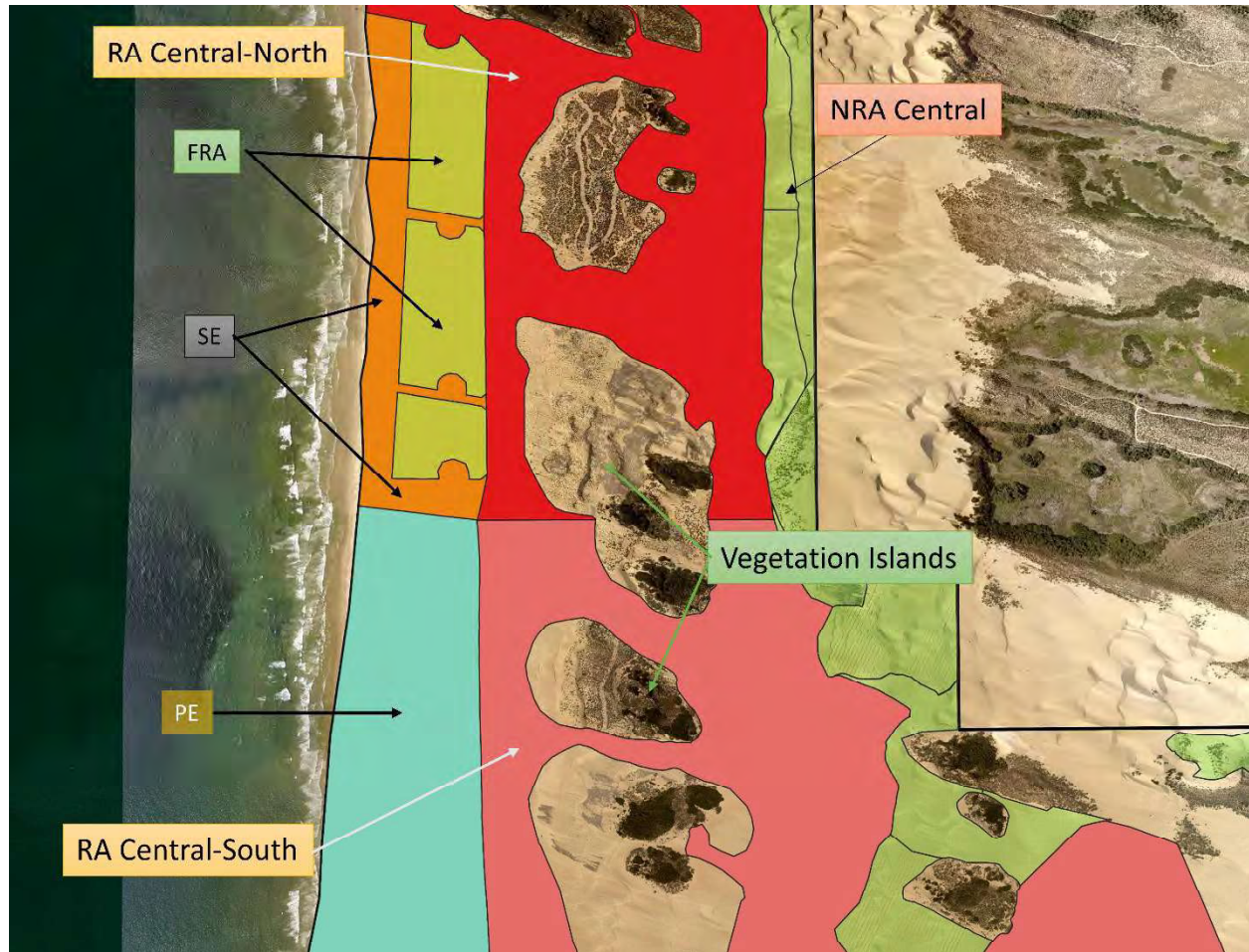
Figure 16: Outlines of the Foredune Restoration Area (FRA; pale green), Plover Exclosure (PE; teal), and the Seasonal Exclosure (SE: orange) areas. Portions of the Riding Area (Central-North in bright red; Central-South in salmon red) are also shown. Vegetation Islands are outlined but not colored. The Central zone of the Non-Riding Area borders the western boundary of the park, and it is shaded in transparent green because most of this area was recently converted from open sand to vegetation. Refer to Figure 12 for general location.

The excess emissions framework proposed by SAG (**SAG Memo – Framework for Assessing "Excess Emissions" of PM$_{10}$ from the Oceano Dunes**, January 30, 2023) identifies the need to develop emissions grids for various modeling scenarios. This requires development of emissivity relations for each of the zones and sub-regions identified above, based on PI-SWERL measurement that are clustered or pooled accordingly.

For Current (2024) Conditions, it is recommended that the ODSVRA area be subdivided into eight polygons (Figure 17) and a series of vegetation polygons (i.e., treated areas), as follows:
1. Riding Area Central-North Sub-Region
2. Riding Area Central-South Sub-Region
3. Non-Riding Area North Zone
4. Non-Riding Area Central Zone
5. Non-Riding Area South Zone
6. Foredune Restoration Area (FRA)
7. Plover Exclosure (PE)
8. Seasonal Exclosures (SE)
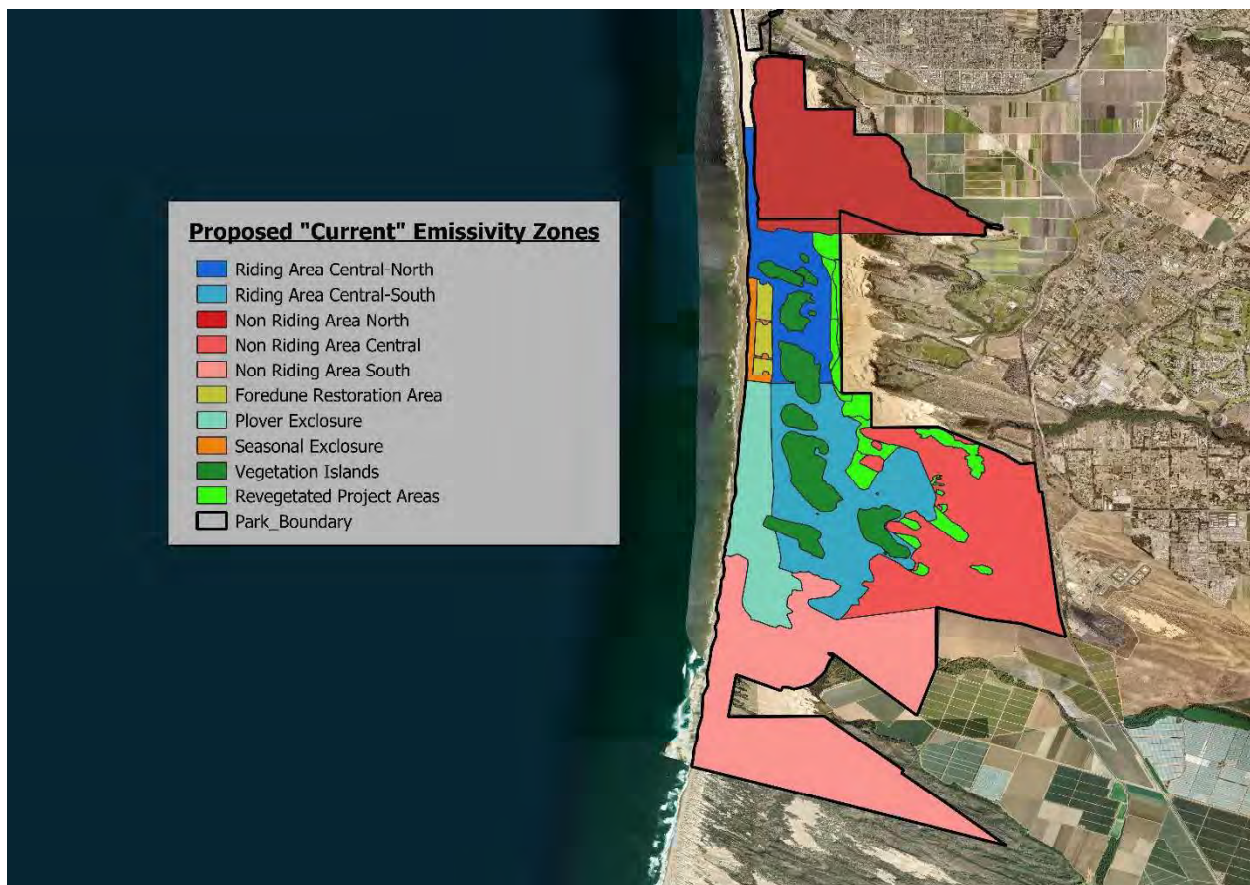9. Vegetation Islands (VI) and Revegetated Project Areas (RPA).

Figure 17: Proposed emissivity polygons for modeling the 'Current' landscape conditions (2024 and future). Emissivity power relations are developed for each of these zones. Vegetation masks (with zero emissivity) are to be superimposed on this zonation.

For the Pre-Disturbance (1939) scenario, it is recommended that the ODSVRA be subdivided into three large NRA zones (North, Central, and South), as delineated by the boundaries shown in Figure 14 (between North and Central) and Figure 15 (between Central and South). Each of the three zones (Figure 18) will have a different emissions relation. The North zone is essentially the same as the Dune Preserve, which has not had OHV access for a long time. Similarly, the South zone encompasses the Oso Flaco area for which there has been no recent riding allowed. The Central zone, which currently has a mix of zones and riding access, will be classified in its entirety as non-riding for the pre-disturbance scenario, and only non-riding data from NRA Central will be used to characterize the emissivity relation. The 1939 vegetation cover mask developed by UCSB should be applied to this modeling scenario, yielding four distinct modeling zones (North, Central, South, Vegetation) all of which have non-riding characteristics.
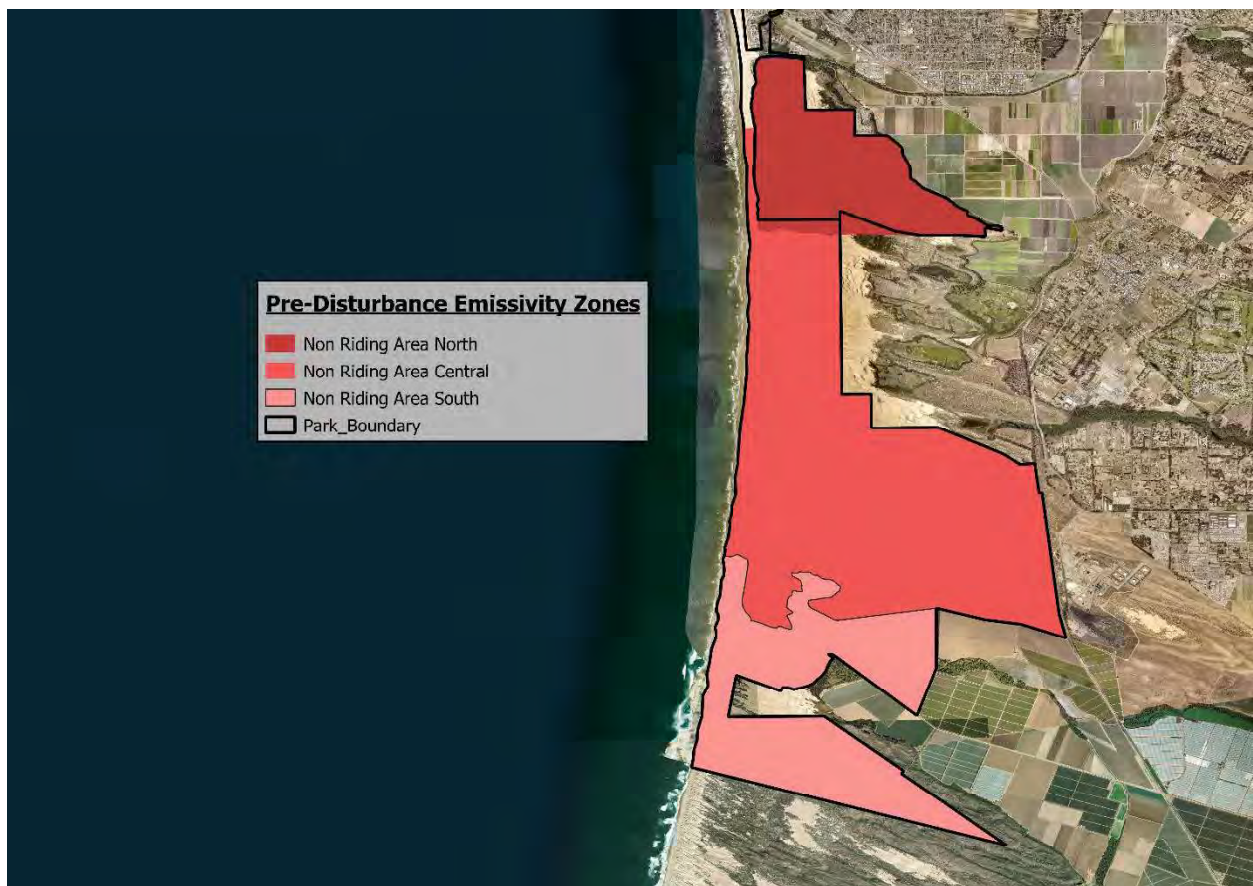

Figure 18: Emissivity zone polygons proposed for modeling the Pre-Disturbance (1939) scenarios. Note that there are three large zones (i.e., three shades of red) with the Central zone comprising multiple sub-zones that are different in the 'Current' landscape scenario shown in Figure 17. Vegetation cover mask from 1939 to be superimposed.

Emissivity Curves

General Considerations

For each of the proposed zones and sub-regions identified above, emissivity relations will need to be assigned for purposes of modeling. These relations take the form of a power function:

$$F = a\, u_*{}^b$$

where F is the emissive flux (mg m^{-2} s^{-1}), u_* is shear velocity (m s^{-1}), a and b are coefficients from regression analysis of the PI-SWERL results for the three rotational speeds (Etyemezian et al., 2007). Such emissivity relations are deemed to be representative of the entire zone or sub-region, regardless of intra-area variations in surface characteristics (e.g., texture, mineralogy, slope, aspect, moisture content, degree of disturbance). Accounting for all such micro-scale controls is logistically impractical. Fortunately, there are a very large number of PI-SWERL measurements across the entire park area, making a statistical approach viable.

In past modeling efforts, emissivity grids were developed for both the 2013 and then the 2019 PI-SWERL measurement campaigns using a spatial interpolation algorithm superimposed on a 20 m by 20 m grid for the entire modeling domain covering the ODSVRA and bordering areas. Each grid cell was given a different emissivity relation based on the spatially interpolated emissivity surface derived from the PI-SWERL measurements at unevenly distributed point locations. **The proposal for moving forward is to define emissivity relations for each of the zones and sub-regions rather than for the 20 m by 20 m interpolated grids used earlier.** Since each of the zones and sub-regions includes multiple measurements, a statistical approach implies using some measure of central tendency (e.g., mean, mode, median) to quantify a representative emissivity value for each of the RPM speeds (shear velocities) of the PI-SWERL measurements.

Figure 19 shows two characteristic data distributions based on all the measurements (2013-2022) in the RA Central-North and RA Central-South Sub-Regions. It is apparent that the data distributions are heavily skewed, with a large number of measurements falling at the low end of the emissivity range and a handful of measurements at the extreme high end of the emissivity range. Tests for normality consistently yielded negative results, and as a consequence, standardized parameters used to describe Gaussian distributions (e.g., mean, standard deviation) are not strictly applicable.

Although non-parametric statistics typically have reduced explanatory power, **it is recommended that future emissivity relations be based on the median** rather than the mean. The median is defined as the 'middle' value of the distribution, which is arguably more representative of the typical emissivity because it is not influenced by a few extreme values to the same extent as is the mean. Figure 19 indicates that for the PI-SWERL data, the median is marginally smaller than the mean, although in some cases the mean can be considerably larger when skewed by a few measurements with extremely large emissivity values. This difference between using the median rather than the mean will yield updated values for modeled emissions and PM$_{10}$ concentrations at specific measurement sites, but when applied to both the pre-

disturbance and present conditions uniformly, this approach will facilitate a direct comparison of emissions for purposes of assessing the effectiveness of dust control measures.
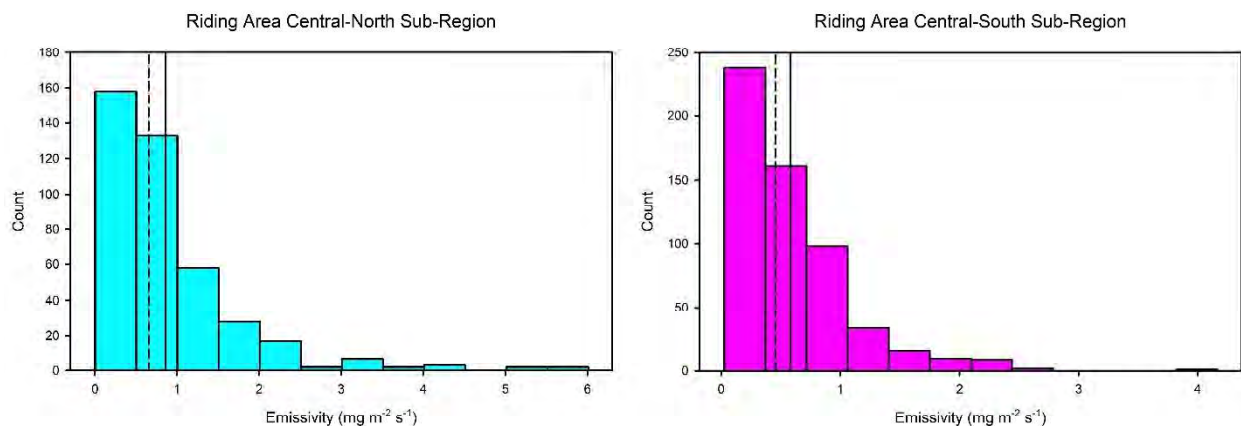
Figure 19: Histograms of PI-SWERL emissivity values (Hi-RPM setting) for Central-North Sub-Region (left) and Central-South Sub-Region (right)of the Riding Area for all measurements from 2013 to 2022. Solid vertical line is the arithmetic mean; dashed vertical line is the median.

For purposes of curve-fitting, it is recommended that non-linear least-squares regression be used to derive the coefficients of the power relation. For the present analysis, a software package called **SigmaPlot**© was used, but any other package that offers a non-linear fitting routine will suffice. Note that **Microsoft Excel**© is not recommended for the purpose of fitting power relations because it uses an algorithm that initially log-transforms the original data and then performs linear least-squares regression, which is computationally efficient but less reliable in ensuring an optimal fit to the data at large values within the range. In contrast, an iterative optimization algorithm that does not transform the data and performs non-linear regression will minimize the residual sum of squares (of deviations) across the entire range of values equally, thereby producing more reliable fits at large values than the approach implemented within **Excel**.

Riding and Non-Riding Areas (including FRA and PE)

The following recommendations are made in regard to assigning emissivity curves to the various zones and sub-regions in the Riding and Non-Riding areas:

<u>**Current (2024) Conditions Scenarios**</u>

Zone or Sub-Region	*Emissivity curves based on data from…*
NRA North	All 2013-2022 PI-SWERL measurements located in NRA North Zone
NRA Central	All 2013-2022 PI-SWERL measurements located in NRA Central Zone **(not including FRA, PE, SE)**
NRA South	All 2013-2022 PI-SWERL measurements located in NRA South Zone
RA Central-North	All 2013-2022 PI-SWERL measurements located in RA Central-North Sub-Region **(not including points in FRA and SE when seasonally managed)**
RA Central-South	All 2013-2022 PI-SWERL measurements located in RA Central-South Sub-Region **(not including points in PE when seasonally managed)**
FRA	Only 2022 PI-SWERL measurements located in the FRA
PE	Only 2022 PI-SWERL measurements located in the PE
SE	Weighted average of riding and non-riding measurements in SE areas (see below for details)

<u>**Pre-Disturbance (1939) Scenario**</u>

Zone or Sub-Region	*Emissivity curves based on data from…*
North (same as NRA North)	All 2013-2022 PI-SWERL measurements located in NRA North Zone
Central (same as NRA Central but also including footprint of RA areas between the north and south boundaries as well as footprint of FRA, PE, SE, and Vegetation Islands)	All 2013-2022 PI-SWERL measurements located in NRA Central Zone **(not including FRA, PE, SE)**
South (same as NRA South)	All 2013-2022 PI-SWERL measurements located in NRA South Zone

Note that for both the Current Conditions and Pre-Disturbance Scenarios, **the recommendation is to take advantage of the complete set of PI-SWERL measurements between 2013 and 2022 listed in Table 1 (with updates in the future after new measurement campaigns are complete)**. Despite 2013 having demonstrably large emissivity values (refer to discussion of Figures 1, 3 and 7), perhaps due to dry moisture conditions, it is recognized that dry years are part of the normal climatology of the region and that prolonged droughts are projected to become more frequent in the future. There is no defensible reason to exclude the 2013 data from consideration, and they help to define the natural variability in the system, which should be accounted for when considering model uncertainty. Similarly, there are no defensible reasons for excluding any of the other PI-SWERL measurements (e.g., inordinately small or large emissivity) because they have been thoroughly quality controlled for errors associated with instrumental failure and transcription/coding inaccuracies by DRI personnel.

Table 3 provides the results for the emissivity relations developed for the Non-Riding and Riding Areas as well as the Foredune Restoration Area and Plover Exclosure area, based on the recommendations presented above. The total number of points is 1509, which is slightly smaller than the total number of measurements listed in Table 1 (1516) because there were seven (7) cases when measurements were not recorded for some of PI-SWERL speed settings. Graphic renditions of the data and power relations are shown in Figure 20. The same axis scaling is used for quick visual comparison, and it is apparent that the RA Central-North sub-region has the largest median emissivity. Interestingly, the RA Central-South sub-region has median values that are not too dissimilar from the NRA North zone and NRA South zone, despite OHV restrictions in the latter two zones. The PE and FRA have the smallest median emissivity.

Table 3: Data used in developing emissivity relations. Flux magnitudes for each PI-SWERL speed are median values (mg m^{-2} s^{-1}). Power function coefficients (a, b) are shown at the bottom. Results generated using SigmaPlot© software.

	Non-Riding Areas			Riding Areas		FRA	PE
	North	Central	South	Central-North	Central-South		
n =	111	221	67	403	574	110	23
u$_*$ (m s^{-1})							
0.381	0.039	0.021	0.001	0.094	0.024	0.006	0.003
0.534	0.307	0.193	0.142	0.640	0.432	0.068	0.032
0.607	0.932	0.610	0.388	1.349	0.964	0.192	0.107
F = a (u$_*$)^b							
a	66.376	51.649	20.786	24.340	24.395	10.710	11.416
b	8.547	8.893	7.972	5.795	6.466	8.060	9.355
r^2	.999	.999	.999	1.000	0.999	1.000	1.000
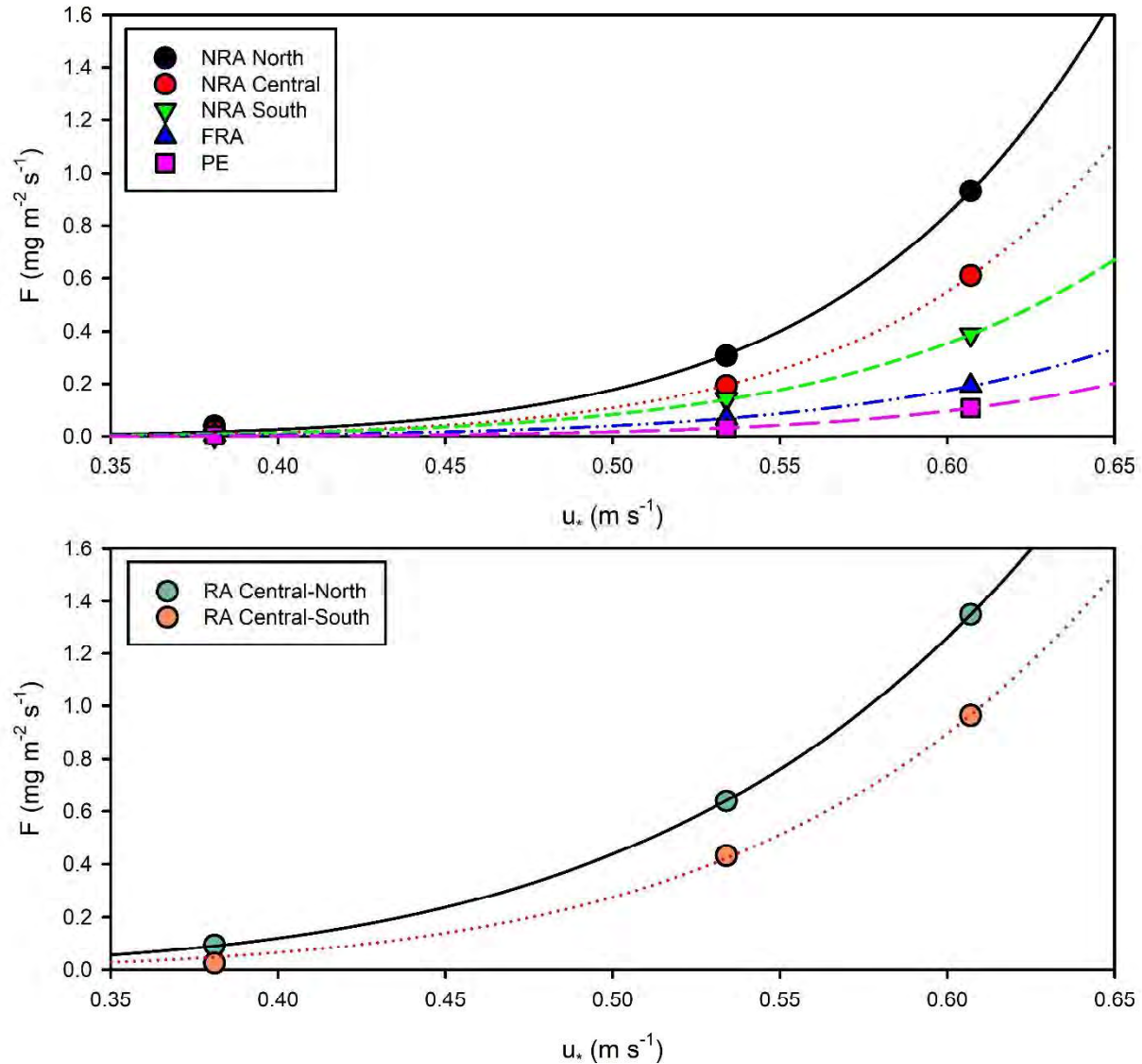
Figure 20: Emissivity relations for various zones in future modeling scenarios. Refer to Table 3 for details.

Seasonal Exclosure (SE) Areas

As mentioned previously, the Seasonal Exclosure areas require separate treatment because they are neither exclusively 'riding' nor 'non-riding.' There are two sub-zones within the current SE area (see Figure 16): (1) a continuous narrow beach strip that lies to the west of the FRA; and (2) two access corridors that divide parts of the FRA and a third access corridor between the PE and FRA. The beach strip is closed to OHV use between March 1 and September 30, but accessible for OHV recreational use between October 1 and February 28. The corridors are managed similarly with the exception of the eastern entry areas that provide year-around rider access to toilet facilities.

A total of 69 PI-SWERL measurements were taken along the beach and corridor areas on September 30, 2022, which is at the end of the exclosure period. Thus, these measurements are thought to be characteristic of the sand surface at the conclusion of the non-riding season after a 7-month period of continual post-riding adjustment. However, some of these measurements were made in the year-around entry areas to the toilets, where OHV access was allowed, and therefore these measurements were considered to be characteristic of the riding period. Several other measurements were made in corridors where it was noted that there had been recent disturbance of the surface by bulldozers as part of regular park maintenance. Therefore, of the 69 PI-SWERL measurements made in the SE area, 24 were classified as 'riding' whereas 45 were considered to be representative of 'non-riding' conditions. The 'riding' measurements were supplemented with another 34 measurements that were taken in the footprint of the SE area between 2013 and 2019 when OHV riding was allowed all year (i.e., before seasonal closure). These 34 measurements were extracted from the data set used to characterize RA Central-North using a GIS map to locate the relevant points. Table 4 presents the data and power function exponents, whereas Figure 21 shows the curves in graphical form.

Because there is a 'riding' period and a 'non-riding' period, each with different emissivity relations, it is necessary, for the purposes of modeling, to combine these into a single relation that characterizes the SE area. Several approaches were explored to yield a weighted average using relaxation and ramp-up factors in an attempt to quantify the adjustments taking place on the landscape as the surface transitions from one emissive state at the end of the riding period (February 28) to another emissive state at the end of the non-riding period (September 30). Little is known about how rapidly these transitions occur and how they are influenced by meteorological conditions. Thus, a simple averaging approach was adopted, to yield a third relation based on the average of the two (2) medians for the riding and non-riding relations. The results from this approach are shown in Table 4 and Figure 21.

Table 4: Data used in developing emissivity relations for the Seasonal Exclosure area. Power function coefficients (a, b) are shown at the bottom.

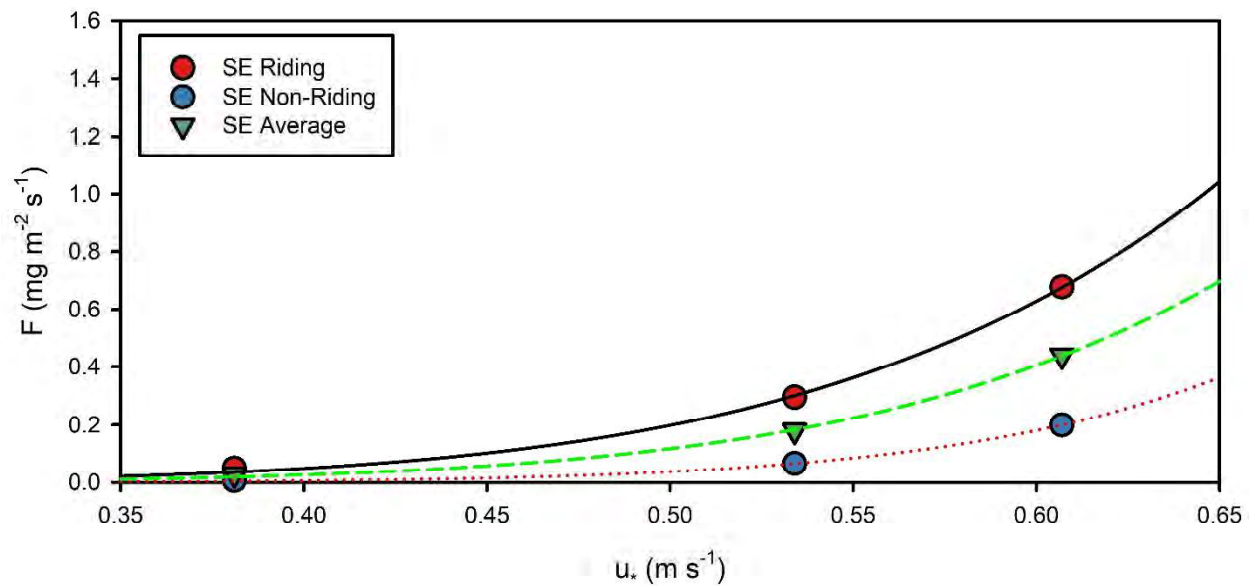|	Riding Affected Period (2013-2022)	Non-Riding Period (Sep 2022)	Average
n =	58	45	2
u_* (m s^{-1})			
0.381	0.049	0.006	0.028
0.534	0.295	0.065	0.180
0.607	0.678	0.200	0.439
$F = a(u_*)^b$			
a	15.875	15.450	13.042
b	6.322	8.709	6.798
r^2	.999	1.000	.999

Figure 21: Emissivity relations for the Seasonal Exclosure area. Refer to Table 4 for details.

Additional Comments and Recommendations

For purposes of defining emissivity relations that characterize the Pre-Disturbance (1939) surface, it is recommended that all PI-SWERL measurements (2013-2022) from the NRA North zone be pooled to define a single power relation that applies to that zone only. Similarly, the emissivity relations for the NRA Central zone and NRA South zone would be based on the 2013-2022 non-riding area measurements in those two zones, respectively. The pre-disturbance landscape would not have had zones equivalent to the FRA, PE, or SE, and there would have been limited impacts from vehicular traffic. Therefore, the measurements from the FRA, PE, and SE should not be included in the pooled data that defines the NRA Central.

The FRA, PE, and SE areas are all managed landscapes in one way or another. The FRA, for example, has six different treatments (species, planting densities, surface pre-treatments) and it is not known with certainty how these varying surfaces, which are in continual stages of evolution, relate to a pre-disturbance condition. There is evidence from the air-photo reconstruction of the 1939 surface that foredunes were a component of the landscape. Given limited resolution and exposure in this early imagery, it is difficult to identify the exact extent of these areas, and there is no information on plant densities or heights from that time, which are critical factors in quantifying the sand-trapping and dust-retention characteristics of these former vegetated surfaces. More monitoring is needed over the next decade to better understand how the FRA will evolve and how the emissions characteristics will change. This does not undermine the use of the 2022 PI-SWERL measurements for the purposes of modeling the current (2024) landscape in the FRA (and PE), which are the only data available characterizing the emissivity potential of these areas since closure. **Another measurement campaign is being planned for 2024, and these data will need to be integrated into the global data set to yield updated emissivity relations. Additional measurement campaigns beyond 2024 are recommended.**

The PE surface is a recently adjusted surface that is managed for bird habitat, and the introduction of large woody debris has, combined with emergent vegetation, lead to the development of appreciable incipient nebkha dune cover. One can imagine similar surfaces having evolved in the pre-disturbance environment after a major storm event that caused coastal inundation and erosion. But it would likely still take a decade or longer for a disturbed sand surface to return to a completely natural state. This would involve multiple meteorological events across a range of speeds, directions, temperatures, and moisture conditions that serve to reorganize the sand surface in terms of texture, vegetation cover, and dune development, but not yet reaching the stage of foredune development with mature plant communities. Thus, there is uncertainty as to how the measurements taken in the PE in 2022 might apply to a pre-disturbance landscape, which is why they are not included in the data subset that defines that NRA Central emissivity power relation.

The SE surface clearly has no counterpart in a pre-disturbance landscape given that it is seasonally subjected to OHV disturbance, so these measurements should not be used to characterize the pre-disturbance landscape in the NRA Central.

At this time, all vegetated areas (natural or treated) are represented identically in the current DRI model, with zero dust emissions. It is recommended that this practice be followed in the near future for both the pre-disturbance and current conditions scenarios. This assumption is admittedly simplistic because there are areas in the ODSVRA that are densely vegetated (for which the assumption is clearly valid) and other areas that are sparsely vegetated, inundated by sand from upwind, or recently planted (for which there is likely to be some dust emission from open sand surfaces between plants, especially under extreme wind events). However, in most of the managed areas where recent planting has taken place (with the exception of the FRA), it has been standard practice to spread straw on the surface, which prevents dust emissions for several years until the plant cover spreads or, alternatively, the straw deteriorates. There is relatively little understanding of how different plant species and assemblages prevent saltation and dust emissions even though it is generally appreciated that there is a dependency on plant height and stem density. Thus, given current uncertainty surrounding this issue, invoking a more complex dust emission scheme for vegetated areas that accounts for plant characteristics (species, density, height, seasonal cycles, senescence, rooting structure) across the treated surfaces is not yet viable nor recommended.

Model Zonation

Figures 22 and 23 show complete renditions of the proposed emissivity grids to be used in future modeling efforts leading to assessments of dust (mass) emissions from the ODSVRA, as per the Stipulated Order of Abatement (modified 2022). Each of these zones is to be characterized by emissivity power relations according to the discussion above. The total acreages for the pre-disturbance and current scenarios are equivalent—only the internal zonation differs. **These proposed zones do not include the large areas adjacent to, but outside, of the ODSVRA boundaries, which would be critical to represent when modeling PM$_{10}$ concentrations at monitoring stations such as CDF, Mesa2, and Oso Flaco.** A much more extensive conversation would be required to reach decisions on how to characterize the emissivity

characteristics of these external areas, many of which are privately owned and inaccessible for purposes of PI-SWERL measurements.

Figure 22 (see also Appendix III) shows the proposed zonation for the Pre-Disturbance scenario for the purpose of defining 'naturally occurring emissions' as per the SOA. There are three large zones (North, Central, South) shown in red shades, with the North (crimson red) and South (pinkish red) zones being equivalent to NRA North (Dune Preserve) and NRA South (Oso Flaco), respectively. The Central zone (salmon red) has a footprint that covers several different 'current' zones (RA Central-North, RA Central-South, NRA Central, FRA, PE, and SE).
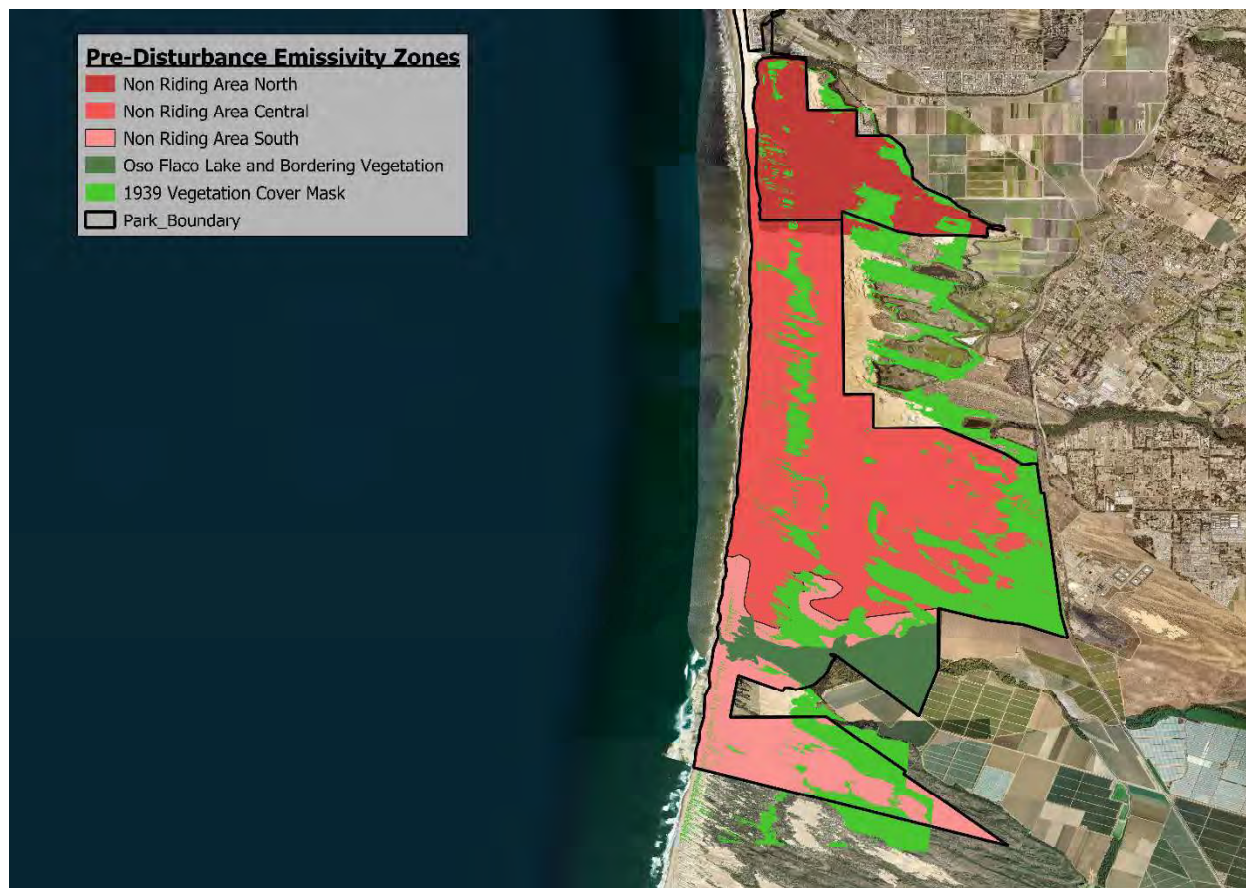
Figure 22: Proposed zonation for the Pre-Disturbance (1939) modeling scenario with three emissivity zones (refer to Figure 18) and superposed vegetation cover masks.

The 1939 vegetation cover mask (light green) from the air-photo analysis undertaken by the University of California – Santa Barbara (Swet et al., 2022) is superimposed on the three zones of the Pre-Disturbance emissivity grid. Note that the vegetation mask extends outside the boundaries of the ODSVRA in some places, but this is irrelevant to modeling mass emissions from within the ODSVRA. The extended coverage may be useful in emission-dispersion modeling that predicts PM_{10} concentrations at CDF or Mesa2. **There is an olive-green area covering Oso Flaco Lake (within the ODSVRA) and the bordering vegetated areas (including some agricultural fields to the east of the lake also within the ODSVRA) that needs to be parameterized separately because this area was excluded from the UCSB air-**

photo analysis due to technical challenges with classification (see report by Swet et al., 2022). The olive-green polygon was digitized to outline those areas with dense vegetation cover and water surfaces (lake and ponds with stream outlet to the ocean) in the vicinity of Oso Flaco Lake, as judged qualitatively from recent Google Earth imagery. The entire polygon is assigned an emissivity value of zero. Examination of the 1939 air photo indicates that the vegetation cover within the boundaries of this polygon have not changed significantly.

Figure 23 shows the proposed zonation for the 'Current' landscape scenario for the purpose of defining mass emissions from the present-day (and future) ODSVRA. There are eight large management areas (RA Central-North, RA Central-South, NRA North, NRA Central, NRA South, as well as the Foredune Restoration Area, Plover Exclosure, and Seasonal Exclosure). Each of these areas has a specific emissivity power relation assigned to it, as described in the table above (Current Conditions (2024) Scenarios) and quantified in Tables 3 and 4
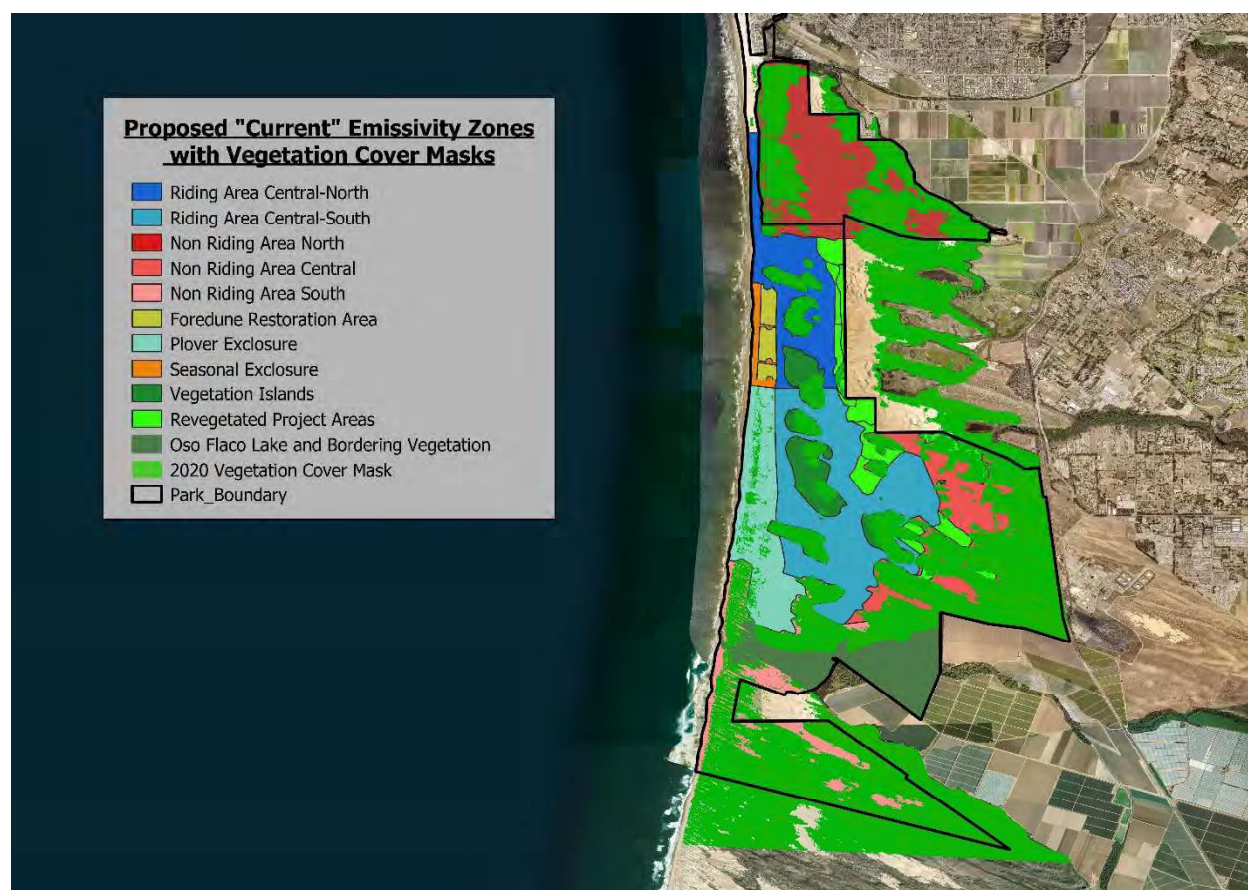
Figure 23: Proposed zonation for the 'Current' Landscape (2024) modeling scenario with eight emissivity zones, superposed 2020 vegetation cover mask, and three additional vegetation zones.

The vegetation covered areas for the 'Current' Landscape scenario are more complex than for the Pre-Disturbance scenario, covering a larger portion of the ODSVRA, in part because of natural greening trends, but also because of dust-mitigation efforts by CDPR.

There are series of vegetation islands (dark green) that are mapped separately, and each island consists of a core of long-established vegetation (e.g., thick, woody shrubs) and fringing vegetation assemblages that often include recent plantings with straw treatments. There are additional areas that were treated and planted in recent years, referred to as 'Revegetated Project Areas' and shown in neon green. These are discussed in detail in recent Annual Report and Work Plans. Superimposed on these zones is a 2020 vegetation cover mask (grass green) from the air-photo analysis undertaken by the University of California – Santa Barbara (Swet et al., 2022), which is the most recent mask available. And finally, there is the olive-green polygon covering Oso Flaco Lake and bordering vegetation that is identical to the one used for the Pre-Disturbance scenario. All vegetated areas are assigned an emissivity value of zero.

CONCLUDING REMARKS

The purpose of this memo is to present a detailed analysis of the PI-SWERL data collected to date, and to offer several recommendations that will assist in satisfying the conditions outlined in the Stipulated Order of Abatement (filed October 18, 2022). In particular, Section 3.c. of the SOA requires that,

> "Emissions shall be calculated using...a representative emissivity grid derived from PI-SWERL measurements as recommended by the SAG, ..."

The analysis presented in this memo provides the rationale for the proposed emissivity grids, which consist of (1) subdivision of the ODSVRA into a series of zones and sub-regions, each with similar and internally consistent usage and management activities; and (2) a set of emissivity power relations developed from the PI-SWERL measurements from 2013 through 2022 for each of the zones and sub-regions.

The proposed emissivity grids for the Pre-Disturbance (1939) Scenario and the Current (2024) Landscape Scenario are to be incorporated into the latest predictive models (managed by DRI) for purposes of assessing whether "emissions in excess of naturally occurring emissions from the ODSVRA" have been eliminated, as per Section 3.b. of the SOA.

Future PI-SWERL campaigns (beyond 2024) are recommended in order to parameterize the emissivity characteristics of the proposed management zones with greater confidence.

Appendix I. Linear Theil Regression Analysis

Linear Theil regression (Theil, 1950; Wilcox, 2005) was performed on the PI-SWERL data to evaluate changes in emissivity over time. Theil regression is a non-parametric method that fits a line to data by computing the median of the slopes of all the possible combinations of pairs of data points. An advantage of the Theil regression is its insensitivity to outliers. The regression was performed on PI-SWERL data from 2013 through 2022, aggregated by percentile for both riding and non-riding areas (see Figures 1 and 3, respectively). Kendall tau statistics were used to determine statistical significance; a statistically significant trend was assumed at the 99% significance level (p< 0.01), meaning there is a 99% chance that the slope was not due to random chance.

Results for the three PI-SWERL speeds are shown in Tables A1 and A2 for the riding and non-riding areas, respectively. **None of the trends were statistically significant (p<0.01).**

Table A1. Regression results for temporal trend analysis for PI-SWERL data for the **riding areas**. The percentile corresponds to the data distribution, the slope (mg m^{-2} s^{-1} day^{-1}) corresponds to data from 2013 through 2022, and p is the statistical significance. Three speeds (u_* is shear velocity) were used in the PI-SWERL instrument.

	$u_* = 0.381$ m s^{-1}		$u_* = 0.534$ m s^{-1}		$u_* = 0.607$ m s^{-1}	
Percentile	slope	p	slope	p	slope	p
5	3.8E-07	0.02	-1.3E-05	1.00	-3.0E-05	0.62
10	4.1E-07	0.09	-4.3E-05	0.46	-3.5E-05	0.46
25	-4.5E-06	0.71	-5.5E-05	0.22	-4.3E-05	0.46
50	-1.7E-05	0.32	-1.1E-04	0.32	-2.2E-04	0.14
75	-5.5E-05	0.32	-1.9E-04	0.22	-2.2E-04	0.32
90	-1.0E-04	0.05	-2.8E-04	0.08	-5.2E-04	0.14
95	-1.3E-04	0.05	-3.7E-04	0.22	-3.2E-04	0.46

Table A2. Regression results for temporal trend analysis for PI-SWERL data for the **non-riding areas**. The percentile corresponds to the data distribution, the slope (mg m^{-2} s^{-1} day^{-1}) corresponds to data from 2013 through 2019, and p is the statistical significance. Three speeds (u_* is shear velocity) were used in the PI-SWERL instrument.

	$u_* = 0.381$ m s^{-1}		$u_* = 0.534$ m s^{-1}		$u_* = 0.607$ m s^{-1}	
Percentile	slope	p	slope	p	slope	p
5	0	0.71	-2.5E-05	0.05	-5.7E-05	0.29
10	4.4E-07	0.64	-2.6E-05	0.02	-8.4E-05	0.10
25	-2.5E-06	0.54	-3.3E-05	0.05	-9.8E-05	0.05
50	-5.9E-06	0.29	-4.3E-05	0.18	-1.8E-04	0.18
75	-5.9E-06	0.18	-7.0E-05	0.18	-2.0E-04	0.29
90	-1.5E-06	0.88	-6.7E-06	0.65	-9.0E-05	0.45
95	3.2E-06	0.65	-5.2E-05	0.65	7.3E-05	0.65

Appendix II. West-East Transects and Point Clusters

Early assessments of PI-SWERL measurements noted a decrease in emissivity from north to south within the ODSVRA, ostensibly due to mean particle size differences. Gillies and Etyemezian (2015), for example, reported that the mean particle size in the north is about 225 μm whereas in the south it is about 400 μm. These prior observations prompted a detailed investigation of north-south zonation, which was incorporated into the proposed emissivity grids, as discussed (above) in this document.

General understanding of coastal beach-dune systems indicates that there is typically a gradient in mean particle size from a poorly-sorted population with coarse mean size at the foreshore and beach to well-sorted, fine material in the lee of the foredune and beyond. This expectation serves as motivation to explore whether there were west-east trends in emissivity within the ODSVRA. At the outset, it was recognized that there was little logic to assessing west-east trends within the Non-Riding Area (NRA) data for the following reasons:

(1) The NRA North and NRA South are distinct zones with internal homogeneity. There seems little obvious advantage to (or need for) dividing these two zones into smaller areas since they are treated equally for the pre-disturbance and current scenarios in the model.

(2) The NRA Central is very narrow longitudinally in the north, and there are few measurements to assess west-east trends. Although this zone widens in the south, there are very few sampling locations that are aligned in west-east transects. Rather the measurements are spatially sparse, and there are large vegetation patches and treatment areas that interrupt west-east process continuity along transects.

(3) Attempts at pooling the data in the west-east direction using lines of longitude are confounded by the bias introduced by the strong north-south trends in emissivity, with the north having significantly greater emissivity than the south.

The focus was therefore exclusively on the Riding Area (RA) data from 2013 through 2022. As a first step, the RA data were pooled according to a somewhat arbitrary west-east division at a line of longitude (-120.62°) that coincides roughly with the fence line separating the riding and non-riding areas in the La Grande Tract. Contrary to expectation, the western zone had slightly greater mean and median values for emissivity than the eastern zone, and despite considerable overlap in the distributions the sample differences were statistically significant (p<0.001) for all three PI-SWERL speeds. The challenge with this crude assessment, however, is that there are also north-south differences that skew the outcome because most of the measurements in the RA Central-North happen to fall west of the division line whereas in the NRA Central-South there are measurements on both sides of the longitudinal division line. Thus, the RA Central-North data, with known greater emissivity, bias the sample distribution for the western half. There are few corresponding data from the NRA Central-North east of the division line to counter-balance this bias. Despite statistical significance, not much credence can be placed on a simple west-east division of the pooled data extending from the north to south boundaries of the ODSVRA. The next step in the analysis was to pool the data into quadrants. The same line of longitude (-120.62°) was used to separate west from east, and the line of latitude (35.62°) that was used earlier to separate north from south was applied to the quadrants. The results were mixed. The

north-west quadrant has a smaller mean and median emissivity than the north-east quadrant, but the differences are not statistically significant. In part, this is due to the differences in medians being small, but also because there were only 31 measurements in the north-east quadrant compared to 394 in the north-west quadrant. The south-west quadrant (n=177), in contrast, had slightly greater mean and median emissivity than the south-east quadrant (n=409), with the differences being statistically significant for Medium and High RPM settings ($p<0.003$) but not for the Low RPM setting ($p=0.115$).

It was suggested that there might be some value in examining the trends along PI-SWERL transects that follow the prevailing wind direction. Most of these PI-SWERL transects extend from the upper beach eastward into the non-riding area, and often along their course they are interrupted by vegetation islands or treatment areas. It makes little sense to compare emissivity values that cross the boundary between riding and non-riding areas because these data are already pooled separately into distinct zones. Transects that are interrupted by patches of vegetation would be anticipated to have different particle size and emissivity tendencies in the downwind direction, so they too are to be avoided.

Two transects were identified in the global data set that were continuous across the span of the riding area and uninterrupted by vegetation patches (see Figure A_1). These transects are simply identified as 'North Transect' and 'South Transect', and both were measured originally in 2013 and then again in 2015 (north) and 2019 (south).

Figure A_1: PI-SWERL measurement transects used to assess potential west-east trends. Only the data points from 2013 are represented, but virtually identical locations were sampled again in 2015 and 2019.

Figure A_2 shows the longitudinal trends along the north and south transects for all three PI-SWERL settings and according to measurement campaign. Several things are apparent, consistent with the data analysis discussed in the main body of this memorandum. For example, the 2013 emissivity values are greater than those measured in 2015 and 2019 (c.f., Figure 1). Also, the emissivity values along the north transect are generally greater than along the south transect (c.f., Figures 10 and 11). The spatial trends along the transects appear to be consistent across all three PI-SWERL settings for any particular measurement campaign (i.e., bumps and valleys in the lines are consistently reflected in the trendlines), however, there is little consistency between measurement campaigns. Sampling locations that had large emissivity in 2013 are not necessarily places where there was large emissivity in 2015 or 2019. Indeed, there appears to be rather large variance in the data around the mean trend line (shown as dashed lines), especially for the High RPM setting. The regression lines also indicate mixed results with regard to the expected inland increase in emissivity. The 2013 data for the North transect show an overall decrease in emissivity with inland distance whereas the 2015 data show a gradual increase. In contrast, the 2013 data for the South transect show a gradual increase in emissivity inland, but the 2019 data show a decrease. It should be noted also that the regression lines have very low R^2 values (less than 0.15 except in one instance). Thus, very little can be concluded from this transect analysis regarding west-east trends.
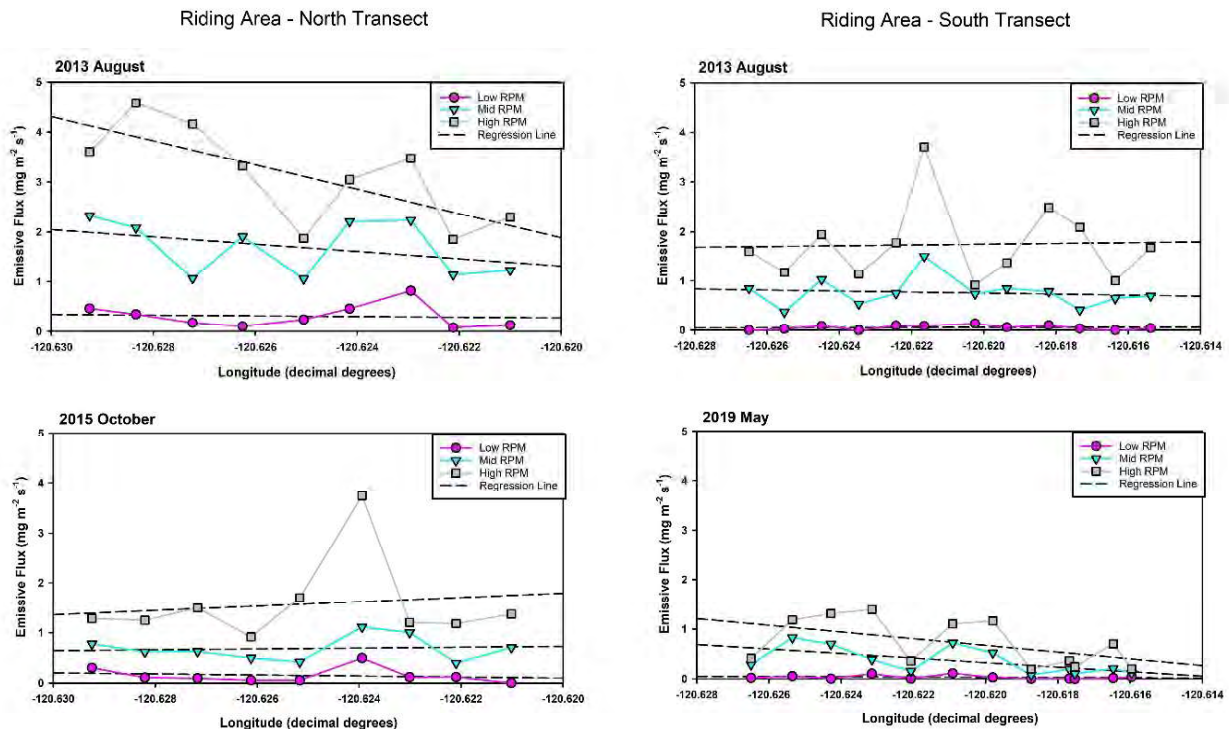

Figure A_2: West-east trends in emissivity according to longitude for the North and South transects.

One of the factors that may contribute to the mixed results and uncertainty in west-east trends in emissivity is the relatively large variance in emissive flux across very small distances. The PI-SWERL measurement protocols call for repeat measurements in certain locations in order to

confirm the proper operation of the field instruments. Figure A_3 (left panel) shows a clip of the NRA North (Dune Preserve) with the 2013 PI-SWERL sampling locations. Circles identify multiple measurements in a spatial cluster, and the photo on the right shows a close-up of the measurements within the green circle. The spatial separation between points is a few meters or less.
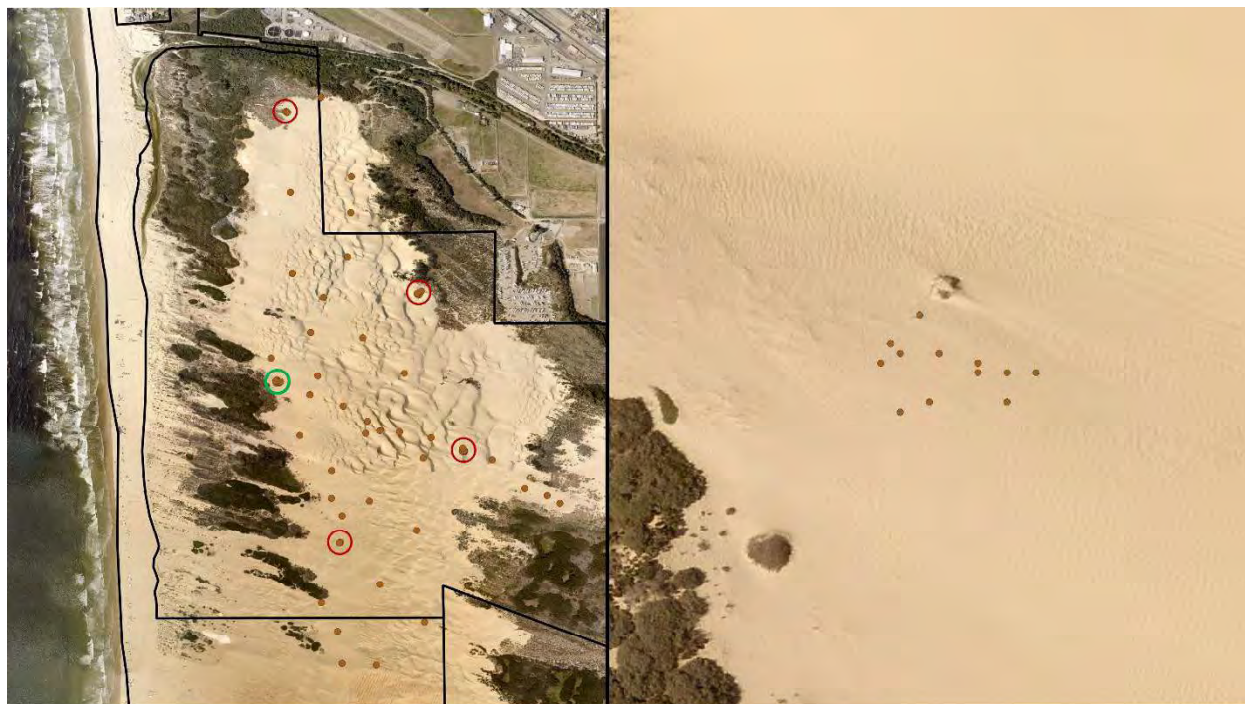

Figure A_3: Examples of PI-SWERL measurement clusters in the NRA North (Dune Preserve) indicated by circles (left panel), and a close-up of the cluster within the green circle (right panel).

A small number of clusters from the non-riding area were selected randomly, spanning the north, central, and south regions, and for two measurement campaigns (2013 and 2019). The data distributions in emissive flux for the three PI-SWERL settings are shown in Figure A_4. These are simply examples, and they are not intended to suggest analytical comprehensiveness. But what becomes apparent is that even over small spatial separation distances there can be large variations in emissive flux. At the High RPM setting, the measurements typically span approximately 1 mg m^{-2} s^{-1}. This suggests that at least some of the uncertainty associated with analyzing west-east trends along transects (as represented in Figure A_2) is due to relatively large variance in emissive flux in the immediate vicinity of the PI-SWERL measurement locations. These localized variances are due to differences in mean particle size and grain sorting associated with dynamic aeolian processes at multiple scales and as influenced by multiple spatial-temporal controls. Thus, the precise value of emissivity used to characterize any particular sampling location within the ODSVRA depends not only on the geographical position of that sampling location (i.e., latitude and longitude coordinates) but also on the precise placement of the PI-SWERL instrument within a relatively small area (of the order of 10 m^2) at

that sampling location, which will be random and arbitrary. Logistically it is unreasonable to make multiple measurements at every sampling location because of time and effort.
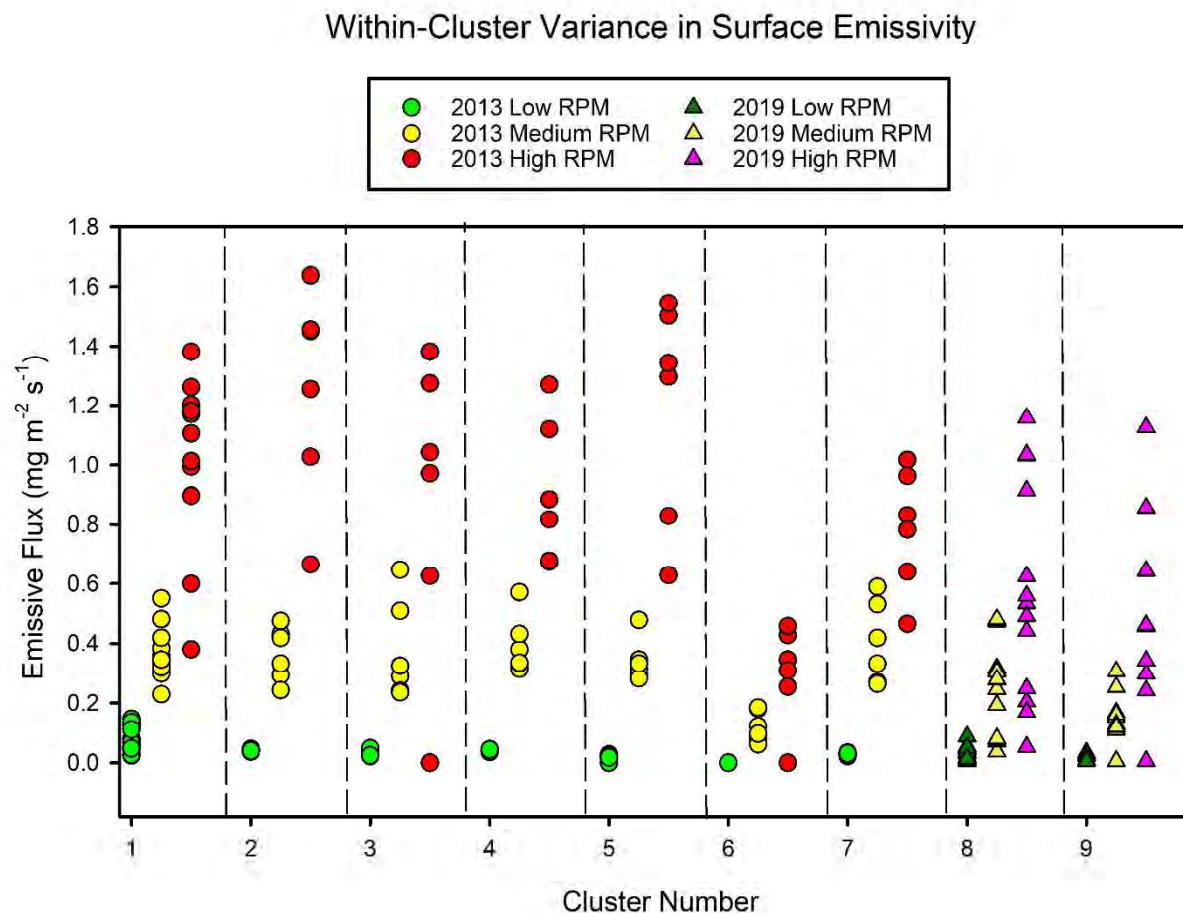
Figure A_4: Variance in emissive flux within spatial clusters. A total of nine (9) clusters are represented, with circles (triangles) corresponding to 2013 (2019) measurement campaigns. PI-SWERL settings are color-coded.

In summary, there is very little rationale for west-east zonation within the ODSVRA. The current landscape scenario already comprises eight (8) distinct zones and sub-regions with additional areas associated with vegetation islands, treatment projects, and vegetation masks. Many of these are already oriented in a north-south direction, and therefore there is an inherent west-east zonation according to management zones. Additional complexity in zonation seems unwarranted given the weak statistical foundation for west-east segregation of the PI-SWERL data.

Appendix III. Side-by-Side Comparison of Proposed Emissivity Grids.

Pre-Disturbance Emissivity Zones

Legend:
- Non Riding Area North
- Non Riding Area Central
- Non Riding Area South
- Oso Flaco Lake and Bordering Vegetation
- 1939 Vegetation Cover Mask
- Park Boundary

Proposed "Current" Emissivity Zones with Vegetation Cover Masks

Legend:
- Riding Area Central-North
- Riding Area Central-South
- Non Riding Area North
- Non Riding Area Central
- Non Riding Area South
- Foredune Restoration Area
- Plover Exclosure
- Seasonal Exclosure
- Vegetation Islands
- Revegetated Project Areas
- Oso Flaco Lake and Bordering Vegetation
- 2020 Vegetation Cover Mask
- Park Boundary

References

Etyemezian, V., Nikolich, G., Ahonen, S., Pitchford, M., Sweeney, M., Purcell, R., Gillies, J., Kuhns, H., 2007. The Portable In-Situ Wind ERosion Laboratory (PI-SWERL): a new method to measure PM10 windblown dust properties and potential for emissions. **Atmos. Environ**. 41 (18), 3789–3796. https://doi.org/10.1016/j.atmosenv.2007.01.018.)

Gillies, J.A., Etyemezian, V., 2015. Addendum to the PI-SWERL Report of Etyemezian et al. (2014) Particle Size Distribution Characteristics and PI-SWERL PM_{10} Emission Measurements: Ocean Dunes State Vehicular Recreation Area. Report prepared by the Desert Research Institute for Off-Highway Motor Vehicular Recreation Division, California State Parks, 1725 23d Street, Suite 200, Sacramento, CA 95816, July 13, 2015 (available upon request).

Gillies, J.A., Furtak,-Cole, E., Nikolich, G., Etyemezian, V., 2022, The role of off-highway activity in augmenting dust emissions at the Oceano Dunes State Vehicular Recreation Area, Oceano, CA. **Atmospheric Environment**, X 13 (2022) 100146.
https://doi.org/10.1016/j.aeaoa.2021.100146

Mejia, J.F., Gillies, J.A., Etyemezian, V., Glick. R., 2019, A very-high resolution (20m) measurement-based dust emissions and dispersion modeling approach for the Oceano Dunes, California, **Atmospheric Environment** 218 (2019) 116977.
https://doi/org/10.1016/jatmosenv.2019.116977.

Swet, N., Hilgendorf, Z., and Walker, I., 2022. UCSB Historical Vegetation Cover Change Analysis (1930-2020) within the Ocean Dunes SVRA. Report prepared for California Department of Parks and Recreation. 86 pages.

Thiel, H., 1950, A rank-invariant method of linear and polynomial regression analysis, **Proc. Kon. Ned. Akad. V. Wetensch. A**. 53, 386-392, 521-525, 1397-1412.

Wilcox, R., 2005, *"10.2 Theil–Sen Estimator", **Introduction to Robust Estimation and Hypothesis Testing**, Academic Press, pp. 423–427, ISBN 978-0-12-751542-7*)

ODSVRA Dust Control Program Draft 2024 ARWP

ATTACHMENT 09

Modeling to Determine the Conditions of Excess Emissions for 2023 ODSVRA (DRI Documents)

THIS PAGE WAS INTENTIONALLY LEFT BLANK.

Modeling to Determine the Condition of Excess Emissions for 2023 ODSVRA

J.A. Gillies and J. Mejia, Division of Atmospheric Sciences, Desert Research Institute, Reno, NV

Staff, Oceano Dunes State Vehicular Recreation Area, Oceano, CA

The second amendment to the Stipulated Order of Abatement (SOA), adopted in October 2022, modified the key mass emissions and concentration reduction requirements from the original SOA that had formed the basis for State Parks' Dust Control Program and 2019-2022 ARWP documents. Specifically, the October 2022 SOA amendments replaced the requirement to reduce baseline PM_{10} emissions by 50% and achieve absolute ambient air quality standards with a new requirement that is "designed to eliminate emissions in excess of naturally occurring emissions from the ODSVRA that contribute to downwind violations of the state and federal PM_{10} air quality standards".

To determine if the ODSVRA is, or is not, in a condition of excess emissions required major modifications to the DRI emissions modeling process (Mejia et al., 2019) and model inputs. The changes to the model were developed principally by the Scientific Advisory Group (SAG) and were presented to California Department of Parks and Recreation (CDPR) on December 19th, 2023*.

These recommendations were:

1. In the model, the ODSVRA is to be divided into emissivity zones based on location (non-riding area north, riding south, etc.) instead of using the 21 m by 21 m grid that had been used in the past.

2. All PI-SWERL data from 2013 to 2022 will be used for both the current and pre-disturbance modeling scenarios (Table 1, below).

3. The median of the emissivity values (E, mg m^{-2} s^{-1}) from the distribution of emissivity values for each of the (three) PI-SWERL test friction velocities (u$_*$ m s^{-1}) will be used to derive an emissivity relation of the form $E = a\, u_*^b$ that characterizes the emissivity in the designated zones for both the current and the pre-disturbance scenarios.

4. The pre-disturbance scenario will be based on the non-riding area emissivity overlain on the riding area for three defined zones identified in Table 1 and as shown in Fig. 1 (below). The current year scenario will be based on the emissivity of the zones identified in Table 1 and as shown in Fig. 2 (below).

On Feb. 8, 2024, the SLOCAPCD conditionally approved the SAG recommendations and CDPR instructed DRI to carry out a modeling exercise based on application of these recommendations within the emission model to evaluate the condition of being in excess of emissions between the current year ODSVRA (i.e., emissivity zones, dust emission control zones, and vegetation cover as of 2023) and 1939, representing the naturally occurring emissions case.

This report describes the changes to the DRI emission model that were required to estimate the emissions in metric tons per day from the defined zones (Table 1) and the total emissions, i.e., the summation of emissions from the zones representing the current conditions and the

Table 1. The defined zones of emissivity and the data source for deriving the emissivity relations.

Zones for Current Year	Emission Source Data for Emissivity Relation
Non-Riding Area (NRA) North	All 2013-2022 PI-SWERL measurements located in NRA North Zone
Non-Riding Area (NRA) Central	All 2013-2022 PI-SWERL measurements located in NRA Central Zone (not including FRA, PE, SE)
Non-Riding Area (NRA) South	All 2013-2022 PI-SWERL measurements located in NRA South Zone
Riding Area (RA) Central-North	All 2013-2022 PI-SWERL measurements located in RA Central-North Sub-Region
Riding Area (RA) Central-South	All 2013-2022 PI-SWERL measurements located in RA Central-South Sub-Region
Foredune Restoration Area (FRA)	Only 2022 PI-SWERL measurements located in the FRA
Plover Exclosure (PE)	Only 2022 PI-SWERL measurements located in the PE
Seasonal Exclosure (SE)	Weighted average of riding and non-riding measurements in SE areas
Zones for Pre-Disturbance (1939)	
North (same as NRA North)	All 2013-2022 PI-SWERL measurements located in NRA North Zone
Central (same as NRA Central but also including footprint of RA areas between the north and south boundaries, and the FRA, PE, and SE areas)	All 2013-2022 PI-SWERL measurements located in NRA Central Zone (not including measurements from FRA, PE, SE)
South (same as NRA South)	All 2013-2022 PI-SWERL measurements located in NRA South Zone

conditions of 1939. The difference in the total mass emissions is used to evaluate if the current condition is, or is not, in a state of excess emissions.
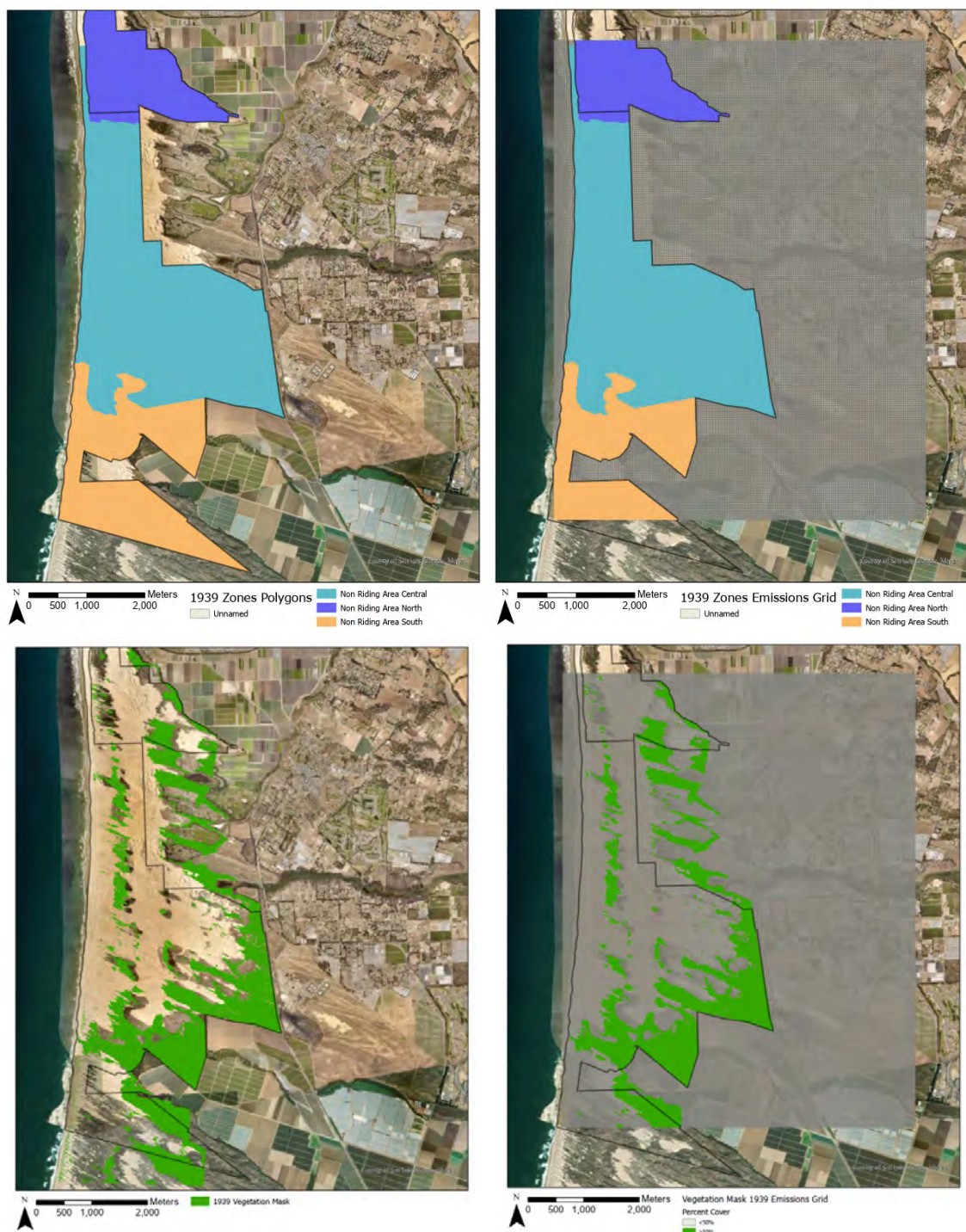
Figure 1. The emissivity zones (upper panels) and vegetation cover zones (lower panels) representing conditions in 1939. Maps show the SAG-provided polygons (left) compared with the grid-defined zones (right). Gray rectangle shown in the maps on the right defines the modeling domain.

Figure 2. The emissivity and dust control zones (upper panels), and vegetation cover zones (lower panels) of the current ODSVRA. Maps show the SAG-provided polygons (left) compared with the grid-defined zones (right). Gray rectangle shown in the maps on the right defines the modeling domain.
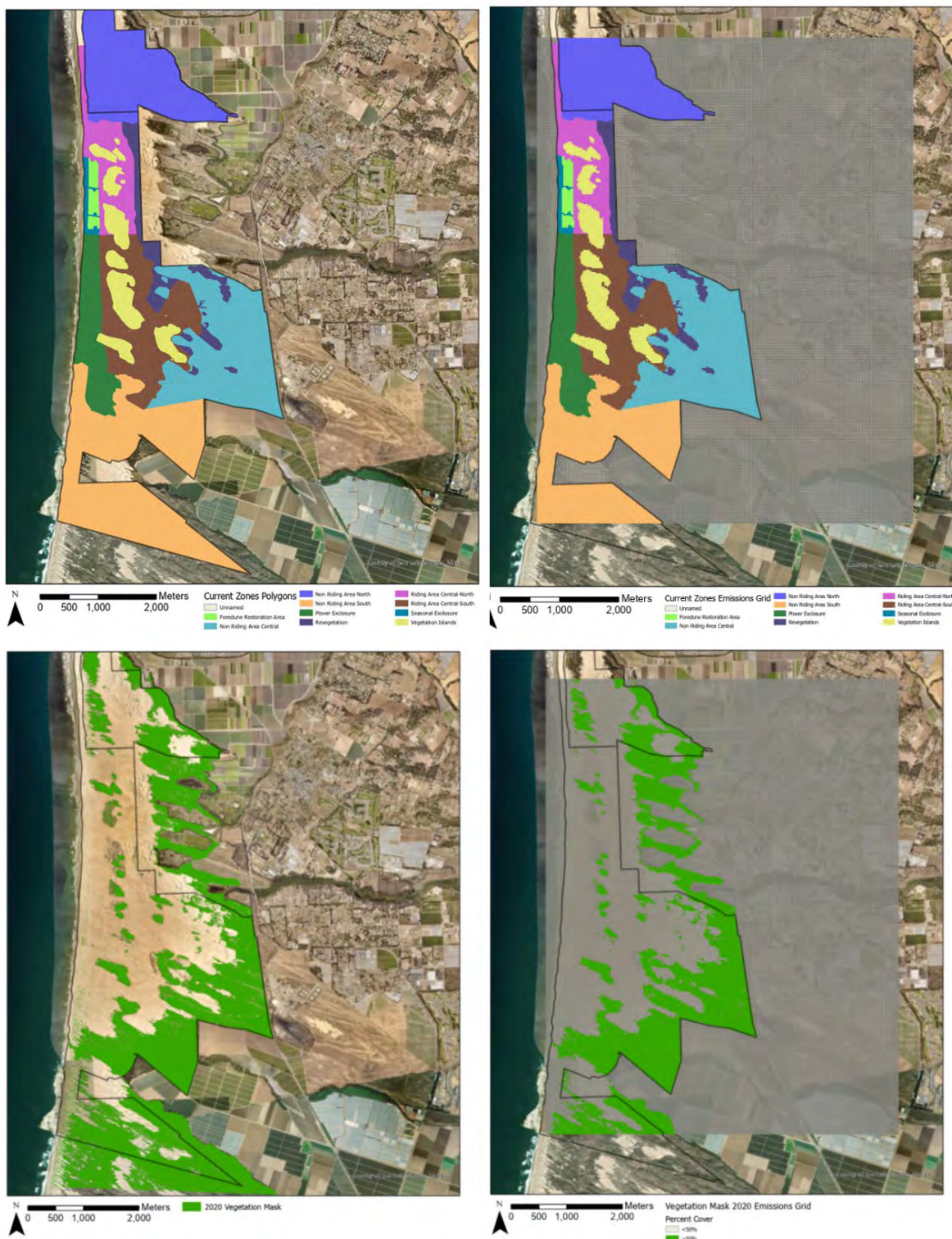
Defining the Zones within the DRI Emission Model

The switch to zones with different emissivity relations as opposed to the interpolated/extrapolated scheme used previously for modeling mass emissions from the ODSVRA created an unforeseen challenge to define the zones within the DRI emission model. The emission model written in Python could not handle the conversion to a zone-based approach basically for lack of Geographic Information System (GIS)-capability to deal with the complexity of zones within zones (e.g., a vegetation zone embedded within an emission zone), which caused the model to crash. To rectify the problem, it was necessary to convert the SAG-provided polygons created in a GIS program to an emissions grid using ArcGIS Pro.

To accomplish this the following steps were taken:

1) Using the X, Y coordinates of the underlying 21 m × 21 m grid cells (see Fig. 1 or 2) and associated tabular data from the DRI emission model, a projected point file was created in WGS1984 UTM Zone 10 N so that the points were equidistant.

2) A polygon file was created and the edges were snapped to the four distal corners of the domain grid to create a single large rectangle.

3) Each of the grid cells in the original DRI emission model has a defined center point for each 21 m × 21 m square. The Fishnet Tool in ArcGIS Pro was used to create a set of identical square polygons that filled the large rectangular polygon (step 2), and each square within the polygon had a coordinate referenced to the middle position of the original domain.

4) A "spatial join" in ArcGIS was used to label each square grid polygon with associated tabular data (e.g., emissivity coefficients, dust control status, etc.) for the point coordinates from the DRI emission model to create a shapefile.

5) To create the SAG-defined zones for the current and 1939 landscapes the SAG-provided polygon files were modified using the Intersect tool in ArcGIS Pro that assigned the square grids to an associated polygon zone.

6) As the underlying grid was composed of squares, at known borders (e.g., park boundary) it was necessary to define whether a square was interior or exterior to the park. If a grid square, by area, was ≥50% within the defined boundary that cut across the square, the square was considered to be in the park and within its specified zone.

7) The same process needed to be undertaken for the vegetation masks (current and 1939). The vegetation cover polygons (from UCSB and as modified by the SAG) were modified using the Intersect tool in ArcGIS Pro to estimate the percent cover in each square grid. If a grid square, by area, was ≥50% covered by vegetation it was considered to be non-emitting. If a grid square was <50% covered it was assigned the emissivity of the zone it was within. This 50% grid square area threshold has been used in previous reports and tested for uncertainty.

8) The fully attributed grids (i.e., zones, vegetation, dust control areas, etc.) were exported from ArcGIS Pro in the form of a shapefile and CSV that could be used within the DRI emission model.

This GIS processing of the SAG-provided polygons defining the zones and the vegetation cover polygons (UCSB with SAG modifications) results in different sized zones once converted to the square grid format that can be brought into the DRI emission model. Table 2 shows the change in area in each of the zones that results from the GIS processing of the original polygons. The processing results in the total area decreasing by approximately 8.8% for GIS modified grid cell zones compared with the SAG-provided polygons.

Table 2. The area of the zones as provided by the SAG compared with the GIS modified grid cell zones by area and % difference. The area of each GIS-modified Grid Cell zone minus the vegetation cover is also provided, based on the Grid Cell zones and vegetation layer.

	Original Polygons	GIS Modified Grid Cell Zones	% Difference	After Removing Vegetation Cover
Zone Designation (1939)	**Acres**	**Acres**		**Acres**
Non Riding Area Central	2526.3	2525.8	-0.02	1915.5
Non Riding Area North	729.6	595.5	-18.38	498.7
Non Riding Area South	1169.3	914.0	-21.84	464.0
Sum	4425.2	4035.3	-8.81	2878.2
	Original Polygons	**GIS Modified Grid Cell Zones**	**% Difference**	
Zone Designation (current)	**Acres**	**Acres**		
Foredune Restoration Area	48.0	49.3	2.62	49.3
Non Riding Area Central	819.4	820.1	0.09	269.7
Non Riding Area North	729.6	595.5	-18.38	389.6
Non Riding Area South	1169.3	914.0	-21.84	303.5
Plover Exclosure	309.7	309.5	-0.08	309.5
Revegetation	207.7	207.3	-0.19	200.6
Riding Area Central-North	251.1	249.3	-0.72	249.2
Riding Area Central-South	546.8	547.2	0.07	546.7
Seasonal Exclosure	34.5	34.0	-1.54	34.0
Vegetation Islands	309.1	309.2	0.01	194.2
Sum	4425.2	4035.3	-8.81	2546.3

There is an underlying model domain issue that remains to be addressed as the new excess emission framework is adopted. This issue is the areal extent of the model domain (gray polygon shown in Figs. 1 and 2), which was initially adopted for evaluating the total emissions from the ODSVRA riding area and estimation of mass concentration of PM_{10} at the SLOCAPCD monitoring stations CDF and Mesa2. This model domain does not cover the entire area of the ODSVRA as designated by the zones listed in Table 2. The size of the original domain was limited due to computational issues related to memory restrictions for running CALMET to generate the wind field. This is not a hardware limitation, but a software limitation to allocate memory within the Fortran code that was used to construct CALMET. The fidelity of the original grid (i.e., individual grid cell size and total number of cells) was balanced against exceeding the memory allocation restrictions to arrive at the size of the original domain.

The size of the domain can be changed to include all the zones, but it will require investigating how to expand CALMET capacity for the larger domain while keeping the 21 m × 21 m grid cell size, or the grid cells will have to be greater than 21 m × 21 m. Changing the size of the domain will also have consequences for other parts of the model output, with the greatest impact on the wind field that drives the emissions. Increasing the size of the domain and introducing new topography will influence the development of the modeled wind field. The model will need to calculate the wind friction velocity (i.e., u_*) for each grid cell in the newly included areas in the larger domain. Adding new areas may also result in changes in wind speed and direction, most prominently at the borders where the newly incorporated areas bound the older domain area, which could also affect the calculation of u_* in these previously defined border zones. DRI acknowledges that these changes can be undertaken, but it will require significant resources to make these modifications and require agreement by the stakeholders (i.e., Parks, APCD, and SAG) on the model modification process. It was not feasible to make these changes in the time frame of reporting the model results in the excess emissions framework by March 2024. Given the directive, these changes could be accomplished before the end of 2024.

The Emissivity Relations Associated with the Zones

The emissivity relations, of the form $E = a\,u_*^b$, associated with the defined zones used for the modeling were drawn from the SAG (2023) memo represented in their Table 4. The non-linear regression used to calculate the a and b coefficients was carried out using the agreed upon software package SigmaPlot. The coefficients for the power relations for the zones used in the DRI emission model are reproduced from SAG (2023) Table 4 in this report as Table 3.

Zones identified as being under re-vegetated dust control or are identified as grid cells with ≥50% vegetation cover are assigned an emissivity of zero under all wind conditions.

Table 3. Data used in developing the emissivity relations. The number of available PI-SWERL tests (n), the u_* values for the three PI-SWERL test settings, the median emissivity values as a function of u_* are shown in the top half of the Table. The power function coefficients (a, b) for the zones are shown in the bottom half of the Table with the correlation coefficient (r^2) indicating the goodness of fit of the power relation in each case.

	Non-Riding Areas			Riding Areas		FRA	PE	Avg. SE
	North	Central	South	Central-North	Central-South			
n=	111	221	67	403	574	110	23	103
u_* (m s^{-1})								
0.381	0.039	0.021	0.001	0.094	0.024	0.006	0.003	0.028
0.534	0.307	0.193	0.142	0.640	0.432	0.068	0.032	0.180
0.607	0.932	0.610	0.388	1.349	0.964	0.192	0.107	0.439
E (mg m^{-2} s^{-1})=$a\,u_*^b$								
a	66.376	51.649	20.786	24.34	24.395	10.71	11.416	13.042
b	8.547	8.893	7.972	5.795	6.466	8.060	9.355	6.798
r^2	0.999	0.999	0.999	1.000	0.999	1.000	1.000	0.999

The Wind Field Driving the Emissions Model

This aspect of the modeling has remained unchanged in the excess emission framework. The development of the wind field is described in detail in Mejia et al. (2019). The wind field applied to the current and 1939 model runs are representative of the amalgamation of the wind field data generated for the 10 highest PM_{10} emitting days that occurred in May 2013. This wind field has been used in the model estimates provided in all the Annual Report and Work Plans (ARWP) through to the 2023 ARWP.

Modeling Results

Maps of emissions created by the meteorology of the 10 highest emission days from May 2013 applied to the zones for the current year and 1939 are shown in Fig. 3. Table 4 provides the model-derived estimates of total mass emissions in metric tons per day for each of the zones in the current year and 1939 and for the sum of total emissions for the equivalently sized areas (4035.3 acres), i.e., the three zones of 1939 and the ten zones of the current year. Note that the vegetation cover is different between the two years, so different sized areas within the total area (i.e., 4035.3 acres) have zero emissions due to the difference in vegetation cover (Table 2).

Based on the summation of the polygons, for equivalent areas for the two scenarios, the current ODSVRA is not in excess of emissions compared to 1939. The pre-disturbance landscape had a modeled emission of 166 metric tons per day whereas the current landscape had a modeled emission of 148 metric tons per day, with a difference buffer of 18 metric tons per day.

Next Phase

In 2024 additional PI-SWERL emissivity data will be collected in May covering as much as possible the test locations that were sampled in 2019 in the riding and non-riding areas. The foredune restoration area and plover exclosure will be sampled in October duplicating the sampling points of October 2022 as much as possible. In October DRI will also select a subset of the May 2024 sampling grid and repeat PI-SWERL measurements at these locations as controls.

The May and October 2024 PI-SWERL data will be QA/QCed by DRI and the emissivity (mg m^{-2} s^{-1}) for each PI-SWERL test for the three u_* set points will be provided to the SAG to add to the PI-SWERL emissivity database as a function of the established zones. Using SigmaPlot, the SAG will update the emissivity relations (Table 2). These updated emissivity relations and any other updated model input data (e.g., current vegetation cover, changes in dust control areas) will be used as input into the model to determine if compliance with the SOA excess emissions mandate is achieved for the conditions of 2024. This could likely be accomplished by the end of December 2024.
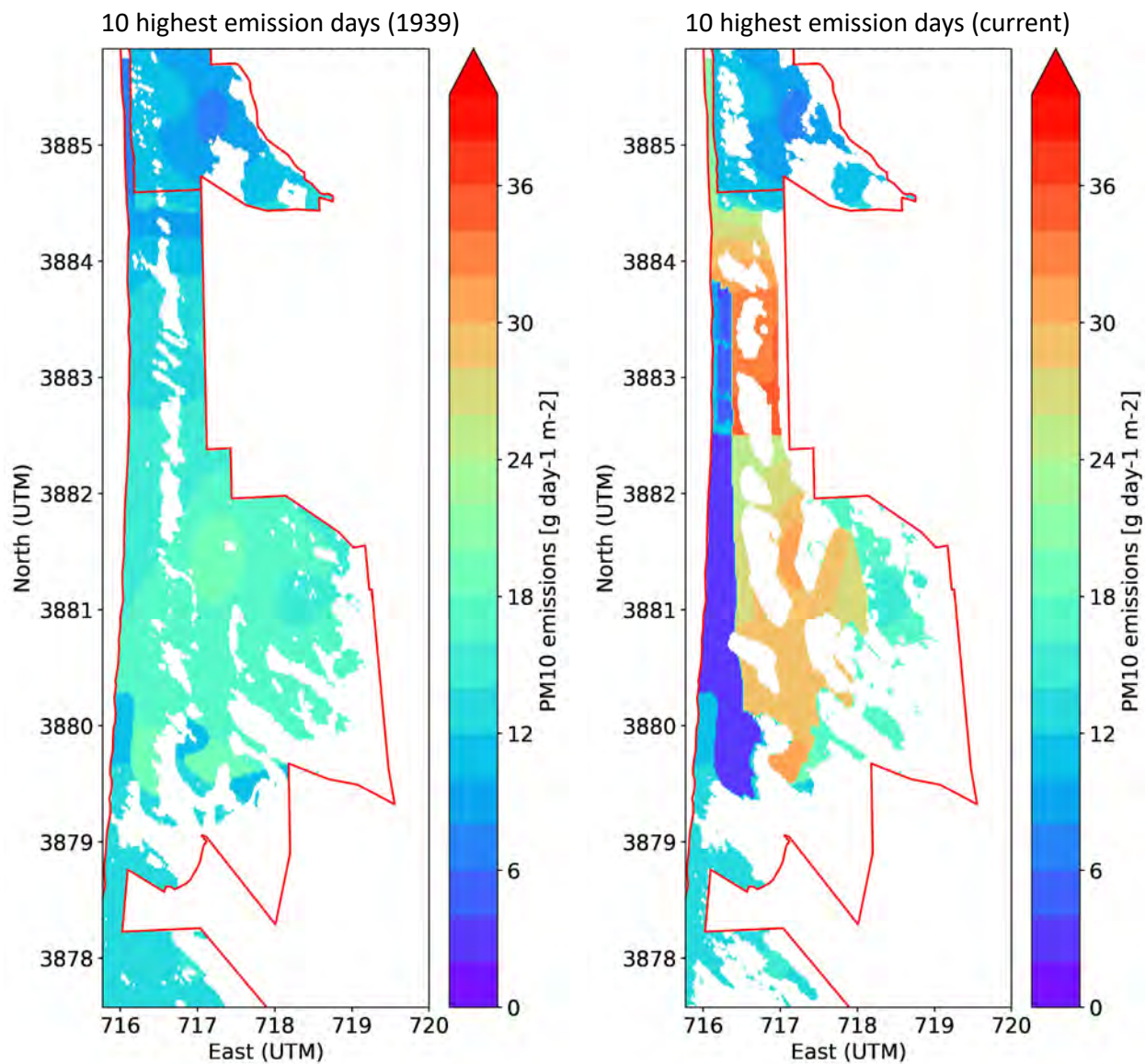
Figure 3. The distribution of emissivity (E= g m^{-2} day^{-1}) for 1939 (left panel) and the current year (right panel) based on the meteorology of the 10 highest PM$_{10}$ emission days, May 2013.

Table 3. Model-derived estimates of total mass emissions in metric tons per day for each of the zones in the current year and 1939 and for the sum of total emissions for the equivalently sized areas.

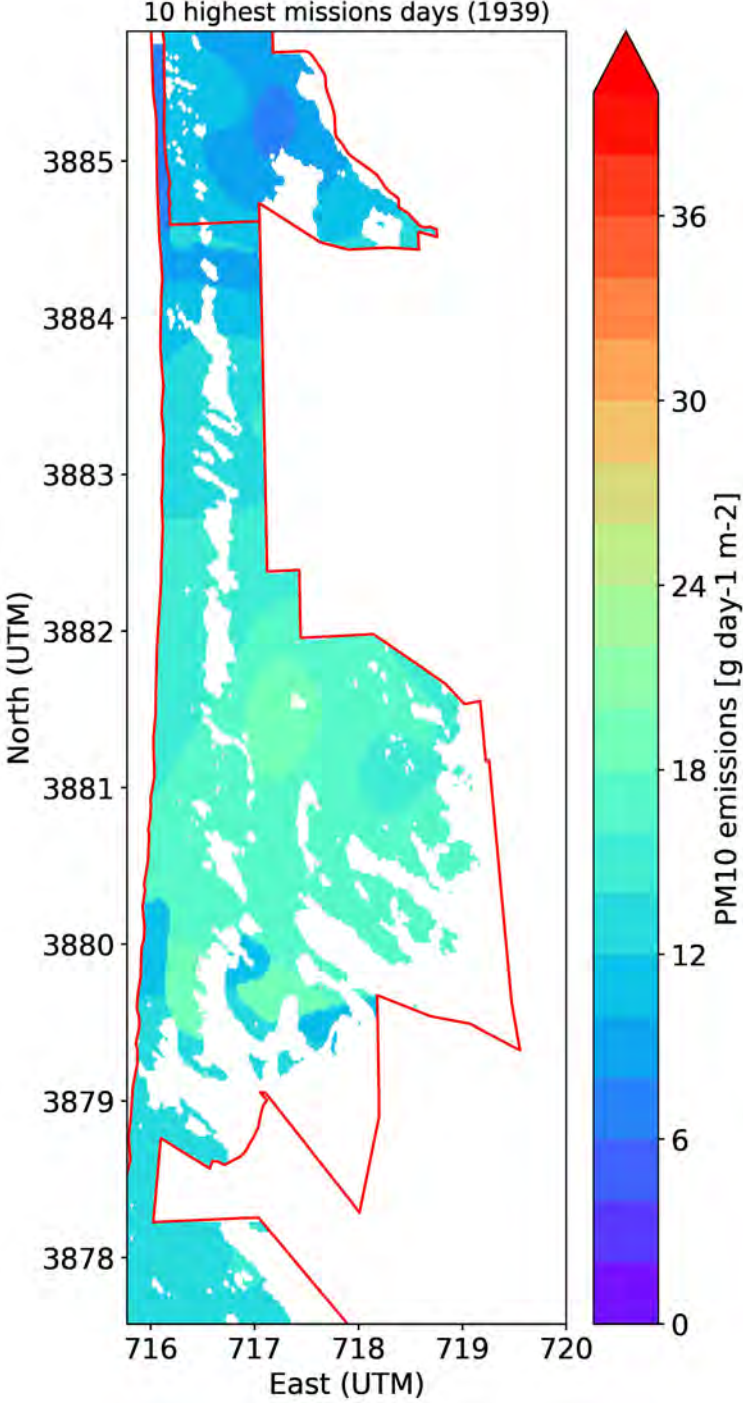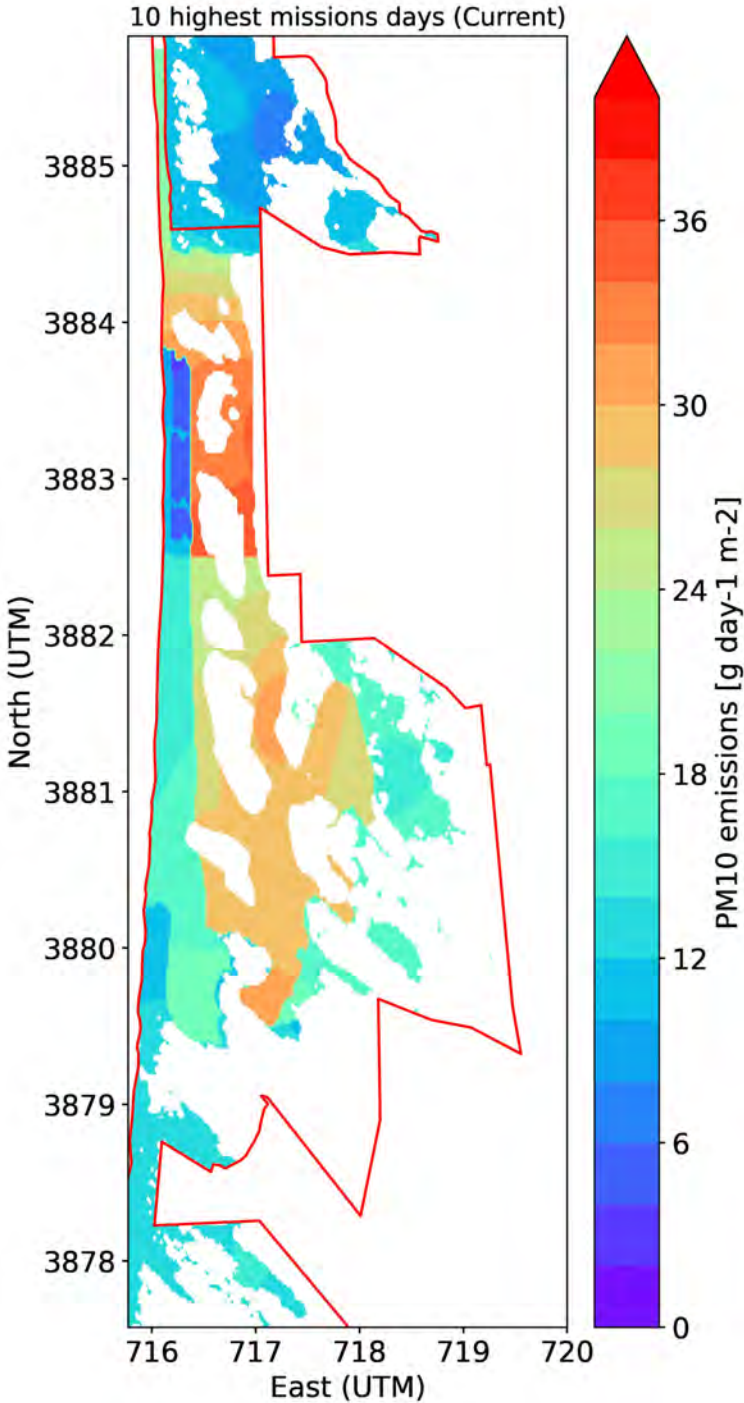| Zone	Total Emissions metric tons/day (10 Highest Emissivity Days May 2013)
1939	
Non Riding Area Central	122
Non Riding Area North	20
Non Riding Area South	24
Total	**166**
Current	
Foredune Restoration Area	1
Non Riding Area Central	18
Non Riding Area North	16
Non Riding Area South	16
Plover Exclosure	4
Riding Area Central-North	30
Riding Area Central-South	63
Seasonal Exclosure	1
Vegetation Islands	0
Revegetation	0
Total	**148**

References

Mejia, J.F., J.A. Gillies, V. Etyemezian, R. Glick (2019). A very-high resolution (20 m) measurement-based dust emissions and dispersion modeling approach for the Oceano Dunes, California. *Atmospheric Environment*, 218, 116977, doi: 10.1016/j.atmosenv.2019.116977.

SAG (2023). *Updated SAG Recommendations for Establishing Emissivity Grids to be used in Modeling of Pre-Disturbance Conditions and Future Excess Emissions Reductions*. Memo from SAG to California Department of Parks and Recreation and San Luis Obispo County Air Pollution Control District, December 19, 2023.

SLOCAPCD (2024). *Approval of California Department of Parks and Recreation's Modeling Assumptions to be used in their 2024 Annual Report and Work Plan in Response to Stipulated Order of Abatement Number 17-01*. Memo from San Luis Obispo County Air Pollution Control District to California Department of Parks and Recreation, February 8, 2024.

10 highest emission days: PE into Non Riding Area Central

Metric Tons/day)	10 highest	May 22
Current	165.5	229.9
1939	166	243

10 highest missions days (Current)

10 highest missions days (1939)

1939

Emissions by zone [Metric Tons/day]	Area [acres] of contributing grid points	10 highest days	22-May
Non Riding Area Central	1915.53	121.94	181.14
Non Riding Area North	498.77	20.10	22.58
Non Riding Area South	464.01	23.85	39.21
Total	**2878.3**	**165.9**	**242.9**

Current (PE into Non Riding Area Central)

Emissions by zone [Metric Tons/day]	Area [acres] of contributing grid points	10 highest days	22-May
Foredune Restoration Area	49.3	0.84	1.23
Non Riding Area Central	269.7	18.12	26.39
Non Riding Area North	389.6	15.67	17.61
Non Riding Area South	303.5	15.63	25.72
Plover Exclosure into Non Riding Area Central	309.5	21.0	33.1
Riding Area Central-North	249.2	30.08	38.17
Riding Area Central-South	546.7	62.81	85.74
Seasonal Exclosure	34.0	1.42	1.96
Vegetation Islands	194.2	0.00	0.00
Revegetation	200.6	0.00	0.00
Total	**2546.3**	**165.5**	**229.9**

Current would be approx. same as emissions as in 1939 for 10 highest days

ODSVRA Dust Control Program Draft 2024 ARWP

ATTACHMENT 10

2024 PMRP Evaluation Metrics

THIS PAGE WAS INTENTIONALLY LEFT BLANK.

PMRP Evaluation Metrics – Annual Record 2023-24

In 2021, the SAG, in consultation with State Parks, updated the PMRP evaluation metrics used to track dust control progress. The updated metrics provide a more streamlined dashboard that make it easier to track progress and to inform adaptive management. "Dust Mitigation Targets" refer to evaluation metrics with specific measurable endpoints. "Dust Mitigation Indicators" refer to values indicating progress but for which specific targets are not defined.

In 2022, the SOA amendments updated the metric for evaluating dust control progress, establishing a new excess emissions framework.

This attachment reports on metrics both from the original SOA (for continuity with prior ARWPs, see Table 1 and Table 3) and the October 2022 amendments to the SOA (for the new excess emissions framework, see Table 2).

Evaluation Metric table notes are provided at the end of this document.

DUST MITIGATION TARGETS TABLE 1: EMISSIONS WITH PREVIOUS METHODOLOGY

Dust mitigation treatments		2013 baseline	2019	2020	2021	2022	2023	2024[1]
A. Cumulative area under treatment within ODSVRA, as of July 31 of current year, relative to 2013 baseline (acres)	A1. Total	0	137.8	230.2	322.5	740.1	740.1	740.1
	A2. Back dunes inside riding area	0	103.1	195.5	213.2	288.3	288.3	288.3
	A3. Back dunes outside riding area	4.7	34.7	34.7	61.3	75.9	75.9	75.9
	A4. Foredunes	0	0.0	48.0	48.0	48.0	48.0	48.0
	A5. Nesting exclosure	0	0.0	0.0	0.0	293.3	293.3	293.3
	A6. Foredune beach and corridor	0	0.0	0.0	0.0	34.6	34.6	34.6
PM_{10} mass emissions		2013 baseline[2]	2019	2020	2021	2022	2023[3]	2024[4]
B. Riding area mean PM_{10} emissions for 10 baseline days - modeled	B1. Mass emissions (metric tons / day)	182.8	135.0	131.6	123.9	103.8	100.9	99.9
	B2. Relative to 2013	100%	73.9%	72.0%	67.8%	56.7%	55.2%	54.6%

DUST MITIGATION TARGETS TABLE 2: EXCESS EMISSIONS FRAMEWORK

PM_{10} mass emissions		2019	2020	2021	2022	2023	2024[5]
A. Mean PM_{10} emissions in all zones for 10 highest emission days - modeled	1939 Pre-disturbance scenario			N/A			166
	Current scenario			N/A			148

EVALUATION METRICS TABLE 3: DUST MITIGATION INDICATORS

Air quality indicators		2013 baseline	2019	2020	2021	2022	2023	2024
1. Actual number of high wind event days[6]		59	30	55	51	64	72	51
2. Actual number of exceedances of California air quality standard[7]	2a. at CDF	58	12	30	54	54	16	13
	2b. at Mesa2	43	14	28	38	38	11	11
3. Actual number of exceedances of Federal air quality standard[8]	3a. at CDF	1	0	0	0	0	0	0
	3b. at Mesa2	0	0	0	0	0	0	0
Foredune restoration		2013 baseline	2019	2020	2021	2022	2023	2024
4. Foredune plant fractional cover, at time of spring survey (%)	4a. Treatment 1	N/A	N/A	N/A	0	0	0	0
	4b. Treatment 2				0.1	1.9	2.7	3.1
	4c. Treatment 3				4.0	12.3	10.1	6.7
	4d. Treatment 4				0.8	5.7	5.1	7.9
	4e. Treatment 5				0.4	2.1	6.4	11.3
	4f. Treatment 6				3.6	12.7	13.8	17.8
5. Foredune species richness index relative to Oso Flaco site (10 species in 2021)[9]	5a. Treatment 1	N/A	N/A	N/A	0	0	20	80
	5b. Treatment 2				33	40	30	50
	5c. Treatment 3				50	50	40	70
	5d. Treatment 4				100	60	70	100
	5e. Treatment 5				110	100	90	90
	5f. Treatment 6				110	80	100	100
6. Foredune sand volume, current spring survey relative to previous fall survey ($m^3 \, m^{-2} \, mo^{-1}$)[10]	6a. Treatment 1	N/A	N/A	N/A	0.4	0.8	-0.7	0.0
	6b. Treatment 2				0.5	0.8	0.6	0.0
	6c. Treatment 3				0.6	0.7	1.0	0.0
	6d. Treatment 4				0.2	0.4	0.8	0.1
	6e. Treatment 5				0.1	0.3	0.8	0.1
	6f. Treatment 6				0.0	0.4	0.8	0.1

Back dune stabilization		2013 baseline	2019	2020	2021	2022	2023	2024
7. Cumulative area of back dune stabilization within ODSVRA, as of July 31 of current year (acres)	7a. Planting area	TBD[11]	89.2	109.6	168.5	287.1	314.4	351.9
	7b. Fencing area	0	48.6	53.7	72.8	53.0	32.5	0
	7c. Straw bales area	0	0	18.9	27.3	24.1	17.3	12.3
	7d. Temporary vehicle exclusion areas	0	0	0	5.9	0.0	0.0	0
	7e. Stabilized vegetation surface area	TBD[12]	137.8	182.2	274.5	364.2	364.2	364.2
8. Native seed harvest for all plants during current ARWP reporting period (kilograms/year)		N/A	203.2	307.3	193.0	252.6	234.5	241.9
9. Plant species cultivation for all plants during current ARWP reporting period (#/year)			106,350	89,433	127,464	125,380	121,724	116,112

EVALUATION METRIC TABLE NOTES

[1] 2024 dust mitigation treatment acreage values are based on State Parks 2024 ARWP, Chapter 3, and are subject to change.

[2] The 2013 "Riding area mean PM_{10} emissions for 10 baseline days – modeled" value of 182.8 metric tons per day is based on the original SOA methodology and is based on 2013 PI-SWERL data only.

[3] State Parks 2023 ARWP, Table 2-7, provided an estimate of progress made toward achieving the original SOA's requirements to achieve a 50% reduction in 2013 modeled baseline 24-hour PM_{10} emissions. As shown in this table, State Parks had, as of July 31, 2023, reduced 24-hour PM_{10} emissions from 182.8 metric tons per day to 100.9 metric tons per day, a reduction of 81.9 metric tons per day, and an approximately 44.8 reduction in modeled baseline 24-hour PM_{10} emissions. This estimate was based on the "revised" DRI air quality model that incorporated the 2019 emissivity grid in all areas except the foredune restoration area and the nesting exclosure, which used actual 2022 PI-SWERL observations measured in those areas, and the seasonal foredune beach and transportation corridors, which incorporated a weighted average emissivity relation based on measurements made when these areas were open and closed to vehicular recreation. The "revised" DRI air quality model is described in Section 2.2.1.1 of State Parks' 2023 ARWP.

[4] State Parks 2023 ARWP, Section 3.5.1, estimated the 2023 Work Plan (37.5 acres of converted dust control measures) would reduce 24-hour PM_{10} emissions by one metric ton per day. Therefore, the 2023 Work Plan would reduce 24-hour PM_{10} emissions from 182.8 metric tons per day to 99.9 metric tons per day, a reduction of 82.9 metric tons per day, and an approximately 45.4 reduction in modeled baseline 24-hour PM_{10} emissions.

[5] Pre-disturbance and current scenario emissions under the new excess emissions modeling are from 2024 ARWP Table 2-9.

[6] Values are determined using the ARWP definition of "high wind event day", defined, in consultation with the SAG, as any day when the 3 p.m. PST hourly wind speed at CDF exceeds 8 mph and the 1 p.m. PST hourly wind direction is between 290 and 360°. The period of consideration is January 1 - July 24, 2024. Data may be preliminary and subject to change. The ARWP definition of high wind event days may differ from the SLOAPCD's definition used in SLOACPD reports and studies.

[7] The California Ambient Air Quality Standard is a mean value of 50 $\mu g/m^3$ over a 24-hour period. The period of consideration is January 1 - June 26, 2024. Data may be preliminary and subject to change.

[8] The National Ambient Air Quality Standard is a mean value of 150 $\mu g/m^3$ over a 24-hour period. The period of consideration is January 1 - June 26, 2024. Data may be preliminary and subject to change.

[9] The number of native plant species recorded for each treatment area as compared to reference site at Oso Flaco (10 species in 2021). Long term goal is to have a stable or increasing richness value versus reference site.

[10] 2021 – 2023 normalized volumetric change by total area per month obtained from 2024 ARWP Table 2-3. Values represent the change between spring (February UAS survey) of the column year and fall (October UAS survey) of the previous year. For example, the estimate of foredune sand volume for 2022 for treatment 2 (0.008 m^3 m^{-2} mo^{-1}) is based on Table 2-3 column "Oct. 2021 – Feb. 2022".

[11] The baseline 2013 back dune stabilization "planting area" metric may be estimated from UCSB's historic vegetation report; however, the SAG has not established the methodology for establishing baseline vegetation conditions. State Parks will coordinate with the SAG to finalize the methodology for determining baseline 2013 back dune stabilization planting areas. Currently, the yearly estimates of planting area for the Dust Control Program (e.g., 89.2 acres in 2019) are based on the amount of back dune vegetation planted under the Dust Control Program (i.e., excludes foredune vegetation and non-vegetation projects such as wind fencing).

[12] The baseline 2013 back dune "stabilized vegetation surface area" metric may be estimated from vegetation coverage estimates determined from aerial imagery; however, the SAG has not established the methodology for establishing baseline vegetation conditions. State Parks will coordinate with the SAG to finalize the methodology for determining baseline 2013 back dune stabilization planting areas. Currently, the yearly estimates of stabilized vegetation surface area for the Dust Control Program (e.g., 137.8 acres in 2019) reflect the sum of the stabilization approaches in metrics 7a to 7d.

ODSVRA Dust Control Program Draft 2024 ARWP

ATTACHMENT 11

Updated Scientific Review Process

THIS PAGE WAS INTENTIONALLY LEFT BLANK.

Scientific Review Process for the ODSVRA Dust Control Program

This document describes the process for the review of scientific documents (e.g., reports, public outreach materials) related to dust/particulate matter, beach-dune geomorphology and ecology, windblown (aeolian) processes, dust emission and dispersion, dune restoration, and dust mitigation strategies at Oceano Dunes State Vehicular Recreation Area (ODSVRA).

Background and Goal: There has been, and continues to be, substantial research at the ODSVRA to better understand the science of dust emissions, dust controls, and dune restoration at the park. A standardized approach was adopted by the California Department of Parks and Recreation (CDPR) and by the Scientific Advisory Group (SAG) in August 2021 (see 2022 ARWP, Attachment 07) for the review of scientific documents commissioned by and submitted to CDPR that are relevant to dust mitigation efforts at ODSVRA. In April, 2024, the CDPR and the SAG entered into discussion leading to an update of the protocols. Below is an updated description of the established process by which the scientific review process should proceed, with guidelines for timelines and responsibilities of the SAG, CDPR, and third-party contractors. The primary focus is on when and how the SAG is asked to provide peer review of a research study, prior to steps taken by CDPR to release a document to the public.

For clarity, this review process only applies to research products commissioned by or produced by CDPR that are relevant to the mandates prescribed in the SOA. **Manuscripts submitted to scientific journals for publication, which undergo peer review managed by journal editorial teams, are not subject to the review processes outlined herein.** Such manuscripts developed by third-party contractors are typically based on reports submitted to CDPR as per contract stipulations, and therefore will have been subject to initial review by the SAG for scientific accuracy. Scientific reports directly produced by the SAG, which is an independent entity established by the SOA, are not subject to this review process. Nevertheless, it is generally the case that SAG reports destined for public distribution will be provided a courtesy review by CDPR and SLOAPCD.

The over-riding objective of this review process is to streamline and standardize the manner in which reports are reviewed to ensure that all research products related to dust mitigation efforts in the ODSVRA receive consistent levels of expert review in timely fashion, in order to ensure that all scientific findings (and recommendations flowing from them) are robust and as defensible as possible before they enter the public domain.

Steps in the Review Process for CDPR-Commissioned Reports:

1. CDPR commissions study by a third-party researcher related to SOA mandate. Third-party researcher conducts research and submits report to CDPR.

2. CDPR informs the SAG that a report has been submitted, and may opt to inform the SLOAPCD of the report, as needed. No actions by the SAG are triggered at this stage.

3. CDPR performs preliminary review of third-party report, **normally within 3 weeks of receipt.** CDPR may request that the third-party contractor present report findings verbally to CDPR personnel or to a technical group to address methodological and analytical issues.

4. After preliminary review, CDPR may request that the third-party contractor revise and resubmit the report with clear guidelines as to required changes within a set timeline established through discussion with third-party contractor. Although the third-party contractor retains discretion as to how they choose to address comments from CDPR, the researcher is expected to ensure that the results of the study are scientifically robust and to work with CDPR toward developing a clear public message regarding the research findings.

5. After the report has been reviewed by CDPR (and revisions have been made, if requested and as appropriate), **a request is made to the SAG for a scientific review of the report**. The document continues to remain confidential at this stage and is not to be shared with anyone outside of the SAG.

6. The SAG undertakes a thorough scientific review and produces an assessment document that outlines concerns and makes recommendations for improvement. The review document is submitted to CDPR, **normally within 10 working days**.

7. CDPR shares the SAG review with the third-party contractor and provides guidance as to requested changes and edits to the draft report in timely fashion. The third-party contractor has discretion as to how to address the comments from the SAG, but there is an expectation that all comments will be addressed in some fashion. **The timelines for revision and reply are to be negotiated between CDPR and the third-party contractor**, reflecting the extent of requested changes as well as anticipated scheduling challenges.

8. Third-party researcher submits updated version of report to CDPR, along with summary of how various comments were addressed (or not).

9. At this point, CDPR has several options:

    (a) to accept the revised report as submitted;

    (b) to request additional changes, primarily editorial rather than scientifically substantive;

    (c) to seek a second review by the SAG with clear direction as to which scientific issues need to be addressed; or

    (d) to seek further review by outside parties (e.g., subject matter experts, APCD or CARB personnel).

Note that options c-d would be invoked only under highly unusual and particularly contentious circumstances. The third-party contractor would complete additional changes to the draft report, as deemed necessary, and resubmit to CDPR. Requests by CDPR for further changes and refinement of the report would not normally include the SAG beyond an unusual second round of review undertaken under (c).

10. Upon completion of the review process, the final document will be communicated to the SAG, along with either a letter outlining how SAG comments were addressed, or with the SAG reviewed draft along with responses embedded in the document.

11. Public release of the final document typically happens through the ARWP process, but may also include a presentation at an OHMVR Commission meeting along with posting the documents on the CDPR website. For the ARWP, the final version of the contractor's report as well as the SAG comments on the original draft report will be included as Appendices to the ARWP. However, there are several steps internal to CDPR that may need to be completed prior to public release, including but not limited to:

    i. CDPR may choose to develop a summary document and/or staff report related to the findings of this report. If so, the third-party researcher may be asked to assist in developing these materials.

    ii. CDPR summary document and/or staff report may need to be submitted to CDPR Executive Team for review. Determination is made whether additional review is needed at higher levels (e.g. Natural Resource Agency, Governor's Office).

12. Once the document is public, the third-party contractor is free to distribute and publicly comment on the findings of their report as well as to publish materials derived from the report. The SAG is also free to comment publicly on the report, either verbally or in written form.

13. Throughout this process, all terms and conditions of contracts between third parties and CDPR take precedence, including procedures for CDPR comment and public release. Nonetheless, all entities (CDPR, SAG, third-party contractors) will make reasonable efforts to respect the process as outlined here.

14. **Throughout the scientific review process, all parties will aim to provide comments, edits in response to comments, and approvals in timely fashion. Parties will notify each other of expected significant delays beyond this timeline.**

THIS PAGE WAS INTENTIONALLY LEFT BLANK.

ODSVRA Dust Control Program Draft 2024 ARWP

ATTACHMENT 12

2024/2025 ODSVRA Dust Control Program Vegetation Restoration Projects

THIS PAGE WAS INTENTIONALLY LEFT BLANK.

2024-2025 Project List (subject to change)						
Project Name	**Project Acreage**	**Total Plants**	**Plants Per Acre**	**Native Seed (lbs)**	**Native Seed (lbs per Acre)**	**Large Straw Bales (3X4X8 ft)**
New Planting Areas						
East Moy Mell 2022-ST-01	12.3	33,644	2,735	138	11.2	133
Subtotal	**12.3**	**33,644**	**2,735**	**138**	**11.2**	**133**
Supplemental Areas						
Sand Highway (east) 2022-VG-01	14.6	46,605	3,192	214	14.7	175
Sand Highway (west) 2022-VG-02	11.3	30,173	2,670	116	10.3	136
BBQ Flats 2019-VG-01	3.0	8,229	2,743	44	14.7	36
Subtotal	**28.9**	**85,007**	2,941	**374**	**12.9**	**347**
Total	**41.2**	**118,651**	**2,880**	**512**	**12.4**	**480**

THIS PAGE WAS INTENTIONALLY LEFT BLANK.